A STUDY OF THE POLYMORPHISM OF 4-METHYL-2-NITROACETANILIDE AND RELATED COMPOUNDS

A thesis submitted for the degree of Doctor of Philosophy

by

Alan Yeadon

Department of Chemistry, Brunel University

April 1985

ABSTRACT

The full crystal structures of three polymorphs of 4-methyl-2-nitroacetanilide (MNA) are described. The white form (MNA-1), is the most stable form. The least stable form is the amber form (MNA-2). The yellow form (MNA-3) has been found to change in a topotactic manner into the white form.

The relationships between the three polymorphs are discussed and possible mechanisms to account for the topotactic phase changes are presented.

The polymorphs show different i.r. and Raman spectra in the solid state. These spectra, and those of deuterated analogues are interpreted and their differences explained.

A study of the proton and 13-C n.m.r. spectra show that the conformation of flexible MNA molecules is markedly dependent on the nature of the solvent.

The ability of other o-nitroacetanilides to exist in a white (intermolecular) and yellow (intramolecular hydrogen bonded) forms has been examined.

Finally, details of the synthesis of these compounds and an account of the examination of MNA polymorphs by differential scanning calorimetry (d.s.c) are described.

A description of computer programs used, including one in BASIC which will enable the contents of unit cell(s) to be viewed, is given.

Acknowledgements

I gratefully acknowledge the help and guidance from my supervisor Dr. David N. Waters and the helpful co-operation and work by John C. Moore, School of Physics, Slough College of Higher Education who determined the crystal structures of three polymorphs of MNA at Birkbeck College, London.

I would also like to thank Mr Robert W. Lancaster, Glaxo Research, Greenford, Middlesex for providing facilities for the determination of infrared spectra at low temperature and to Mr Martin Kipps, ICI Plant Protection, Bracknell who recorded the 400 MHz n.m.r. spectrum of MNA.

I gratefully acknowledge the encouragement and financial support given to me during the period from 1976 to 1985 by Berkshire Education Committee and all involved in the Staff Development Scheme. Finally, I express my gratitude to the Science Department secretarial staff for their unflagging assistance and to all my colleagues for their encouragement and patience.

Contents

Appendices.

1. The unit cell parameters for 2,4-dinitroacetanilide.

2. The unit cell parameters for 2-nitroacetanilide.

3. References to other computer programs which have been used in the preparation of this thesis.

4. A BASIC computer programme using high resolution graphics which may be used to view a unit cell(s) before or after rotation around specified axes.

5. A dynamic display showing the phase change yellow (MNA-3) to white (MNA-1).

CHAPTER ONE

A survey of previous work on the structures and spectra of amides and anilides.

Infrared Spectra of secondary amides

The CO-NH group could possibly adopt trans or cis forms

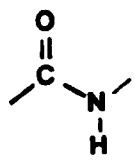

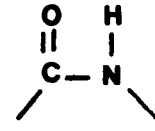

This grouping in N-methylacetamide has been shown to adopt the trans form in gaseous, liquid and solid states as well as in aqueous solutions.[1,2,3,4] X-ray examinations[5] made on many molecules containing the peptide group also show that this group takes only the trans form. From a study of stretching vibrations, however, Russell and Thompson[6] suggested that both the trans and cis forms co-existed. Jones[7] concluded that the molecule of N-methylformamide is in the cis form in the gaseous state rather than the trans form. Secondary amides which are anilides contain the group

—CONHPh

A wide variety of anilides have been examined by infrared spectroscopy. Suzuki[8] and co-workers have examined the infrared spectra and apparent dipole

moments of acetanilide and formanilide and concluded that acetanilide exists in the trans form in solution whereas formanilide exists in the trans and cis forms.

The Raman spectra of formamides and deuterated formamides have been examined by Miyazawa[9] and Suzuki[10] and also by Smith and Thompson[11]. Some assignments due to the latter workers are listed in TABLE 1.

TABLE 1

Vibrational Mode Assignments to Observed Raman Bands

	$HCONH_2$	deuterated formamides
ν(CH)	2896	ν (C-D) 2177 in $DCOND_2$
ν(OCN)	1393	
ν(OCN)	1672	ν(OCN) 1639 in HCOND2
		cis δ(N-D) 1123 in $HCOND_2$
		trans δ(N-H) 1215 in HCONHD
		trans δ(N-H) 1215 om HCONHD
		cis δ(N-H) 1444 IN HCONHD

In Suzuki's[12] work on N-methylacetamide the band at 943cm^{-1} has considerable δ(ND) character. Miyazawa, Shimanouchi and Mizushima[3] have considered the band at 977 cm^{-1} to be almost pure δ(N-D). Smith and Thompson[11] found evidence for cis and trans forms of HCONHD and DCONHD.

Many papers have been published concerning the infrared spectra of secondary amides. Work on this subject is summarised and extended by Miyazawa *et al.*[9] and their results are as follows:

1. The 1650cm^{-1} band (amide I) does not change in position and intensity on deuteration and is mainly νC=O.
2. The 1550cm^{-1} band (amide II) disappears on deuteration.
3. A strong band in the region 1300-1200 (amide III) disappears on deuteration.
4. In N-deuterated compounds a new band appears at 1450cm^{-1} and 950cm^{-1}. These bands were called amide II' and amide III' respectively.
5. Molecules containing the group CH_2CONH give rise to a strong band near 620cm^{-1} (amide IV). The position hardly changed on deuteration.
6. Monosubstituted amides in the *trans* form show a band in the region 700-750cm^{-1} (amide V). This band was assigned to γ(N-H). γ(N-D) produced a band in the region 510-570cm^{-1} (amide V').
7. Another characteristic vibration of molecules containing the group CH_2CONH is observed near 600cm^{-1} (amide VI). After deuteration the amide VI' band overlaps with the amide IV' band.
8 The amide I, III and IV bands can be observed in the Raman spectra as lines with strong or medium intensity, whereas lines due to amide II, V and VI appear as weak lines.

Miyazawa *et al.*[9] have assigned amide bands to molecular vibrations. Thus, amide I is assigned to ν(C=O)with a small contribution from δ(NH). However, the assignment of the amide II band has given rise to much controversy[13]. Richards and Thompson[14] assigned it to N-H in-plane-bending vibration. Randall, Fowler, Fuson and Dangle[15] have assigned ν(C-N) to the amide II band. Letow and Gropp[16] have assigned amide II to ν(C-N). Frazer and Price[17] have suggested that the vibrations ν(C=O), δ(N-H), and ν(C-N) have considerable interaction among each other. Kessler and Sutherland[18] have assigned the band near 720cm^{-1} to the N-H out-of-plane bending vibration.

Vibrations in *cis*-amides have been assigned by Miyazawa[3]. A band near 840.cm^{-1} to γ(NH) which on deuteration shifts to 652cm^{-1} [γ(ND)]. It was considered in the *cis* form, that coupling between δ(NH) and ν(OCN) is small and bands occur near 1440 cm-1 and 1350cm^{-1}. However, in the *trans* form interaction is considerable. Hence amide II was assigned to a combination of δ(NH) and ν(CN) and amide III to a combination ν(CN) and δ(NH). The assignments due to Miyazawa are presented in TABLE II.

TABLE II

Summary of amide vibrations in trans N-methylacetamide

Amide	Wavenumber	Assignment	Raman
I	1650	ν(O=C-N) and δ(NH)	medium
II	1560	δ(NH) and ν(O=C-N)	weak
III	1300	ν(O=C-N) and δ(NH)	strong
IV	630	skeletal vibration CH_2CON	strong
V	754	γ(NH)	weak
VI	610	γ(CO) and γ(NH)	weak

The position of bands in lactams has been calculated using a "consistent force field" method by Warshel, Levitt and Lifson[19]. These workers agree with Miyazawa et al. that amide II is absent from cis amides. Two bands at 1422cm^{-1} and 1375cm^{-1} in 2-pyrrolidone have δ(NH) and ν(CN) character. The assignments of bands in deuterated pyrrolidone and deutererated caprolactam are based on different combinations of vibrations. In caprolactam, bands of medium intensity disappear after deuteration and several new bands occur. Interpretation of these changes is difficult since bands change their characteristics as, for example, δ(N-H) is coupled to ν(CN) and also to CH_2 vibrations in different combinations. δ(N-H) is associated in varying degrees with nine bands and δ(N-D) with ten bands. In deuterated caprolactam, bands at 1170cm^{-1} and 1085cm^{-1} are mainly due to δ(N-D). Bands containing a contribution from ν(C-N) also contain considerable contributions from CH_2 vibrations.

The infrared spectra of acetanilide and deuteroacetanilide have been studied by Abbott and Elliott[20] in 1956. Earlier work using infrared analysis had been carried out by Crooks[21], Mann and Thompson[22], and Bamford[23] et al. and Gierer[24]. The Raman and infrared spectra of acetanilide and deuteroacetanilide have been studied in detail by Chalapathi and Ramiah[25]. These molecules were subjected to normal co-ordinate treatment and the mixing of the amide vibrations has been determined and is listed in TABLE III.

TABLE III

Acetanilide			Deuteroacetanilide
Wavenumber/cm^{-1}		Assignment	
IR	RAMAN		
1658	1640	ν(C=O)	1640
1558	1550	δ(NH)	1410
1258	1269	ν(C-N)	1080
1017	1025	ν(N-Ph)	958
650	632	δ(O=C=N)	645
843	850	ν(C-CH_3)	820
3305		νN-H ν(N-D)	2500 (near)

The assignments given to the bands at 1410cm^{-1} and 1080cm^{-1} in deuteroacetanilide are inconsistent in this work. For example, it is stated that in the 1080cm^{-1} band of deuteroacetanilide "there is no contribution from C-N stretching vibration". However the band at 1080cm^{-1} is assigned to ν(C-N). If the assignments of bands at 1410cm^{-1} and 1080cm^{-1} were reversed i.e. 1410cm^{-1} to ν(CN) and 1080cm^{-1}to δ(N-D) then these conclusions would be in accordance with those of Miyazawa. The amide V band in acetanilide is assigned to a band near 600 cm^{-1} and γ(N-D) to a band at 520cm^{-1}. These bands do not differ by a factor of $\sqrt{2}$ which is expected for a pure vibration in which D has replaced H. The band at 745cm^{-1} has a distinct shoulder which disappears on deuteration. It seems likely that the amide V band in acetanilide is obscured by the 745cm^{-1} band and it may be coupled to aromatic γ(CH) vibrations. This might explain the changes in intensity in the bands near 750cm^{-1} and 700cm^{-1} on deuteration.

The infrared spectra of anilides have been measured by Forbes, Morgan and Newton[26]. By observing the wavenumbers of bands near 3300cm^{-1} and 1700cm^{-1} these workers were able to detect intramolecular hydrogen bonding in the solid form as well as in solution. Generally, a band at a wavenumber 1700cm^{-1} was taken to indicate a free non-hydrogen bonded C=O group, whereas a band about 1670cm^{-1} indicated a hydrogen bonded C=O group.

In general, o-nitroacetanilides are intramolecularly hydrogen bonded [ν(NH) 3370 $\pm$ 20cm^{-1} in chloroform] and could be distinguished from non-bonded p-nitro and unsubstituted compounds [ν (N-H) 3440 $\pm$ 20cm^{-1} in chloroform]. Intramolecular hydrogen bonding does not occur in 2-methyl-6-nitroacetanilide and in 2,4-dimethyl-6-nitro acetanilide in the solid state as revealed by their typically bonded N-H and C=O bands. The nature of the hydrogen band in some nitronaphthalides is also discussed.

The interaction of nitro and amino groups in nitroanilines and nitronaphthylamines has been examined in detail[27].

The infrared spectra of anilides has been examined by Peltier, Pichevin and Bonnin[28]. Mono and disubstituted aniled show a band near 1710cm^{-1} due to ν(C=O). This value was compared with that for acetanilide (1705cm^{-1}) and N-methylacetamide [1686cm^{-1} (s) and 1712cm^{-1} (w)] . Conjugation of the N atom with the ring should increase the value of ν(C=O). Since a lowering in wavenumber is apparent, Peltier et al. proposed a hydrogen bonding effect which would lower ν(C=O).

In I the vibration νC=O is restricted by the proximity of H-6. In 2, 6-dinitro-4-methylacetanilide and 2,4-dichloroacetanilide the band due to ν C=O occurs near 1740 cm^{-1}. (doublet). Hence the presence of II was inferred and dipole-dipole repulsion was the suggested explanation. Anilides containing an ortho ester group were found to be strongly hydrogen bonded as indicated in III

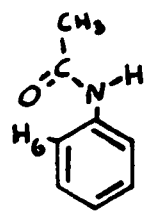

I

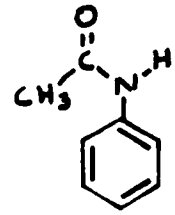

II

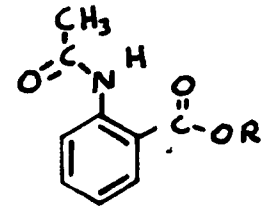

III

Gomel and Lumbroso[29] have measured the dipole moments of acetanilides. In certain benzene solutions acetanilide was present as open chain dimers IV.

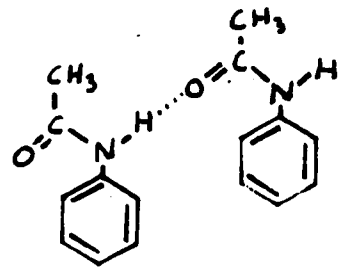

IV

In general the results once more indicated the trans arrangement for the amide group. o-chloroacetanilide appeared to be unassociated due to intramolecular hydrogen bonding whereas o-methylacetanilide was strongly associated, with both molecules having the amide group as in I. Smith has also measured the dipole moments of anilides[30]. Small amounts of the form II have been detected[31,32] and Siddall [33] has reported the isolation of cis and trans

forms of o-methylformanilide. For formanilides[34] the value of the rotational barrier is about 76 kJ mol $^{-1}$

Some investigators have considered the acetamido group as a substituent in aromatic systems. Dyall and Kemp[32] examined the infrared spectra of about six ortho and six para substituted anilides in solvents. The shift of the ν (N-H) band was measured and compared with that observed for acetanilide. Evidence for various forms of anilides was obtained. Two bands due to ν (N-H) (about 45 cm^{-1} apart) were observed in non-basic solvents but only one in basic solvents. These bands also differ in intensity, the stronger one at higher frequency is attributed to the trans isomer. The frequency separation has been described by Moritz[35] as being due to the direct field effect of the C=O group. For an ortho substituted anilide, four conformations are possible, and the infrared spectrum of o-methylacetanilide shows 4 bands due to ν(N-H). Ortho substituents which can hydrogen bond to the amide group have only one ν(NH) band which moved to lower wavenumbers in more basic solvents. From the linear plots of ν(NH) of a compound against ν(NH) acetanilide [BELLAMY PLOT][36] evidence for hydrogen bonding was obtained. However, similar plots were obtained for o-methylacetanilide where intramolecular hydrogen bonding is not possible. It was concluded that intramolecular hydrogen bonds can be broken by the more basic solvents.

The Nuclear Magnetic Resonance Spectra of Amides

Structure of the Amide Group

Amides have been extensively studied by n.m.r. since the amide linkage is of interest to biochemists, theoretical chemists and organic chemists. Most of the chapter headings in a popular high level textbook[37] can be directly applied to amides. Application has ranged from a study of internal rotations of amides, finger-printing, confirmation of structure and the electronic structure of the amide bond.

This short review will refer to studies which show the conformation and flexibility of the amide group in secondary amides since rotation around the C-N bond and around the R^2-N bond could lead to polymorphism in anilides.

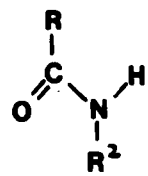

Nomenclature for the geometrical isomerism in secondary amides

Authors have used the terms cis/trans, endo/exo and E/Z to describe the two possible arrangements around the amide bond. Geometrical isomerism is possible since the amide group is resonance stabilised.

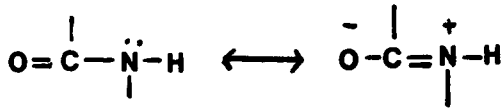

The C-N bond achieves partial double bond character and hence rotation around the C-N bond is restricted and the amide group has a stiff planar structure.

In aliphatic secondary amides the two possible geometrical isomers are as follows

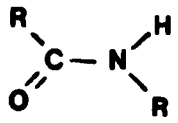

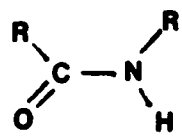

In anilides, the possible arrangements are as follows:

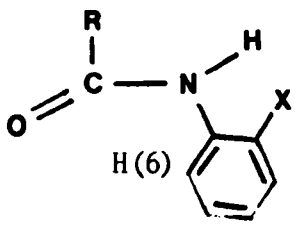

I=Z

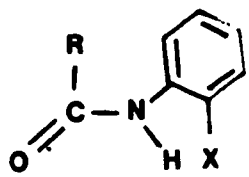

II

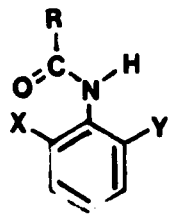

III

The relative positions of the O and H atoms in the amide group are shown in I and II. It is proposed in this thesis to use the terms E and Z to describe the arrangements. The term Z refers to the structure (I) in which the O and aromatic ring lie on the same side of the (partial) double bond as each other. In anilides the problem of the positions of the planes occupied by the amide group and aromatic ring arises. Extreme cases arise where the rings can be either coplanar or at right angles to each other. If the group X (I, II and III) can hydrogen bond to the amide group then the rings will be coplanar. However, in III the rings will be perpendicular whether or not X (or Y) is capable of hydrogen bonding to the secondary amide group.

An important feature of structure I is that the oxygen atom in the carbonyl group must lie very close to H-(6) if the ring is coplanar with the amide group. Such proximity is revealed by protons H-(6) having a much greater chemical shift than expected from mesomeric and inductive effects. Other ring protons are affected to a much lesser extent. In some cases H-(5) is coupled to N-H[38].

Anisotropic Effects in Amides

The shielding and deshielding areas have been determined by Paulsen and Todt[39]. Generally, protons are deshielded when held in the plane of the amide and shielded when out of the amide plane[40,41].

Comprehensive reviews of the n.m.r. spectra of amides, covering the literature to 1970 are available[42,43].

Bartels-Keith and Cieciuch[38] have examined the n.m.r. spectra of a range of ortho substituted nitroacetanilides. The high chemical shift for the H-(6) proton and the effect of change of solvent on this parameter enabled these workers to estimate the relative strength of the intramolecular hydrogen bond in compounds where the group ortho to the amide group was nitro and the group para to the amide was either methyl or methoxy or hydrogen. The greater the change in chemical shift in $CDCl_3$ to CD_3CN, the weaker the intramolecular hydrogen bond was assumed to be. By this means it was possible to conclude that the order of hydrogen bond strengths was 5-methyl-2-nitroacetanilide>o-nitroacetanilide>4-methyl-2-nitroacetanilide>4-methoxy-2-nitroacetanilide.

Since the chemical shift of H-(6) in o-acetylacetanilide was not solvent dependent the $COCH_3$ group may be assumed to form a stronger hydrogen bond to the $NHCOCH_3$ group than a nitro group does.

Rae and co-workers measured acylation shifts for a series of 4-substituted-2-nitroacetanilides and a good correlation with σ values of the substituents was found[44].

Lynch[45] has used the anisotropic effect of the C=O group to analyse the n.m.r. spectra of a series of 2-nitroacetanilides. In the intramolecularly hydrogen

bonded molecules the deshielding effect of the C=O group is larger than in non-planar anilides. Hence such studies can provide evidence for hydrogen bonding whereas infrared spectra may not provide such unequivocal evidence[46].

Conformation and Structure of Anilides

The n.m.r. spectra of formanilides have been studied by Carter[47]. The stereochemistry of formanilides is rather easier to measure by n.m.r. since the formyl proton is on an adjacent atom to the N-H group and its coupling constant is either about 2 Hz (J cis) or 10 Hz (J trans)

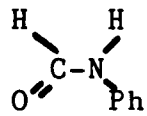

cis

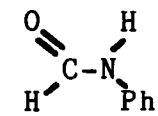

trans

In the case of the trans formyl proton it is possible to relate the chemical shift to the dihedral angle between the amide and benzene ring planes[48]. Carter[47], found that appreciable amounts of Z and E forms exist in solution and since it is possible to assign signals due to each of these isomers, quantitative results could be obtained. It has been possible to isolate stable Z and E isomers[49]. Also rotational barriers can be found and these are of the order of 18 kcal/mole at about 350K.

In formanilide, the amount of E isomer increases on dilution perhaps due to the stabilisation of dimers[50].

Appreciable amounts of both E and Z forms are reported for acetanilide, 4-methylacetanilide and 4-butylacetanilide in $CDCl_3$ (Ref.6 p.528). Acetanilide in solution appears to exist mainly in the Z form and changing the alkyl substituent on the carbonyl group does not alter the isomer ratio[51,52,53,40]. A bulky ortho substituent increases the stability of the E form[51] and is greatest when the ortho substituent is t-butyl[54]. Such groups increase the barrier to rotation of the Z and E isomers and such isomers of 2,4,6-tri-(t-butyl) acetanilide can be separated by TLC[55] and crystals of the pure E form obtained from ethanol.

Studies on the rotation around the Aryl-N bond in anilides

The early work on this subject has been reviewed by Adams[56]. In general, ortho substituted anilides show signals due to E and Z forms. 2,6-di-isopropylacetanilide shows signals due to the CH_3 group in the acetyl group in different orientations.

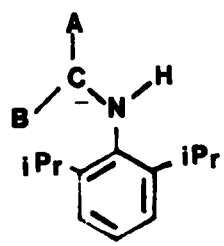

A = Me or O
B = O or Me

Kessler[57] has measured the E/Z ratios of this anilide in various solvents. The Z isomer predominates in solvents of high dielectric constant. In solvents of low dielectric constant the proportion of E isomer increases up to a maximum of 26:74 in C_6D_6

Siddall and Stewart[58] have measured the energy barrier to rotation of the Ar-N bond in some ortho substituted acetanilides and obtained values of the order of Ea=20 kcal/mole and ΔG^{*}, the free energy of activation, slightly greater. Some data are presented for 0.3M CH_3CONH-2,6$(2Pr)_2C_6H_3$ in $CHBr_3$:-

for rotation around amide bond = 19.3 kcal/mole(105°C)

for rotation around benzene ring-nitrogen bond in E isomer = 18.9 kcal/mole(75°C)

for rotation around benzene ring-nitrogen bond in Z isomer = 11.8 kcal/mole(-60°)

Conformations of N-methylacetanilide

In contrast to the preferred Z arrangement of the amide group in 2° amides, N-methylacetanilide has been shown to exist mainly in the E form[59]. The n.m.r. spectrum of this compound in pyridine solution consisted of large peaks at 112 Hz and 195 Hz with smaller peaks at 126 Hz and 177 Hz. This corresponds to an E/Z ratio of 99.5/0.5. The E arrangement in N-methylacetanilide has been inferred by Thomson and Hollberg[60] from dipole moment measurements. Gutowsky and Holm[61] detected only one isomer in benzene solution but were unable to decide whether the E or Z arrangement was present. Carter has compared the n.m.r. spectra of acetanilide and N-methylacetanilide[52].

Conformations adopted by thioamides

S
"

In thioacetanilides, the thioamide (NHCR) was shown by n.m.r. experiments to lie in the plane of the benzene ring only if intramolecular hydrogen bonding is possible[62]. By measuring the acylation shift i.e. the difference in chemical shift of the H-(6) proton in the amide and parent amine, it is possible to deduce whether the C=S (or C=O) is adjacent to H-(6). If this is the case, then the acylation shift is relatively high. Thus in 2,5-dimethoxyacetanilide the acylation shift of H-(6) is 163 Hz which is a large value and hence the following conformer should exist:

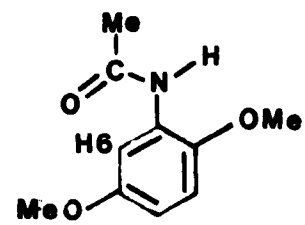

An acylation shift of 64 Hz in 4-methylthiopivanilide indicates that the E isomer exists in $CDCl_3$ colution.

The anisotropic effect of the C=O group in a heterocyclic compound

The chemical shift of H-(3) of the heterocyclic compound 2-acetoacetamido-4-methylpyridine is 7.99 ppm ($CDCL_3$)[63]. This position corresponded to a large "acylation shift" thus the conformation shown must be the favoured one i.e. the C=O group lies near H-(3).

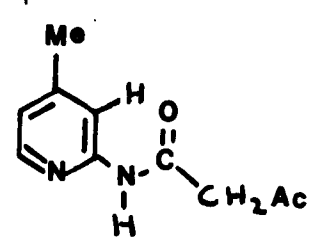

^{13}C n.m.r. spectra on anilides

Solvent effects on the ^{13}C n.m.r. spectra of anilides have not been reported. These spectra, which should prove to be complementary to ^{1}H n.m.r. should also show solvent dependence due to the change in electron density at the ortho and para positions (relative to the amide group) as the dihedral angle between the benzene ring and amide group changes. Several such series of spectra have been recorded[64].

Rae[65] has examined the n.m.r. spectra of 1,3-diacylphenylenediamines.

The acylation shifts for ring protons in such compounds were only slightly smaller than those predicted on the basis that each of the amide groups acts independently.

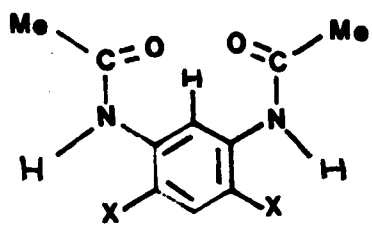

The following acylation shifts were assumed (a) 1.0 ppm for protons ortho to the amide group (b) 0.2 ppm, meta and (c) 0.4 ppm, para.

When substituents which are capable of hydrogen bonding are introduced in the 4 and 6 positions acylation shifts of about 4 ppm are recorded for H-2.

Hydrogen bonding must maintain the planarity of the whole molecule in spite of a severe dipole-dipole repulsion.

A low field shift due to anisotropic shielding of an N-acetyl group has been reported by Brugel in 2-acetylaminopyridine (I), in N-acetyl derivatives of benzimidazoles (II) and purines and 4-N-acetylpyrimidine.

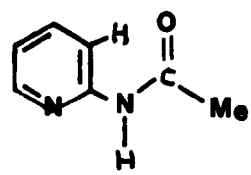

I

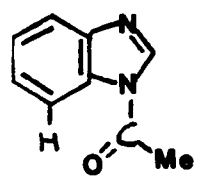

II

The crystal structure of anilides

The first anilide examined by X-ray diffraction techniques was acetanilide[67]. A further refinement of this work improved the overall regularity of the molecule and corrected a mistake in the earlier paper in which the value for the dihedral angle between the amide and ring planes was given as 37°54'. The recalculated[68] value was 17.6°. Pedersen and Pedersen[69] examined the structure of N-methylacetanilide and found the amide group existed in the E conformation, in contrast to the Z conformation adopted by acetanilide, and that the amide-ring dihedral angle was 90°.

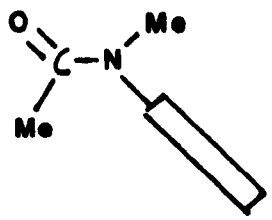

Ring viewed edge on.

The ^{1}H chemical shifts in these compounds have been correlated with electron density by Carter who assumed that the molecules had the same conformation in solution as in the solid state[70].

Some monosubstituted anilides have been examined by X-ray diffraction and these include p-aminoacetanilide,[71] p-methylacetanilide,[72] p-hydroxyacetanilide,[73] p-chloracetanilide,[74] and p-bromoacetanilide.[75] The crystal structure of benzanilide has recently been determined and its structure compared with poly(p-phenyleneterephthalimide)[KEVLAR] and poly(m-phenyleneisophthalamide)(NOMEX].[76] A dominant feature of all these structures is the Z conformation of the amide (H-N-C=O) system which allows linear chains of intramolecularly hydrogen bonded molecules to be constructed.

A computer search of the data files at the Centre for Crystallographic Data, University of Cambridge was carried out on 9th March 1978. Thirty five compounds containing the fragment PhN(C=O)C which were listed by the computer are presented in Table IV. A complementary computer search of Chemical Abstract Indexes using the key words FORM, AMIDE and ANILIDE revealed that few anilides which exist in polymorphic forms have been examined by X-ray crystallography. The search did reveal that the crystal structures of polymorphic forms of p-methylacetanilide[72] and p-hydroxyacetanilide[73] had been reported.

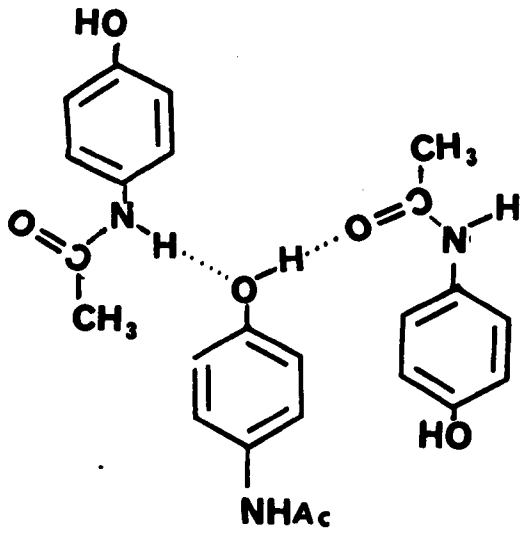

In the former compound, two forms exist. One form contains molecules stacked in a parallel (orthorhombic) and the other contains molecules stacked in an antiparallel (monoclinic) manner. An interesting feature of the crystal structure of p-hydroxyacetanilide is that the hydroxyl group can form hydrogen bonds to the amide group.

The crystal structure of several N-methylamides was determined by Leiserowitz and Tuval.[77] The molecular packing of N-methyl derivatives of propiolamide, tetrolamide, banzamide, cinnamide and sorbamide were determined and compared with other secondary amides whose structures had been determined by other workers. The types of structures found were classified as follows:-

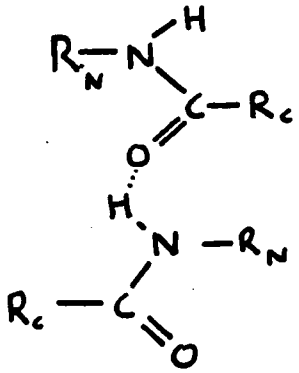

1(a)

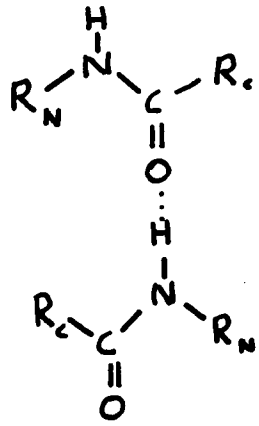

1(b)

Type 1 (2_1 axis or glide)

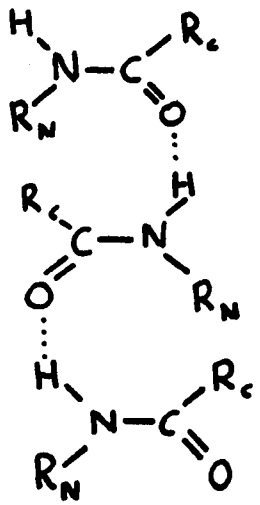

Type 1(c)

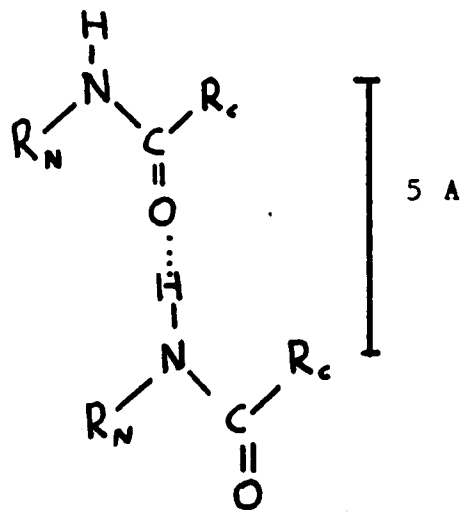

Type 2. (Translation type)

It was noted in monoamides where Rn and Rc differ in size e.g. p-bromoacetanilde. that the molecules tend to interlink via the glide or 2_1 axis. Acetanilide links as in 1a with the phenyl groups arranged around a 2_1 axis which coincides with the hydrogen bonding chain. In this way contact between the bulky groups is avoided. In type 2 the group Rc...Rc and Rn...Rn would be forced to be the same distance apart along the hydrogen bond axis i.e. about 5Å apart. N-bromoacetamide packs according to 1c. N-propyldipropylacetamide packs according to 2. P-bromoacetanilide and p-chlororacetanilide pack according to 1a which has hydrogen bonded molecules related by a glide. [A glide translation consists of a reflection through a plane parallel to the hydrogen bonding followed by a translation along the axis of the hydrogen bond]. Secondary diamides tend to form hydrogen bonds by translation e.g. N,N-diethyladipamide along the axis in the direction of the hydrogen bond. This effect places adjacent hydrogen bonded molecules about 5Å apart.

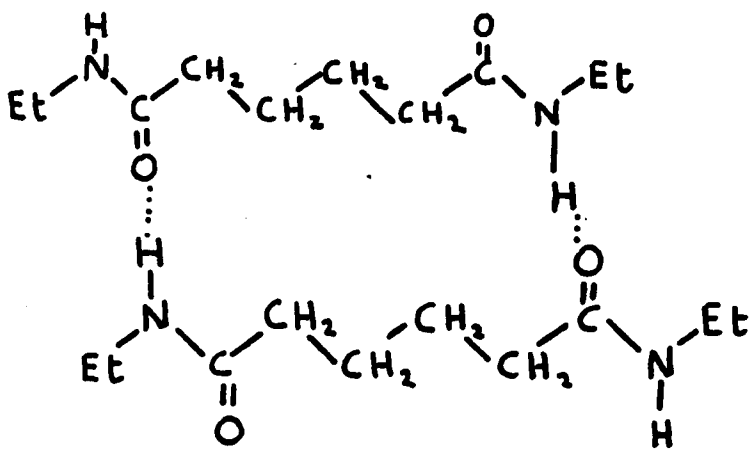

Secondary cis (or E) amides may be interlinked by N-H....O bonds in two ways; (a) as hydrogen bonded pairs

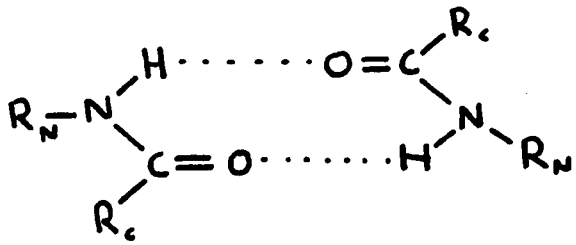

or (b) by simple N-H....O=C bonds along a 2_1 axis thus linking molecules by a helical arrangement of hydrogen bonds.

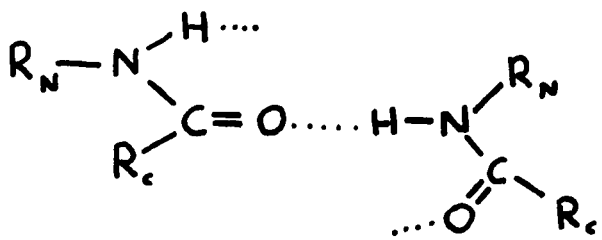

An example of type (b) is α-pyridone and an example of (a) is succinimide. In such compounds the N-H....O distances are close to 2.84Å thus demonstrating that the length of the N-H....O bond in secondary amides does not seem to depend on a Z or E arrangement of the amide group.

TABLE IV

Anilides of known crystal structure

acetanilide[67]

N,O-diacetyl-5-p-chloroanilino-4-hydrocypenta-2,4-dienal[73]

p-acetotoluidide[72]

3-amino-3-chloro-2-cyano-acrylic acid anilide[79]

N-acetyl-l-tyrosine-p-nitroanilide[80]

2,2'-bis(2-bromoacetylaminoanilino)-benzalazine benzene solvate[81]

2-bromo-5-trifluoromethyl-dipropylacetanilide[82]

(-)-N-(2-benzylmethylamino)propyl) propionanilide hydrobromide[83]

N(1')-carboxybiotin di(p-bromoanilide)[84]

4-chloro-di-N-propylacetanilide[85]

2-chloro-5-trifluoromethyl-diethylacetanilide[86]

p-chloroacetanilide[74]

2-chloro-isonitrosoacetanilide[87]

N-((6-chloro-4-oxo-4H-3,1-benzoaxin-2-yl)methyleneamino) -N-phenylacetamide[88]

desoxycholic acid p-bromoanilide[89]

3,4-dichloro-isobutyranilide[90]

N,N-diphenylacetamide[91]

4-ethoxy-isonitrosoacetanilide[92]

2-ethoxy-isonitrosoacetanilide[93]

N-(1-(-3(p-fluorobenzoyl)propyl)-4-piperidy)propionanilide[94]

p-hydrocyacetanilide (orthorhombic form)[73a]

p-hydroxyacetanilide (monoclinic form)[73b]

2-(isopopylidineamino-oxy)propion-p-bromoanilide isonitrosoacetanilide[95]

2-diethylamino-2',6'acetoxlidide[96]

lidocainebis(p-nitrophenyl) phosphate[97]

lidocaine hydrohexafluoroarsenate (2-diethylamino-2',6'-acetoxylidide hydrohexafluoroarsenate)[98]

lidocaine hydrochloride monohydrate[99]

2-methyl-4-(N-acetanilino)-6-bromo-1,2,3,4-tetrahydroquinoline[100]

N-methylacetanilide[69]

3-methyl-N-ethylisonitrosoacetanilide[101]

2-methoxy-isonitroso-acetanilide[102]

alpha-dibromo-alpha-(4-methyl-2-nitrophenylazo) acetanilide[103]

N-methyl-piperidinium-(O-methyl-acetanilide) iodide[104]

N-methylpiperidinium acet-p-nitroanilide iodide[105]

2-(1-methylpiperidino-(1))-2'-chloroacetanilide iodide[106]

N-methylpiperidinium-m-chloroacetanilide[107]

N-methylpiperidinium acet-p-bromoanilide iodide monohydrate[108]

N-methyl-2,4,6-trinitroacetanilide[109]

4-methoxy-isonitroso-acetanilide[110]

N-(4-methoxymethyl)-1-(2-phenylethyl)-4-piperidinyl)-N-phenyl-propanamide[112]

alpha-(2-nitro-4-chlorophenylazo)acetoacetanilide[113]

(N-methylimidazole)-(dioxygen)-tetrapivalamidophenyl)-(porphinato) iron (II)[114]

1,1-bis(N-phenylcarbamoyl)-2-(p-chlorophenyl)-ethylene

piperidinoacetic acid o-chloroanilide[115]

(N-piperidino-acetyl)-m-bromoanilide[116]

2,3-dihydro-1,3-diphenyl-2-oxoindol-3-yl

diphenyl (phenylcarbamoyl)methyl sulphide[117]

ionylidene acetyl p-bromoanilide[118]

rifamycin p-iodoanilide acetone pentahydrate[119]

rifamycin p-iodoanilide DMSO solvate[120]

tetrahydrothiophene-(dioxygen)-(pivalamidophenyl)-

porphinato-

iron(II) tetrahydrothiophene solvate[121]

p-bromoacetanilide[75]

CHAPTER TWO

A review of the polymorphism of amides and the topotactic changes of organic compounds.

Polymorphism, conformational polymorphism and topotactic changes in organic compounds

A polymorph is a solid crystalline phase of a given compound resulting from the possibility of at least two different arrangements of the molecules of that compound in the solid state. The molecular conformation in each polymorph may be the same or different. If the relationship between the molecules in the different forms is one involving tautomerism or geometrical isomerism then this does not constitute polymorphism. Polymorphism can result from identical molecules being packed in different types of crystalline structures or from molecules having different conformations being packed in similar or different ways. Such changes in conformation may result from rotation of parts of the molecule around certain bonds and this is usually accompanied by small differences in bond lengths and bond angles so that equivalent intramolecular and intermolecular distances can be markedly different.

Polymorphism is the ability of any element or compound to crystallise as more than one distinct crystal species. An example of polymorphism is shown by the ability of carbon to exist either as graphite (hexagonal) or diamond (cubic). Different polymorphs of a given compound are often different in structure and properties as the crystals of two different compounds.

Thus density, colour, solubility, melting point, crystal shape, crystal symmetry, hardness, vapour pressure, optical, electrical and biological properties can vary with the polymorphic form. The latter property makes the study of polymorphism in drugs an important topic in the pharmaceutical industry. In addition, the preparation of individual polymorphs of drugs may be protected by patents. The pharmaceutical industry is also interested in polymorphic changes which occur during the preparation of tablets or polymorphic changes which occur during the storage of drugs. Also drug dosage is dependent on polymorphic form. Applications of polymorphism in the pharmaceutical industry have been reviewed by Haleblain and McCrone and this review contains references to the polymorphism of steroids, barbiturates, antihistamines, and sulphonamides.[122] The subject of polymorphism has been covered in several texts including those by Jenkins,[123] O'Connor[124] Hartshorne and Stuart,[125] Kofler and Kofler,[126] McCrone,[127] and Verma and Krishna[128].

Deffet[129] has published a comprehensive compilation of organic compounds which show polymorphism and the amides included in his survey are listed in Table V. The most recent reference is cited.

TABLE V

Polymorphic amides and anilides listed by Deffet[129]

acetamide

dichloroacetamide

malonamide

lactamide

succinimide

asparagine

sulphanilamide

formanilide

benzamide

acetanilide

2,4-dibromoacetanilide

1-nitro-3-bromo-4-acetanilide

valeranilide

p-toluenesulphanilide

4-nitrobenzoyl-2-chloro-4-bromanilide

p-chloroacetanilide

p-bromoacetanilide

p-iodoacetanilide

2-chloro-4-bromoacetanilide

4-chloro-2-bromoacetanilide

2-nitro-6-methylacetanilide

2-nitro-4-methylacetanilide

3-chloro-4-methylacetanilide

p-bromopropio-anilide

p-iodopropio-anilide

N-butyranilide

p-acetophenetidine

N-alkylvanillamides

A historical account of the polymorphism of 4-methyl-2-nitroacetanilide

In 1885 Gattermann[130] reported the occurence of polymorphic forms for 4-methyl-2-nitroacetanilide. Subsequent workers examined the physical properties of the white and yellow forms of this compound. Schenck[131] found the melting point of the yellow form (91.58°C) and the white form (93.32°C). Auwers[132] measured the molecular weight of several amides and found that some amides especially formamides, showed anomalous behaviour in that the molecular weight was higher than the formula weight. However, 4-methyl-2-nitroacetanilide did not show this behaviour indicating that the compound was not associated in solution. Baly, Tuck and Marsden[133] examined the absorption spectrum of 4-methyl-2-nitroacetanilide. Hantzsch[134] commented on several compounds, including 4-methyl-2-nitroacetanilide and a dichloro-dihydroxy derivative of diethyl phthalate, which did not obey Beer's Law. Later Hantzsch[135] examined the UV spectra of several nitro compounds and found that the UV spectra of 4-methyl-2-nitroacetanilide was solvent dependent in addition to its deviation from Beer's Law. It was suggested that these properties were related to the existence of coloured isomers.

Muller[136] examined over twenty five compounds which had been found to exist in polymorphic forms. The amides mentioned in this work included acetamide, acetanilide, benzamide, formanilide and 4-methyl-2-nitroacetanilide.

Schaum[137] listed a wide variety of compounds which showed polymorphism and grouped these compounds into various categories of polymorphism.

The association of amides was studied by Hunter and Chaplin[138] using cryogenic and wet melting point techniques. It was found that 2,6-disubstituted anilides associate even in the presence of an ortho nitro group which was capable of forming an intramolecular hydrogen bond and hence preventing intermolecular association. Compounds such as

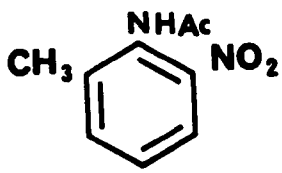

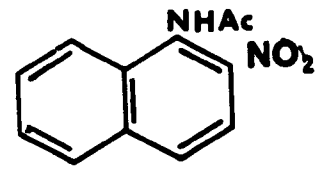

associate and have low solubility in hydrocarbon solvents whereas the compounds

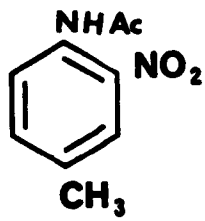

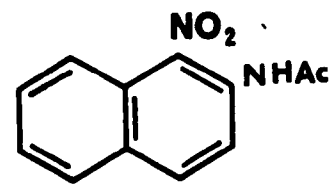

were found to be soluble in hydrocarbon solvents and unimolecular. These properties were explained on the basis that the latter compounds contained intramolecular hydrogen bonds. These workers also discussed the possibility of optical activity in 2,6-disubstituted anilides. Although optical activity would be predicted in such molecules due to restricted rotation of the amide group this was not realised in practice. This

inability to show optical activity was explained in terms of a low barrier to rotation of the amide group which would result in rapid racemisation. Skulski[139] examined the UV spectra and infrared spectra of some o-nitroacetanilides in pyridine:cyclohexane mixtures. The changes in UV spectra with solvent were explained in terms of the relative strengths of the intramolecular hydrogen bond viz. o-nitroacetanilide = 4-methyl-2-nitroacetanilide > 1-nitro-2-acetonaphthalide > 2,6-dimethyl-6-nitroacetanilide. Since the UV spectrum of 4-mthyl-2-nitroacetanilide in cyclohexane was very similar to that of the yellow form and the infrared spectrum of N-methyl-4-methyl-2-nitroacetanilide was similar to the white form, it was concluded that the yellow form contained intramolecular hydrogen bonds and the white form contained intermolecular hydrogen bonds. This view was confirmed by the infrared spectra of the yellow and white forms (KBr disc). The yellow form showed bands near 3400 cm^{-1} and 1710 cm^{-1} whereas the white form showed bands near 3300 cm^{-1} and 1690 cm^{-1}. These bands were assigned to ν N-H and νC=O respectively. It was also noted that after grinding the yellow form for about five minutes with KBr the spectrum of the white form was obtained whcih was known to be the stable form. No other compound mentioned showed this behaviour. This technique offers a method for detecting polymorphism when the phenomenon depends on the presence of a weak hydrogen bond which can change to a more stable system involving intermolecular hydrogen bonds.

Skulski[140] has examined the ultraviolet absorption spectra of several o-nitroacetanilides including o-nitroacetanilide, 4-methyl-2-nitroacetanilide, and 1-nitro-2-acetamidonaphthalene. The UV spectra of these compounds changed considerably with solvents whereas no change was observed with the N-methyl analogues of these compounds. It was concluded that these compounds were intramolecularly hydrogen bonded in cyclohexane but addition of a solvent, such as methanol, caused the formation of a noncoplanar species since the solvent could compete with the nitro group for the formation of hydrogen bonds with the amide group.

Extensive studies of the solvent dependance of the ultraviolet absorption spectra of numerous nitroacetanilides and a few nitrophenols led Skulski to conclude that the nature of the hydrogen bond in such molecules was obtained better with aid of UV spectroscopy than by other physical techniques such as infrared spectroscopy.

The infrared and ultraviolet spectra of two polymorphic forms of 4-amino-2-nitroacetanilide were examined and Skulski concluded that the red form contained an intramolecular hydrogen bond whereas the yellow form contained an intermolecular hydrogen bond.

Identification of polymorphic forms of crystals by infrared spectroscopy

The use of infrared spectroscopy to recognise polymorphic forms is well established and is complementary to other techniques available for this task such as X-ray analysis of powders, optical microscopy, and electron microscopy. The infrared technique offers advantages such as the use of samples of the order of 1mg, the analysis is rapid and the detailed character of the spectrum can be used as a permanent record for characterisation and comparative purposes. Kendall in 1953 reported on the use of infrared spectroscopy to identify polymorphic forms of dyes and titanium dioxide in the form of mulls.[141] In the case of dyes, which often occur as powders rather than crystals, the use of the microscope is not possible. However, by means of infrared spectroscopy Kendall was able to determine polymorphic forms qualitatively and quantitatively present in mixtures to the level of about 1%. Mesley[142] has examined the solid state infrared spectra of 35 steroids and investigated the various polymorphic forms. About 20 of these steroids showed polymorphism and this could be ascribed to the formation of different types of hydrogen bonds. Examples of some other compounds, mainly of pharmaceutical interest, which have been examined for polymorphism by infrared spectroscopy are trimethorprim,[143] sulphonamides,[144] steroids,[145] cephaloridine,[146] phenobarbitone[147] and acetohexamide.[148]

The occurence of polymorphism has been detected in steroids by means of a technique which involves comparison of the infrared spectra after melting and resolidification with that of the original solid.[149] In this procedure polymorphic forms of the same compound, treated under the same conditions of melting and cooling, will revert to that single polymorph favoured by energy consideration. This approach requires complete melting, identical cooling rates, and the absence of foreign matter that could provide nucleation sites favouring a particular polymorph.

Since polymorphic transitions can be induced by the grinding process involved in making potassium bromide discs and since polymorphism is a phenomenon of wide occurence the resulting infrared spectra may not correspond to the original material. In order to test for possible changes occurring during the preparation of a disc the spectrum given by the disc and that produced by a mull made under as mild conditions as possible should be compared. If no changes occur then the crystals have not undergone a polymorphic transition. However, it cannot be assumed that if a certain crystalline solid does not change on grinding that the compound does not show polymorphism. Several examples of variations between mull and pellet spectra have been reported by Baker[150] and warnings of different spectra from different polymorphs are given in textbooks on practical infrared spectroscopy.[151]

Polymorphism and molecular conformation

The technique of X-ray diffraction has been used to solve the crystal structures of polymorphs and several polymorphic amides have been examined. Using this technique exact values of bond angles, bond lengths and molecular contacts can be found. Haisa and co-workers have examined the crystal structures of the polymorphs of p-methylacetanilide(PMA)[72] and p-hydroxyacetanilide(PHA).[73] Orthorhombic(O) and monoclinic(M) forms of each polymorph were examined. The main difference between the polymorphic forms of each compound is that molecular packing, as revealed by the space group, is different whereas there are only minor differences in intramolecular bond lengths and bond angles. A comparison of the crystal structures of these polymorphs is presented in Table VI.

TABLE VI

A comparison of the crystal structures of p-methylacetanilide and p-hydroxyacetanilide

	PMA	PMA	PHA	PHA
Space group	$P2_1/c$	Pna2	Pcab	$P2_1/a$
(A)	2_1	a glide	b glide	a glide+c translation
(B)	N(amide)	N(amide)	O(hydroxy)	O(hydroxy)
(C)O...D(Å)	2.923	2.904	2.724	2.663
O...H(Å)	2.05	1.97	1.91	1.80
O...H-D(°)	178	174	171	165
C=O...H(°)	142	166	128	136
(D)	b	a	b	[102]
(E)	antiparallel		parallel	O(OH)...H-N
O(OH)...H-N				
	molecular stacking	molecular stacking	hydrogen bond	hydrogen bond
(F)	inversion	c translation	a glide	a glide
(G)	(100)	(010)	(001)	(010)
(H)	a	b	c	b

The characteristic feature of the crystal structures of p-methylacetanilide and p-hydroxyacetanilide are summarised in Table VI under items (A) to (H). The molecules related by (A) are linked by the hydrogen bond C=O...H-(B) with dimensions (C) to form a chain along (D). The chains are held together by (E) between molecules related by (F) to form a sheet parallel to (G). The sheets are stacked along (H) by van der Waal's interactions. The torsion angles around C(1)-N, where C(1) is the ring atom joined to the amide group, is -19.6° (PMA(m)), -8.3° (PMA(O)), 17.8° (PHA(O)), 23.5° (PHA(M)). The resonance interaction between the ring and amide group depends on this torsion angle. This effect could account for the slight changes in molecular geometry between the polymorphs. Haisa did not report on any aspect of infrared spectroscopy in his work on PMA and PHA.

Conformational Polymorphism

Structural investigations consistently show that bond angles and bond lengths do not differ significantly between polymorphs as was indicted in the case of the polymorphic forms of p-methylacetanilide and p-hydrocyacetanilide. Large deviations are not expected since relatively large energies are required to bring about changes in these quantities. For example, in the case of aromatic nitro compounds and anilides, groups such as nitro or amide would be expected to be very nearly in the same place as the benzene ring so as to maximise the overlap of the p-orbitals. This is not the case with single bonds where the energy involved in the torsional parameter is of the order of 4-8 $kJmol^{-1}$. This value is of the same order as the energy difference between crystalline forms. Since it is the torsional parameters which determine the conformation of molecules, for molecules with torsional degrees of freedom, various polymorphs may exhibit significantly different molecular conformations. Several examples of such cases have been reported and these include 2,2',4,4'6,6'-hexanitroazobenzene,[152] the antiviral agent virazole,[153] and, adenosine 5'-monophosphate.[154]

The development of advanced computational technology has led to much work on the prediction of crystal structures and comparisons of the energies of hypothetical structures. The parameters which must be considered in such calculations have been summarised by Kitaigorodsky,[155] and Kaloustian.[156].

It is interesting to note that Kitaigorodsky states that "Most conformational calculations are conducted on free molecules" and that "the crystal field does not affect the lengths of the bonds in any way and alters but insignificantly the values of the valence angles".

Bernstein and Hagler[157] have termed the occurrence of polymorphism due to molecules adopting different conformations in different crystalline forms as "conformational polymorphism". In such cases the differences in molecular conformation must be directly related to intermolecular or crystal forces since this is the only variable in the system. Hence conformational polymorphism provides excellent opportunities for investigating the relationship between crystal forces and molecular conformation.

The work of Bernstein and Hagler on the conformational polymorphism of N-(p-chlorobenzylidene)-p-chloroaniline(BACL) has been reported.[158] Bar and Bernstein have examined the conformational polymorphism of p-methyl-N-(p-methylbenzylidene)-aniline (BAME).[159]

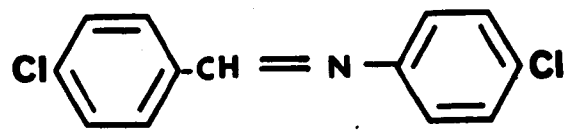

BACL

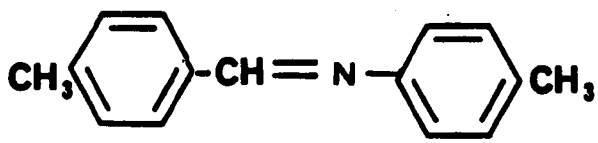

BAME

These compounds were chosen since their lattice paramaters were known (BACL)[160]. (BAME)[161]. The molecules are relatively small and can be reasonably compared with model compounds which are amenable to ab initio calculations. Also the conformation of the molecules is defined by two exocyclic torsion angles. Since the crystal structures do not contain molecules of solvation the crystal structure is determined by interactions between like molecules. Finally the molecular conformation in the two polymorphs of BACL differ significantly. In one form (triclinic space group P1) the molecule is essentially planar while in the second form (orthorhombic space group Pccn) the exocyclic torsion angles are each 24.8°with rings rotated in opposite senses with respect to the four atoms in the central bridge.

Lattice energy calculations were performed using "6-12","6-9" and an exponential function. The charges on atoms for calculating the electrostatic contribution to the total energy were estimated from values obtained from ab initio calculations (STO-3G basis set) as was the difference in molecular energy due to rotations about the N-phenyl and CH-phenyl bonds. These calculations let to the result that the triclinic form was the more stable structure (which is in agreement with experiment). However, the triclinic form contains the more highly energetic planar form and, in order to discover why the molecule does not pack in the crystal in which the intramolecular energy is a minimum,

calculations were performed on a system in which the dichloro compound (BACL) was placed in the crystal structure of the dimethyl compound (BAME). The latter compound is trimorphic and in one form the molecules have the low energy conformation and it was this crystal structure which was used in the calculations. The analysis of the results showed the lack of stability to arise from the relatively unfavourable energetic environments of the aniline ring (including its Cl) as compared with its environment in the observed crystal.

The examples discussed above show that it is now possible to calculate crystal structures and to compare these with known structures. Polymorphic structures can by analysed in detail and subtle differences in packing and conformation can be studied and if necessary, hypothetical structures can be constructed and analysed in order to achieve a deeper understanding of forces which are operating in crystals. Such an approach is possible using the crystal structures of the trimorphic 4-methyl-2-nitroacetanilide which will be described in a subsequent chapter and an additional feature in this case would be the contribution that the various types of hydrogen bonding would make to the lattice energy.

Transformation of polymorphic forms in the solid state

The formation of polymorphic forms of crystal is usually associated with recrystallisation procedures i.e. the crystalline form of a compound is dependent to some extent on the type of recrystallisation solvent. One polymorph may crystallise from non-polar solvents, another from polar solvents, and perhaps even a third one from hydrogen bonded solvents. Another manner in whcih polmorphs may arise is a solid state transformation which may occur at ambient temperature or more rapidly on heating. During the latter process the extent of "reaction" may be observed as a band or front moving through the parent crystal. The daughter crystal may be formed in a random manner with no preferential orientation but some changes occur with strong orientational growth. The latter type of growth is described as a topotactic growth and can be recognised by optical microscopy, electron microscopy, or by X-ray diffraction techniques.

In this research 4-methyl-2-nitroacetanilide has been obtained in the following three forms:-

(i) a dark yellow or amber polymorph (MNA-2),

(ii) a yellow polymorph (MNA-3), and,

(iii) a white polymorph (MNA-1)

It has been found that the following solid state phase changes occur:-

(a) MNA-2 changes to MNA-3 on standing at ambient temperature for a few days or in several minutes in a te mperature range 60° to 90°;

(b) MNA-3 has been observed to change to MNA-1 over a period of several weeks. (However, some sample of MNA-3 have remained stable for over three years at ambient temperature);

(c) MNA-3 has been observed to change to MNA-1 on maintaining the temperature of the sample in the range 80-90°C.

The crystal to crystal phase changes observed in (b) and (c) occur with new growth either directed along the long axis of the filament or in a direction at approximately 45° to the filament. Similar behaviour has been observed with other compounds and a brief account of such examples follows.

Studies of the solid state phase change

A review of thermal reactions in the solid state by Curtin et al. was published in 1979.[162] In some of the examples cited in this review a chemical change occurs in the solid phase so that one or two compounds are formed whereas the other examples involve the formation of a new conformation i.e. a polymorphic transition (or phase transition) has occurred. Where changes in the type of hydrogen bonding occur, as in a change involving a transition from intramolecular to intermolecular hydrogen bonding, it is not obvious whether such changes should be considered as solid state reactions or a polymorphic transition. In the former type of changes the distance between the reacting centre and orientation of molecules is critical. This has led to the synthesis, by the strategem of "crystal engineering", of stereochemically pure products, and also of single crystal, extended chain polymers, both of which are difficult if not impossible to prepare by solution techniques. Examples of such reactions have been presented in review articles by Schmidt[163] and Cohen.[164] Reactions in which the product shows one or a small number of crystallographically equivalent, definite orientations relative to the lattice of the parent crystal and where the reaction has proceded through the bulk of the reactant are said to be topotactic. Topotactic reactions and topology in the solid state have been discussed in a comprehensive manner by Thomas.[165]

In surveying reactions of crystals Curtin has considered two hypothetical mechanisms. The first type is designated the "homogeneous mechanism" and involves the conversions of "A" molecules of the starting material in the initial crystal lattice to "B" molecules which remain in place at the sites previously occupied by the "A" molecules from which they were formed. Thus the reaction proceeds through a continuous series of solid solutions and the reaction would be topotactic.

In the second hypothetical mechanism, the "heterogeneous mechanism", the reaction starts at one or several sites and reaction fronts spread through the crystal. No mixing of A and B structures occurs. If the orientation of growth of the new lattice is determined by the old lattice at the interface it is possible that the reaction proceeding by the "heterogeneous mechanism" could be topotactic.

A likely candidate for the homogeneous mechanism is the phase transition of the perchlorate (P) since a crystal of the β-form, stable at 25°C, after structure determination at that temperature gave on cooling to 3°C single crystals of the α-form which was a second

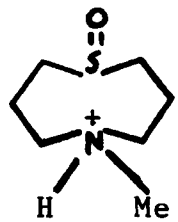

ClO_4^- P

polymorphic form of the compound and this new crystal was used to determine the new crystal structure.[166]

The polymorphic change was explained in terms of inversions and rotations but an alternative mechanism based on the idea of simple planar shear has been proposed.[167]

The reversible change of red crystals of the anil (A) at room temperature to colourless at liquid air temperature has been interpreted as an equilibrium of tautomeric forms.[168]

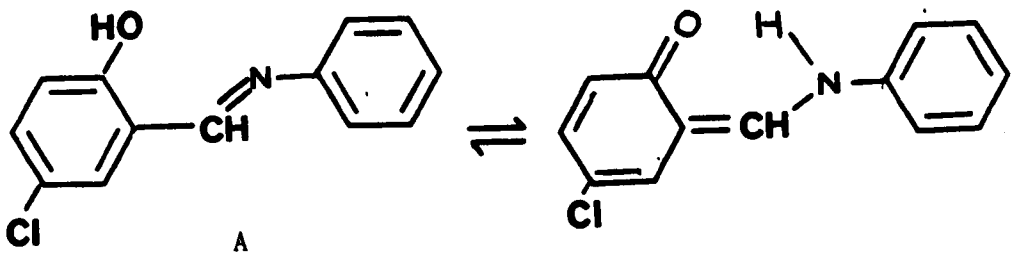

A

The thermal rearrangement of 2,2'-diiodobenzoyl peroxide has been extensively investigated.[169] Single crystals of the compound slowly transform at room temperature to single crystals of (B) over a period of several weeks. The relationship between the new crystallographic axes and the old ones has been discussed. However, the reaction mechanism cannot be homogeneous in spite of the observed topotaxy.

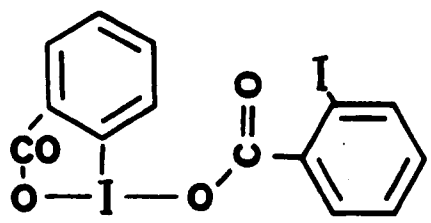

B

In the heterogeneous mechanism the reaction begins at one or more nucleation sites and is characterised by the spread of well defined reaction fronts through the crystal. Certain phase changes involving small or no change in crystal shape have been studied in detail and that of the conversion of α - and β-p-dichlorobenzene has been carefully examined.[170] The transformation only involves reorientation of molecules. The thermal transformation of the metastable β-phase of p-nitrophenol to the stable α -phase has been found to occur with the phase boundary moving perpendicular to the axis of the needle shaped crystal.[171] The structural change in this transformation involves a twist of rings in adjacent linkgs in the chains of molecules.

The conversation of the yellow form of 3,6-dichloro2,5-dihydroxyterephthalate (C) to a white form of the sampe compound has been examined in detail bu Curtin and Byrn.[172]

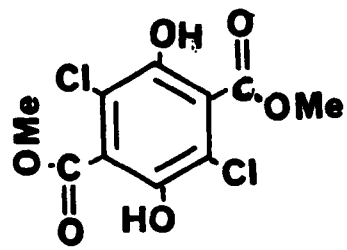

C

The change involves a rotation of phenolic hydroxyl groups together with a change of intramolecular hydrogen bonding in the yellow form to intermolecular hydrogen bonding in the white form.

In addition, the plane of the ester groups changes from a position of being coplanar with the ring to one where the ring and ester groups are approximately at right angles. Also each ring has to rotate round an axis by 180°. A description of the changes as observed using an optical microscope has been recorded.[173] This thermal rearrangement has also been studied by spectroscopic means by Swiatkiewicz and Prasad.[174] The rearrangement has been found to start as a homogeneous process but becomes heterogeneous as product forms. A temperature-dependence study of the Raman phonon spectra suggests that the rearrangement may be defect controlled rather than phonon assisted.

Colour changes are also observed in the solid state conversion of 2-(4'-methoxyphenyl)-1,4-benzoquinone.[175] On heating the yellow form changes to a red form. Single crystals rearrange by a process which begins at a number of nucleation sites in the crystal and spreads by migration of well defined fronts. The yellow and the red constituent molecules are related to each other as diastereoisomers. The difference in colour is accounted for by the stacking of the molecules in the yellow form with overlap between the adjacent quinone rings, whereas in the red form there is π complexing between the quinone and anisyl rings.

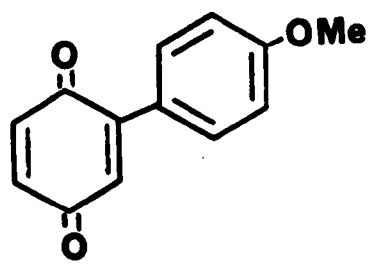

The structures of the yellow and orange forms of diethyl-2,5-diaminoterephthalate (D ;R=H) have been determined by X-ray crystallography and the rearrangement of single crystals studied.[176]

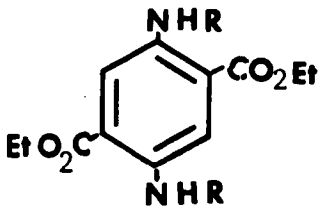

D

The structural results show that the reaction involves major changes in hydrogen bonding and also significant molecular reorientation. The reaction was shown by studies using an optical microscope to be heterogeneous with nucleation at one or more sites followed by spread of the reaction through the crystal. The heterogeneous thermal transformation of the orange diethyl NN'-diphenyl-12,5-diaminoterephthalate (D ;R=Ph) has been studied by Mann, Curtin and Paul.[177] The orange form contains benzene which becomes included in the complex when the parent compound is recrystallised from benzene. On heating, a red benzene-free crystalline solid is formed. The reaction normally began at a side face of the crystal but naturally occurring defects or pin pricks could influence the start of the reaction.

Naphthazarine (E) exists in three polymorphic forms:- a green form (A), a dark red form (B), and a light red form (C).

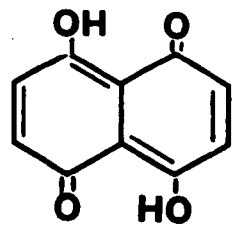

E

The green form (A) changes to the red form (C) on cooling to -20°C. The two structures differ in their edge-to-edge molecular contacts. The reaction belongs to the heterogeneous class and the reaction front spreads along the needle axis of the crystal.[178] .

o-Acetamidobenzamide has been found to crystallise in at least two distinct forms, both of which undergo complex thermal solid-state transformations which result in the formation of 2-methylquinazol-4-one (F).[179]

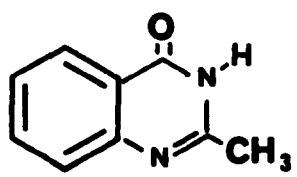

F

The polymorphic transformation occurs at 150°C and involves loss of an intramolecular N-H...O hydrogen bond and formation of a new intermolecular N-H...O hydrogen bond. The polymorphic transformation occurs simultaneously with the cyclodehydration reaction. Different phases were characterised by infrared spectroscopy and by differential scanning calorimetry curves.

Although this next example does not involve transformation of polymorphic forms it is included because it is a solid state reaction which has been shown to proceed at a faster rate in the crystal than in solution or in the melt. Methyl-p-dimethylaminobenzenesulphonate rearranges to p-trimethylammoniumbenzenesulphonate.

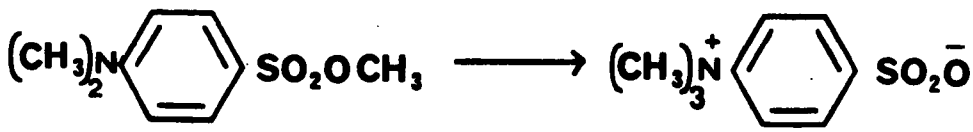

The structure of the starting material was determined by X-ray crystallography and showed that the molecules in the crystal are ideally orientated for the given reaction.[180] This example emphasises that rapid changes in crystals are possible if the correct topology is present.

Another rare example of a reaction which occurs more rapidly in the solid phase than in the liquid phase is formation of compounds containing azetidione groups from isocyanate groups in 4,4'-methylenebis(phenyl isocyanate) ($OCNC_6H_4-CH_2-C_6H_4-NCO$) known in industry as MDI.[181]

An important feature of the crystal structure of this compound is that adjacent molecules have isocyanate groups related by an inversion centre with intermolecular contacts of only 3.146(2) Å and with adjacent antiparallel N=C atom pairs forming an approximate square.

Octahydro-1,3,5,7-tetranitro-1,3,5,7-tetrazocine(HMX) is an important monopropellant material and is known to exist in four solid-state polymorphs labelled α, β, γ, and δ. X-ray crystal structure determinations on the α-,[182] β-,[183] and δ-[184] forms have been carried out. α-HMX and δ-HMX are quite similar to one another as far as the conformation of the HMX molecule is concerned, but differ in the positioning of the molecules relative to one another in the lattice. The conformation of the ring is a "boat" form. β-HMX exists more in the "chair" form giving the entire molecule a centre of symmetry.

The laser Raman spectra of the four polymorphs have been recorded and anlysed by Goetz and Brill.[185] Thermally induced phase transitions could be readily detected by Raman spectroscopy.

The intramolecular and intermolecular interactions in these polymorphs have been examined in great detail by Brill and Reese[186] with a view to understanding the known properties of this material. Brill and Karpowicz[187] have reported a Fourier transform infrared method to study the rates of solid-solid phase transitions in HMX.

A rare example of a solid state rearrangement of an organometallic compound has been reported by Etter and Siedle.[188]

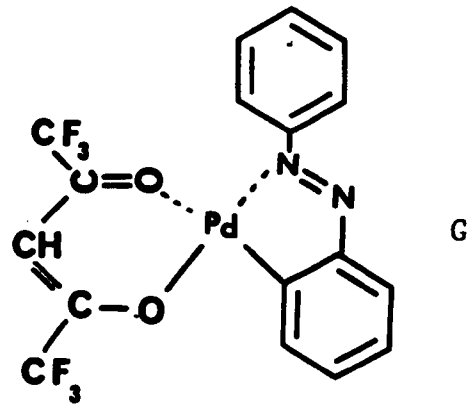

G

(Phenylazophenyl)palladium hexafluoroacetylacetonate (G) crystallises from hexane solution in the form of yellow needles which on heating to approximately 90°C undergo an expansion of about 10% along the needle axis. On further heating a red phase front develops at one end of the crystal and moves along the needle until the entire crystal is an opaque red colour. Weissenberg patterns indicated that the red solid formed from single crystals of the yellow form was microcrystalline. On the basis of their known structures and their relationship to the observed crystal expansion it was proposed that molecular stacks slip together as in a Martensitic transformation.

CHAPTER THREE

The first part of this chapter contains an account of the crystal and molecular structure of the white (MNA-1) and yellow (MNA-3) polymorphs of 4-methyl-2-nitroacetanilide.

The second part contains the crystal and molecular structure of the amber polymorph (MNA-2).

The X-ray diffraction experiments described in this chapter were performed by John C. Moore at Birkbeck College, Malet Street, London WC1E 7HX. Mr. Moore processed the diffractometer data to obtain the atomic coordinates of the three polymorphs.

Abstract

The crystal and molecular structure of white (MNA-1) and yellow (MNA-3) forms of 4-methyl-2-nitroacetanilide have been determined by X-ray diffraction techniques.[196] The crystals of MNA-1 are monoclinic, a = 10.421(2), b = 9.980(2), c = 9.568(2)Å, β = 99.51(5)°, space group $P2_1/c$(14), Z = 4. Crystals of MNA-3 are triclinic, a = 17.956(2), b = 12.908(2), c = 4.039(1)Å, α = 93.13(5)°, β = 83.71(5)°, γ = 90.77(5)°, space group $P\bar{1}$ (2), Z = 4. Both structures were solved by direct methods using the SHELX-76 system of programs and refined using full matrix least squares. The numbers of unique reflexions used in refinement and the final R values are MNA-1, 1545, 0.0674; MNA-3, 3127, 0.0654. The two distinct molecules in MNA-3 have intramolecular hydrogen bonds, different molecular conformations, although both are fairly planar, and each type is closely packed in columns of parallel molecules along the c direction. In MNA-1 the C=O...H-N geometry is indicative of intermolecular hydrogen bonding and the molecules adopt a conformation in which the nitro and amide groups lie in planes at approximately 45° to the benzene ring.

Introduction

White and yellow polymorphs of MNA ($C_9H_{10}N_2O_3$) were first reported by Gatterman[130], and Skulski[139] proposed that intermolecular hydrogen bonding was present in the white form and intramolecular in the yellow form. During the present investigation a third (amber) polymorph of MNA has been found to exist and four different types of solid state transformations have been observed to take place at room temperature.

X-ray analyses of the white and yellow polymorphs have been completed and quite different molecular conformations have been found in the two structures. It has been verified that fairly strong intermolecular hydrogen bonding is present in the most stable (white) polymorph and in the yellow form the amide hydrogens are situated such that an intra hydrogen bond is indicated.

The objectives of this work were to establish confirmation, or otherwise, of Skulski's proposal; to obtain further information on possible conformations of nitro groups, viz. when close to an amide group; ultimately to use this example of polymorphism to study the relationships between crystal forces and molecular conformation after the manner of Bernstein[157, 158, 189], to study a rare example of solid state phase transformations and to explain the actual mechanism of the topotactic transformation from yellow to white form.

This present paper reports the structures of the most stable (white) form, MNA-1, which has been found to be monoclinic ($P2_1/c(14)$) and of the next most stable (yellow) form, MNA-3, which is triclinic ($P\bar{1}(2)$).

The structure of the relatively unstable (amber) form, MNA-2 (also monoclinic, $P2_1/c$) and an account of the mechanisms and energy changes of the transformations will be published later.

Experimental

The crystals were grown by slow evaporation, MNA-1 forming white tabular crystals from aqueous ethanol and MNA-3 forming very long filamentary yellow crystals from petrol (boiling range 60°-80°C) or from carbon disulphide. The MNA-3 crystals have longitudinal/transverse dimensional ratios 10:1 to 10^2:1 and great difficulty was experienced in trying to obtain approximately equi-dimensional crystals, suitable for X-ray diffraction data collection, until a dominant cleavage plane was discovered at approximately 65° to the longitudinal axis. All other attempted methods for reducing the crystal length resulted in excessive cracking and initiation of the phase transformation from MNA-3 to MNA-1.

Unit cell and space group data were obtained from rotation and Weissenberg films. Accurate cell dimensions were determined by least squares refinements of θ, χ and ϕ values measured on a four circle diffractometer. For structure analysis purposes, integrated intensities were measured by step scanning in the ω/θ mode. Lorentz and polarisation factors were applied in the usual manner, and semi-empirical absorption corrections were made using the method of North, Phillips and Mathews [193] modified according to Kopfmann and Huber [192] and Tickle.[194]

Crystal data and details of diffractometer data collection are recorded in Table 3.1.

Structure Determination and Refinement

Both structures were solved by direct methods using the program SHELX-76. The E-maps produced gave all the non-hydrogen atoms of MNA-1 and all except three non-hydrogen atoms of the bimolecular asymmetric unit of MNA-3. An electron density map then gave all the missing non-hydrogen atoms of MNA-3. For each structure, three cycles of isotropic least squares refinement were then completed, with hydrogen atoms in theoretical positions, before using a difference electron density map to actually locate the non-methyl hydrogens. Although the difference maps gave indications of significant electron densities present in all methyl hydrogen regions, the peak locations given did not correlate to ideal methyl hydrogen geometries, neither relative to each other nor relative to the carbon atoms. The final R values were then achieved by further least squares refinements, using anisotropic temperature factors for the non-hydrogen atoms and isotropic factors for all the hydrogens, with methyl hydrogens refined as rigid groups. However, when three hydrogen atoms, each with a site occupation factor of unity, were placed in each methyl group, exceptionally high isotropic thermal parameters were obtained for those hydrogens. When six hydrogens per rigid methyl group were considered, symmetrically orientated and each with a site occupation factor of 0.5, more reasonable isotropic parameters were obtained together with reductions in R and R_w values, which were shown to be significant by application of Hamilton's tests [190]. It was thus concluded that some appreciable degree of methyl hydrogen disorder is present in both structures.

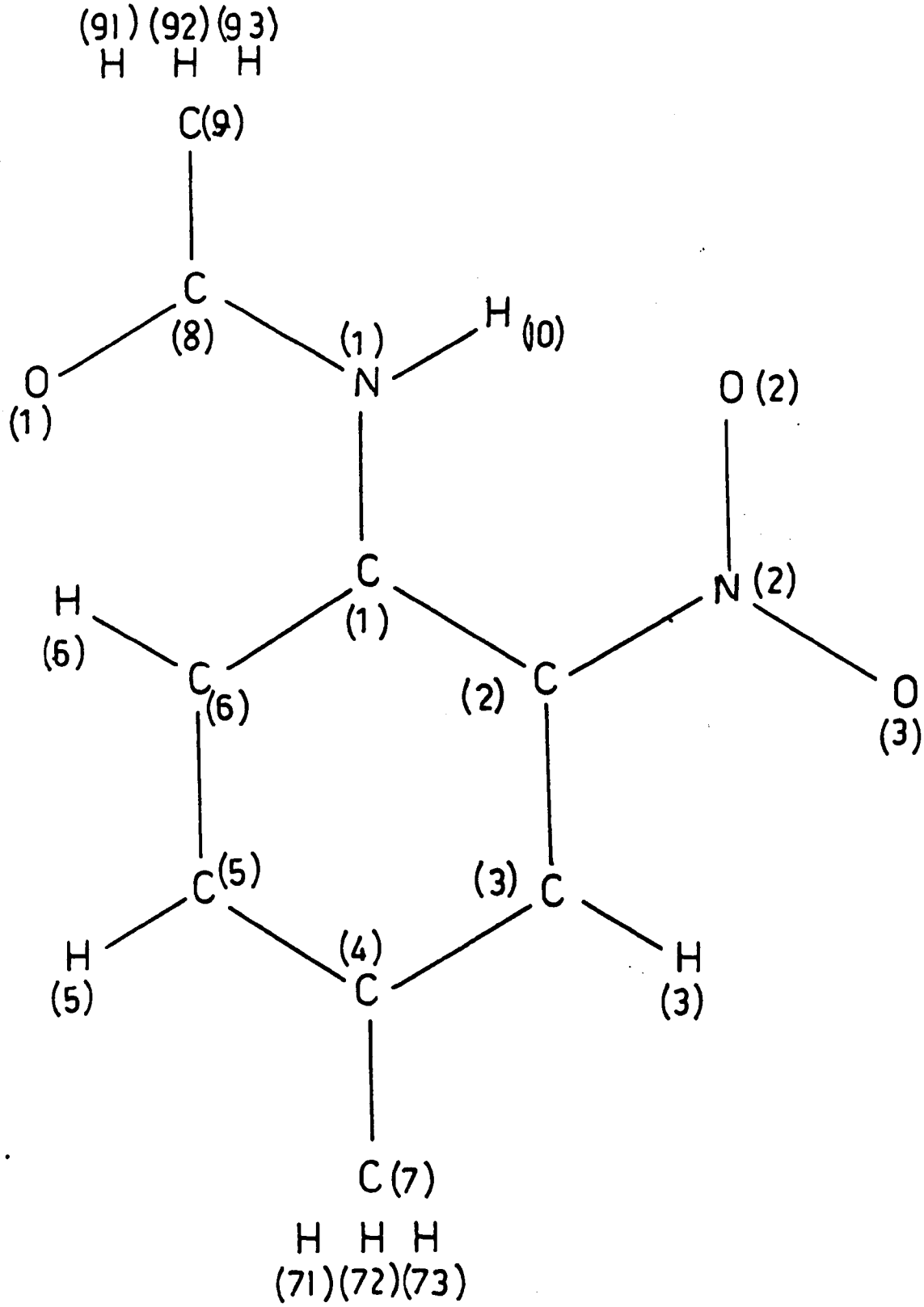

The numbering system for MNA which is used in all polymorphic forms. This system is used in crystal structures and general discussions.

Fig. 3.1

Results

The atom identity scheme is shown in Fig.3.1, corresponding bond lengths and bond angles are presented in Table 3.3, mean plane equations, interplanar angles and deviations of atoms from the planes are given in Table 3.4. Atom co-ordinates and isotropic thermal parameters, with e.s.d. values are in table 3.5.

MNA-1 Structure:

The results confirm Skulski's proposal that intermolecular hydrogen bonding is present in the stable, white, MNA-1 and this has been found to be due to strong C=O.....H-N bond between the molecules which are c-glide related, to form chains along the c direction. The chains are held together by anti-parallel molecular stacking involving molecules related by inversion, thus forming a sheet structure parallel to (100).

The intermolecular hydrogen bond geometry of this structure is such that the O....H distance is 1.947 (38)Å, the O....H-N angle is 172.8 (2.5)°, the O....N distance is 2.859(4)Å and the C=O....H-N torsion angle is 165.4(2.5)°, where C=O are at x, y, z and H-N are at x, $\frac{1}{2}$-y,$-\frac{1}{2}$+z.

The next closest intermolecular contacts are as follows:

(i) 2.37 (8)Å between H(10) at x, y, z and a methyl hydrogen of C(7) at 1-x, 1-y, 1-z.

(ii) 2.49 (8)Å between a methyl hydrogen of C(7) at x, y, z and a methyl hydrogen of C(9) at −1+x, y, z.

MNA-3 Structure:

In this polymorph there is no significant intermolecular bonding but there are indications of intramolecular effects.

The results show that the shortest distances for possible intramolecular interactions, involving the amide hydrogens, are 1.950 (35)Å and 1.976 (38)Å and both of these are H(10)...O(2) distances (within molecules 1 and 2 respectively). With respect to possible intermolecular interactions, the shortest distance is between H(10), molecule 1, and O(2), molecule 2, and this is 2.625(35)Å, the next shortest intermolecular distance being 3.050 (38)Å between H(10), molecule 2, and O(2) molecule 1 (x, y, z+1). Since such intermolecular closest contacts are larger than the sum of the van der Waal's radii, intermolecular hydrogen bonding considerations can thus be discounted.

The packing arrangement may be described as columnar, the columns consisting of either type 1 or type 2 molecules. The columnar direction is parallel to c and along each column the stacking

arrangement consists of x, y, z or -x, -y, -z molecular types, the benzene ring planes being inclined to the c direction at an angle of 31.6° for molecule 1 columns and 29.2° for molecule 2 columns. This dominant columnar structure in the c direction would account for the pronounced filamentary or needle shape of the crystals, particularly since the longitudinal axis of the macro crystal coincides with the short c direction.

The average ring-ring interplanar spacings are 3.43 Å (molecule 1 columns) and 3.52 Å (molecule 2 columns), the overlapping of the rings presumably being stabilised by the weak bonding forces such as those operating in π molecular complexes. Another interesting feature of the columnar structure is that the C=O and N(2)-O(2) bonds lie nearly perpendicular to c, thus maximising the distances between the amide-amide groups and nitro-nitro groups along the c direction.

It has also been found that type 1 molecules at translation $1+\bar{x}$, $1+\bar{y}$, $3+\bar{z}$ have ring planes which are essentially co-planar with the ring planes of the type 1 molecules (x, y, z) and this would explain the occurrence of the most intense X-ray reflexion in the diffraction pattern, $d(3\bar{1}1) = 3.432$Å. Not only are the ring-ring interplanar spacings of molecules of type 1 equal to 3.43Å, as previously stated, but the angle between the normal to the ring planes and the normal to the $(3\bar{1}1)$ planes is only 2.4°.

The parallel sets of rings of type 2 molecules account for the second most intense reflexion, corresponding to $d(021) = 3.329$Å, the angle between the normals to these planes and type 2 rings being 5.4°.

FIG 3.2

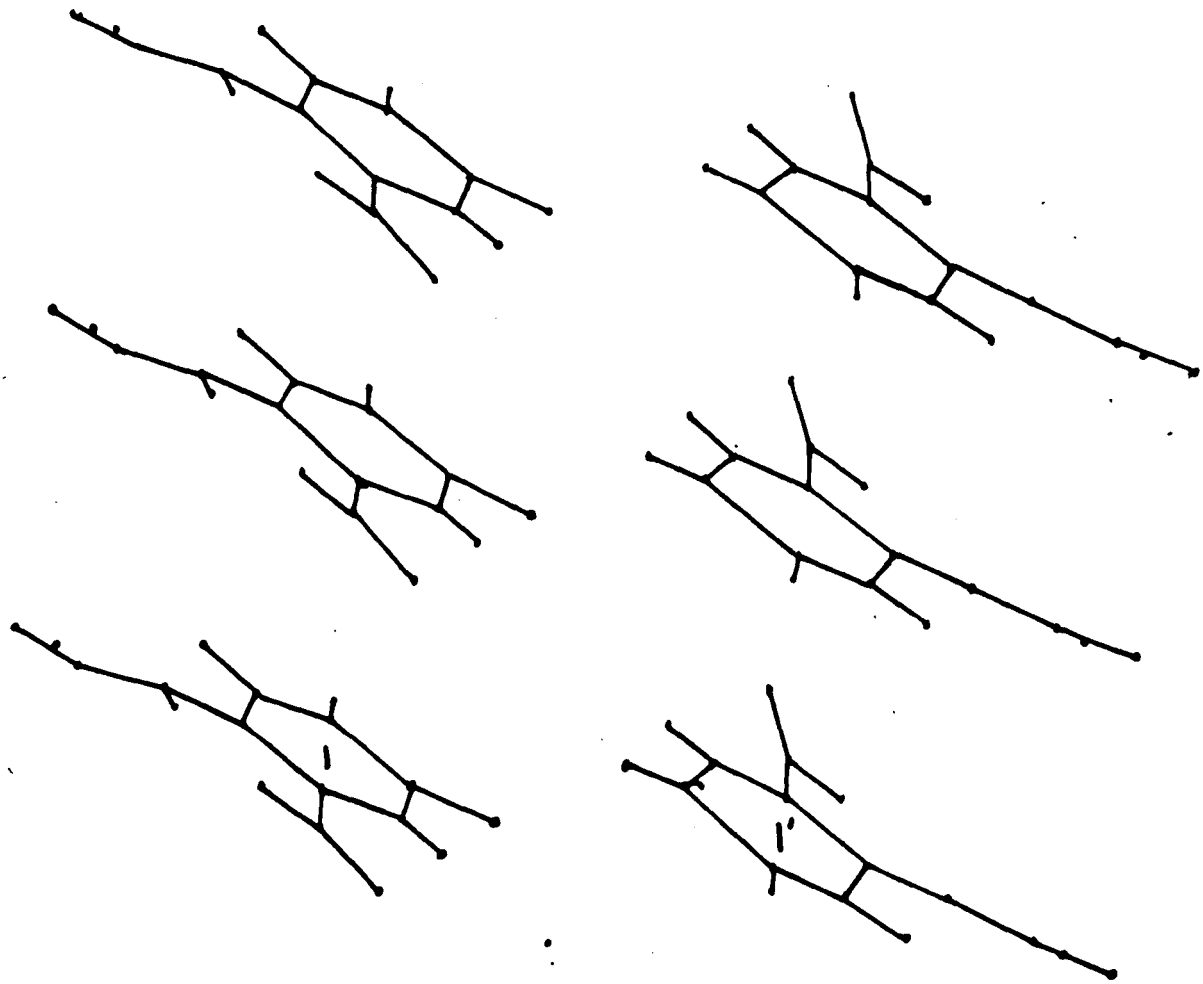

A view along Y showing the arrangement of molecules 1 and 1' in MNA-3 (orthonormal coordinates)

The packing arrangement is such that π-π' interactions between amide groups and between benzene rings is particularly favoured by the degree of overlap which occurs in the columnar stacking of type 2 molecules. However, the reduced degree of overlap of type 1 molecules, and hence less favourable π-π interactions, does increase the possibility of a stronger intramolecular amide-nitro group interaction, i.e. an increased intramolecular hydrogen bond effect, resulting in a more planar molecule.

Discussion

In both polymorphs the molecules contain essentially planar amide groups in trans (Z) form and the benzene rings are also reasonably planar, Table 3.4. However, together with the nitro groups, no overall molecular planarity exists in either form with the molecule of MNA-I having significantly greater interplanar angles than even the least planar molecule of MNA-3, Table 3.4b.

The nitro group angle relative to the benzene ring is, for MNA-I in particular, quite different to the general trend of non-sterically hindered aromatic nitro groups as reported by Holden and Dickinson (1977) and the O(2)-N(2)-O(3) bond angles in both structures are smaller than the equilibrium value of 126.4° suggested by the same authors, thus suggesting that significant steric hindrance is present.

The results show that several bond lengths and angles are dependent on the conformation of the nitro and amide groups. In the single conformation of MNA-1 and both conformations of MNA-3, the C(3)-C(4) and C(5)-C(6) bonds are the relatively short ones in the ring, Table 3.3, and the lengths of the C(1)-N(1) and the longer C(2)-N(2) bonds

remain very nearly the same. However, the length of the C(1)-N(1) bond is shorter than the corresponding bond in acetanilide (1.426 Å) (Brown and Corbridge [67]) and in eight other anilides examined by Haisa and co-worker [71, 72] (average bond length 1.420 Å). This indicates that there is a significant contribution from the canonical form (Figure 3.3) in all three conformations. The approximately constant N(2)-C(2) bond length is in accordance with the reported lack of correlation between C-N bond lengths and angles of nitro group rotations out of ring planes.

There are distinct differences in the geometrics of the amide groups in MNA-1 and MNA-3, Table 3.3 and these are consistent with the idea of competition for the N(1) lone pair electrons, either by the adjacent carbonyl group or by the ring and nitro group. In MNA-1, interaction by the carbonyl group predominates so that the amide group geometry is similar to that in acetanilide. In MNA-3 interaction between the N(1) lone pair electrons and the ring and the nitro group predominates, but in molecule 2 the conjugation between the nitro and amide groups is reduced due to the increased rotation of the amide and nitro groups relative to the ring plane and also due to weak $\pi-\pi$ interaction between the overlapped, parallel amide groups. These effects would explain why the amide group in MNA-3, molecule 2, is the most planar amide group of all three molecular conformations reported in this work.

Electron withdrawal by the nitro groups (in both MNA-3 molecules) causes the N(1)-C(8) bonds to be longer and the C(8)-O(1) bonds to be shorter, Table 3.3 than is generally observed in anilides (Brown and Corbridge, [67]; Haisa et al., [71, 72]).

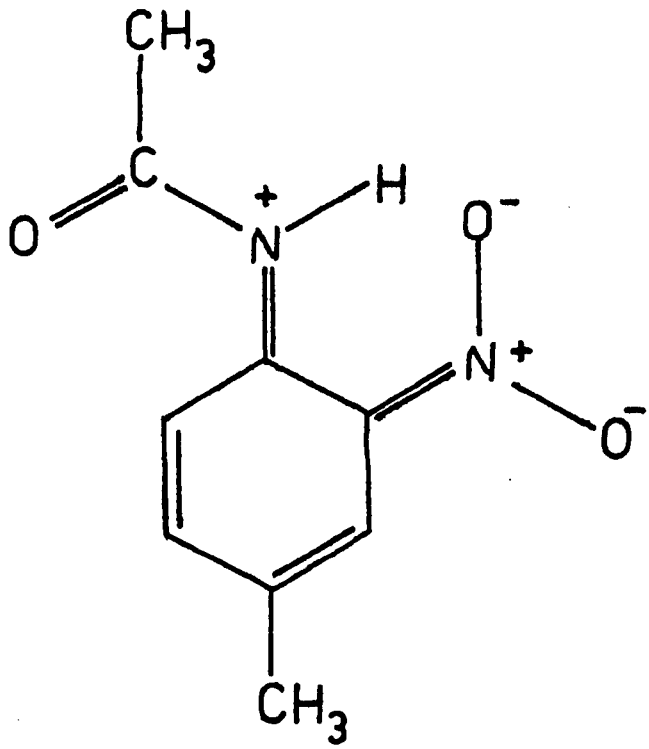

Fig. 3.3

A canonical form for MNA.

The shortening of the C(8)-C(9) bonds in all three molecules is presumably due to hyperconjugation and an increased hyperconjugative effect may also explain the indicated shortening of the C(4)-C(7) bond in MNA-3, molecule 2, which would then offset the reduced conjugation of the ring with the nitro and amide groups.

Coplanarity of the amide group and benzene ring is prevented by steric hindrance, either by the nitro group in MNA-1 (N(2)....O(1), 2.69 Å, O(2)....O(1), 2.97 Å and O(3)....O(1), 3.10 Å) or by H(6) in MNA-3 (H(6)....O(1), 2.26 Å, molecule 1 and 2.32 Å, molecule 2).

In all three molecules, maximum resonance interaction between the NH and CO groups is prevented by the displacement of the amide hydrogen out of the amide plane, towards the plane of the benzene ring.

In both molecules of MNA-3, the displacement of the amide group, due to H(6)-O(1) steric hindrance, is also accompanied by a displacement of the nitro group in such a way that an intramolecular H(10)....O(2) interaction is indicated (H(10)....O(2) being 1.95 Å and 1.98 Å in molecules 1 and 2 respectively).

The displacements of the carbon atoms from the mean plane of the benzene ring in MNA-1 reveal a slight boat conformation, C(2) and C(5) being out of the ring plane, Table 3.4c A similar but far less significant effect is observed in both benzene rings of MNA-3, with C(1) and C(4) being the atoms with maximum displacement from the mean plane.

Stereo pair illustrations of the structure of MNA-1 and MNA-3 are presented in Figures 3.4 a and 3.4 b respectively.

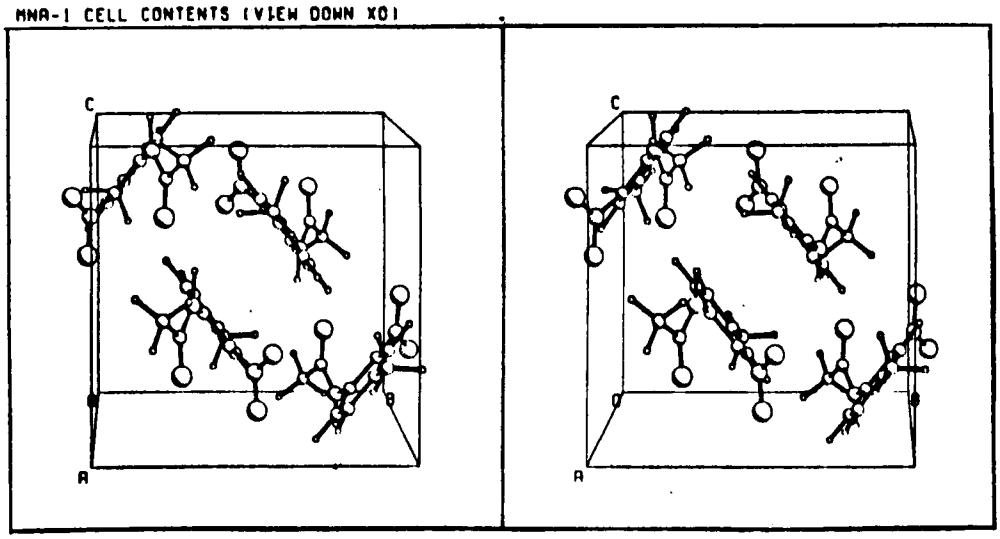

Fig. 3.4 a

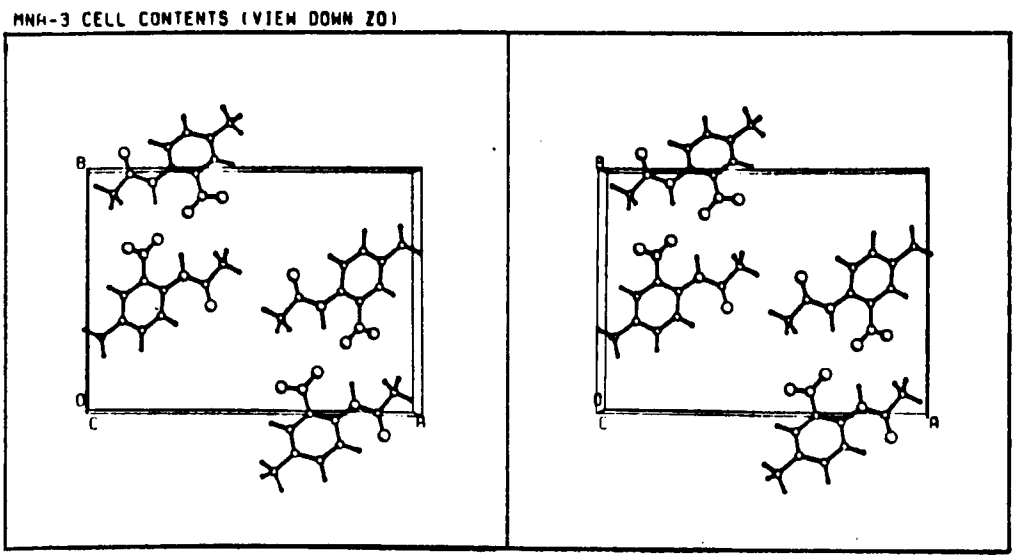

Fig. 3.4 b

Stereo Pair views of MNA-1 (upper) and MNA-3 (lower)

Stereopair MNA-1

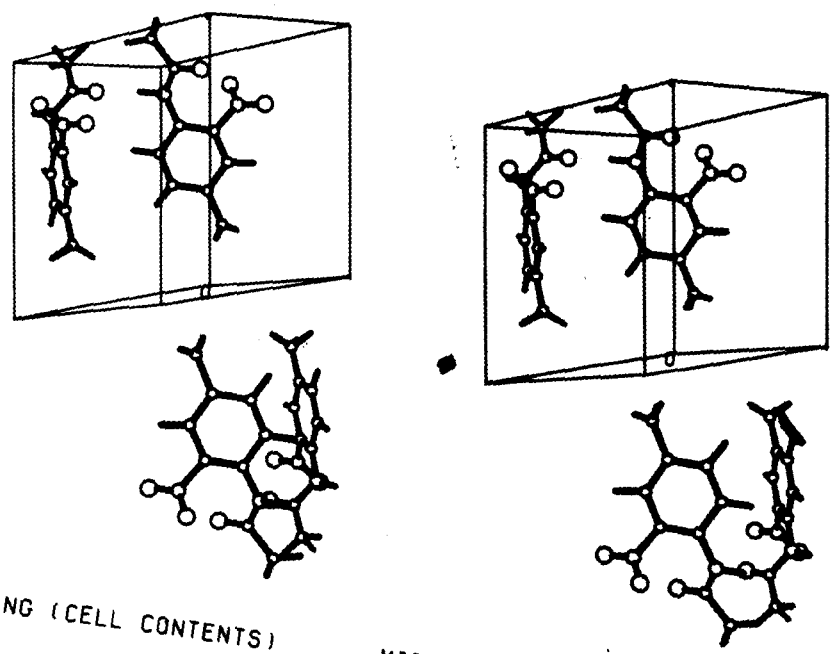

VIEW PERP. TO RING (CELL CONTENTS)

VIEW PERP. TO RING (CELL CONTENTS)

Fig. 3.4 c

FIG 3.5

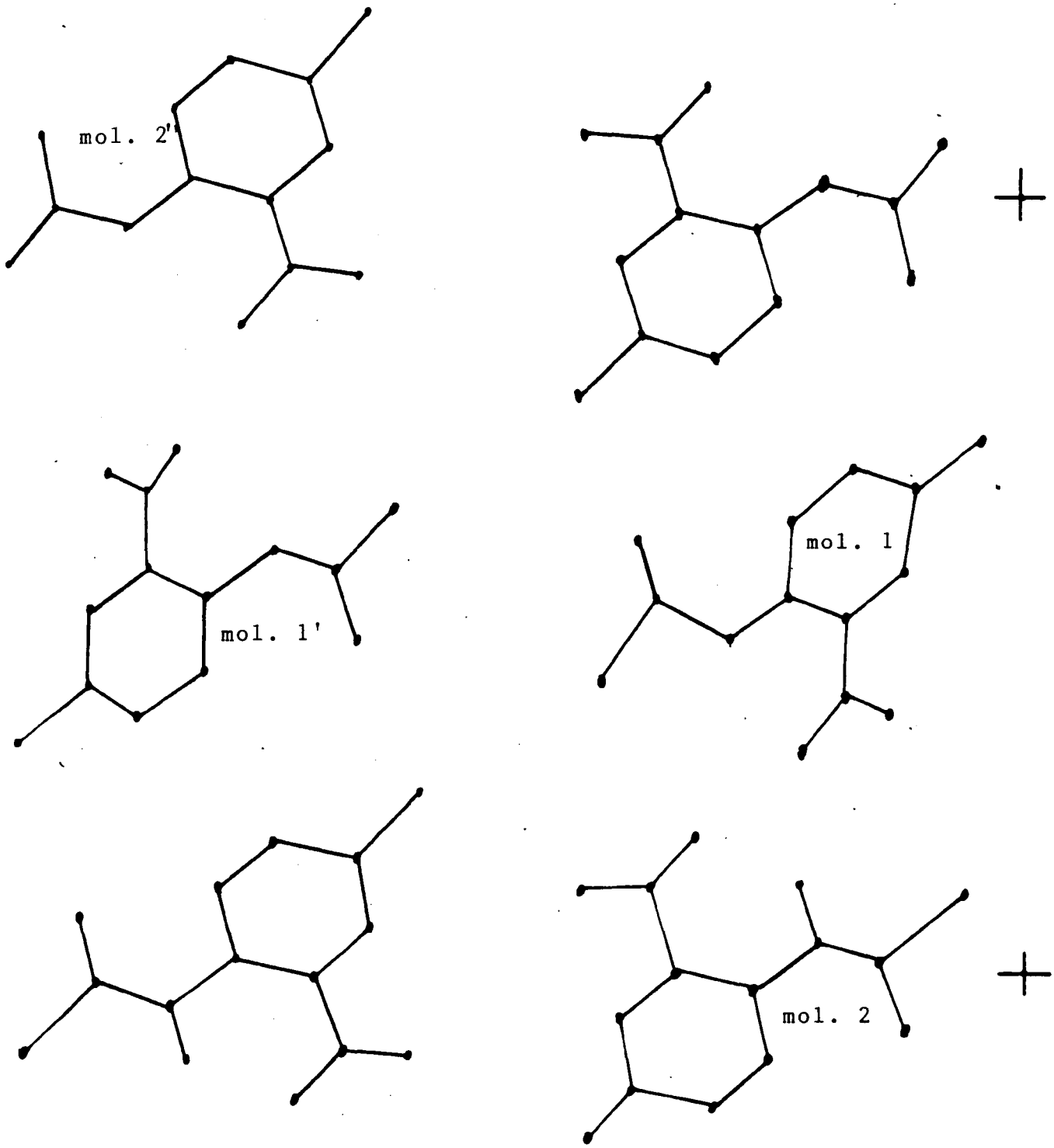

A view down z of the arrangement of molecules in MNA-3 (orthonormal coordinates).

FIG. 3.5b

MNA-3

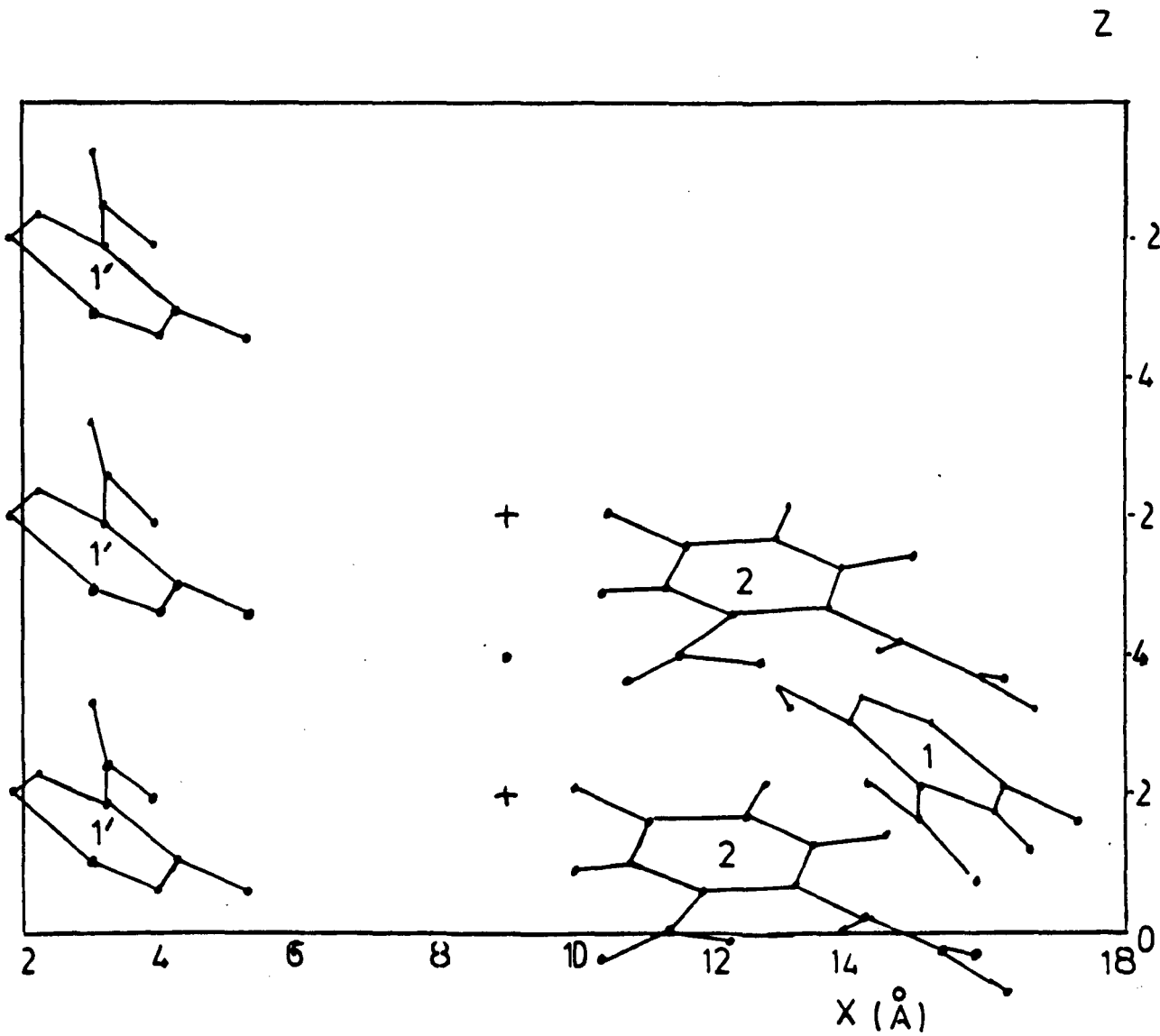

N.B. SOME GROUPS OMITTED FOR CLARITY

ORTHOGONAL CO-ORDINATES USED

A view of molecules 1,1',2, and 2' in MNA-3 (yellow)

Note the coplanarity of molecules 1 and 1' (1-x,1-y,3-z).

The view is down y.

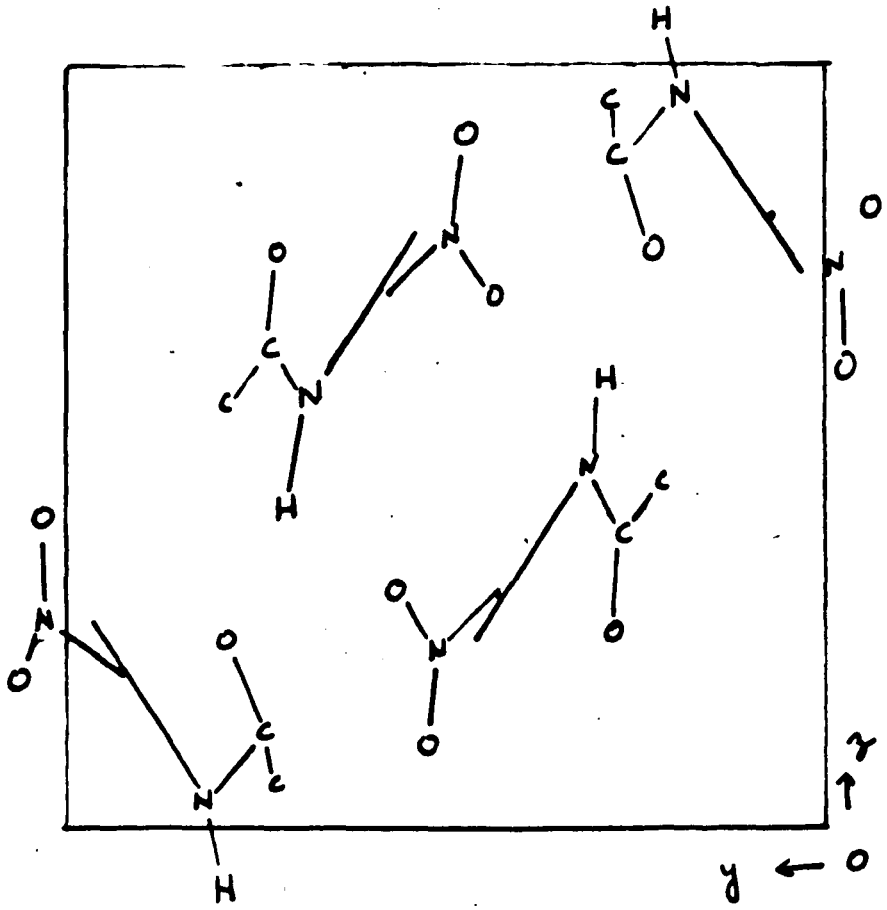

Fig. 3.6 View of MNA-1 down x. Benzene rings are represented by lines since they are viewed (approximately) parallel to the ring plane.

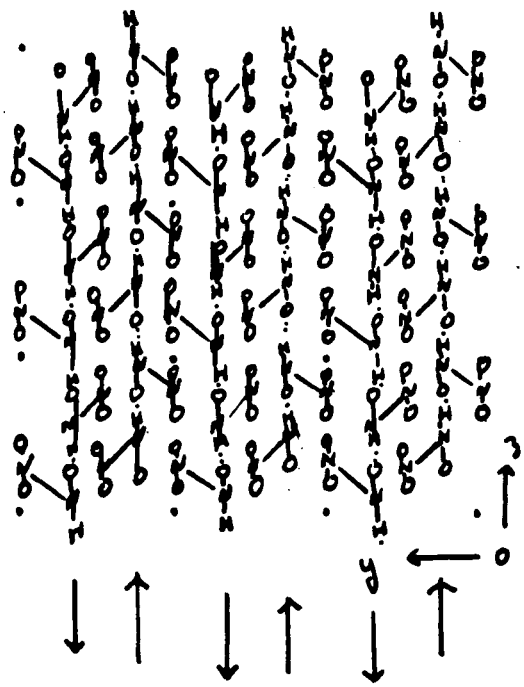

Fig. 3.7 9 unit cells of MNA-1 viewed down x. The diagram shows the parallel lines of hydrogen bonded amide groups at y = 0.25 and y = 0.75 lying parallel to the z axis.

TABLE 3.1- Crystal Data and Experimental Details

(Molecular formula: $C_9H_{10}N_2O_3$, Rel. mol. mass: 194.1

	MNA-1	MNA-3
Crystal system	Monoclinic	Triclinic
Habit	White, tabular	Yellow, filamentary
a,b,c (Å)	10.421(2), 9.980(2), 9.568(2)	17.956(2), 12.908(2), 4.039(1)
α,β,γ (deg)	90, 99.51(5), 90	93.13(5), 83.71(5), 90.77(5)
V (Å^3)	981.4	929.1
Z	4	4
D_{calc}	1.31	1.39
D_m	1.30	1.38
Flotation mixture	aqu. KI	aqu. KI
Crystal size (mm)	0.3 x 0.3 x 0.1	0.35 x 0.3 x 0.15
λ, Cu-Kα(Å)	1.5418	1.5418
ϕ axis	C*	C_o
Max θ (deg)	70	70
h,k,l limits	-12 -8 -11 12 12 8	-21 -15 -3 21 15 4
Total reflexions	4665	5858
Unique reflexions	1545 (1293 with $I>3\sigma I$)	3127 (2443 with $I>3\sigma I$)
F (000)	408.0	408.0
Systematic absences	0k0, k=2n+1 h01, l=2n+1	none
Space group	$P2_1/c$	$P\bar{1}$
$R = \Sigma\|\Delta F\| / \Sigma\|F_o\|$	0.0674	0.0654
$R_w = \Sigma\|\Delta F\|\omega^{1/2} / \Sigma\|F_o\|\omega^{1/2}$	0.1027	0.0920
Max. residual electron density (e Å^{-3})	0.2	0.3

TABLE 3.2

U_{ISO}, R and R_w values obtained using different CH_3 group specifications:

a) three H atoms per group, each with unity site occupation factor.

b) six H atoms per group, each with 0.5 site occupation factor.

	MNA-1	MNA-3	
		Molecule 1	Molecule 2
U_{ISO} - H(7) group (a)	0.215	0.157	0.200
U_{ISO} - H(7) group (b)	0.098	0.069	0.082
(U_{ISO} - C(7)	0.084	0.078	0.071)
U_{ISO} - H(9) group (a)	0.237	0.188	0.157
U_{ISO} - H(9) group (b)	0.091	0.109	0.092
(U_{ISO} - C(9)	0.078	0.088	0.070)
R(a)	0.075	0.072	
R(b)	0.067	0.065	
R_w(a)	0.107	0.098	
R_w(b)	0.103	0.092	
$\mathcal{R}$ (=R_w(a)/R_w(b))	1.039	1.065	
$\mathcal{R}_{4,1389,0.005}$	1.005	.....	
$\mathcal{R}_{8,2817,0.005}$	.....	1.004	

TABLE 3.3 Corresponding Bond Lengths and Bond Angles for MNA-1 and MNA-3, molecules 1 and 2, (with esd's, $10^3\sigma$ /Å or σ/deg, in parentheses)

Bond Length/Angle	MNA-1	MNA-3 (1)	MNA-3 (2)
C(1)-C(2)	1.391 (4)	1.405 (3)	1.405 (3)
C(1)-C(2)-C(3)	121.7 (.3)	121.9 (.2)	122.2 (.2)
C(1)-C(2)-N(2)	121.3 (.2)	122.1 (.2)	121.6 (.2)
C(2)-N(2)	1.460 (4)	1.454 (3)	1.459 (3)
C(2)-N(2)-O(2)	118.6 (.3)	120.8 (.2)	119.7 (.2)
C(2)-N(2)-O(3)	117.4 (.3)	118.5 (.2)	118.8 (.2)
N(2)-O(2)	1.208 (3)	1.204 (3)	1.205 (3)
N(2)-O(3)	1.231 (3)*	1.211 (3)	1.218 (3)
O(2)-N(2)-O(3)	123.9 (.3)*	120.7 (.2)	121.5 (.2)
N(2)-C(2)-C(3)	116.8 (.3)	116.0 (.2)	116.2 (.2)
C(2)-C(3)	1.390 (4)	1.388 (3)	1.386 (3)
C(2)-C(3)-C(4)	120.9 (.3)	121.4 (.2)	121.2 (.2)
C(2)-C(3)-H(3)	119.5 (2.1)	120.7 (1.7)	118.0 (1.6)
C(3)-H(3)	.961 (39)	.866 (28)	.916 (26)
H(3)-C(3)-C(4)	119.4 (2.1)	117.9 (1.7)	120.8 (1.6)
C(3)-C(4)	1.378 (4)	1.372 (4)	1.383 (3)
C(3)-C(4)-C(5)	117.4 (.3)	117.3 (.2)	116.5 (.2)
C(3)-C(4)-C(7)	120.6 (.3)	121.9 (.2)	122.0 (.2)
C(4)-C(7)	1.507 (4)	1.512 (3)	1.499 (3)
C(7)-C(4)-C(5)	122.0 (.3)	120.8 (.2)	121.4 (.2)
C(4)-C(5)	1.384 (5)	1.397 (4)	1.392 (3)
C(4)-C(5)-C(6)	122.0 (.3)	121.7 (.2)	122.8 (.2)
C(4)-C(5)-H(5)	117.3 (2.0)	121.7 (1.7)	115.8 (1.4)
C(5)-H(5)	.990 (35)	.988 (32)	.978 (26)
H(5)-C(5)-C(6)	120.6 (2.1)	116.6 (1.7)	121.4 (1.4)

Continued/.....

TABLE 3.3 Continued.....

Bond Length Angle	MNA-1	MNA-3 (1)	MNA-3 (2)
C(5)-C(6)	1.370 (4)	1.367 (3)	1.373 (3)
C(5)-C(6)-C(1)	121.5 (.3)	122.0 (.3)	121.3 (.2)
C(5)-C(6)-H(6)	118.2 (1.9)	118.2 (1.6)	120.3 (1.7)
C(6)-H(6)	.957 (33)	.904 (28)	.998 (28)
H(6)-C(6)-C(1)	120.0 (1.9)	119.8 (1.6)	118.3 (1.7)
C(6)-C(1)	1.391 (4)	1.403 (3)	1.393 (3)
C(6)-C(1)-C(2)	116.5 (.3)	115.6 (.2)	115.9 (.2)
C(6)-C(1)-N(1)	119.1 (.3)*	121.5 (.2)	121.3 (.2)
C(2)-C(1)-N(1)	124.3 (.3)*	122.9 (.2)	122.8 (.2)
C(1)-N(1)	1.410 (4)	1.396 (3)	1.400 (3)
C(1)-N(1)-C(8)	124.8 (.2)*	127.2 (.2)	126.5 (.2)
C(1)-N(1)-H(10)	117.1 (2.1)	114.0 (1.8)	115.3 (2.2)
N(1)-H(10)	.918 (38)	.948 (32)	.899 (35)
H(10)-N(1)-C(8)	115.7 (2.1)	118.7 (1.8)	115.6 (2.2)
N(1)-C(8)	1.346 (4)*	1.366 (3)	1.372 (3)
N(1)-C(8)-O(1)	121.3 (.3)*	123.0 (.3)	122.9 (.2)
N(1)-C(8)-C(9)	116.0 (.3)*	114.6 (.2)	114.5 (.2)
C(8)-O(1)	1.225 (3)*	1.208 (4)	1.211 (3)
O(1)-C(8)-C(9)	122.7 (.3)	122.4 (.3)	122.7 (.2)
C(8)-C(9)	1.490 (4)	1.501 (4)	1.495 (3)

* indicates significant differences between MNA-1 and MNA-3

TABLE 3.4 Mean plane equations, interplanar angles and deviations of atoms from the planes.

(Plane 1 is identified by atoms C(1), C(2), C(3), C(4), C(5)and C(6) Plane 2 by atoms C(2), N(2), O(2), O(3) and Plane 3 by N(1), C(8), O(1), and C(9))

3.4a), Orthonormal equations:-

MNA-1, Plane 1	0.0409(XO) +0.7939(YO) +0.6067(ZO) = 4.7551
Plane 2	-0.5437(XO) +0.8277(YO) +0.1389(ZO) = 0.3724
Plane 3	0.3912(XO) +0.9193(YO) -0.0437(ZO) = 5.8965
MNA-3 (1) Plane 1	0.4584(XO) -0.2547(YO) +0.8515(ZO) = 8.2181
Plane 2	0.6373(XO) -0.2182(YO) +0.7391(ZO) =10.6905
Plane 3	0.3059(XO) +0.0628(YO) +0.9500(ZO) = 8.5229
MNA-3 (2) Plane 1	-0.0648(XO) +0.4831(YO) +0.8732(ZO) = 4.3817
Plane 2	-0.3601(XO) +0.3819(YO) +0.8512(ZO) = 0.7470
Plane 3	0.3235(XO) +0.1319(YO) +0.9370(ZO) =10.1148

3.4b), Interplanar Angles:-

	MNA-1	MNA-3 (1)	MNA-3 (2)
Planes 1 and 2	44.0°	12.3°	18.0°
Planes 1 and 3	44.0°	21.1°	30.6°
Planes 2 and 3	57.2°	28.0°	43.0°

Planes 1, MNA-3 (1) and (2) : 53.8°

Planes 2, MNA-3 (1) and (2) : 71.6°

Planes 3, MNA-3 (1) and (2) : 4.2°

3.4c) Deviations of atoms from planes

Plane	Atom	Deviation (Å) from mean planes		
		MNA-1	MNA-3 (1)	MNA-3 (2)
1	C(1)	-0.0121	-0.0054	-0.0094
	C(2)	0.0169	0.0037	0.0056
	C(3)	-0.0052	0.0014	0.0021
	C(4)	-0.0115	-0.0047	-0.0058
	C(5)	0.0163	0.0029	0.0018
	C(6)	-0.0045	0.0022	0.0059
2	C(2)	0.0042	-0.0006	-0.0001
	N(2)	-0.0150	0.0019	0.0002
	O(2)	0.0055	-0.0007	-0.0001
	O(3)	0.0053	-0.0007	-0.0001
3	N(1)	0.0006	-0.0008	-0.0001
	C(8)	-0.0018	0.0024	0.0002
	O(1)	0.0007	-0.0010	-0.0001
	C(9)	0.0005	-0.0007	0.0000
	H(10)	-0.1465	-0.0770	-0,2093

TABLE 3.5

Atom Co-ordinates and Isotropic Thermal Parameters for MNA-1 and MNA-3, molecules 1 and 2 (with esd's, $10^3\sigma$, or 10^3 (A^2) in parentheses)

3.5a) MNA-1

ATOM	x	y	z	u_{iso}* ($Å^2$)
C(1)	0.6575 (3)	0.3503 (3)	0.4096 (3)	0.049 (2)
C(2)	0.6193 (3)	0.4350 (3)	0.2949 (3)	0.050 (2)
C(3)	0.4889 (3)	0.4599 (3)	0.2431 (3)	0.056 (2)
H(3)	0.4661(34)	0.5216(39)	0.1659(41)	0.080 (10)
C(4)	0.3922 (3)	0.4046 (3)	0.3071 (4)	0.060 (2)
C(5)	0.4304 (3)	0.3248 (3)	0.4249 (4)	0.066 (10)
H(5)	0.3609(33)	0.2850(37)	0.4707(37)	0.075 (2)
C(6)	0.5586 (3)	0.2965 (3)	0.4737 (4)	0.060 (9)
H(6)	0.5795(31)	0.2463(33)	0.5597(36)	0.064 (3)
C(7)	0.2510 (3)	0.4307 (5)	0.2493 (5)	0.084 (2)
N(2)	0.7145 (3)	0.5102 (3)	0.2304 (3)	0.063 (2)
O(2)	0.8039 (2)	0.5634 (3)	0.3071 (3)	0.089 (2)
O(3)	0.6954 (3)	0.5201 (3)	0.1004 (3)	0.085 (2)
N(1)	0.7873 (2)	0.3122 (3)	0.4592 (3)	0.056 (2)
H(10)	0.8085(31)	0.2910(34)	0.5535(41)	0.070 (10)
C(8)	0.8719 (3)	0.2704 (3)	0,3763 (3)	0,056 (2)
O(1)	0.8454 (2)	0.2766 (2)	0.2469 (2)	0.066 (2)
C(9)	0.9984 (3)	0.2176 (5)	0.4516 (4)	0.078 (3)

Lists of structure factors and anisotropic temperature factors have been deposited with the British Lending Division as supplementary publication No. 60415 which contains 34 pages of structure factor tables.

3.5b) (i) MNA-3, molecule 1

ATOM	x	y	z	u_{iso}*(Å^2)
C(1)	0.7671 (1)	0.4992 (2)	0.7456 (6)	0.051 (1)
C(2)	0.8276 (1)	0.4590 (2)	0.5289 (6)	0.054 (1)
C(3)	0.8887 (1)	0.5201 (2)	0.4212 (6)	0.059 (1)
H(3)	0.9252(14)	0.4944(20)	0.2846(70)	0.063 (7)
C(4)	0.8931 (1)	0.6229 (2)	0.5231 (6)	0.060 (1)
C(5)	0.8338 (1)	0.6636 (2)	0.7418 (6)	0.058 (1)
H(5)	0.8333(15)	0.7369(24)	0.8261(73)	0.079 (8)
C(6)	0.7732 (1)	0.6042 (2)	0.8488 (6)	0.056 (1)
H(6)	0.7362(15)	0.6344(20)	0.9899(66)	0.059 (6)
C(7)	0.9585 (2)	0.6908 (2)	0.4003 (8)	0.078 (2)
N(2)	0.8296 (1)	0.3515 (2)	0.4011 (6)	0.065 (1)
O(2)	0.7857 (1)	0.2887 (2)	0.5192 (7)	0.093 (2)
O(3)	0.8762 (1)	0.3265 (2)	0.1716 (7)	0.099 (2)
N(1)	0.7053 (1)	0.4390 (2)	0.8596 (5)	0.059 (1)
H(10)	0.7131(16)	0.3665(25)	0.8272(74)	0.079 (8)
C(8)	0.6362 (1)	0.4736 (2)	0.9910 (8)	0.073 (2)
O(1)	0.6198 (1)	0.5643 (2)	1.0181(11)	0.111 (2)
C(9)	0.5816 (2)	0.3894 (3)	1.0974(10)	0.088 (2)

3.5b) (ii) MNA-3, molecule 2

ATOM	x	y	z	u_{iso}*(Å^2)
C(1)	0.7411 (1)	-0,0198 (2)	1.1673 (6)	0.053 (1)
C(2)	0.6663 (1)	0.0060 (2)	1.1410 (6)	0.053 (1)
C(3)	0,6069 (1)	-0.0577 (2)	1.2497 (6)	0.055 (1)
H(3)	0.5593(15)	-0.0356(20)	1.2311(66)	0.065 (7)
C(4)	0.6186 (1)	-0,1502 (2)	1.3930 (6)	0.055 (1)
C(5)	0.6927 (1)	-0.1748 (2)	1.4239 (6)	0.060 (1)
H(5)	0.7003(13)	-0.2411(21)	1.5210(64)	0.060 (6)
C(6)	0.7520 (1)	-0.1123 (2)	1.3173 (6)	0.059 (1)
H(6)	0.8043(16)	-0.1332(23)	1.3415(73)	0.080 (8)
C(7)	0.5551 (1)	-0.2201 (2)	1.5125 (7)	0.071 (2)
N(2)	0.6469 (1)	0.1015 (2)	0.9939 (6)	0.063 (1)
O(2)	0.6919 (1)	0.1715 (2)	0.9687 (9)	0.103 (2)
O(3)	0.5852 (1)	0.1084 (1)	0.8989 (6)	0.085 (1)
N(1)	0.8017 (1)	0.0426 (2)	1.0514 (6)	0.059 (1)
H(10)	0.7898(18)	0.1070(29)	1.0022(90)	0.097 (10)
C(8)	0.8716 (1)	0.0092 (2)	0.9204 (6)	0.057 (1)
O(1)	0.8899 (1)	-0.0810 (1)	0.9083 (6)	0.074 (1)
C(9)	0.9233 (1)	0.0934 (2)	0.7933 (8)	0.070 (2)

* for non-H atoms

$$u_{iso} = [u_{11}\ u_{22}\ u_{33}]^{\frac{1}{3}}$$

The crystal structure of the amber form (MNA-2)

Abstract

The crystal and molecular structure of a third polymorph of 4-methyl-2-nitroacetanilide has been determined by X-ray diffraction techniques.[196] It crystallises in the monoclinic system, space group $P2_1/c$, Z=4, with a = 10.158(2), b = 11.635(2), and c = 8.041(2) Å, β = 94.55(2)°. Using 1027 unique reflections the structure was solved by the (Patterson) method of vector verification and refined by full matrix least squares which gave convergence to R = 0.080. The structure consists of nearly planar molecules, all approximately parallel to each other with their principal axes being parallel to b. The amide group forms an intramolecular hydrogen bond with the nitro group. Molecules related by c-glide are stacked along c in a very distinct columnar form. The columns are held together by the dipole forces between carbonyl groups of molecules related by an inversion centre and similarly by the nitro groups.

White and yellow polymorphs of 4-methyl-2-nitroacetanilide (MNA) were first reported by Gattermann[130] and Schaum[137] reported the existence of a third unstable variety which was described as dark yellow. X-ray analyses of the white (MNA-1) and yellow (MNA-3) forms have been reported (Moore et al.,[196]) and the intermolecular and intramolecular type of hydrogen bonding proposed by Skulski[139] for the white and yellow forms respectively was confirmed.

In the present work the crystal structure of the third variety, MNA-2 or amber form, was investigated in order to establish the nature of the hydrogen bond and as part of a study of the solid state phase changes of MNA. In fact, the ease with which the amber variety changed form and differences in thermal stability and crystal size between similarly prepared batches of crystals caused some of the difficulties experienced in this work.

Amber crystals of MNA-2 were prepared by partial evaporation of a hot (ca. 60°C) solution of MNA-2 in petrol (boiling range 80-100° C) containing about 10% (v/v) of carbon tetrachloride. Short filamentary crystals were obtained and a cleavage plane was found at approximately 60° to the longitudinal axis.

Unit cell and space group data were obtained from rotation and Weissenberg films. Accurate cell dimensions were determined by least squares refinements of θ, χ, and ϕ values measured on a four circle diffractometer. For structure analysis purposes, integrated intensities were measured by step scanning in the ω/θ mode. All diffractometer work was carried out with the crystal situated in an air stream maintained at 2°C in order to minimise the possibility of a solid state phase transformation which can take place at room temperature. Lorentz and polarisation factors were applied in the usual manner, and semi-empirical absorption corrections were made using the method of North et al.[193] modified by Kopfman and Huber[192] and Tickle[194].

Crystal data and details of diffractometer data collection are recorded in Table 3.6.

Table 3.6 Crystal data and experimental details (molecular formula $C_9H_{10}N_2O_3$, M_r 194.1)

Crystal system	Monoclinic
Habit	Amber, filamentary
a,b,c (Å)	10.158(2),11.635(2),8.041(2)
α, β, γ (deg)	90,94.55(2),90
V_c (Å)^3	947.4
Z	4
D (g cm^{-3})	1.36
D_m (g cm^{-3})	1.35
Flotation mixture	aqueous KI
Crystal size (mm)	0.3 x 0.25 x 0.2
λ, Cu- Kα (Å)	1.5418
ϕ axis	c
Max θ (deg)	52
h,k,l limits	-10 -11 -7
	10 11 8
Total reflections	4586
unique reflections	1027
	(788 with I > 3σI)
F (000)	408.0
Systematic absences	0k0, k = 2n+1
	h0l, l = 2n+1
Space group	$P2_1/c$
$R = \Sigma\|\Delta F\|/\Sigma\|F_o\|$	0.0?8o
$R_w = \Sigma\|\Delta F\|w^{\frac{1}{2}}/\Sigma\|F_o\|w^{\frac{1}{2}}$	0.089
Max. residual electron density (eÅ^{-3})	0.2

Structure determination and refinement

The structure could not be solved by direct methods of the program SHELX-76 nor by MULTAN-78 but the solution was obtained by the method of Patterson search, using a known part of the molecule, as proposed by Braun, Hornstra, and Leenhouts [195]. The molecular fragment used for this vector verification method consisted of atoms located at C(1), C(2), C(3), C(4), C(5), C(6), C(7), N(1), and N(2), Fig. 1, with orthonormal coordinates obtained from earlier work completed on polymorph MNA-1 (Moore et al. [196]). A vector set was found which had an excellent degree of compatibility with the sharpened Patterson function and an electron density map then gave all other nonhydrogen atoms. Three cycles of isotropic least squares refinement, with hydrogen atoms in theoretical positions, preceded a difference electron density map from which all nonmethyl hydrogens were located. With reference to the methyl hydrogens, the difference map only gave indications of significant electron densities present in the appropriate regions, it did not give peak locations which had good correlation with ideal methyl hydrogen geometries.

Final R values were achieved by further least squares refinement, using anisotropic temperature factors for the non-methyl hydrogen atoms and isotropic factors for all the hydrogens, with methyl hydrogens refined as rigid groups. Refinements were obtained with three hydrogen atoms per methyl group, each with a site occupation factor of 1.0, and also with six hydrogen atoms per group, each with a site occupation factor of 0.5. Differences obtained between isotropic thermal

parameters, R and R_w values and application of Hamilton's significance tests [190], Table 3.7 indicate that some appreciable methyl hydrogen disorder is present in this MNA-2 polymorph, in a manner similar to that previously reported for MNA-1 and MNA-3 polymorphs (Moore et al., [196]).

Table 3.7 U_{iso}, R, and R_w values obtained using different CH_3 group specifications.

U_{iso} H(7)[a]	0.201
U_{iso} H(7)[b]	0.079
(U_{iso} C(7)	0.088)
U_{iso} H(9)[a]	0.202
U_{iso} H(9)[b]	0.082
(U_{iso} C(9)	0.084)
R[a]	0.089
R[b]	0.080
R_w[a]	0.101
R_w[b]	0.089
$\mathcal{R}$ (=R_w^a/R_w^b)	1.135
$\mathcal{R}$ 4,871,0.005	1.009

[a] Three H atoms per group, each with unity site occupation factor.

[b] Six H atoms per group, each with 0.5 site occupation factor.

Results

Bond lengths and bond angles are presented in Table 3.8 mean-plane equations, interplanar angles and deviations of atoms from the planes are given in Table 3.9. Atom coordinates and thermal parameters, with esd values, are given in Table 3.10.

Molecular structure

The dimensions and general features of the MNA-2 molecule are similar to those reported for MNA-3 (viz. molecule 1). Thus resonance interaction of the nitro and amide groups would account for the relatively short C(3)-C(4) and C(5)-C(6) bonds. Such interaction of the substituent groups is favoured by the low dihedral angles between the amide and ring and between the ring and nitro groups. The benzene ring is more planar whilst the amide and nitro groups are slightly less planar than were found for MNA-1 and MNA-3. In general terms, all the nonhydrogen atoms lie very nearly in the molecular plane. The dihedral angle (3.9^{o}) between the amide and ring planes is lower than the equivalent angle reported for MNA-1 and MNA-3 as well as for 32 out of 35 other anilides whose structures were retrieved from the data files at the Cambridge Crystallographic Data Centre. Also, the value of the nonbonded distance O(1)-H(6), 2.16(6)Å is lower than that reported for the equivalent distance in MNA-3 and in a series of 4-substituted-anilides (Haisa et al.[72]). The deviation of the angles C(1)-N(1)-C(8), 129.7(.6) and N(1)-C(8)-O(1), 123.4(.5) from 120^{o} and the short O(1)-H(6) distance may be explained on the basis of a

bulky amide group being forced into the plane of the benzene ring. As a further consequence of the same effect the O(2) atom of the nitro group is slightly displaced from the plane of the benzene ring. The H(10)...O(2) distance 1.98(.05)Å is very similar to that found in MNA-3 (molecule 1, 1.95Å and molecule 2, 1.98Å). This, together with the angle C(1)-N(1)-H(10), 111(3.6)° is consistent with a weak intramolecular hydrogen bond between O(2) and H(10).

Intermolecular relationship

The projection of the unit cell contents along Z shows that the molecules are packed in distinct columns parallel to c, with molecular axes parallel to b, and the projection along Y shows the molecular planarity and how parallel they are to each other. Adjacent molecules within the column are glide plane related. The average perpendicular distance of the ring atoms of a molecule x,0.5-y,0.5+z to a molecule x,y,z which is adjacent to it within the column, is 3.40 Å. These molecules are very nearly parallel the angle between the normals to the ring planes being only 0·95°. Presumably molecules within a column are bonded by weak forces such as those operating in π molecular complexes and since the whole molecule is very planar, orbital interaction must occur between amide and benzene ring. This interaction is expected to be at a maximum when charge alternation on adjacent atoms is at a maximum i.e. when the amide and nitro groups are in the plane of the benzene ring.

An adjacent column consists of molecules of symmetry 1-x,1-y,1-z and 1-x,0.5+y,0.5-z. A molecule in the adjacent column at 1-x,0.5+y,1.5-z lies very nearly parallel to that at x,y,z in the first column. The perpendicular distance between the planes occupied by each benzene ring is 0.173 Å and the angle between the planes is 1.42°. Thus an unusual feature of this structure is that all atoms (except for the methyl hydrogens) lie in parallel planes. This feature accounts for the very strong reflection in the diffraction pattern, $d(\bar{2}02)$ = 3.271 Å which is comparable to the distance between the ring planes of

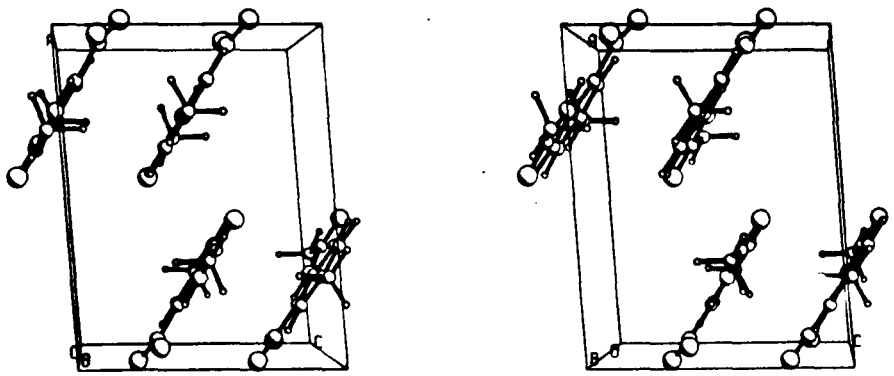

A view down y

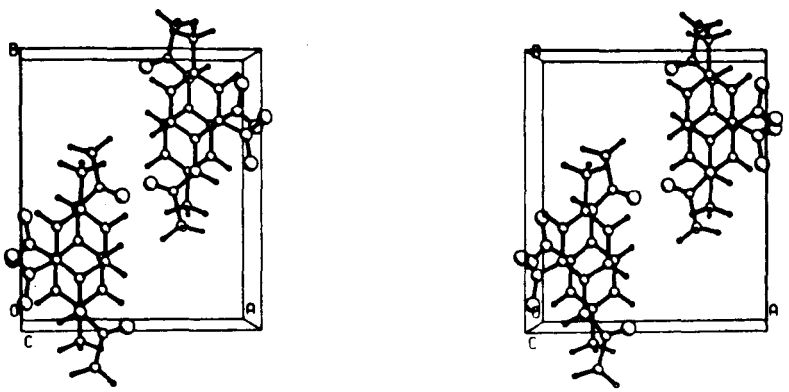

A view down z

Fig. 3.8

Stereo-pair diagrams for the unit cell of MNA-2

FIG. 3.9

MNA-2

VIEW DOWN Y

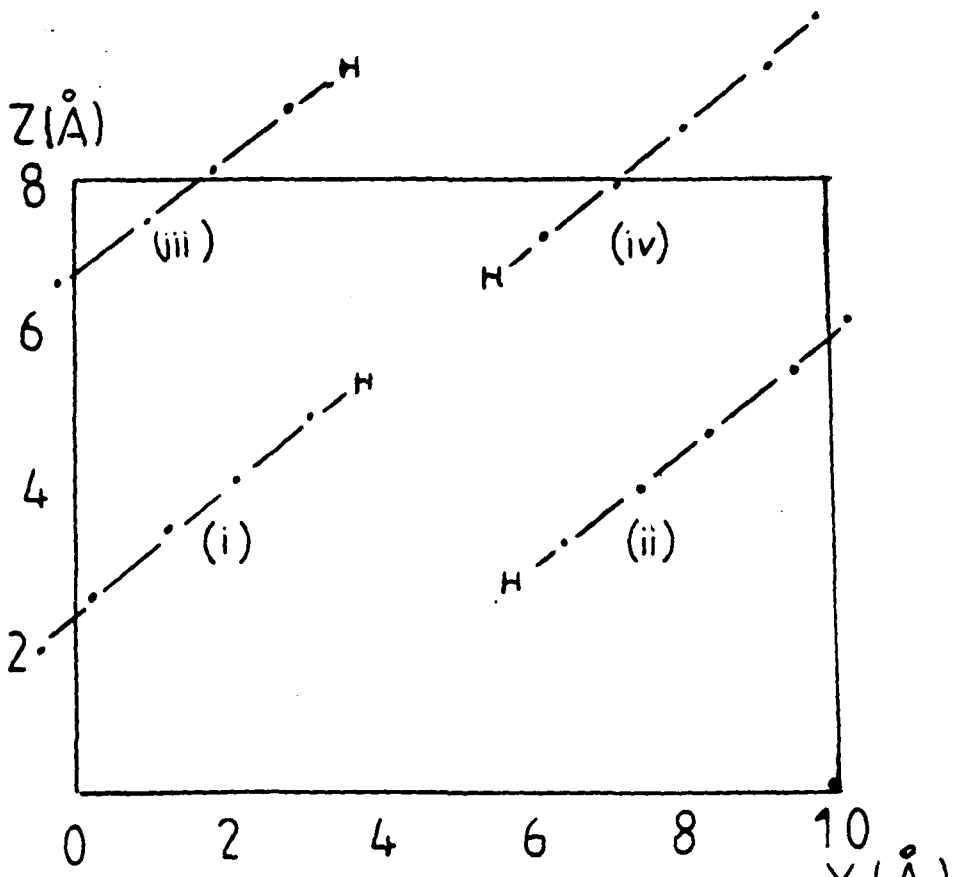

MOLECULES VIEWED DOWN C(7) – N(1) AXIS. BENZENE RING IS END-ON.

(i) = XYZ
(ii) = 1-X, 1-y, 1-Z.
(iii) = X, 0·5-y, 0·5 +Z.
(iv) = 1-X, 0·5+y, 1·5 -Z.

FIG. 3.10

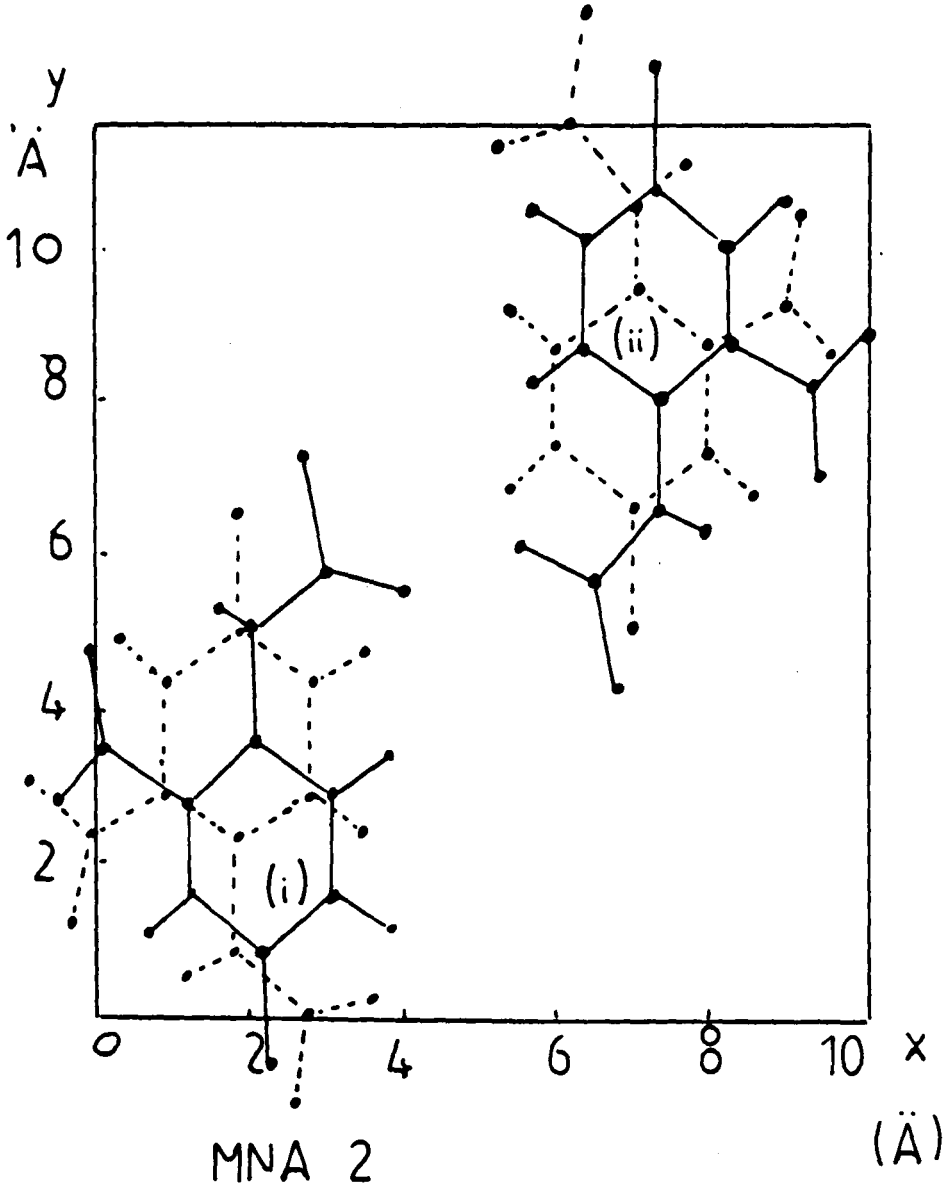

VIEW DOWN Z
(i) xyz
(ii) 1−x 1−y 1−z

the molecules at x,0.5−y,0.5+z and 1−x,0.5+y,1.5−z, i.e. 3.29 Å. Angles between normals to the $\bar{2}02$ plane and molecular planes are 3.5° (plane 1), 7.1° (plane 2), and, 5.5° (plane 3).

The main columnar interactions appear to be of the dipole–dipole type between carbonyl groups across a centre of inversion and a similar interaction for nitro groups. The distance between the oxygen atoms of the carbonyl groups in the molecules of symmetry x,y,z and 1−x,1−y,1−z is 3.25(1) Å and the distance between nitro group oxygen atoms (O(2)...O(2)) in molecules x,y,z and −x,1−y,1−z is 3.52(1) Å. The shortest intermolecular distances involve O(1)[x,y,z] to H(5)[1−x,0.5+y,1.5−z],2.23(6) Å; H(3)[x,y,z] to H on C(7)[−x,−y,1−z], 2.51(9) Å; and O(2)[x,y,z] to H on C(9)[−x,1−y,1−z], 2.55(7) Å.

Table 3.8 Bond lengths and bond angles for MNA-2 (esd's: $10^3\sigma$ (Å^2) for bonds not involving H atoms; $10^2\sigma$ (Å^2) for bonds to H atoms; or σ(deg) for bond angles, in parentheses.)

bond length or angle	Å or degree	bond length or angle	Å or degree
C(1)-C(2)	1.395(6)	C(5)-H(5)	0.93(6)
C(1)-C(2)-C(3)	121.6(0.5)	H(5)-C(5)-C(6)	121.8(3.3)
C(1)-C(2)-N(2)	122.1(0.5)	C(5)-C(6)	1.367(8)
C(2)-N(2)	1.458(6)	C(5)-C(6)-C(1)	121.1(0.5)
C(2)-N(2)-O(2)	120.1(0.5)	C(5)-C(6)-H(6)	120.5(3.4)
C(2)-N(2)-O(3)	118.4(0.5)	C(6)-H(6)	0.95(6)
N(2)-O(2)	1.234(5)	H(6)-C(6)-C(1)	118.4(3.4)
N(2)-O(3)	1.224(5)	C(6)-C(1)	1.401(7)
O(2)-N(2)-O(3)	121.5(0.4)	C(6)-C(1)-C(2)	116.3(0.5)
N(2)-C(2)-C(3)	116.2(0.5)	C(6)-C(1)-N(1)	120.8(0.5)
C(2)-C(3)	1.386(7)	C(2)-C(1)-N(1)	123.0(0.5)
C(2)-C(3)-C(4)	121.8(0.5)	C(1)-N(1)	1.400(7)
C(2)-C(3)-H(3)	120.2(3.3)	C(1)-N(1)-C(8)	129.7(0.6)
C(3)-H(3)	0.88(5)	C(1)-N(1)-H(10)	111.0(3.6)
H(3)-C(3)-C(4)	118.0(3.2)	N(1)-H(10)	0.79(5)
C(3)-C(4)	1.364(7)	H(10)-N(1)-C(8)	119.3(3.6)
C(3)-C(4)-C(5)	116.9(0.5)	N(1)-C(8)	1.368(7)
C(3)-C(4)-C(7)	122.4(0.5)	N(1)-C(8)-O(1)	123.4(0.5)
C(4)-C(7)	1.510(7)	N(1)-C(8)-C(9)	113.8(0.6)
C(7)-C(4)-C(5)	120.7(0.5)	C(8)-O(1)	1.206(6)
C(4)-C(5)	1.393(7)	O(1)-C(8)-C(9)	122.8(0.5)
C(4)-C(5)-C(6)	122.3(0.6)	C(8)-C(9)	1.505(7)
C(4)-C(5)-H(5)	115.9(3.3)		

Table 3.9 Least-squares planes, displacements (Å) of atomsfrom the planes, and interplanar angles (deg).

1 Benzene ring

$-0.5310(X_o) - 0.0051(Y_o) + 0.8473(Z_o) = 2.0083$

C(1)	- 0.002
C(2)	0.001
C(3)	0.000
C(4)	0.000
C(5)	- 0.002
C(6)	0.003

2 Nitro group

$-0.5763(X_o) - 0.1238(Y_o) + 0.8078(Z_o) = 1.4680$

C(2)	0.002
N(2)	- 0.006
O(2)	0.002
O(3)	0.002

3 Amide group

$-0.5182(X_o) + 0.0608(Y_o) + 0.8531(Z_o) = 2.3730$

N(1)	- 0.002
C(8)	0.005
O(1)	- 0.002
C(9)	- 0.002
H(10)[a]	0.056

Dihedral angles between the planes

1 and 2	1 and 3	2 and 3
7.6°	3.9°	11.4°

[a] All atoms within a specified group were used to calculate the respective planes except H(10) in group 3.

Table 3.10 Atom co-ordinates and isotropic thermal paramenters for MNA-2 (with esd's, $10^4\sigma$ or $10^3\sigma$ ($\AA^2$), in parentheses)

Atom	x	y	z	u ($\AA^2$)[a]
C(1)	0.2446(3)	0.3123(3)	0.5147(5)	0.063(3)
C(2)	0.1470(3)	0.2468(3)	0.4277(5)	0.062(3)
C(3)	0.1504(4)	0.1277(4)	0.4296(6)	0.069(3)
H(3)	0.863(39)	0.0879(32)	0.3763(46)	0.071(13)
C(4)	0.2492(4)	0.0686(3)	0.5170(5)	0.070(3)
C(5)	0.3470(34)	0.1335(4)	0.6043(6)	0.077(3)
H(5)	0.4143(43)	0.0922(35)	0.6609(50)	0.078(14)
C(6)	0.3455(4)	0.2510(4)	0.6046(6)	0.069(3)
H(6)	0.4148(48)	0.2932(35)	0.6638(56)	0.092(15)
C(7)	0.2524(5)	-0.0611(4)	0.5239(7)	0.088(4)
N(2)	0.0367(3)	0.2992(4)	0.3281(5)	0.073(3)
O(2)	0.0185(3)	0.4039(3)	0.3344(4)	0.091(3)
O(3)	-0.0375(3)	0.2367(3)	0.2414(4)	0.092(2)
N(1)	0.2450(4)	0.4326(3)	0.5130(5)	0.071(3)
H(10)	0.1837(41)	0.4566(32)	0.4574(45)	0.058(13)
C(8)	0.3360(5)	0.5078(3)	0.5850(6)	0.075(3)
O(1)	0.4328(3)	0.4780(2)	0.6707(5)	0.095(2)
C(9)	0.3056(5)	0.6318(3)	0.5450(7)	0.0844)

[a] for non-hydrogen atoms $u_{iso} = [u_{11} u_{22} u_{33}]^{\frac{1}{3}}$

Some intraplanar distances in MNA-2.

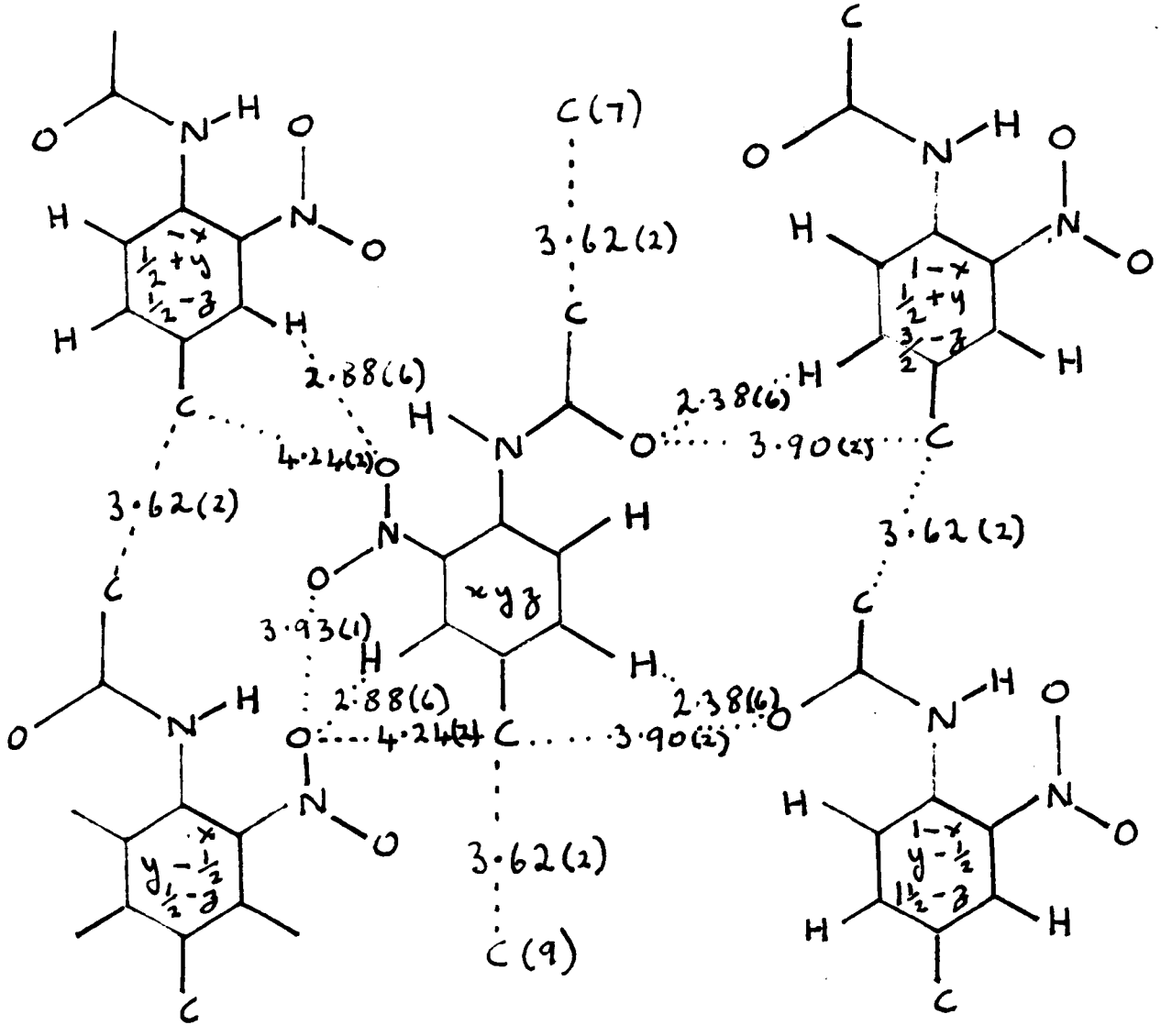

Fig. 3.11
Some intermolecular distances between molecules lying in the $\bar{2}02$ plane in MNA-2. The symmetries of molecules are shown in the ring. The values in parentheses are e.s.ds of the distance.

Some intraplanar distances in MNA-3

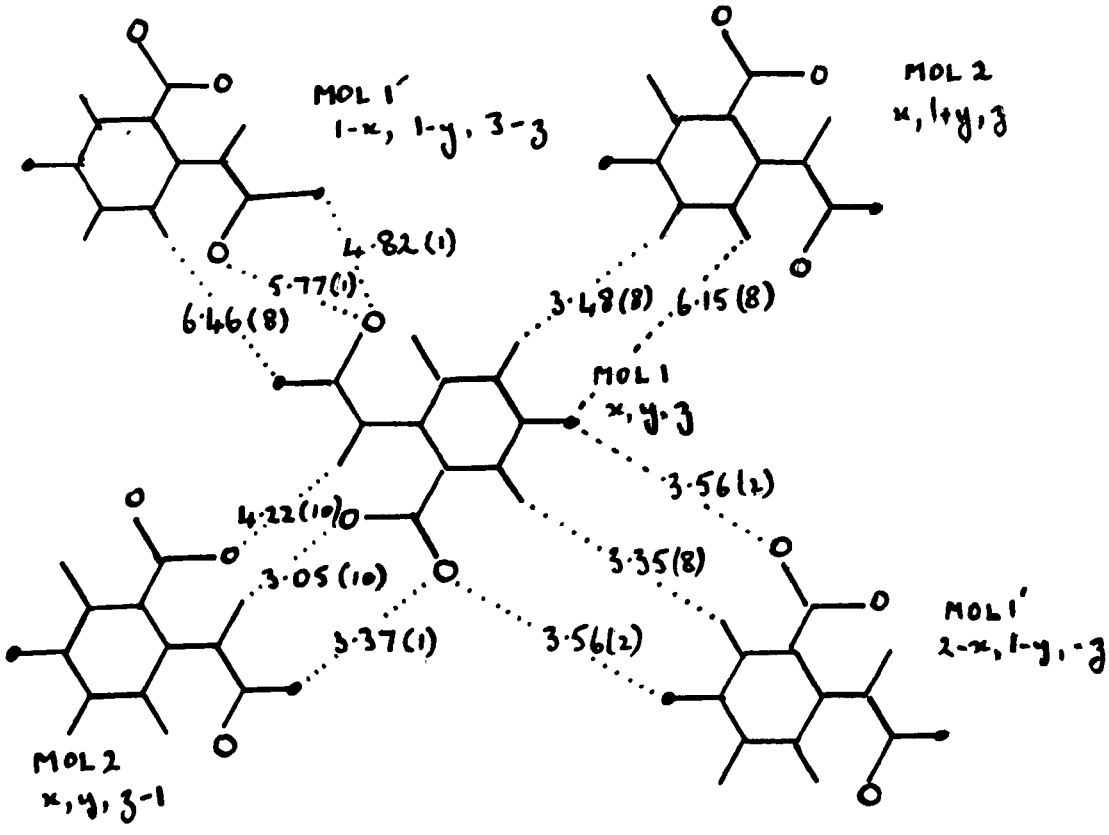

Fig. 3.11a

Some intermolecular distances between molecules of type 1 and 1' which are coplanar in MNA-3. All distances are given in Ångstrom units and values in parentheses are e.s.d values. Some distances from adjacent molecules of type molecule 2 are also given. Molecules of type 1 and 1' lie nearly in the $3\bar{1}1$ plane.

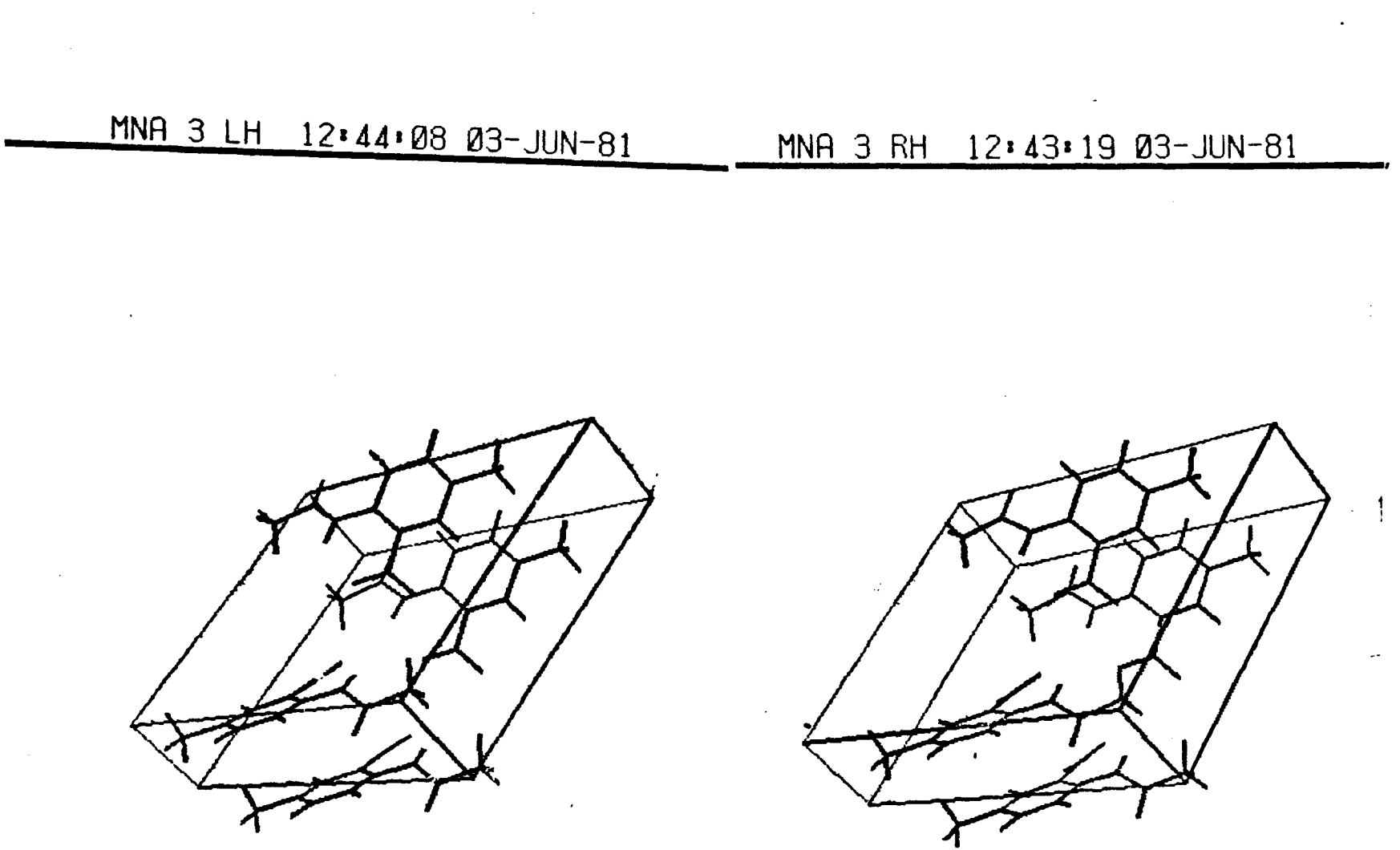

Fig. 3.12 Stereoscopic view of molecules 1 and 2 in MNA-3 (yellow)

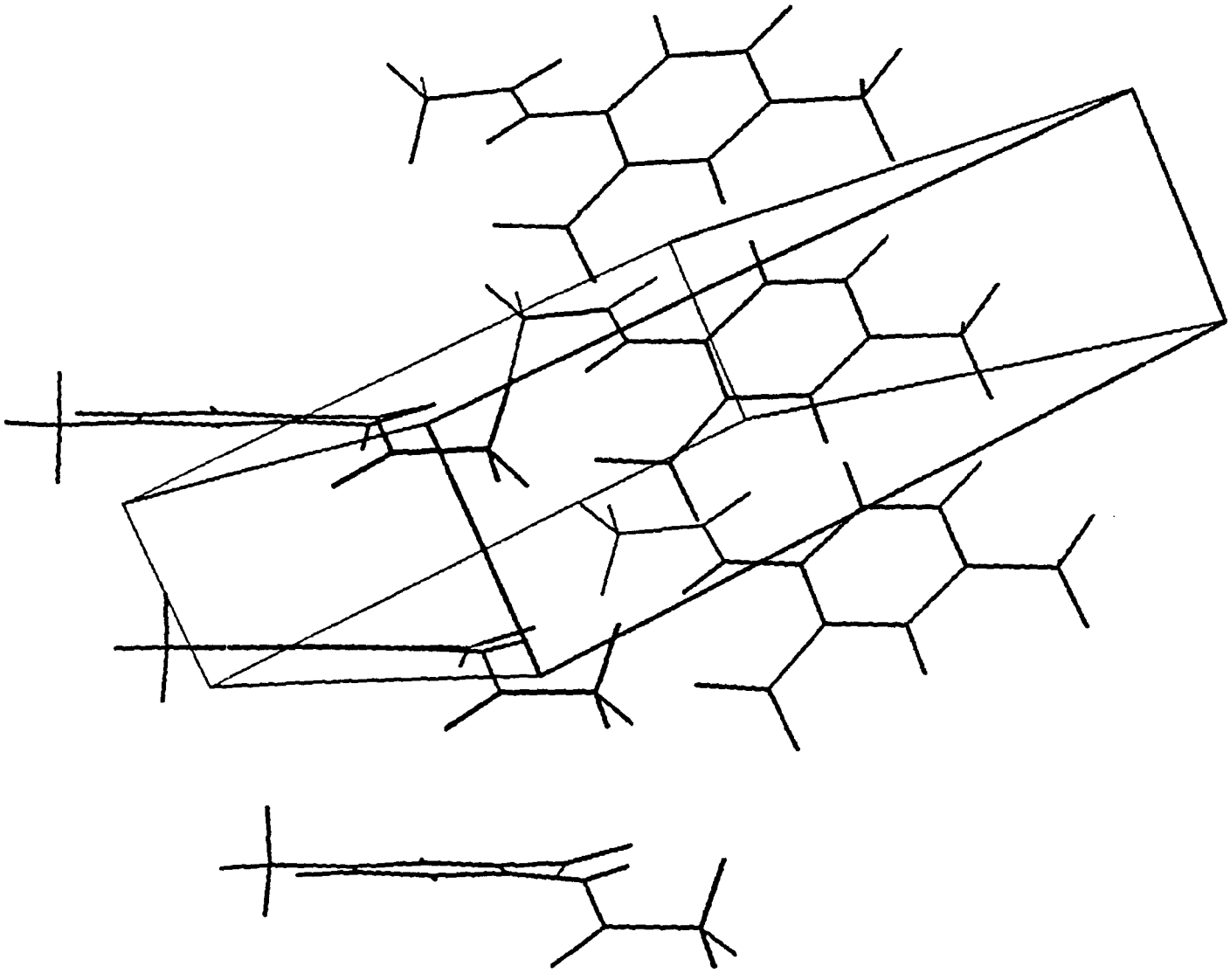

Fig. 3.13 A view of three pairs of molecules 1 and 2 in MNA-3. The outline of the unit cell is shown in perspective.

CHAPTER FOUR

The Topotactic Phase Changes of MNA

An introduction to Chapter 4.

Section 4.1a (page 110)

This section is an account of the morphology of the yellow polymorph (MNA-3) and describes how it can be regarded as a structure of columns which form laths parallel to the z direction. This feature, as well as the presence of a cleavage plane which made analysis by x-ray diffraction possible, are shown in a selection of electron micrographs.

Section 4.1b (page 117)

This section describes the solid state phase change of MNA-3 (yellow) to MNA-1 (white). This change occurs on standing at ambient temperature for periods which may vary from several weeks to several years or more rapidly on heating to about 85°C. The growth of the new phase has strong directional preferences which are illustrated in fig. 4.4 (page 118) and fig. 4.5 (page 119).

Section 4.2 (page 123)

This section describes a hypothetical mechanism for the phase change in which pairs of molecules rotate around axes

which are parallel to the z axes and pass through centres of symmetry (fig. 4.8, page 125). Although this approach yields calculated x and y coordinates which are in good agreement with those found experimentally for MNA-1 (see fig. 5.5 and fig. 5.6 on pages 194 and 195 respectively) a mechanism involving less translational movement is preferred (Section 4.8).

Section 4.3 (page 127)

This section introduces the possibility that the main factor which determines the orientation of the new phase is that their respective flat faces will prefer to be parallel.

Section 4.4 (page 129)

In this section the consequences of possible defects in the column structures are considered.

Section 4.5 (page 137)

This section shows how MNA-2 (amber) and MNA-3 (yellow) can be regarded as crystal structures composed of molecules in closely packed parallel layers.

Section 4.6 (page 146)

This section considers that the phase change of MNA-3 to MNA-1 could occur by a mechansim which involves movement of the contents of parallel planes as in a martensitic transformation.[188]

Section 4.7 (page 150)

This (second) mechanism for the change of MNA-3 to MNA-1 is summarised and criticised in this section.

Section 4.8 (page 152)

A third mechanism for the phase change MNA-3 to MNA-1 is considered in this section. The mechansim involves folding planar molecules found in MNA-3 in such a way that the molecule pivots about N(1) (Fig. 4.20 page 153). Although this mechanism involves movement of benzene rings it explains the orientation of the new phase and shows how a new sheet or layer of molecules of MNA-1 can arise from a layer or sheet of MNA-3 molecules (fig. 4.21, page 156 and 4.22 page 157).

Section 4.9 (page 158)

The phase change MNA-2 (amber) to MNA-3 (yellow) is described and a possible mechanism is proposed and illustrated in fig. 4.27, page 165.

Section 4.10 (page 169)

This section shows how the crystal structures of MNA-2, MNA-3, and MNA-1 can be viewed as structures constructed from molecules lying in parallel planes.

Section 4.1a

The morphology of yellow crystals of MNA-3

Crystals of MNA-3 which are grown from solutions of light petrol form long rod-like structures which fracture readily when attempts are made to cut them. The crystals are not circular in cross section but tend to be flat, and well formed crystals of MNA-3 have an elongated diamond-shaped cross section which is shown below :-

Several electron micrographs of MNA-3 crystals are shown in figs.4.1to 4.5. . It is known from X-ray work that the z-direction is parallel to the long axis of the crystal. The crystals show a cleavage plane which is inclined at about 75° to the z-axis. Ele ctron micrographs of a small section of MNA-3 which was cut from a long section are shown in fig. 4.1. The tendency for the crystal to fracture in planes parallel to the cleavage plane is also revealed. The well defined flat surface of the crystalis shown in fig. 4.3 . Close examination of the flat surface reveals that it is built up from closely packed laths. This feature is probably responsible for the observed property of the crystal to splinter along the length of the crystal.

The stacking of laths parallel to the z-direction is regarded as an important feature of the crystal structure and could account for the observed directions of growth of MNA-1 in the solid state. The strong tendency for MNA-1 to form well developed layers or sheets in the yz plane was emphasised in the previous section.

Following from the ideas of Mnyukh[170] the formation of the strongly layered structure of MNA-1 could be due to the diffusion of MNA molecules across a microcavity and deposition on a flat surface might occur in such a way that the flat layers of MNA-1 grow on the flat layers of MNA-3 so that at an intermediate stage parallel layers of MNA-3 and MNA-1 would co-exist. Hence the orientation of molecules of MNA-3 at the flat surface would be of lesser importance than its flat or planar nature.

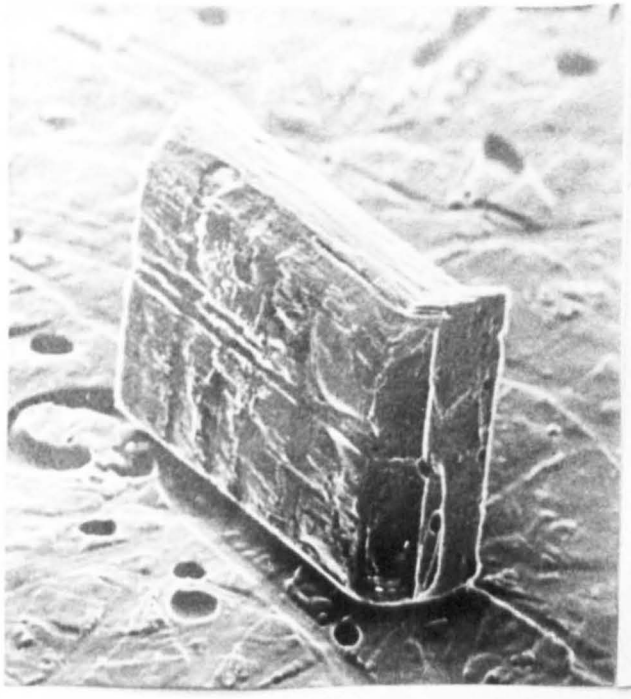

1. x 120

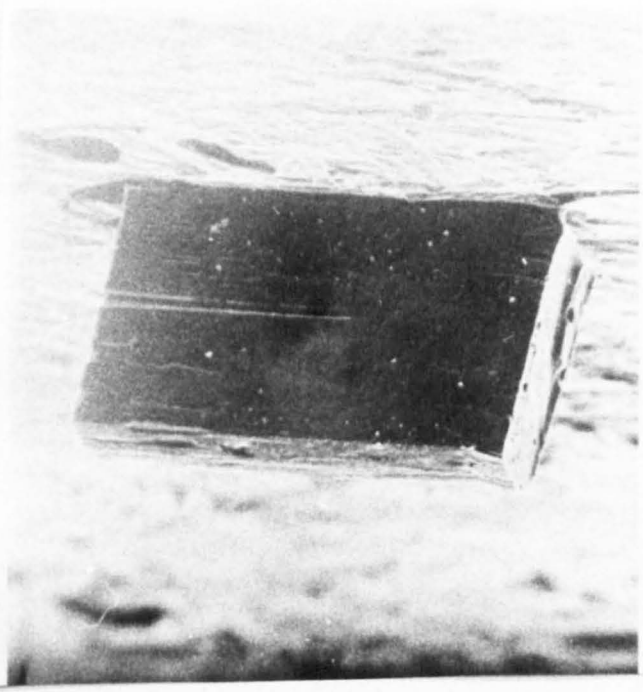

2. x 110

1, 2, and 4 show a cut crystal of MNA-3 (yellow). Note the dislocation on the right-hand end of the crystal as well as 'holes'. 3. shows a surface built from overlapping laths (MNA-3).

3. x 240

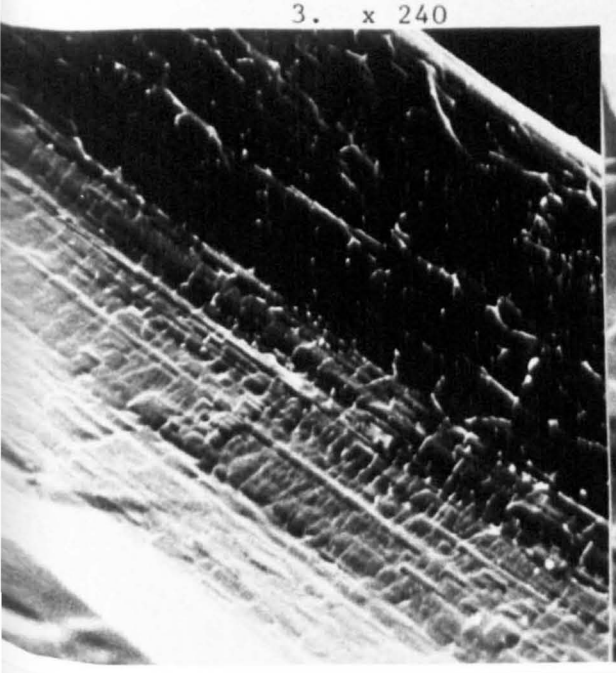

4. x 220

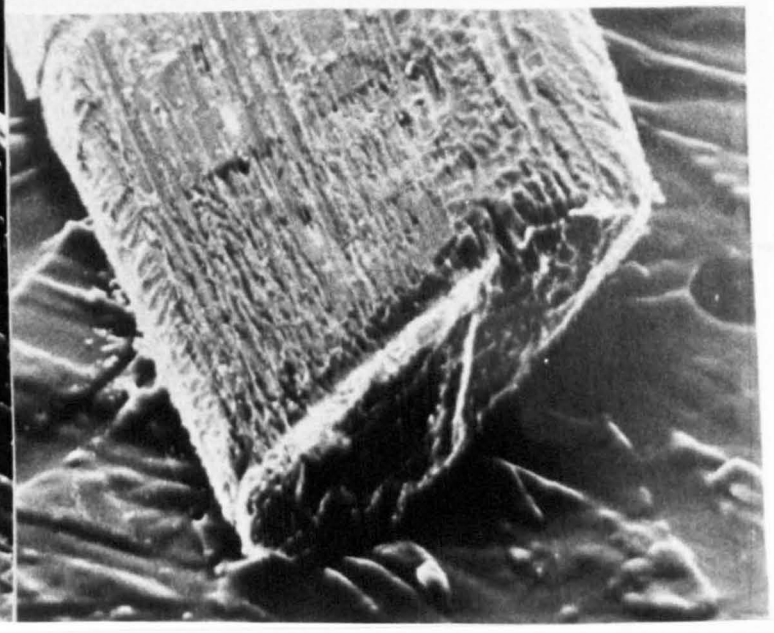

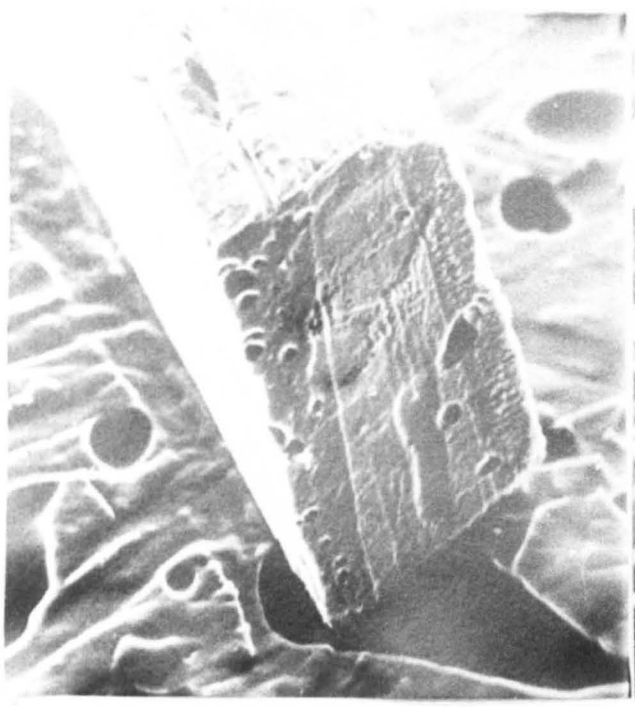

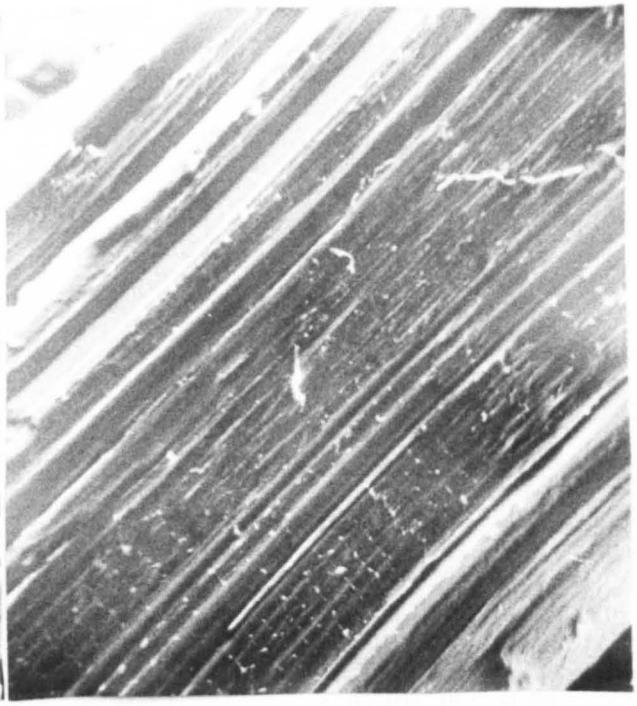

1. x 250 2. x 250

Electron micrographs of MNA-3 (yellow) cut by a razor blade. The clean cleavage is clearly seen (1,3,4).
2. This shows the surface of MNA-3 (yellow). Parallel columns along the diagonal of the photograph are parallel to the z axis.

2. x 250 4. x 250

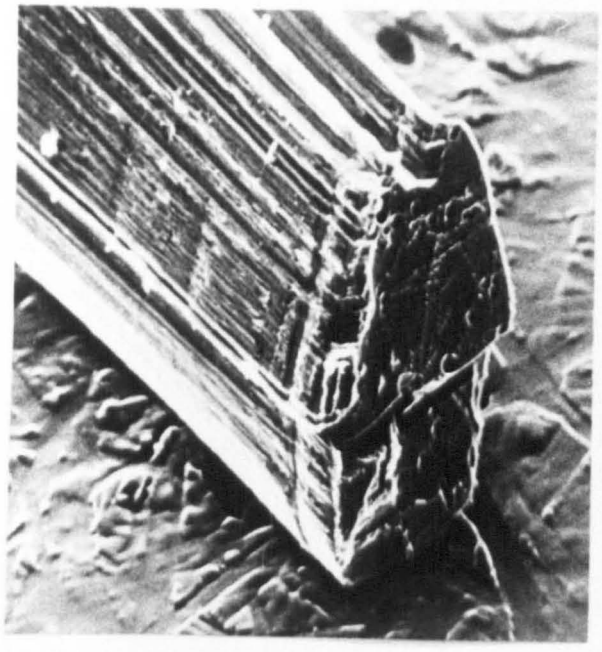

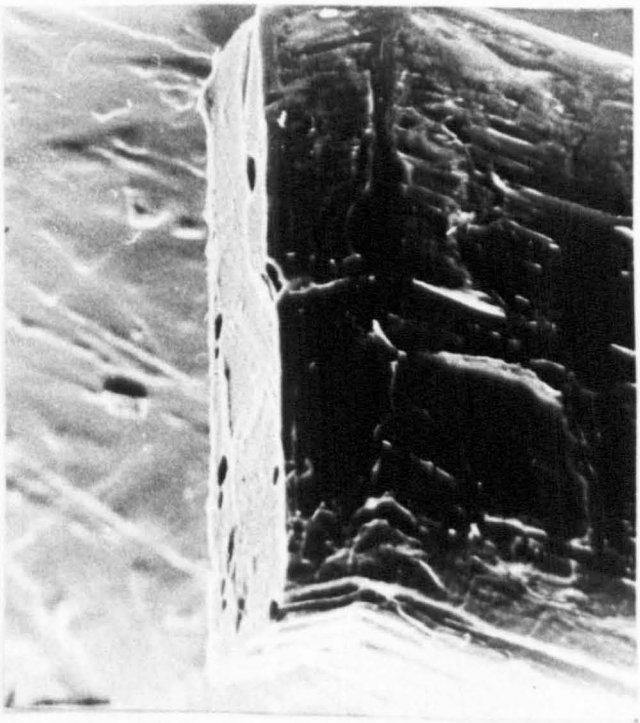

Fig. 4.3

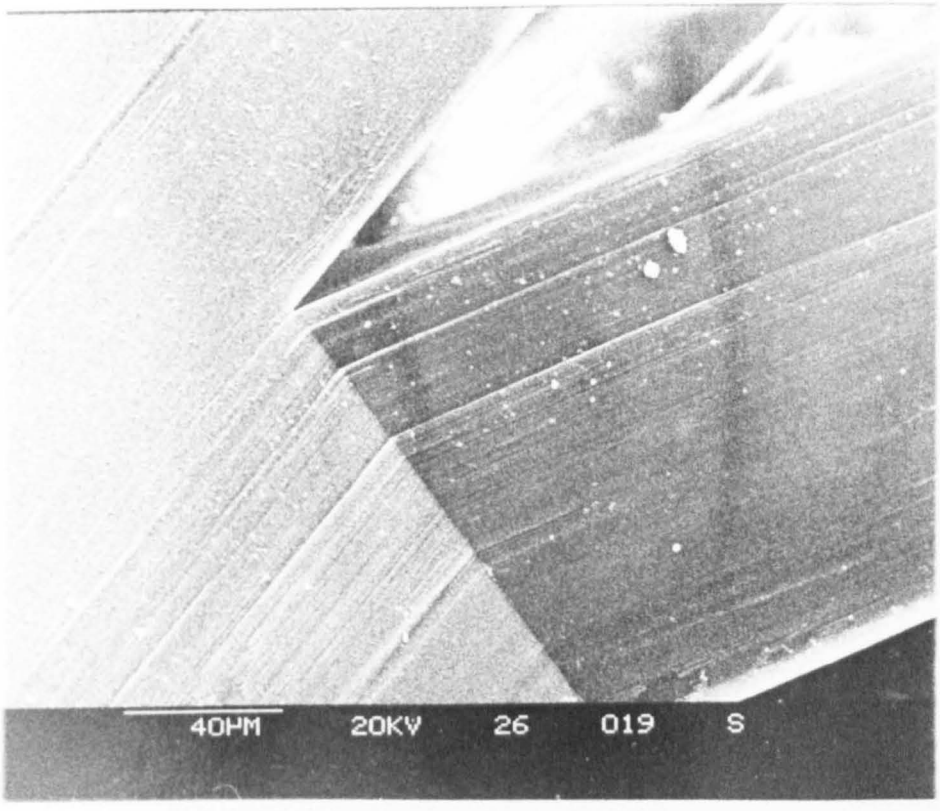

Electron micrographs of a crystal of MNA-3 (yellow) which was splintered by pressing with a spatula end. Stress induced twining has probably occurred. The scale is indicated on each photograph.

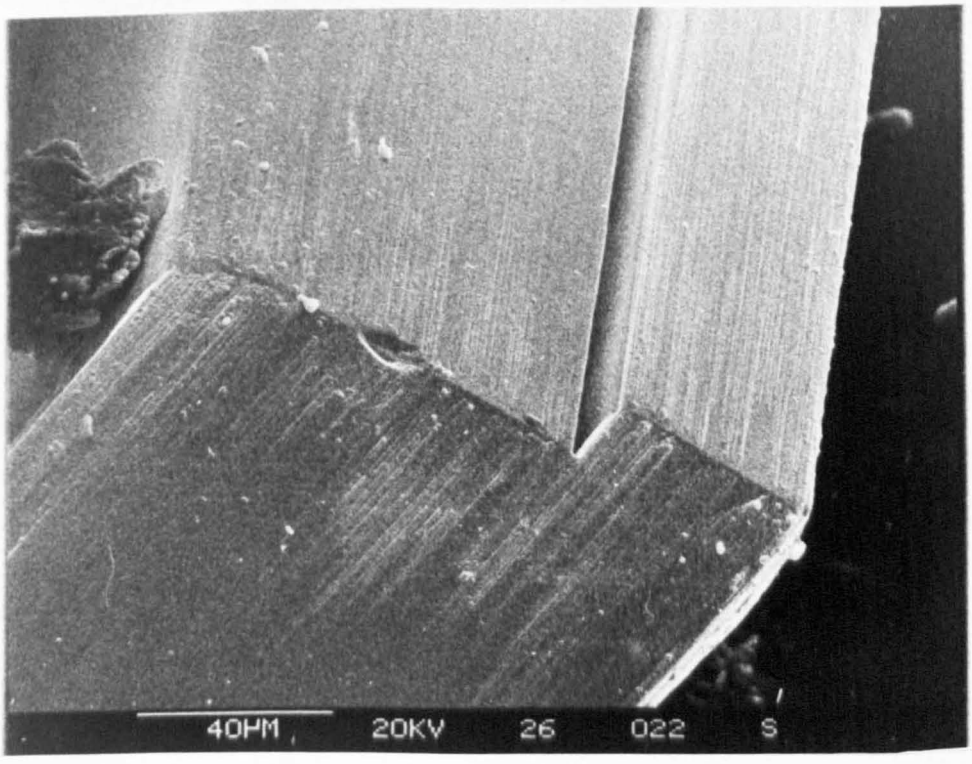

In addition to the electron microscopy work further X-ray work was carried out on single crystals of MNA-3 in order to determine the directions of the a or b axes with respect to the surface of the crystal.

Rotation photographs of MNA-3 crystals were obtained when the crystal was fixed to a glass fibre so that a T-shaped arrangement was present which is shown below :-

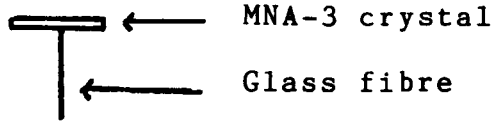

The separation of layer lines suggested that the direction of greatest cross-sectional width corresponded to the a+b axis. The calculated value of the diagonal a + b = 21.9Å whilst the separation of layers lines was **21.95 ± 0.05** Å.

Hence it is concluded that the when the crystals are viewed perpendicular to their flat side (a position which they naturally adopt when placed on a glass plate on the laboratory bench) that the molecular axes N(1)...C(7) are perpendicular to the observer. The orientation of unit cells in a cross section of the crystal is as shown in fig. 5.15

However, if layers of MNA-1 molecules are to grow in the solid state in the observed orientation, then the molecular

axes N(1)...C(7) must change from one of being parallel to MP in fig. 4.18 to one of lying parallel to MA !. Such a re-orientation involves rotation of the molecular axes through about 90 degrees. This possibility will be discussed in the next section.

Section 4.1b

The solid state phase change of MNA-3 to MNA-1

The formation of the white form of MNA from the yellow form i.e. MNA-3 to MNA-1 has been observed to occur in samples which have been stored at ambient temperature or on heating to about 85°C. In the latter case the change can be observed using a Kofler hot-stage microscope. The growth of the new phase can be seen to occur with strong directional preferences and photographs of such growths are shown in the photographs in figs. 4.4 and 4.5.

It can be seen that the crystals of the white form are produced in densely packed clusters of small crystals which have their long axes (which corresponds to the direction in which hydrogen bonds occur) either in the same direction as the needle axis of the yellow form or inclined at an angle of about 45° to this direction.

An attempt has been made to rationalise the formation of the white form and a mechanism for the solid state phase change will be presented.

Tightly packed crystals of MNA-1 (right) formed from MNA-3(left) at ambient temperature in the solid phase. This represents 'vertical' growth of MNA-1 from MNA-3. The MNA-1 and MNA-3 axes are horizontal.

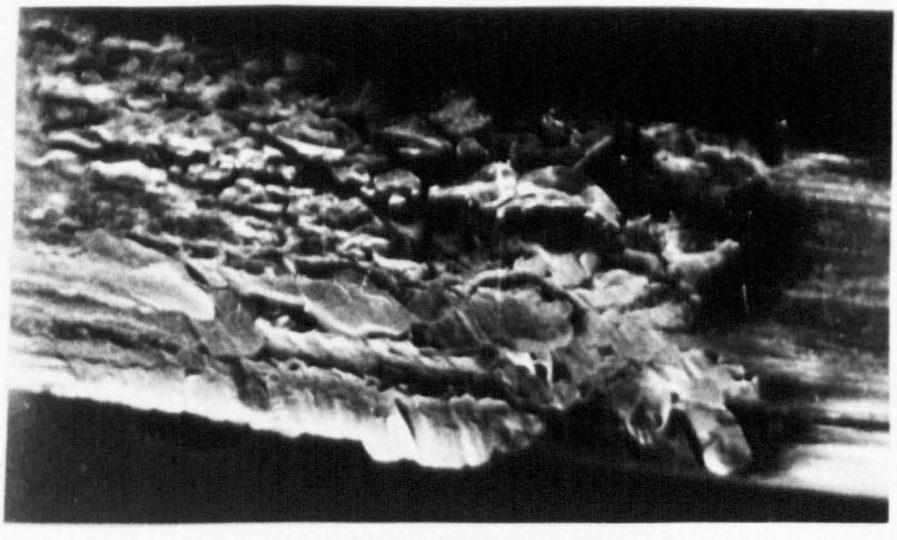

Tightly packed MNA-1 crystals (left) formed in the solid phase from MNA-3 which is just visible on the right of the photograph.

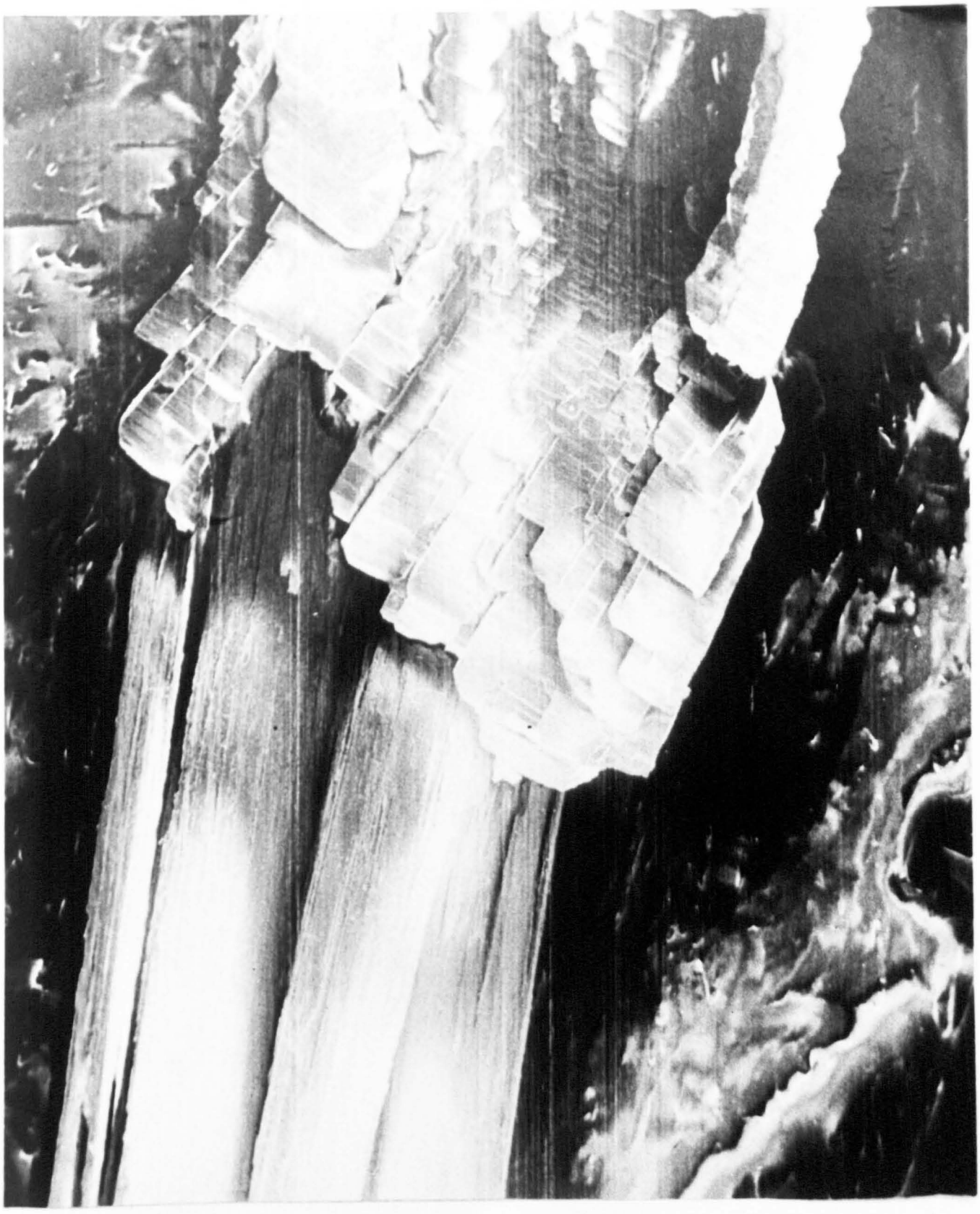

Lateral growth of MNA-1 (upper) occurring on a crystal of MNA-3 (lower). Magnification x 140

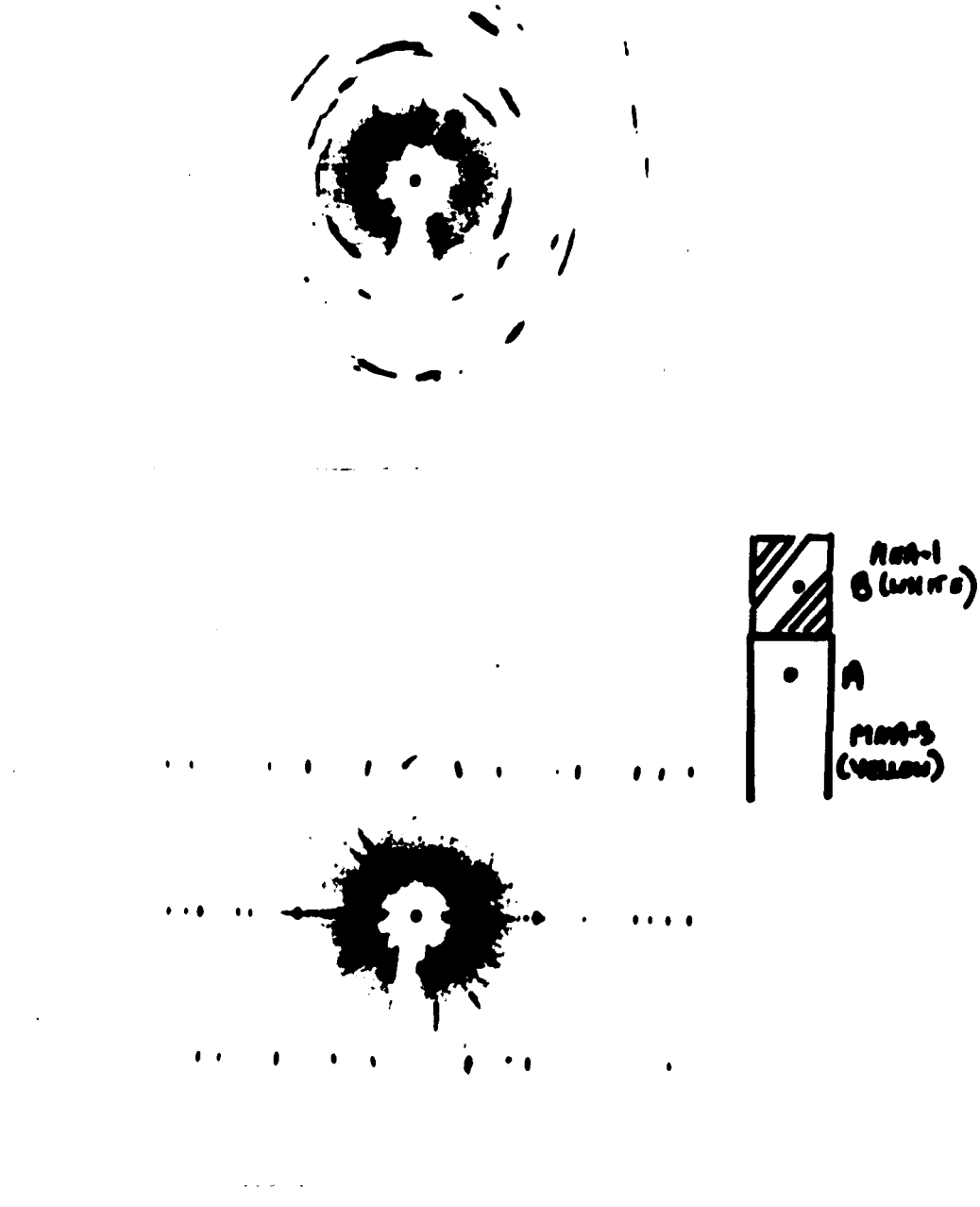

Fig. 4.6a. Oscillation photographs of a single filament of MNA-3 taken at point A and at point B where lateral growth of MNA-1 had occurred which was of the same type as shown in Fig. 4.6. In the lower photograph the layer lines correspond to the 'c' spacing of the triclinic lattice which along the long filamentary axis. The upper rotation photograph shows that the daughter crystallites have grown with preferred orientation but a single crystal, which would have produced horizontal rows of spots, has not been formed. (Stubbens camera, 7.5° oscillation, Cr-Kα radiation)

Fig. 4.6

A view of MNA-1 crystals (upper) formed from MNA-3 (lower) in the solid phase at ambient temperature. (x 500)

1.

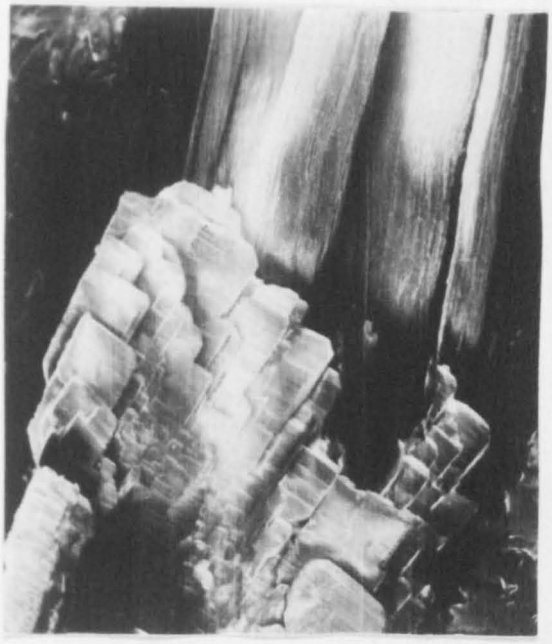

2.

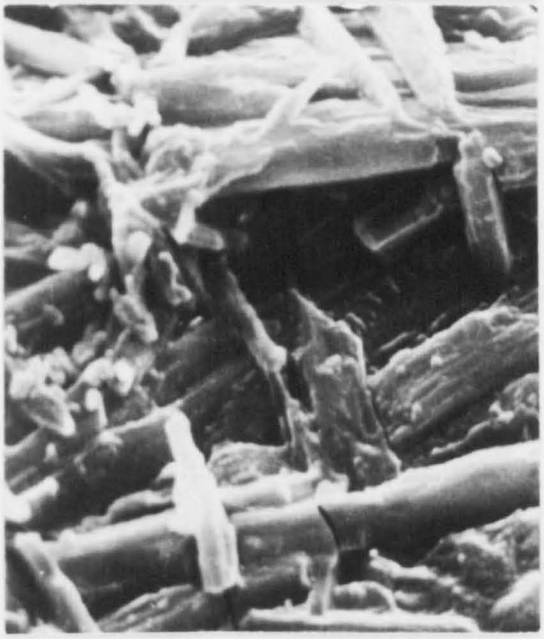

3.

1. A view of MNA-1 crystallites formed in the solid phase from MNA-1.

2. A conglomeration of MNA-1 crystals formed from yellow MNA-3 (upper half of photograph). This shows lateral growth of MNA-1 crystals. Magnification x 375

3. MNA-1 layers (lower half) formed by allowing the amber (MNA-2) form to stand for several weeks.

Section 4.2

A model for the transformation of MNA-3 (yellow) to MNA-1 (white)

The projection of the crystal structure of MNA-3 in the x-y plane shows that the structure is composed of pairs of molecules which are related by an inversion centre. For example, molecules 1 and 1' have an inversion centre at 0.5,0.5,0.5 and molecules 2 and 2' have an inversion centre at 1,1,1. Thus the structure may be viewed as pairs of molecules with members of each pair being related by an inversion centre. The position of the carbonyl groups in these pairs is important since it is probable that dipole-dipole interaction between carbonyl groups helps to stabilise the columnar structure of MNA-3. The relative positions of such pairs of molecules are shown in fig. 4.8 .

The formation of MNA-1 may occur by rotation of these pairs in a clockwise manner around the centre of symmetry. This rotation has been simulated by computer drawn diagrams. A projection of the crystal structure before and after rotation of the pairs of molecules around centres of symmetry is shown in fig. 4.8 , fig.4.9 and fig. 4.10 . The difference between the last two diagrams is that the repeat distance along the x-direction has been reduced by a factor of 0.5. This corresponds to a contraction in this direction. However, the important aspect of this diagram is that

new pairs of molecules are formed which are separated byashort distance of about 4Å and they are related by a centre of symmetry. Such pairs are equivalent to molecules A(x,y,z) and B(1-x,1-y,1-z) in MNA-1. Another important aspect of fig.4.10 is that the pairs of molecules are packed in parallel rows both in the x and y directions. An MNA-1 type of structure can be constructed from this by rotation of the amide groups into directions which are perpendicular to the plane of the diagram so the the old and new z directions are approximately parallel.

The intermolecular hydrogen bonds would be formed parallel to the z axis of MNA-3 i.e. the MNA-1 and MNA-3 z axes would be parallel. Photographs of this type of growth of MNA-1 from MNA-3 in the solid state are shown in fig.4.4 whereas in the case of lateral growth of MNA-1 the z axis of MNA-3 is at 45^{o} to the z axis of MNA-1.

Although the rotation mechanism accounts for the formation of new centres of symmetry the formation of MNA-1 from MNA-3 in two different orientations is, in the opinion of the author, fully explained by the approach discussed in section 4.8 in which the molecules are assumed to pivot about N(1).

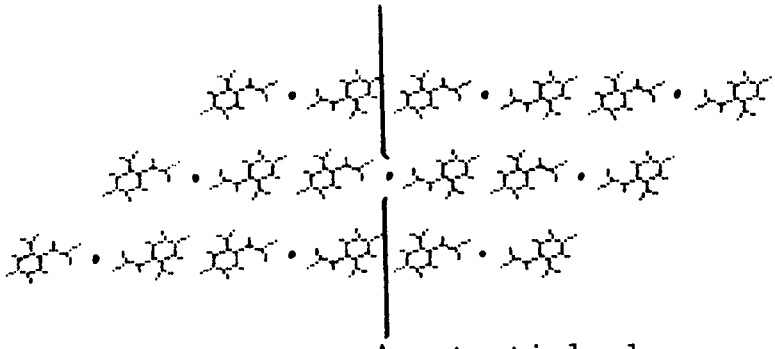

Fig. 4.8
A view of MNA-3 down z showing molecules related by centres of symmetry (•)

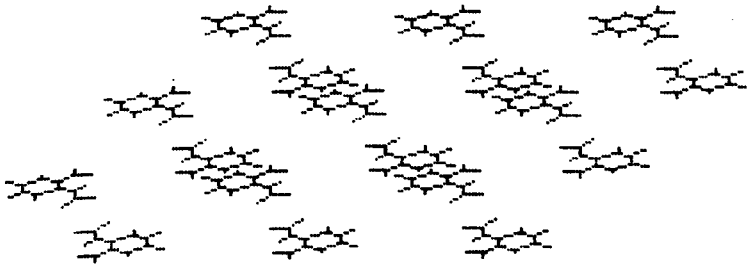

Fig. 4.9
Molecular positions after rotation of each pair around a centre of symmetry by 60°.

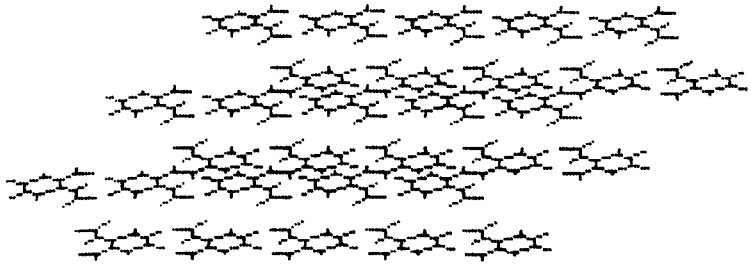

Fig. 4.10
A more dense packing of rotated molecules.

Fig. 4.11 Molecules 1 and 1', and 2 and 2'
The . indicates a centre of inversion.

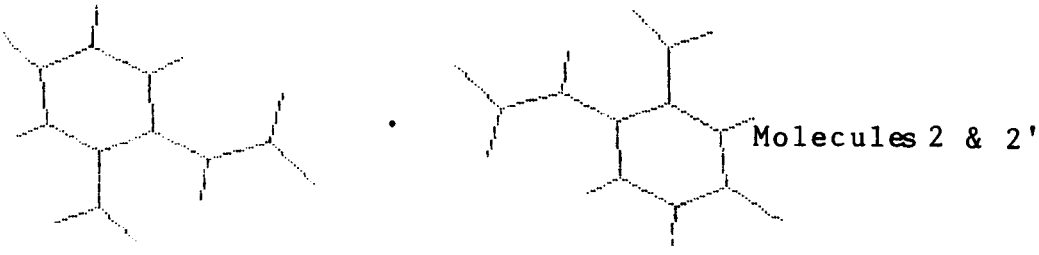

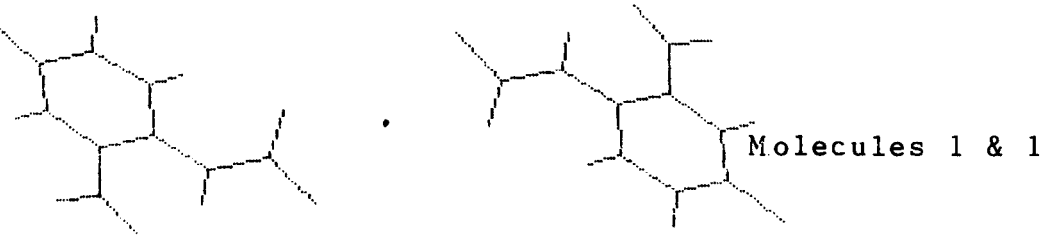

Section 4.3

The validity of a physical interpretation of MNA-3 (yellow) to MNA-1 (white) conversion.

Previous sections of this thesis have described how the MNA-1 (white) crystal structure can be derived from the MNA-3 crystal structure by a clockwise rotation of pairs of molecules which are related by a centre of symmetry and which occupy adjacent positions in the crystal by a dipole-dipole interaction between the carbonyl groups. This interaction is much weaker in MNA-1 (white) since the antiparallel carbonyl groups have an increased separation compared to the MNA-3 (yellow) crystal structure. (The distances O(1)...O(1) in MNA-3 are 4.61 Å (molecule 1) and 4.57 Å (molecule 2); and O(1)...O(1) in MNA-1, 7.69 Å. The molecules in question are at x,y,z and 2-x,-y,1-z and they are related by a centre of symmetry at 1,0,0.5.

One possible interpretation is that rotation of an object can be treated as a mathematical operation in which the coordinates of points in a body are multiplied by a matrix and a comparison of the old and new coordinates may correspond to a convenient physical interpretation involving rotation and perhaps translation. A mathematical relationship between old and new positions does not prove that rotation and translation actually occurred. However,

such an interpretation does remain a possibility.

It is important to stress at this stage that the conversion of MNA-3 (yellow) to MNA-1 (white) is not a phase transformation of a single crystal to a single crystal. This is revealed by examination of transformed crystals under the optical and electron microscopes as well as by the powder pattern obtained by X-ray diffraction of the transformed material. However, the former techniques do clearly show that well formed microcrystals are produced which have grown with strong orientational preferences.

Since MNA-3 and MNA-1 have crystal structures in which distinct layers are present it is possible to apply the ideas of Mnyuch[170] i.e. the transformation could occur from layers of molecules lying parallel to the yz planes across microcavities by a process of sublimation and layers of MNA-1 type crystals might be deposited in such a way that the yz layers (these layers are very pronounced in MNA-1) are laid parallel to the layers of molecules in the yz planes of MNA-3. The mathematical transformation of the MNA-3 to the MNA-1 structure would still be valid because it is based on a feature, namely the close antiparallel C=O groups, which is common to both systems.

Section 4.4

An explanation of the topotactic growth of MNA-1 (white) based on the likely presence of crystal defects in MNA-3 (yellow).

Many batches of crystals of the yellow triclinic form of MNA have been prepared and it has been observed that the stability of these different batches is very variable. For example, a sample which was prepared by crystallisation from light petroleum (boiling range 40-60°) which was collected on a Hirsch funnel and then dried in air, changed completely into the white form on storing in a sample tube for two months. In another case, a sample of the yellow form, which was made by slow cooling of a solution in light petroleum (boiling range 60-80°)containing carbon disulphide, was stable for more than three years although one crystal of the yellow form had changed to the white form. In the latter case the crystals had been made with a view to preparing good crystals for X-ray diffraction experiments and consequently they had been isolated by decantation of the crystallisation solvent and allowed to dry in air. These crystals had grown as well formed spikes or needles which were several centimetres long and 1 to 2 mm thick and many adhered to the sides and bottom of the flask. Hence decantation of the solvent proved to be an easy operation. In fact it was apparent that the stability was increased by careful and gentle handling and that some operations, such as collection on filter funnels,

pressing to remove solvent and packing into sample tubes, should not be attempted.

During the preparation of crystals of MNA-3 for X-ray diffraction is was noticed that the crystals tended to splinter easily when attempts were made to make cuts with a razor blade perpendicular to the length of the crystal. However, the discovery of a cleavage plane, which is mentioned in chapter 3 , enabled clean cuts to be made.

It is therefore possible that crystals of MNA-3 might contain faults or defects in which the long columns of molecules, which are packed along z and parallel to the long filamentary axis of the crystal, have separated. This separation of columns might be of the order of several Angstrom units and the fault would not be detectable by external examination.

It is suggested that a possible line of fracture in the MNA-3 structure is parallel to the line drawn in the projection of the MNA-3 crystal structure which is viewed down z and shown in fig.4.8 .The general direction of the fracture or potential cleavage plane is parallel to the yz-plane. The protruding portions on either side could be members of pairs of 1 and 1' or 2 and 2'. Diagrams of sections parallel to the yz-plane of MNA-3 are shown in figs. 4.12

Fig. 4.12 Views of columns of molecules 1,2,1',2' in MNA-3. Unit cells viewed down y.

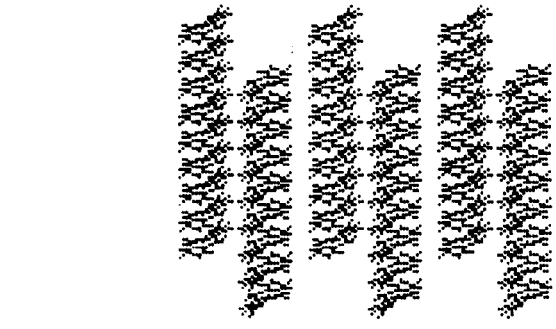

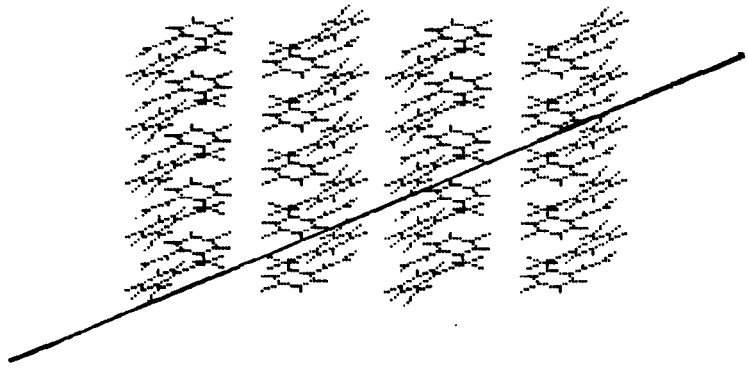

The dark line is a potential cleavage plane.

The plane is viewed edge on.

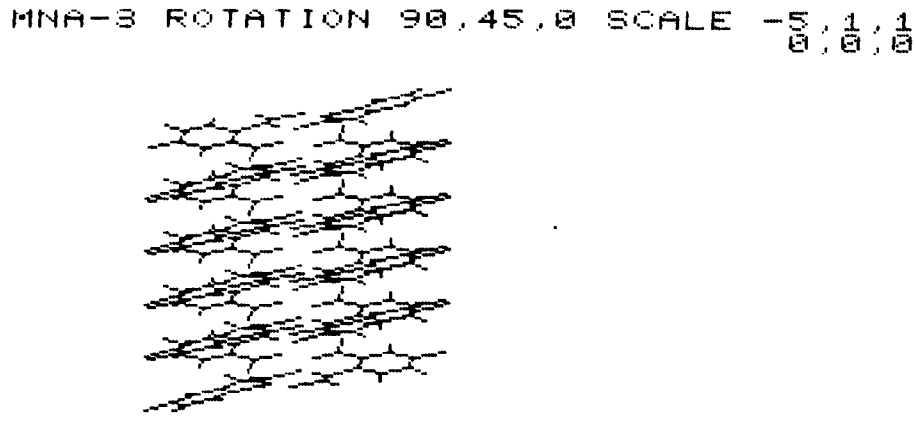

Fig. 4.13

A view of several unit cells stacked along z
The view is perpendicular to the cell diagonal
OP shown in Fig. 4.18.

. It should be noted that these diagrams offer varying degrees of magnification. These diagrams clearly emphasise the columnar arrangement of MNA-3 and it is suggested that the cleavage plane, which proved invaluable for the preparation of suitable samples for X-ray diffraction experiments, corresponds to a section along a plane, viewed edge-on, in fig. 4.12.

This cleavage plane may also be used to explain the shape of twinned crystals of MNA-3. A photograph of a twinned crystal is shown in fig.4.14 and the twinned crystal constructed from the computer generated crystal structure of MNA-3 is shown in fig.4.15. The adjacent molecules on either side of the boundary of the twinned crystals are related by a centre of inversion.

One important aspect of the fracture-plane depicted in fig. 4.8 is that the protruding molecules will be of the 1 and 1' type on one side and 2 and 2' on the other side. If a molecule of MNA in the vapour state attaches itself by dipole-dipole interaction to one of the protruding molecules the two molecules would be related by a centre of inversion and rotation of the amide groups would give molecules equivalent to molecules A (x,y,z) and B (1-x,1-y,1-z) in MNA-1 (white). This pair of molecules would then act as a nucleus for the growth of MNA-1 throughout the entire MNA-3

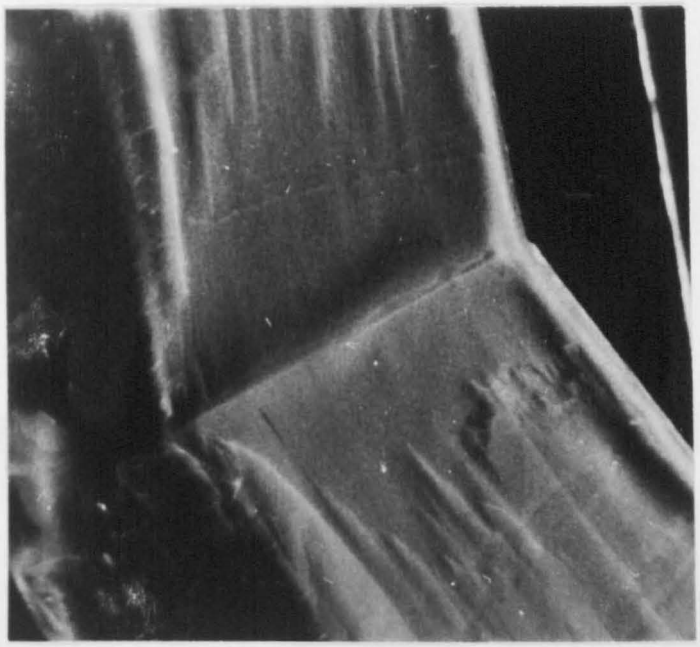

A twinned crystal of MNA-3 (yellow)

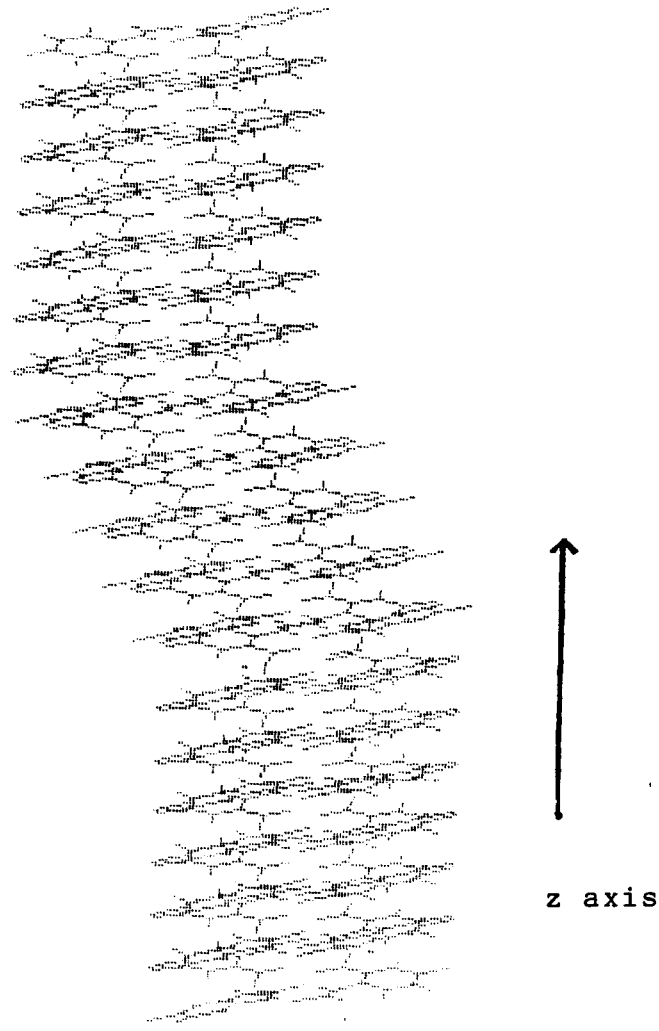

Fig. 4.15 A possible arrangement of molecules in a twinned crystal of MNA-3. Each unit cell is viewed perpendicular to the cell diagonal from 0,0,0 to 1,1,0.

crystal.

According to this hypothesis the orientation of growth of MNA-1 is dictated by (a) the formation of fractures along the crystal axis and parallel to the yz planes and (b) the attachment to a molecule of type 1 or type 2. Attachment to the former would favour growth of MNA-1 with the intermolecular bonds parallel to the long filamentary axis (i.e. vertical growth) and attachment to a molecule of type 2 would favour lateral growth. Since there are the same number of exposed molecules of types 1 and 2 (but on opposite sides of the fracture) there should be an equal probability that vertical and lateral growth occur. This point has not been investigated and examination of many crystal transformations would be necessary to establish this point. However, both lateral and vertical growth of MNA-1 crystals from MNA-3 crystals are commonly observed.

In a perfect crystal of MNA-3 fractures would be absent and spontaneous transformation should not occur. However, the formation of the white form should be observed if small traces of white form are introduced i.e. seeding. Also, if it was possible to make small, well formed crystals of MNA-3 then the sample should show greater stability. It should be noted that small, well formed crystals of MNA-3 are not usually formed from solution where initially fine hair-like

crystals are formed and subsequent growth merely adds to the length to width ratio of 20 or more.

The latter point will be referred to later when the phase change of MNA-2 is discussed since it proved possible to make a thermally stable variety of MNA-3 from MNA-2.

Section 4.5

An alternative model for viewing the changes occurring during phase transformations.

The previous discussion of the mechanism of the phase change concentrated on the structure and organisation of molecules in columns. In this second model, which complements the first model, emphasis is placed on the existence of groups of molecules which occur in planes. For example, all molecules in MNA-2 (amber), are found in parallel planes and fig. 3.8 which gives a view of the structure of MNA-2 down the y-direction, clearly shows that all atoms of a molecule to lie in one plane and all molecules lie in planes parallel to the $\bar{2}02$ plane.

The arrangement of molecules in this plane is shown in fig.4.1 . This diagram was drawn on a hexagonal grid to assist in the construction of hand-drawn hexagons. An additional feature is apparent in that the line diagram fits remarkably well into a pattern which is reminiscent of the crystal structure of graphite. Also the interplanar spacing of MNA-2 (3.4 Å) is very similar to the value found for the interplanar spacing in graphite (3.4 Å). If this diagram is regarded as a projection of the crystal structure then x and y coordinates can be measured from the diagram and z coordinates can be estimated using the following approximation which is based on

the equation for the least-squares plane through the benzene ring :-

$$z = 0.89\ x + 0.3$$

The slope of this line is approximately 41° and hence a reasonable model of MNA-2 can be envisaged by holding fig.4.16 with the y-axis horizontal and at an angle of inclination of about 40° .

The crystal structure of MNA-3 (yellow) can be constructed by rotating alternate rows of molecules, lying parallel to the y-axis, through 180° i.e. a rotation of 180° around an axis formed by an intersection of the glide plane and the plane of the diagram. The resulting structure is shown in fig.4.17 and after adjustment to the hexagonal grid the resulting structure is found in fig. 4.18 . If the parallelogram OABF is regarded as a projection of the unit cell onto the inclined plane then x and y coordinates can be measured. O represents the origin of the unit cell, OA and OB represent the projections of the a and b sides of the unit cell respectively and AM the projection of the c-axis.

Although the molecules marked MOL 1 at x,y,z and 1-x,1-y,3-z are known to be coplanar those marked MOL 2 are not in the same

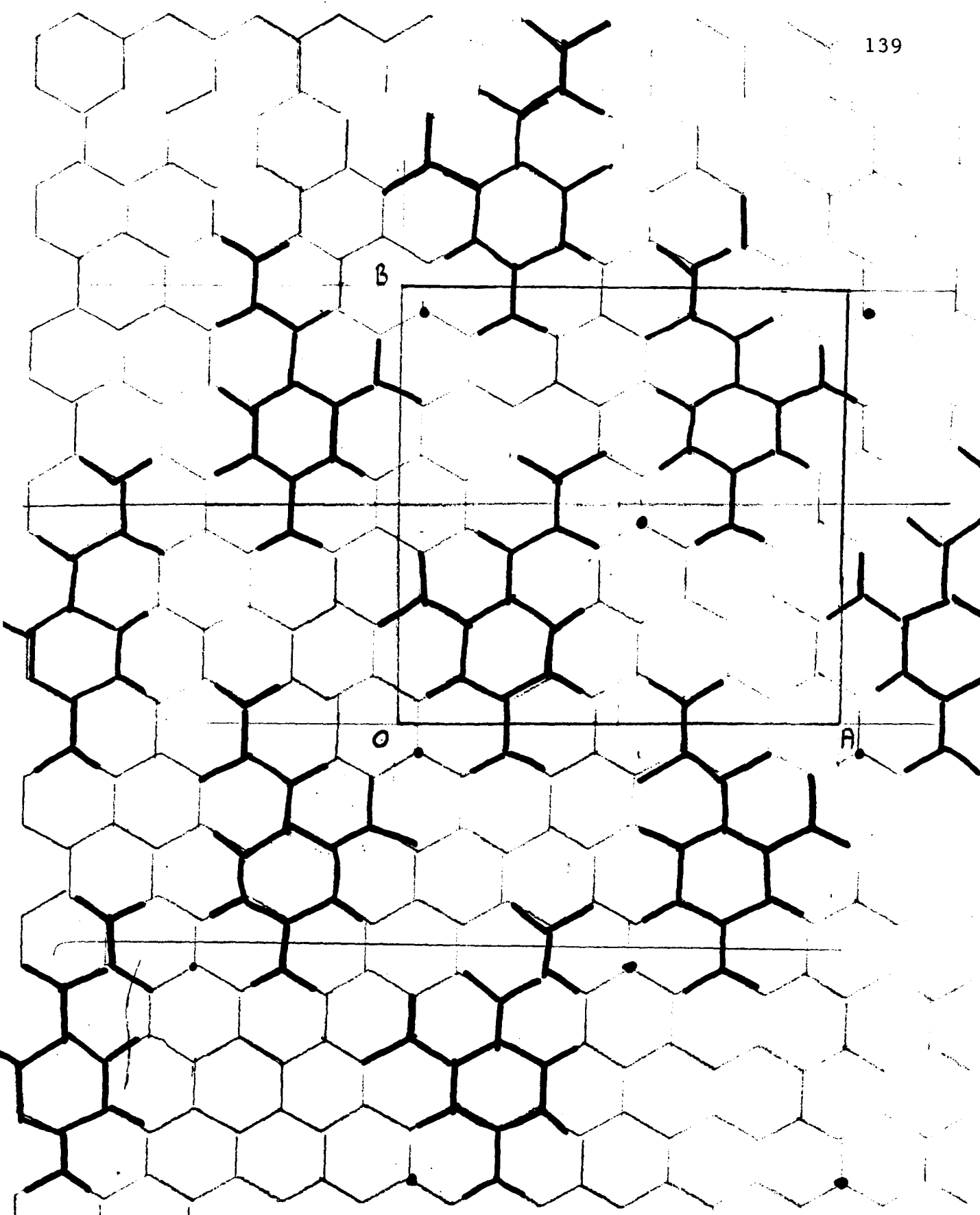

Fig. 4.16 A view of the molecules in one plane, parallel to $\bar{2}02$, in MNA-2, the amber form of MNA.

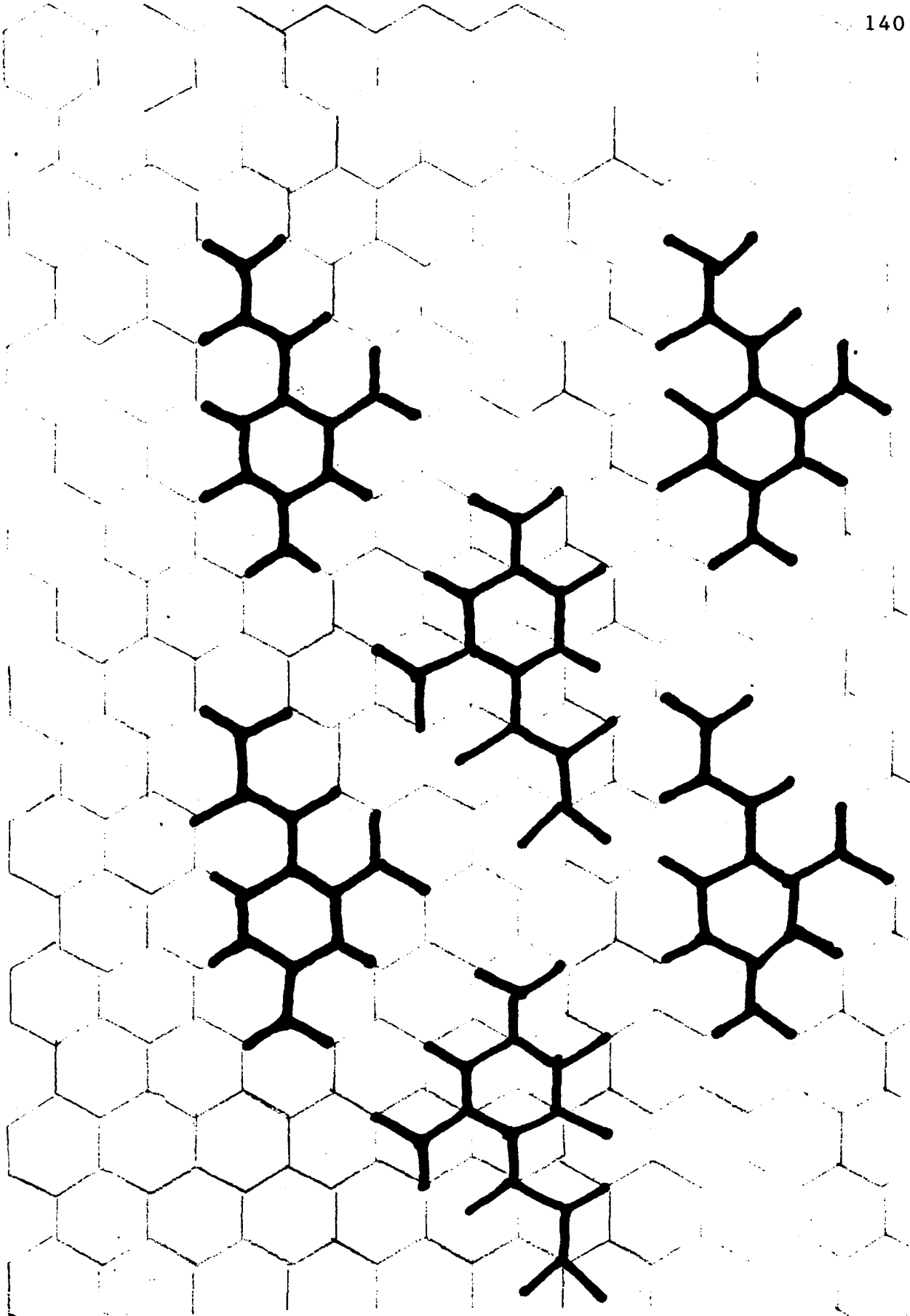

Fig. 4.17 Molecules in the inclined plane after half of them have been rotated.

plane as represented by this diagram. The latter types which are all marked MOL 2 presumably adjust their position to stabilise columns of molecules of type MOL 1 by intermolecular hydrogen bonds but the long axis of the molecule (C(7)....N(1)) remains in the inclined plane. Hence an approximate model of MNA-3 can be constructed by viewing superimposed parallel planes inclined at approximately 40° to the horizontal. A diagram showing the experimentally determined distances in the $3\bar{1}1$ plane is shown in fig.3.11a .

The angle of inclination of the plane of the benzene ring to the z-direction is about 32° and the interplanar spacing is 3.43 Å. The latter value is very nearly the same as that in MNA-2 but the angle of inclination is about 8 degrees smaller. Fractional coordinates measured from fig. 4.18 agree with those from the X-ray diffraction studies to within 0.04 for the x and y values and 0.1 for the z values. The ratio of the lengths OA:OB is 1.24 compared to 1.39 for the found ratio of the unit cell sides a:b.

The general shape of the projection of the unit cell sides a,b, and c onto the inclined plane is consistent with a triclinic unit cell.

In conclusion fig. 4.18 is an approximate representation of the molecules present in the $3\bar{1}1$ plane. One difference is

that all molecules labelled MOL 2 should be rotated around the C(7)...N(1) axis by about 30 degrees and the N(1)....C(7) axes tilted as shown in fig. 5.2.

Fig. 4.18

A structure for MNA-3 obtained from MNA-2 by rotating half the molecules round axes parallel to the z axis. Finally, tilting of the N(1)...C(7) axes as described in Fig. 4.30 occurs to form the found MNA-3 structure.

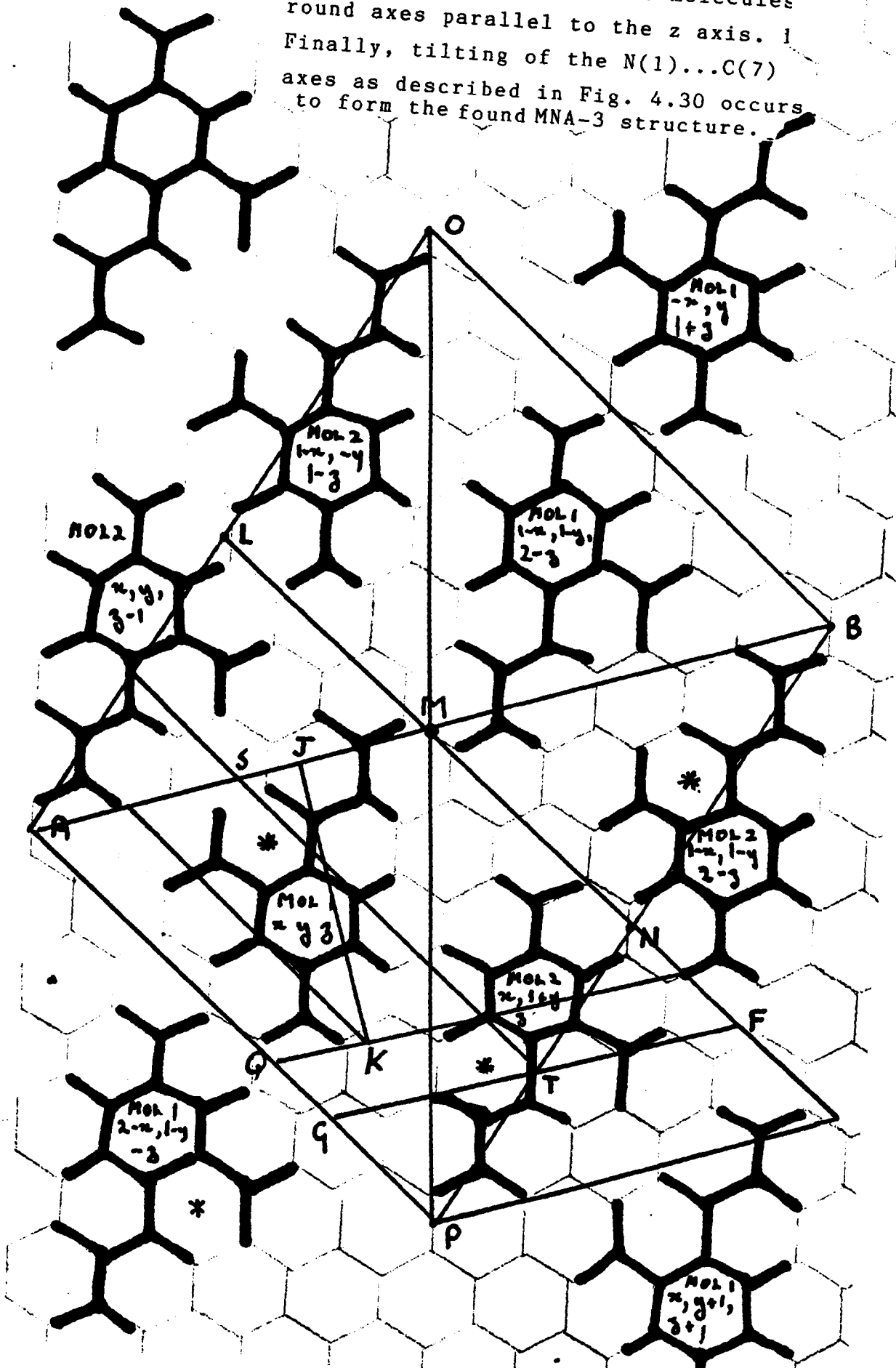

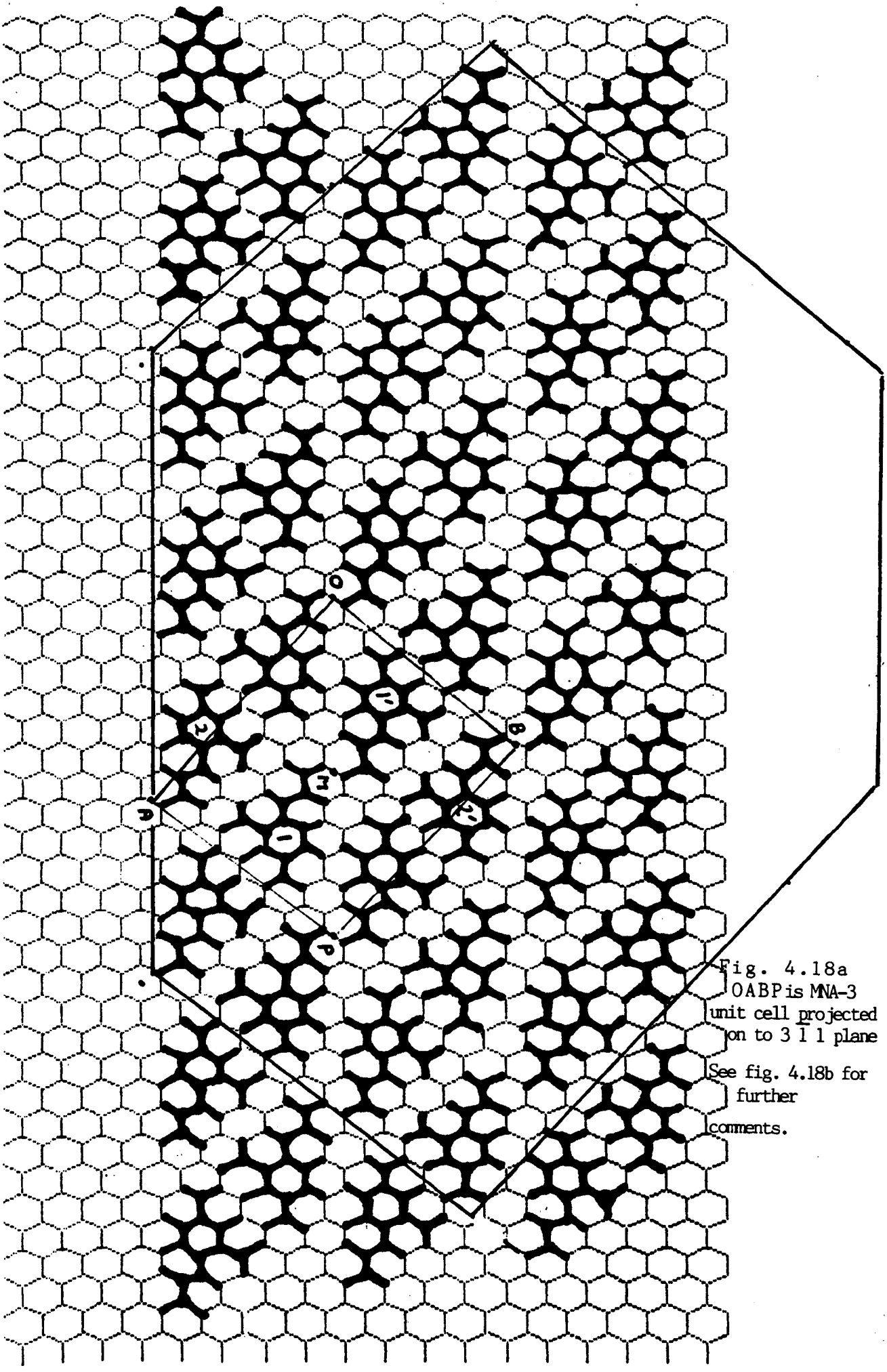

Fig. 4.18a
OABP is MNA-3
unit cell projected
on to 3 1 1 plane

See fig. 4.18b for
further
comments.

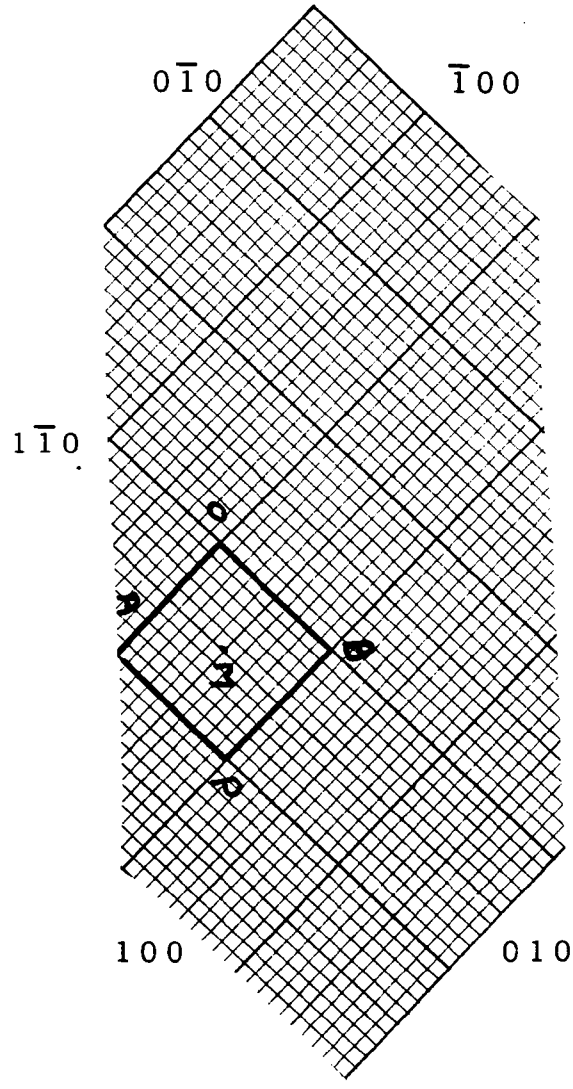

Fig. 4.18b

View of a section through a crystal of MNA-3 (yellow) showing the diamond shaped cross section. The Miller indices of the faces are given. OABP represents the unit cell if the cross section is perpendicular to the z axis which is approximately perpendicular to the plane of this page.

However, the molecules shown in fig. 4.18b should be viewed as lying in the inclined plane (3 $\bar{1}$ 1). In fact, molecules which are of the type molecule 2 and 2' are twisted about their N(1)....C(7) axis, out of this plane so that a molecule 2 in successive planes is linked to a molecule 1 by weak intermolecular hydrogen bonds.

Section 4.6

A mechanism for the transformation of MNA-3 (yellow) to MNA-1 (white) based on interplanar interactions.

This mechanism is based on the premise that the new centres of symmetry, which are necessary for the change to a new space group, are formed between molecules in adjacent inclined planes. For example, a molecule labelled MOL 1, x,y,z and one of the MOL 2 type at x,y,z in the adjacent upper plane could form the two centre molecules in the MNA-1 unit cell i.e. the two molecules at x,y,z, (A) and 1-x,1-y,1-z (B). Similarly molecules at the centre of a new unit cell of the white form would be formed between MOL 2 1-x,1-y,2-z and a molecule in the upper adjacent inclined plane labelled MOL 1 1-x,1-y,3-z.

The shapes outlined by AMNQ, BDMN would correspond to a view of the MNA-1 unit cell perpendicular to the ring plane of the two centre molecules A view of the cell contents of MNA-1 perpendicular to the ring plane of molecule x,y,z is shown in fig. 3.4 c. This view is very similar to that in fig. 4.18 with AMFG as an approximate outline of the MNA-1 unit cell. TS would correspond to the projection of the x-axis onto the inclined plane whilst TF and TG would correspond to the projections of the z and y axes respectively. Thus the directions of the z-axes in MNA-3

(AM) and MNA-1 (TF) are parallel.

The diagram also predicts a contraction of about 25% in the y-direction of MNA-3 (i.e. AP --> AG). MF represents the common edge from 0,0,1 to 1,0,1 between unit cells whilst ASM and GTF are common yz faces between unit cells.

A side view of the inclined plane is shown in fig.4.19. The calculated distances between the ring planes of A type molecules in the cells shown in fig. 4.19 is about -2.13 Å and +2.11 Å. This result would indicate that individual rings have increased their inclination to the z-axis by rotation around the C(7)...N(1) axis. The calculated angles between the individual z-axes and the ring planes are :-

MNA-2	32.03°
MNA-3	29.17°
MNA-1	52.65°

The above results are consistent with the benzene rings being maintained in the same planes in MNA-2 and MNA-3 but in MNA-1 the angle has increased by about 20° . This increase can be accounted for by rotation around the C(7)...N(1) axis as described above and such an increase would allow for a stronger interaction between molecules of types 1 and 2 which are situated in adjacent columns.

Formation of the intermolecular hydrogen bonds

Formation of the intermolecular hydrogen bonds occurs by rotation of the amide groups around the C(1)....N(1) axis by 135 degrees so that the C=O and N-H bonds are directed along the new z-axis which is parallel to the z-axis in MNA-3. The nitro groups of molecules of type MOL 1 remain directed towards AQ and on either side of the new hydrogen bonds that are formed so that a glide plane is formed parallel to the z direction and perpendicular to the y direction.

Similarly intermolecular hydrogen bonds involving molecules of type MOL 2 are formed by rotation of the amide groups around the C(1)...N(1) axis by about 135 degrees and the ring atoms and N(1), N(2), and C(7) remain in the inclined plane.

Thus, adjacent molecules in the columns stacked along z in MNA-3 become connected by hydrogen bonds and each column is linked to each adjacent column by an alternate ring-ring interaction. The arrangement of molecules in the inclined planes can be seen in fig. 4.19 which shows the contents of an assembly of unit cells viewed down the x-axis.

Fig. 4.19 An assembly of MNA-1 unit cells viewed down the x axis.

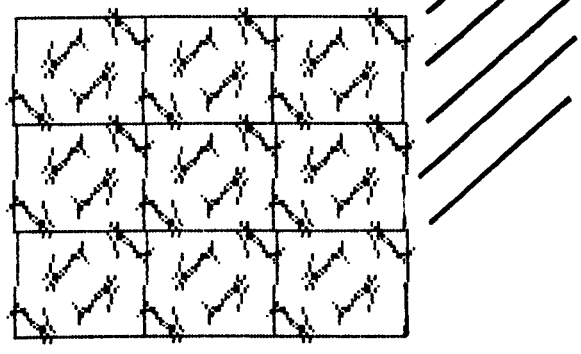

These lines represent edges of the inclined plane.

The molecules in MNA-1 might have their benzene rings still in the original inclined planes. This idea is superceded in section 4.3

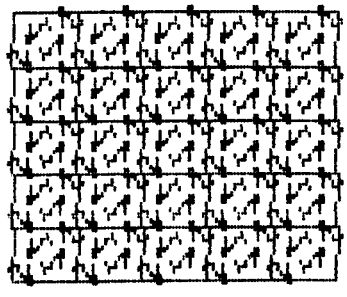

MNA-1 cells viewed down the x axis.
This view is of lower magnification than the above diagram.

Section 4.7

A mechanism for the formation of the white form (MNA-1) from the yellow form (MNA-3).

The second transformation mechanism (summarised below), has the merit of maintaining the direction of the N(1)...C(7) axis and the relative positions of half of the benzene rings.

The proposed changes will be discussed using the molecules described in fig.4.18 and involve the following :-

1. Lateral movement of columns of those molecules labelled * so that the N(1)...C(7) axes would be lined in parallel layers.

2. The a axes of MNA-1 would lie parallel to MF and the c axes parallel to the c axes of the parent MNA-3.

3. Intermolecular hydrogen bonds would be formed by rotating the amide groups through about 135°.
These bonds would be formed from the intracolumnar amide groups.

4. The benzene rings within in a column would interact with those of adjacent columns on an alternate basis.

5. If the rings and N(1)...C(7) axes remained approximately parallel to the original inclined plane then the hydrogen bonds would lie parallel to the c axis of MNA-3 if an amide group of

a. molecule 1 type was involved, or at about 45 degrees to the c axis if a molecule 2 type was involved.

6. In the latter case the sheets of new hydrogen bonds would lie parallel to the plane of the inclined plane of MNA-3.

A diagram showing the formation of sheets or layers of MNA-1 molecules is shown in fig.4.19 and it is important to note that the flat layers of MNA-1 would be formed approximately at right angles to the diagonal (OP) of the MNA-3 unit cells.

This mechanism, which attempts to minimise the movement of the benzene rings during the transformation of MNA-3 to MNA-1 has lead to a result which is not in in accordance with experimental observation which requires the layers of MNA-1 i.e. the sheets of molecules parallel to x, to be parallel to the diagonals (OP) of the MNA-3 unit cells.

However, this discœpancy is absent from the third mechanism which is discussed in section 4.8.

Section 4.8

A mechanism for the solid state conversion of the yellow (MNA-3) into the white (MNA-1) form

A mechansim for the conformational change of MNA.

The crystal structures of the amber and yellow forms of MNA consist of planar arrangements of flat and slightly kinked molecules of MNA respectively whereas the molecular conformation found in MNA-1 is a pronounced folded conformation. From a study of MINIT molecular models it appears that a series of movements of groups could account for the change in conformation. Fig. 4.20 shows the conformation of MNA in the planar form in which intramolecular hydrogen bonding is possible. The arrangement of groups around N(1) consists of a hydrogen atom (H 10), a substituted benzene ring, and an acetyl group. In the molecular model the bond angle between any two of these groups and N(1) is 120 degrees.

Rotation around the N(1)...C(8) bond would give the second structure shown in fig. 4.20 . After this rotation about the nitrogen atom has occurred intramolecular hydrogen bonding is not possible. Other important aspects are that a cis (or E) amide conformation results and the N(1)...C(7) axis has shifted by about 120 degrees. The final change

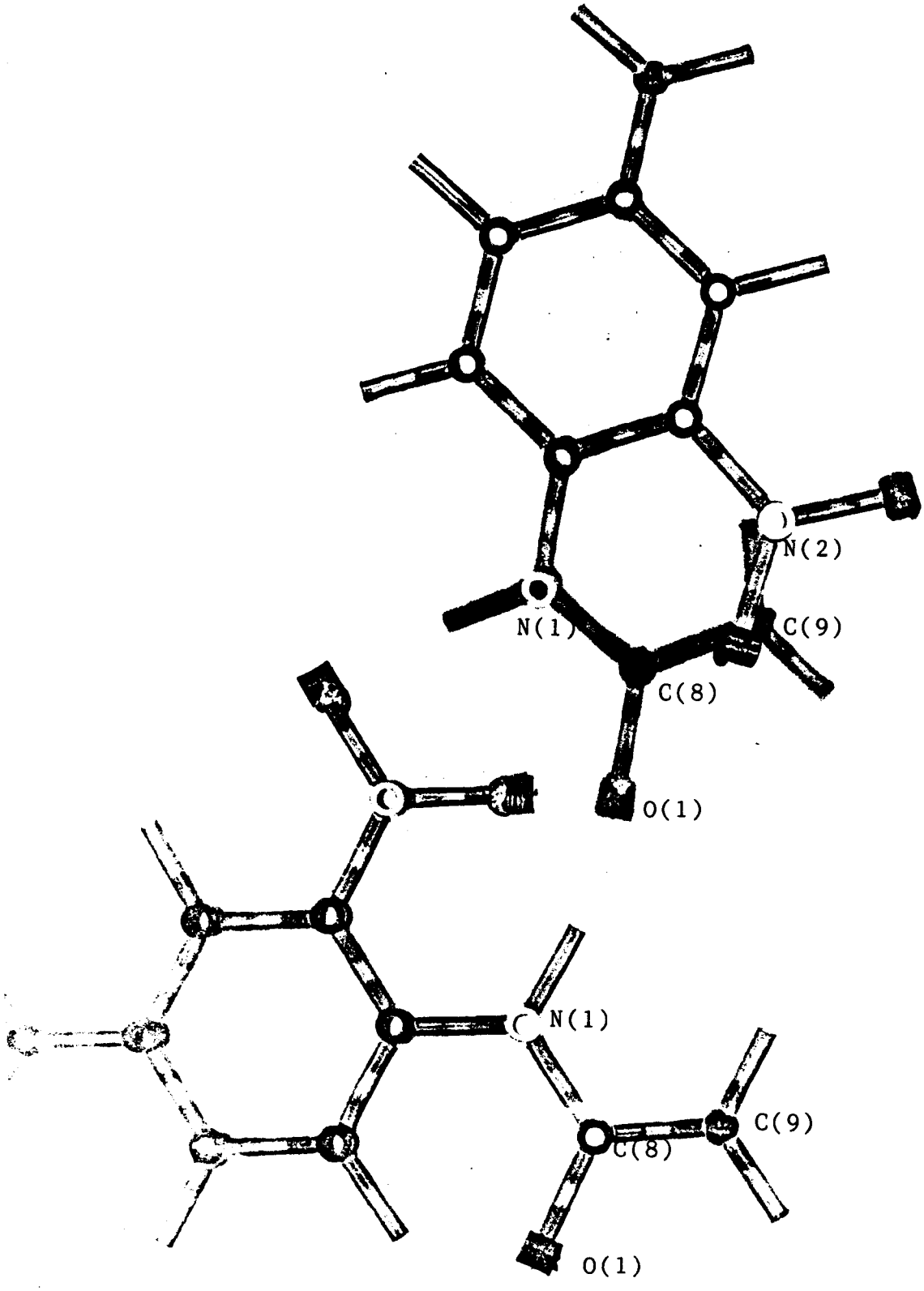

Fig. 4.20 The change from a planar to a folded conformation could occur by a rotation around N(1). The conformation in MNA-3 and MNA-2 is shown in the lower part and that for MNA-1 in the upper part..

consists of a conversion of the amide conformation from cis(E) to trans(Z) and this could occur so that the carbonyl group lies on either side of the nitro group. This would enable enantiomorphic folded conformations to be formed.

Consequences of the conformational change on crystal structure.

Consider a strip of the crystal structure of MNA-3 which lies parallel to the a+b vector (the unit cell diagonal). Such a group could consist of pairs of molecules linked by weak intermolecular hydrogen bonds between nitro and amide groups in molecules 1 (x,y,z) and 2 (x,y,z) and also 1 (2-x,1-y,z) and 2 (2-x,1-y,z) which are shown in fig. 4.21 . Rotation around each N(1) occurring by the sequence of events described in the previous section would produce pairs of folded molecules which are equivalent to molecules A (x,y,z) and B (1-x,1-y,1-z) which occur at the centre of the unit cell of MNA-1. If enantiomorphic pairs were formed from the next layer i.e. of the equivalent symmetry but with z+1 then a layer of C(x,.5-y,.5+z) and D (1-x,.5+y,.5-z) types of molecules would be formed. Hence layers of molecules in MNA-3 which lie perpendicular to the z axis form layers of folded molecules in MNA-1 and the layers are still

perpendicular to the z axis since parent (MNA-3) and daughter (MNA-1) z axes are parallel.

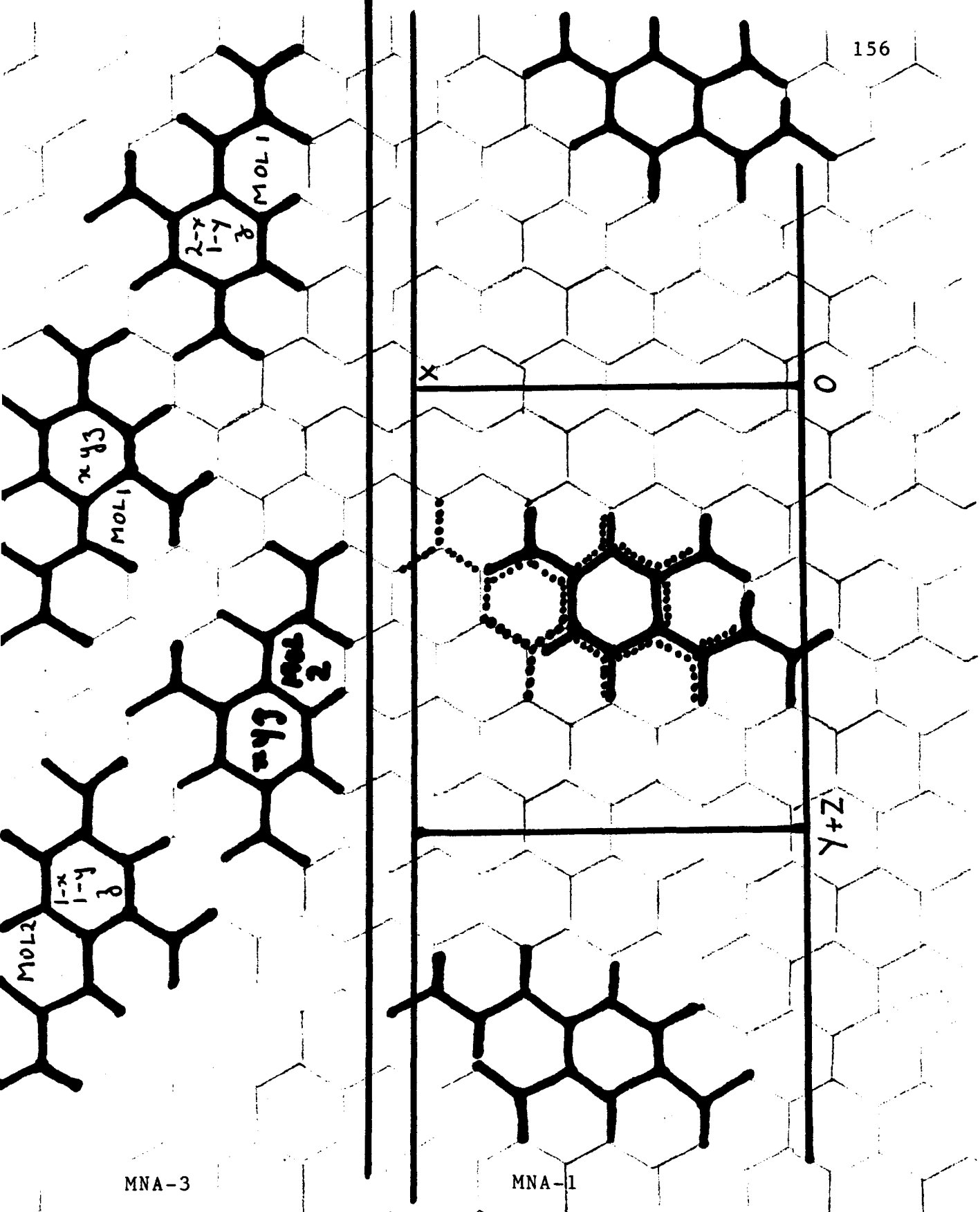

Fig. 4.21

Molecules in MNA-3 with their long axes parallel to the unit cell diagonals.

The folded conformation is achieved by a rotation of the ring about N(1).

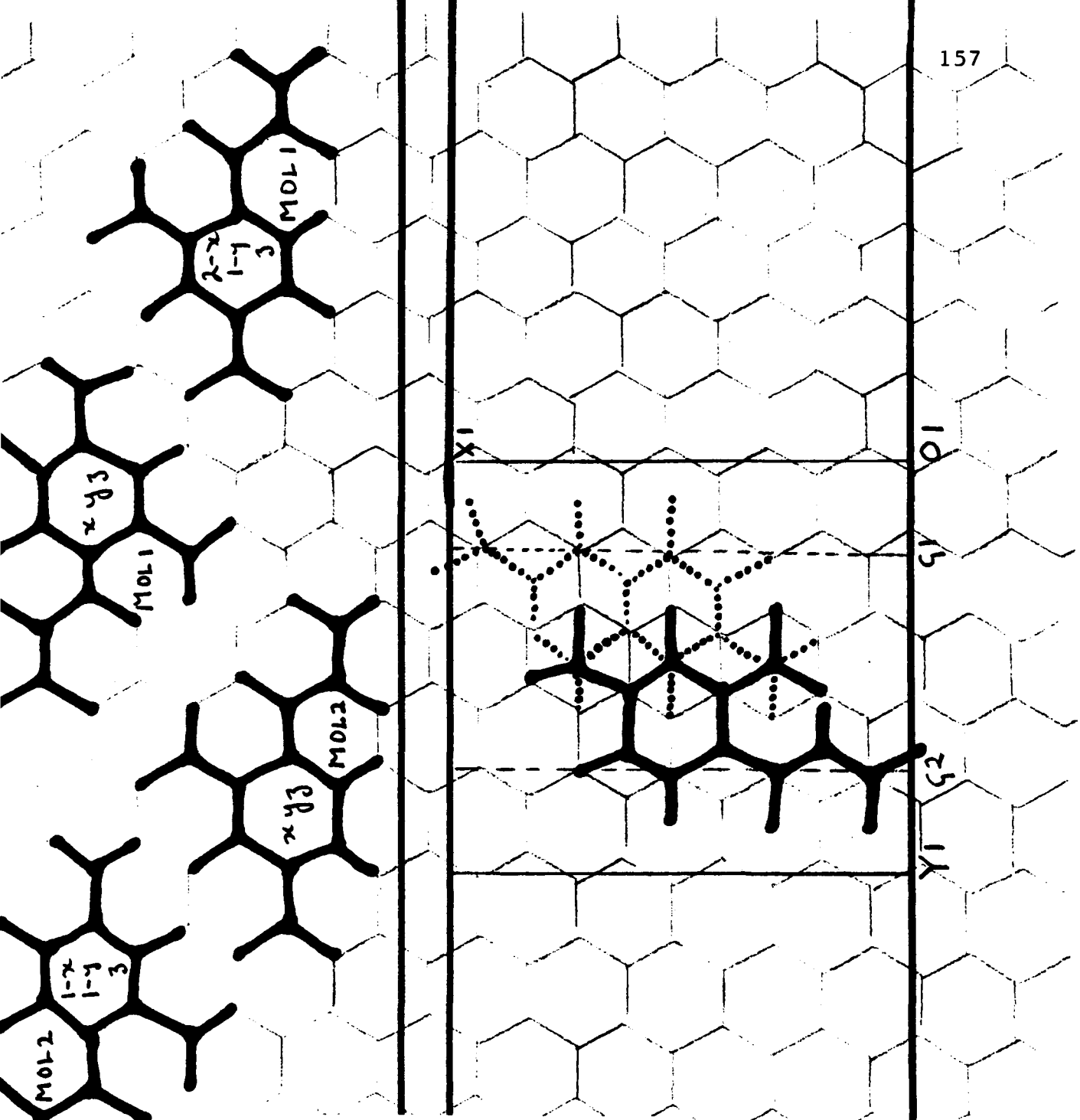

Fig. 4.22

MNA-3 to MNA-1 conversion viewed as involving rotations around N(1) followed by displacements along the direction of the y axis of MNA-1.

The phase change of MNA-2 (amber) to MNA-3 (yellow)

The structure of MNA-2 has been discussed previously in chapter (3). However, some of the main points, which are considered relevant to this phase change, will be restated at this point.

The structure may be regarded as columnar and molecules which are related by the glide plane, which is perpendicular to b, are stacked in columns along c. The crystals of MNA-2 are filamentary but generally are much shorter in length than those of MNA-3. The long axis of the crystals is parallel to the z direction. An unusual feature of the crystal structure is that all molecules lie in parallel planes which are parallel to the plane $\bar{2}02$. This aspect of the crystal structure and the nearly planar shape of the molecules is shown in fig. 3.8 and fig. 3.9 which are views of the crystal structure along the y axis.

A view of the arrangement of molecules in the lower half of several unit cells is shown in fig. 4.23 where molecules at x,y,z and 1-x,1-y,1-z are shown. This arrangement is perpendicular to the long axis of the crystal. The arrangement of molecules which lie in the parallel planes are shown in fig. 4.24and fig. 4.25 .

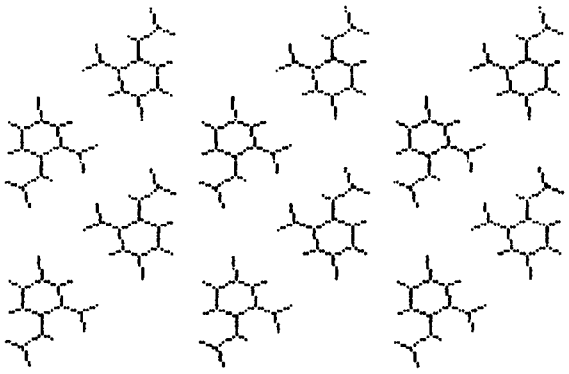

Fig 4.23 A view of MNA-2 down z

MNA-2 IN PLANE ARRANGEMENT OF X,Y,Z AND -X,0.5+Y,0.5-Z

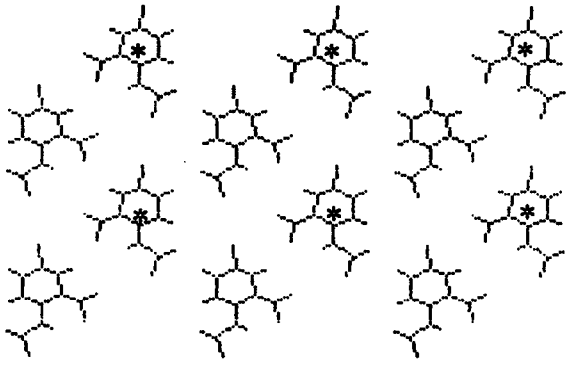

Fig. 4.24 A view of molecules x,y,z and -x,0.5+y,0.5-z which are coplanar.

MNA-2 IN PLANE ARRANGEMENT OF X,0.5-Y,0.5+Z AND 1-X,1-Y,1-Z

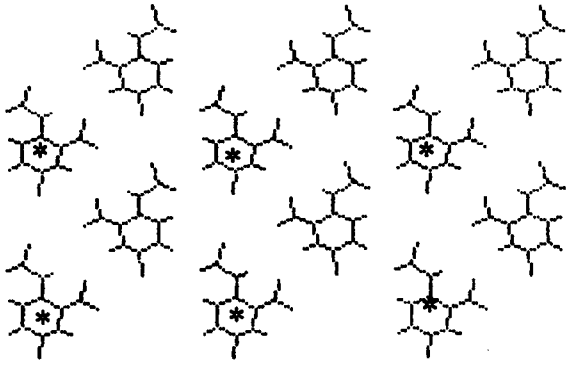

Fig. 4.25 A view of molecules x,0.5-y,0.5+z and 1-x,1-y,1-z which are coplanar.

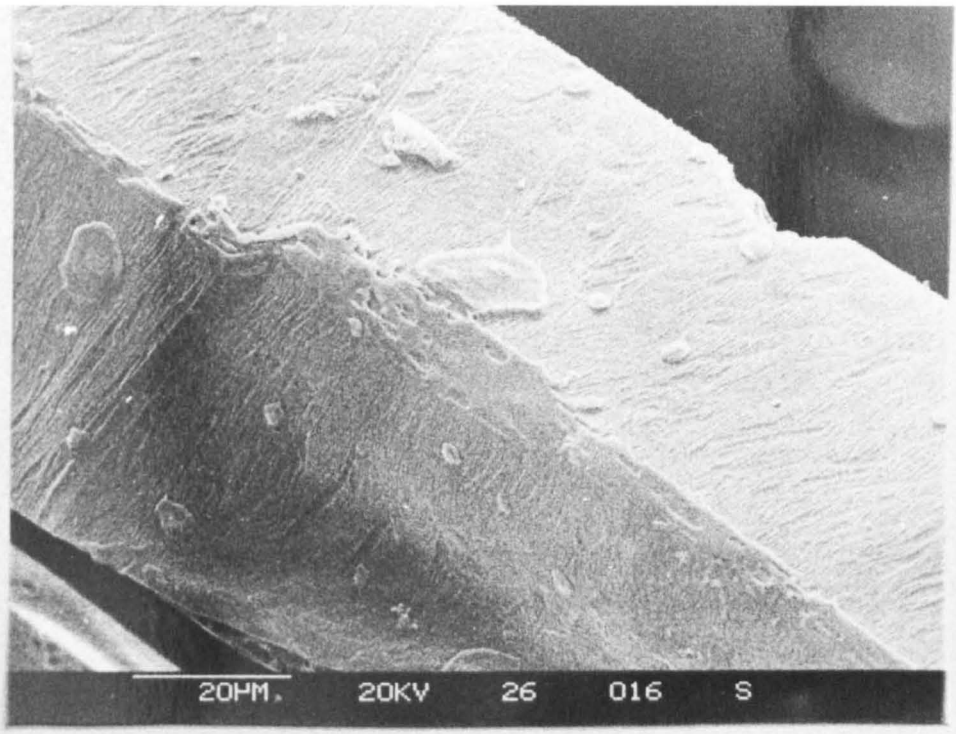

1. A crystal of the amber form (MNA-2). Such crystals have a diamond shaped cross section.
2. A 'ripple' effect caused by the protruding edges of molecules in the parallel $\bar{2}$ 0 2 planes.

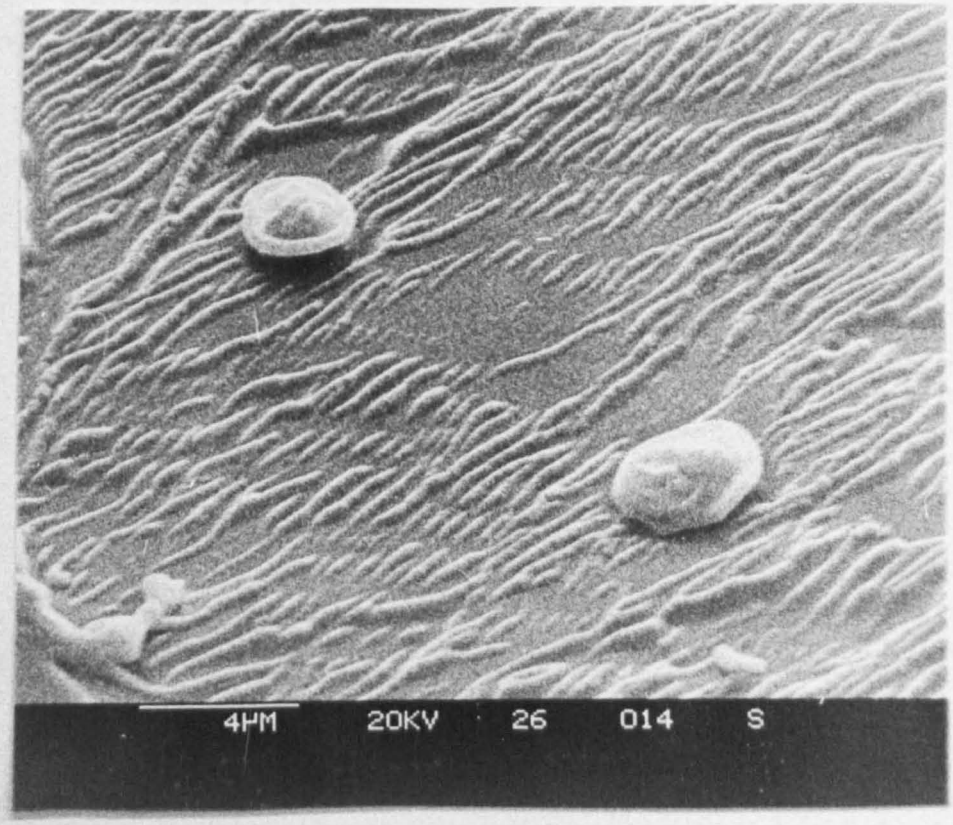

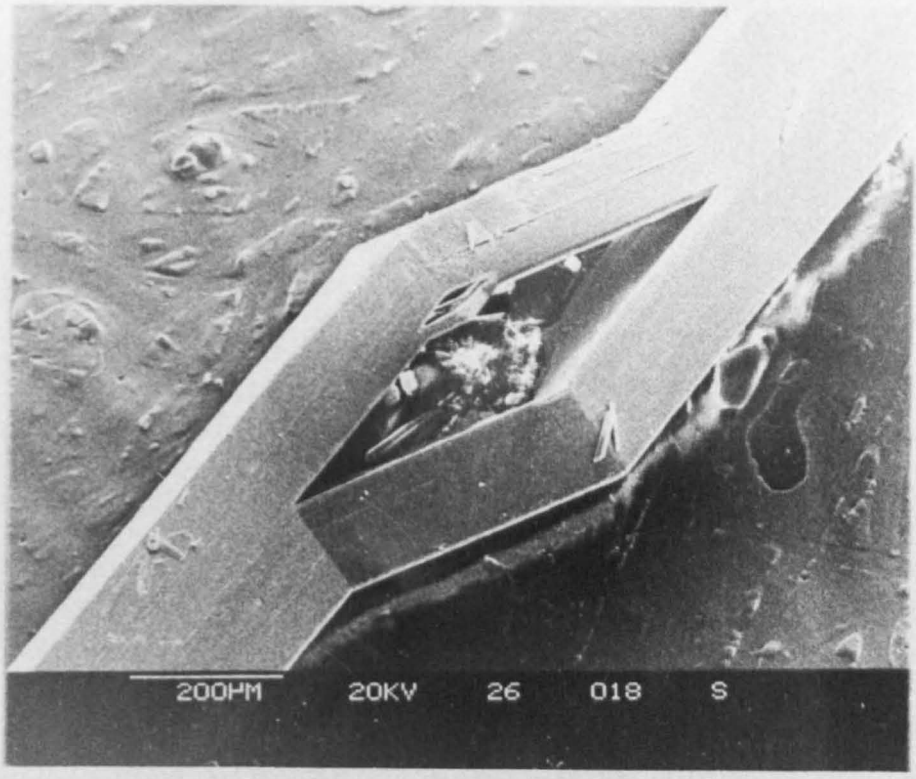

1. A splintered crystal of MNA-3 (yellow).
2. Crystallites of MNA-3 made by heating the amber form at 80°C for several hours. Note the two sets of interlocking crystals.

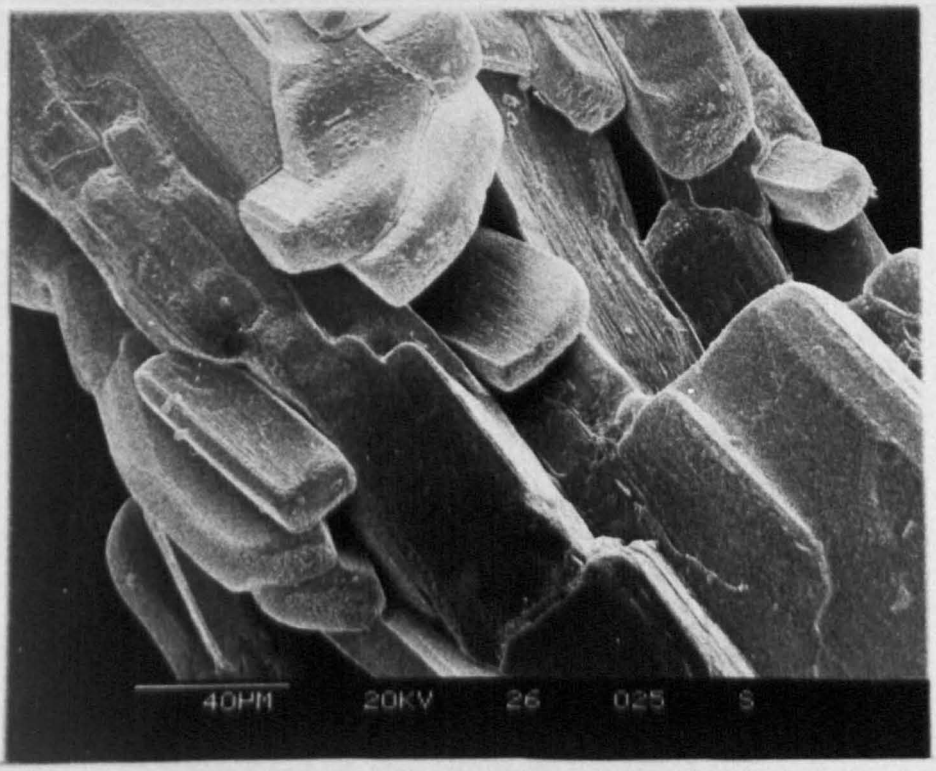

The phase change of MNA-2 (amber) to MNA-3 (yellow) occurs rapidly when the amber crystals are heated to about 85°C. When this process is observed under the microscope on a Kofler hot-stage the clear amber crystals become opaque and yellow. The infrared spectrum and X-ray powder diffraction pattern of the heat treated crystals are identical to that of the MNA-3 polymorph. The dsc curve shown in fig. 9.2 indicates that an exothermic phase change occurs below the melting point when the amber crystals are heated.

It has been observed that amber crystals change, on standing at ambient temperature, to the yellow form which on further standing changes into the white form. For the change amber to yellow, periods of a few days to six months have been recorded as time intervals for the change to occur. The single crystal of MNA-2 which was used in the collection of X-ray diffraction data proved to be stable at ambient temperature for several months after that experiment and hence the maintenance of the crystal at about 2°C during data collection was not essential although at the time it was considered a reasonable precaution against an unwanted phase transition which had occurred in some earlier samples. A plausible explanation for this observed behaviour is that initial samples may have been contaminated with the yellow form. This contamination can occur easily since the amber form was made by allowing hot concentrated solutions of MNA

in petrol (boiling range 60-80° C or 80-100° C) to cool slowly. Initially, the amber form crystallises from the warm (ca 50° C) solution but crystals of the yellow form may suddenly appear and continue to grow rapidly and thus contaminate the amber form. Subsequent batches of crystals were obtained from concentrated solutions of petrol of higher boiling ranges (e.g. 80-100° C and 100-120° C) with carbon tetrachloride. The composition of the solvent mixture was such that a clear solution was obtained below the boiling point of the solvent and amber crystals appeared when the temperature of the solution was about 60° C. If long yellow crystals appeared then the solvent was reheated to dissolve the crystals and more MNA was added. Thus, later batches of MNA-2 were relatively stable at ambient temperature but heat treatment and grinding still rapidly converted the amber form into the yellow form. A mechanism which will account for the observed changes will be discussed.

Two aspects of crystal structure which the amber and yellow form possess are that both structures are columnar and the nitro groups of molecules within any given column are stacked along z (which is parallel to the general direction of the column) so that the coordinates of the atoms in the nitro groups (viz. N(2),O(2),O(3)) of the intracolumnar neighbours have exactly (MNA-3) or nearly the

same (MNA-2) x,y coordinates. The necessary molecular displacements required can be followed by referring to fig.4.24 and fig. 4.25 which show the arrangement of molecules within the parallel planes. If half the molecules (denoted by *) in each plane are rotated around an axis comprising of the N(2)-C(2) bond, then the molecules are in the correct relative positions for the MNA-3 structure. Inspection of a model of the MNA-2 structure shows that there is sufficient room for such a manoeuvre to occur. A diagram of the model considered is shown in fig.4.26 . The new arrangement of molecules within the planes is shown in fig. 4.8 which shows that the NH...O(2) groups in adjacent molecules are close to each other.

The final stage would be the stabilisation of adjacent columns by intermolecular hydrogen bonds so that one column may adopt the MNA-3 (molecule 1 or 1') conformation and the other molecule the MNA-3 (molecule 2 or 2') conformation.

The relationship between the MNA-2 axes and those of MNA-3 are as follows :-

$$c(3) = c(1) * 0.5$$

$$a(3) = a(2) * 2.2$$

$$b(3) = b(2) * 2.2$$

The halving of the c unit cell dimension is a consequence

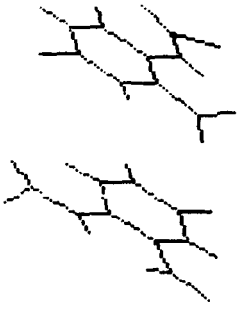

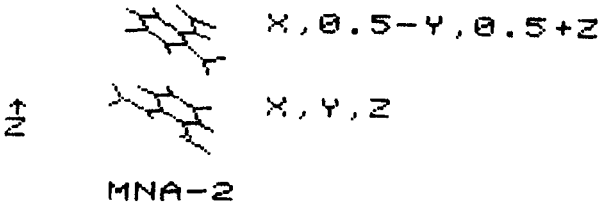

MNA-2

Fig 4.26 Two molecules of MNA in MNA-2 which are stacked along z.

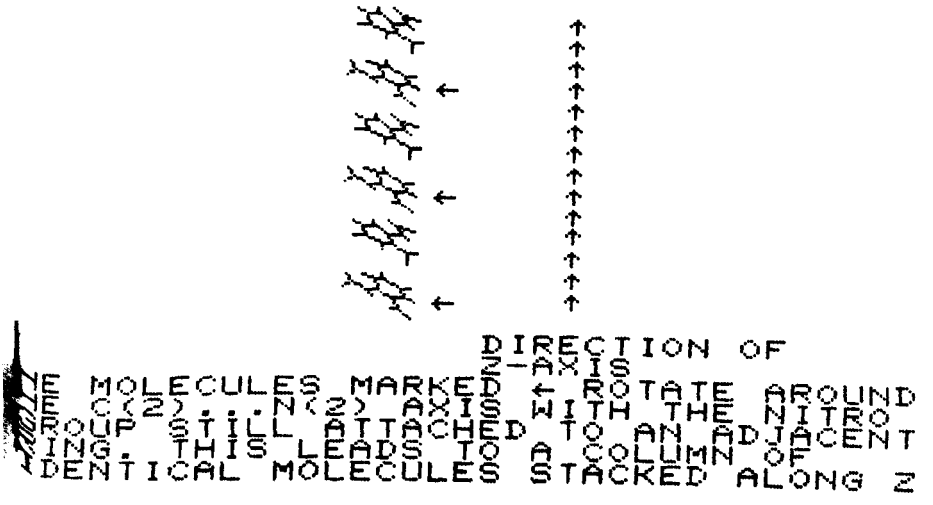

Fig. 4.27 Six molecules of MNA in a column parallel to z. The formation of MNA-3 may occur by a rotation of half the molecules about the C(2).. N(2) axis.

of the removal of the glide plane and the changes in the a and b values of the unit cells is depicted by the resetting of the axes in the xy-plane as shown in fig. 4.28 . Some calculated and observed unit cell dimensions for MNA-3 are as follows :-

observed (Å)	calculated (Å)	
17.956	15.445	a
12.908	15.445	b
4.039	4.021	c

These figures show that an expansion has occurred along the x-direction of MNA-3 whereas a contraction has occurred along the y-direction. The observed and calculated areas for the section through the unit cell in the xy plane are 231.78 $Å^2$ and 238.56 $Å^2$ respectively. Overall, a slight contraction occurs in the xy plane which would account for the small difference in volume of the unit cells of the MNA-2 (947.4 $Å^3$) and MNA-3 (929.1 $Å^3$) This would imply that in MNA-2, the molecules such as those at x,y,z and 1-x,1-y,1-z where the C=O groups are close together, are moving further apart whilst those at x,y,z and -x,0.5+y,0.5-z move closer together. The latter pair would form molecules of the type 1 and 2 in MNA-3 and a further movement towards each other would enable the MNA-1 structure to be formed. Thus the MNA-3 structure can be regarded as a metastable structure

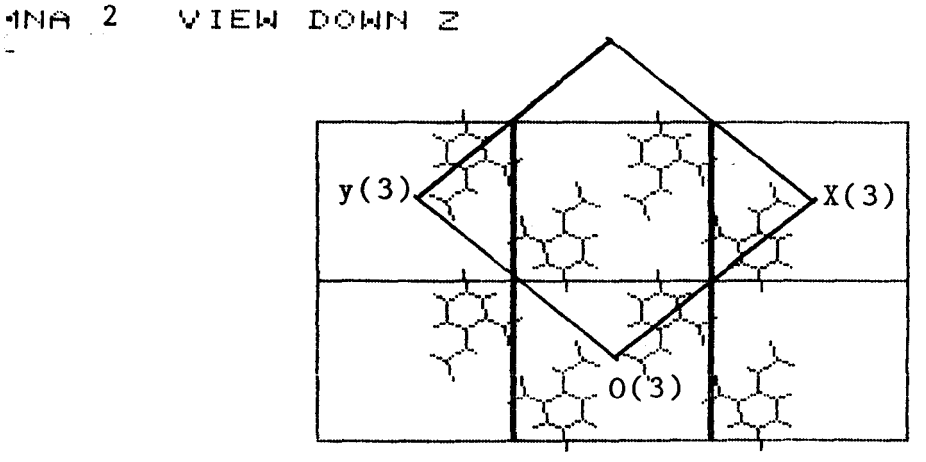

Fig. 4.28 Molecules of MNA in unit cells of MNA-2 are shown by vertical and horizontal axes. The diamond shaped figure is the outline of the unit cell of MNA-3 viewed down z.
O(3)....X(3) represents the x axis of MNA-3.

between the structure (MNA-2) which is favoured at high temperature (ca. 60° C) and the MNA-1 structure, which is favoured at lower temperatures. One of the reasons why this change occurs is likely to be associated with a change in the stability of the amide-nitro system in relation to the benzene ring. At higher temperatures, where increased atomic vibrations can occur, the steric hindrance of the nitro and amide and between the carbonyl oxygen (O1) and a hydrogen atom on the benzene ring (H6), may be accommodated easily but at lower temperatures the concomitant contraction of bonds does not favour a coplanar arrangement of nitro, amide and ring systems. Also, in MNA-2, the angle strain associated with the C(1)N(1)C(8) angle (129.7°) may increase at lower temperatures.

Section 4.10

The following series of diagrams shown in figs. 4.29, 4.30, and 4.31 view the polymorphs MNA-1, MNA-2, and MNA-3 as structures which are constructed from MNA molecules in series of parallel planes.

MNA-2 (amber) is regarded as the 'parent' structure. In this structure all molecules lie in planes parallel to the $\bar{2}$ 0 2 planes. The explanation for the change in inclination of the parallel planes with the z axis is given in fig. 4.30.

The diagrams in fig. 4.29 show how each of the MNA polymorphs can be constructed from parallel planes and this arrangement can be seen in the arrangement MNA-1 unit cells which are orientated in such a way as to produce a lateral growth of MNA-1 from MNA-3.

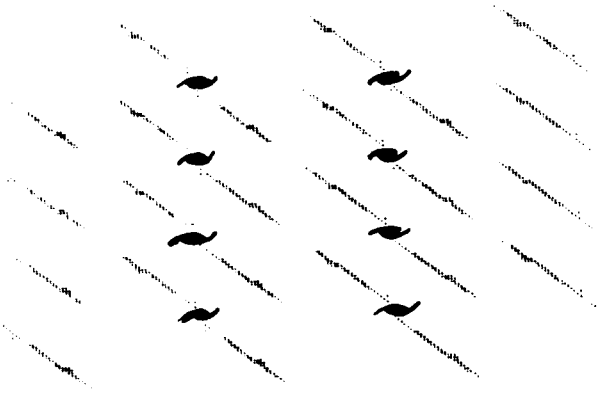

A view of several molecules in MNA-2 which shows molecules in planes parallel to $\bar{2}\ 0\ 2$ plane.

~ represents the position of the twofold screw axis at z=0.25 and z=0.75 along the y axis

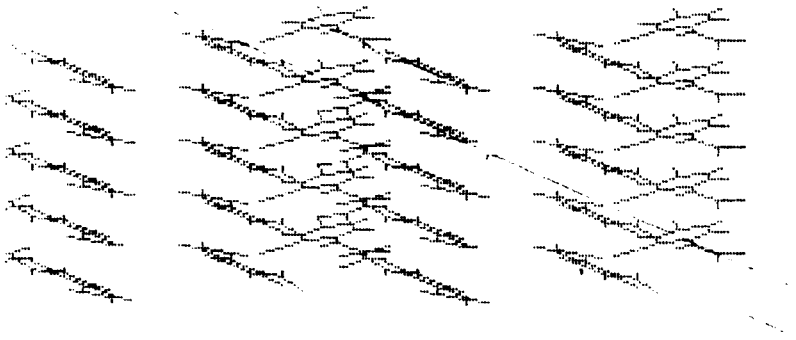

Molecules in $3\ \bar{1}\ 1$ planes emphasised.

A view along the unit cell diagonal towards the origin in several MNA-3 cells.

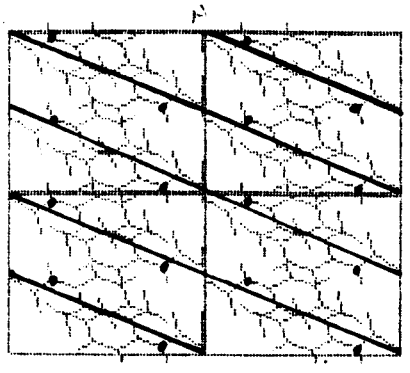

The inserted lines are the edges of $\bar{1}\ 0\ 2$ planes

$d\ \bar{1}\ 0\ 2 = 4.585$ Å

Fig.4.29 A comparison of the MNA-1, MNA-2, and MNA-3 crystal structures which show the arrangement of molecules in parallel planes.

Fig. 4.30

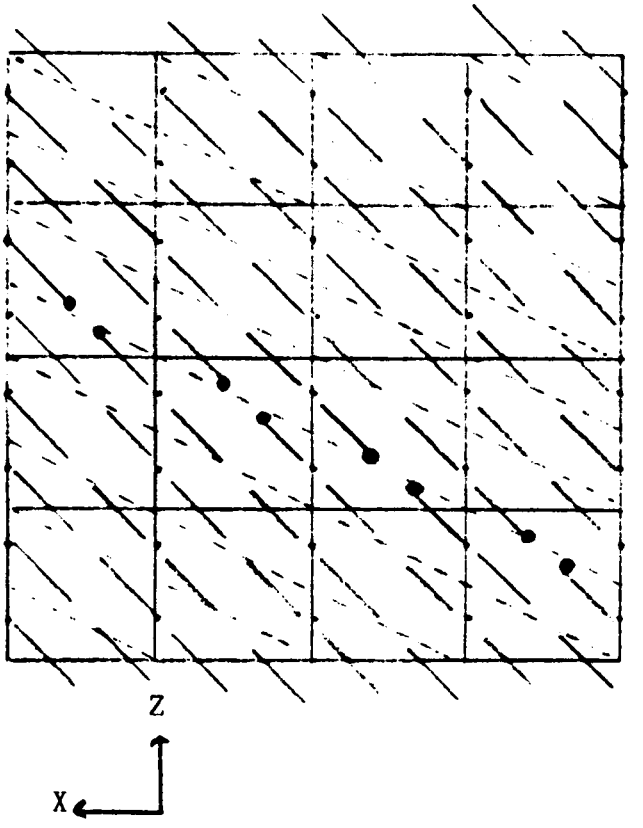

This figure is a diagramatic representation of a 4 x 4 array of MNA-2 unit cells showing the positions of the MNA molecules parallel to the $\bar{2}$ 0 2 planes. The very planar molecules are viewed edge-on. Molecules can become arranged in $\bar{1}$ 0 2 planes by rotation about the emphasised points shown in a representative layer. Thus the nitro groups and amide groups in molecules such as those at x,y,z and -x,1-y,1-z would become close enough to form the intermolecularly hydrogen bonded pairs found in MNA-3. The previous figure (Fig. 4.29) shows the experimentally determined positions of MNA molecules in the three polymorphs viewed so that the arrangement in parallel layers can be seen.

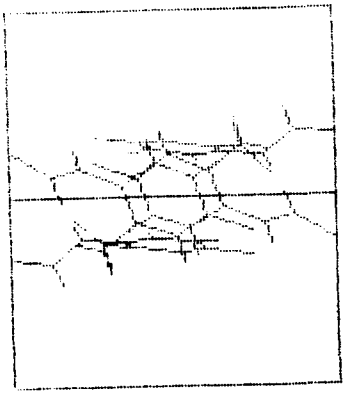

A view of the MNA-1 unit cell perpendicular to the X axis. The cell is orientated in such a way as to give hydrogen bonds at approximately 45° to vertical when viewed down the x axis (see Fig. 5.10 upper)

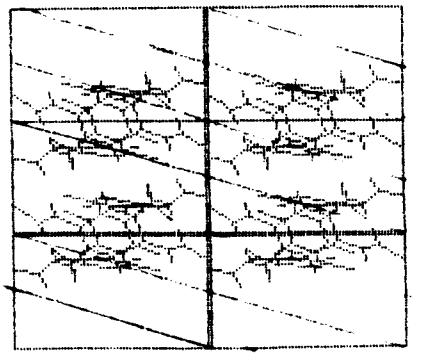

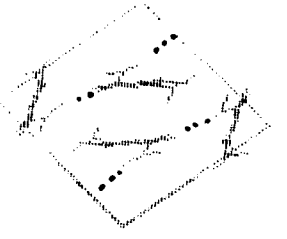

MNA-1 perpendicular to X axis MNA-1 down X

Note the molecules lying in parallel planes i.e. parallel to the $\bar{1}$ 2 2 planes. These parallel planes lie closer than the parallel planes($\bar{1}$ 0 2) shown in Fig. 4.29 where 'vertical' growth of MNA-1 is depicted. d $\bar{1}$ 2 2 = 3.376 Å

d $\bar{1}$ 0 2 = 4.585 Å

Fig. 4.31

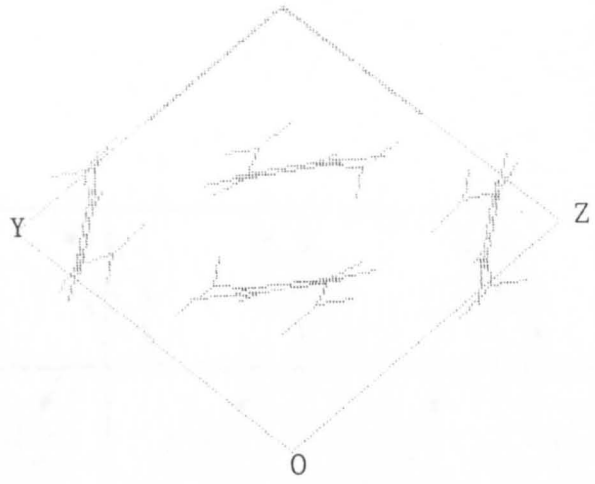

A view of the MNA-1 cell along X. Dotted lines indicate hydrogen bonds.

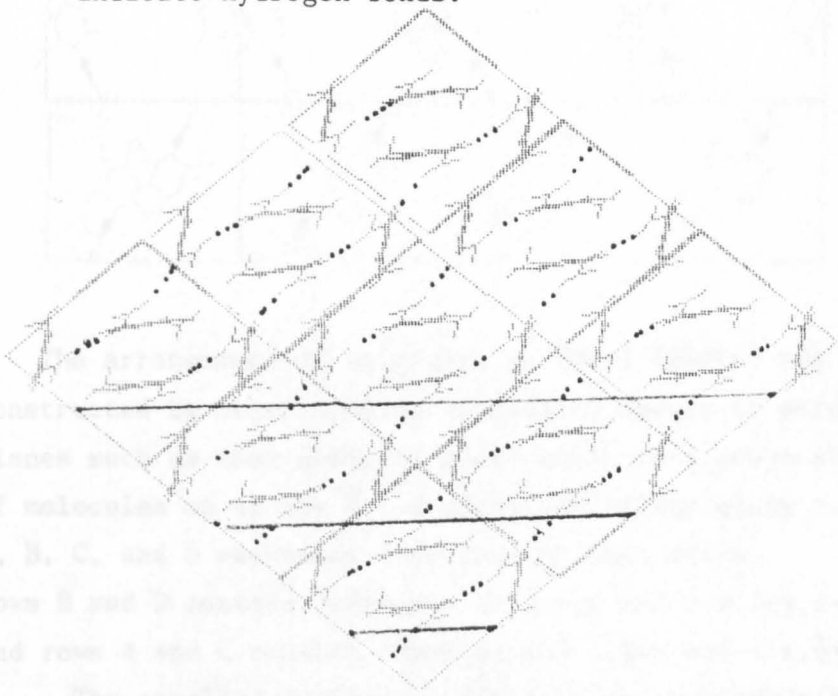

The arrangement of molecules in MNA-1 showing lateral growth of MNA-1 from MNA-3. Note the presence of layers parallel to $\bar{1}$ 2 2 planes. Compare this diagram with the lower diagram in Fig. 5.10

Fig. 4.32

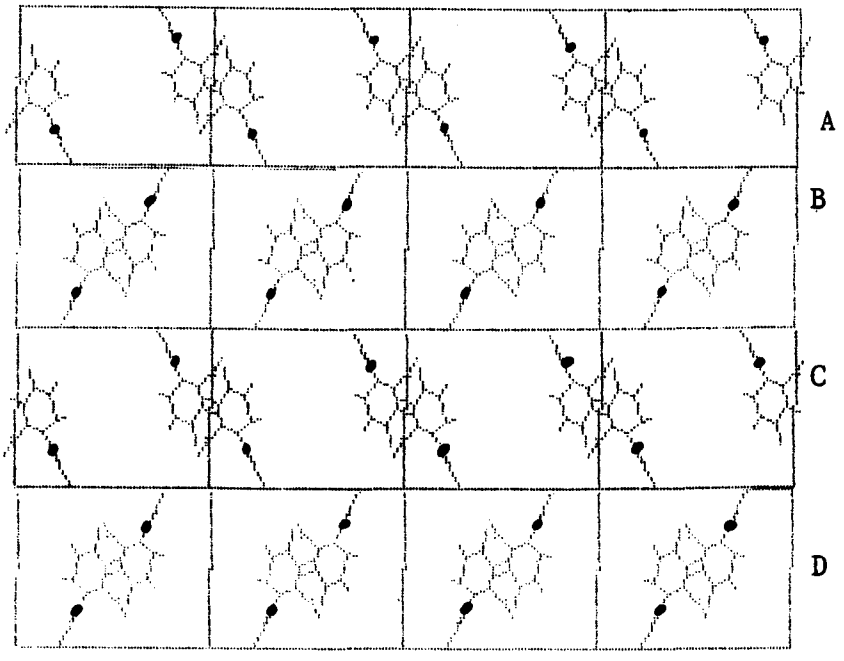

The arrangement of molecules in MNA-1 (white) can be constructed by superimposing successive layers or parallel planes such as that depicted above which is a projection of molecules on to the $\bar{1}$ 0 2 plane and viewed along z.
A, B, C, and D represent four rows of unit cells.
Rows B and D contain molecules at x,y,z and 1-x,1-y,1-z and rows A and C contain those at x,$\frac{1}{2}$-y,$\frac{1}{2}$+z and 1-x,$\frac{1}{2}$+y,$\frac{1}{2}$-z.

The parallel layers are built up by superimposing a row of type C over one of type D and vice versa along the z direction. A side-on view of the structure is shown in Fig. 4.29 (lower diagram).
An important feature of this diagram is that the arrangement of N(1) atoms is very similar to that in the inclined plane (3 $\bar{1}$ 1) in MNA-3 (yellow). N(1) positions emphasised in above diagram.

Fig. 4.33

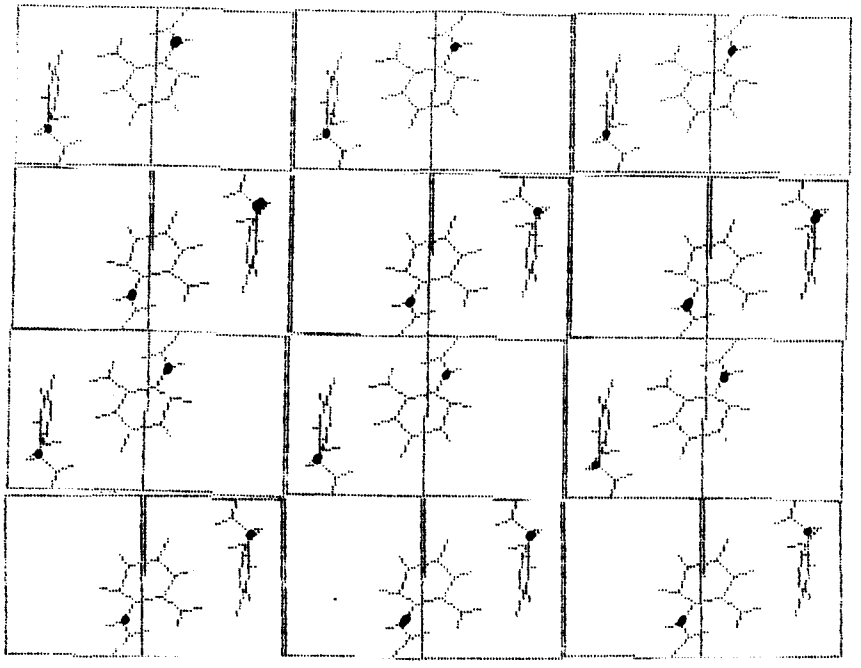

The arrangement of molecules in MNA-1 (white) can also be constructed from parallel layers in such a way that they become equivalent to $\bar{1}$ 2 2 planes. When layers of molecules such as the one shown above are superimposed so that row C and row D alternate along z, the resulting structure becomes equivalent to that of lateral growth of MNA-1 (white) from MNA-3(yellow). See Fig. 4.31 for a side-on view of the above diagram. For any selected row (say) D, the relative arrangement of N(1) in this diagram is very similar to that in Fig. 4.33 which depicts 'vertical' growth of MNA-1 which in turn is similar to the distribution of N(1) in the 3 $\bar{1}$ 1 plane.

Fig. 4.34

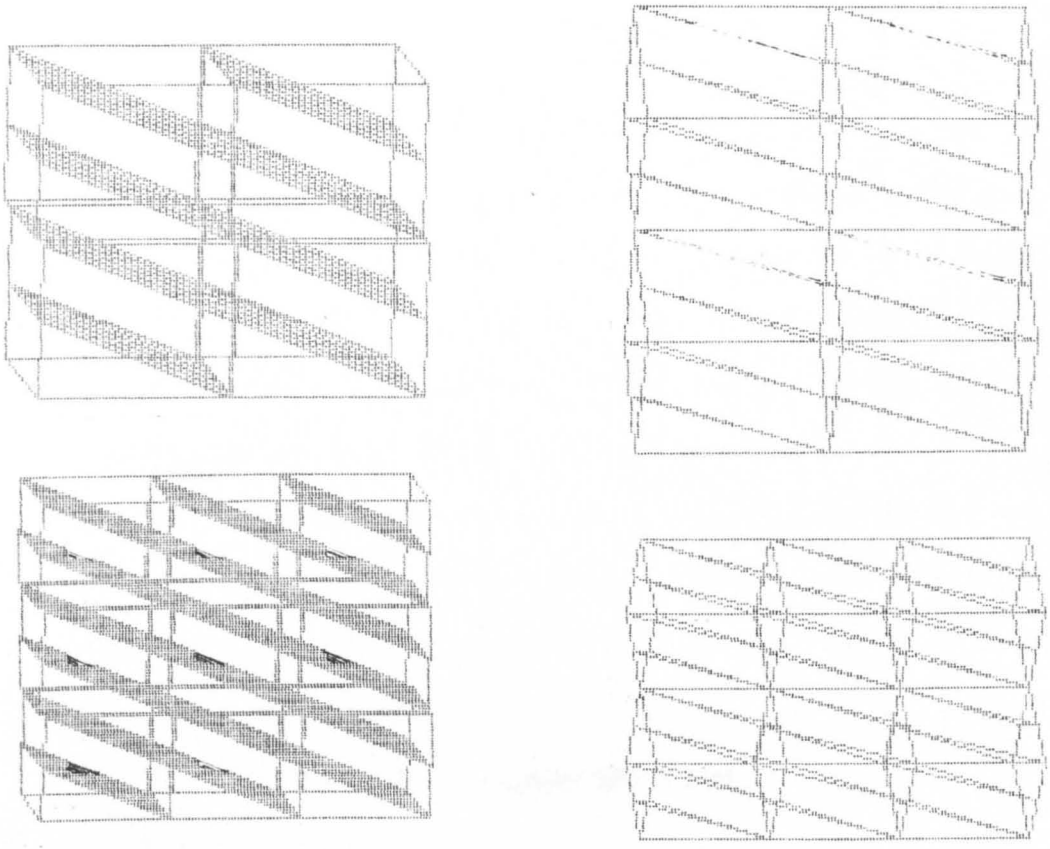

Diagrams showing sets of $\bar{1}$ 0 2 planes (left) and $\bar{1}$ 2 2 planes (right). The former correspond to the arrangment of planes in MNA-1 which originated from the 3 $\bar{1}$ 1 planes in MNA-3 , and give rise to 'vertical' growth of MNA-1. The diagrams on the right correspond to the arrangment of planes and unit cells which give rise to 'lateral' growth of MNA-1 from MNA-3

Fig. 4.35

CHAPTER FIVE

The relationship between the molecular coordinates and orientations in MNA-1, MNA-2, and MNA-3.

Introduction to Chapter 5.

The conversion of MNA-2 to MNA-3 in the solid state occurs readily on heating to about 60°C and more slowly at ambient temperature and the change could occur by a process in which half the molecules rotate about the C(2)...N(2) axis. The other half of the molecules could remain in their original relative positions. The molecules at x,y,z and 1-x,1-y,1-z would become equivalent to molecules 1 and 1' in MNA-3 and a new positioning of the crystallographic axes enables the coordinates of atoms in MNA-2 to be converted to those of molecule 1 and 1' in MNA-3.

The solid state conversion of MNA-3 to MNA-1, which occurs on heating the crystals to about 85°C or at ambient temperature, is accounted for by two approaches. Firstly pairs of molecules in MNA-3 such as 1 and 1' and 2 and 2' could rotate around their respective centres of symmetry in a clockwise manner. Thus molecules of the type 1 and 2 would become physically closer and if they were related by a new centre of inversion, these molecules would become equivalent to molecules A (x,y,z) and B(1-x,1-y,1-z) in MNA-1.

A second approach to the conversion of MNA-3 to MNA-1 involves formation of a folded conformation around N(1) as a pivot so that the relative position of N(1) in MNA-3 and MNA-1 remains the same.

The transformation of MNA-2 coordinates into MNA-3 coordinates by matrix multiplication.

Examination of the projection diagram shown in fig. 5.1 , which is a view down the z-axis of MNA-2, shows that the x and y coordinates of MNA-2 and MNA-3 should be related by a simple geometrical relationship. The relative positions of the x and y axes in relation to each other are shown in fig. 5.1. The figure shows a square within another square. The smaller square represents the MNA-2 unit cell and the larger square represents the MNA-3 unit cell whilst O(2) and O(3) represent the origins of the MNA-2 (amber) unit cell and the latter the origin of the MNA-3 (yellow) unit cell. The transformation requires a change in position of the origin and a change in scale. By means of either vector methods or by transformation geometry it is possible to calculate the x and y coordinates of MNA-3, shown as x(3) and y(3) from the MNA-2 coordinates x(2) and y(2) by the following equations:-

$$x(3) = -0.5x(2) - 0.5y(2) + 1$$

$$y(3) = 0.5x(2) - 0.5y(2) + 0.5$$

Some transformations of points are as follows:-

0,0 ----> 1,0.5

1,0 ----> 0.5,1

0,1 ----> 0.5,0

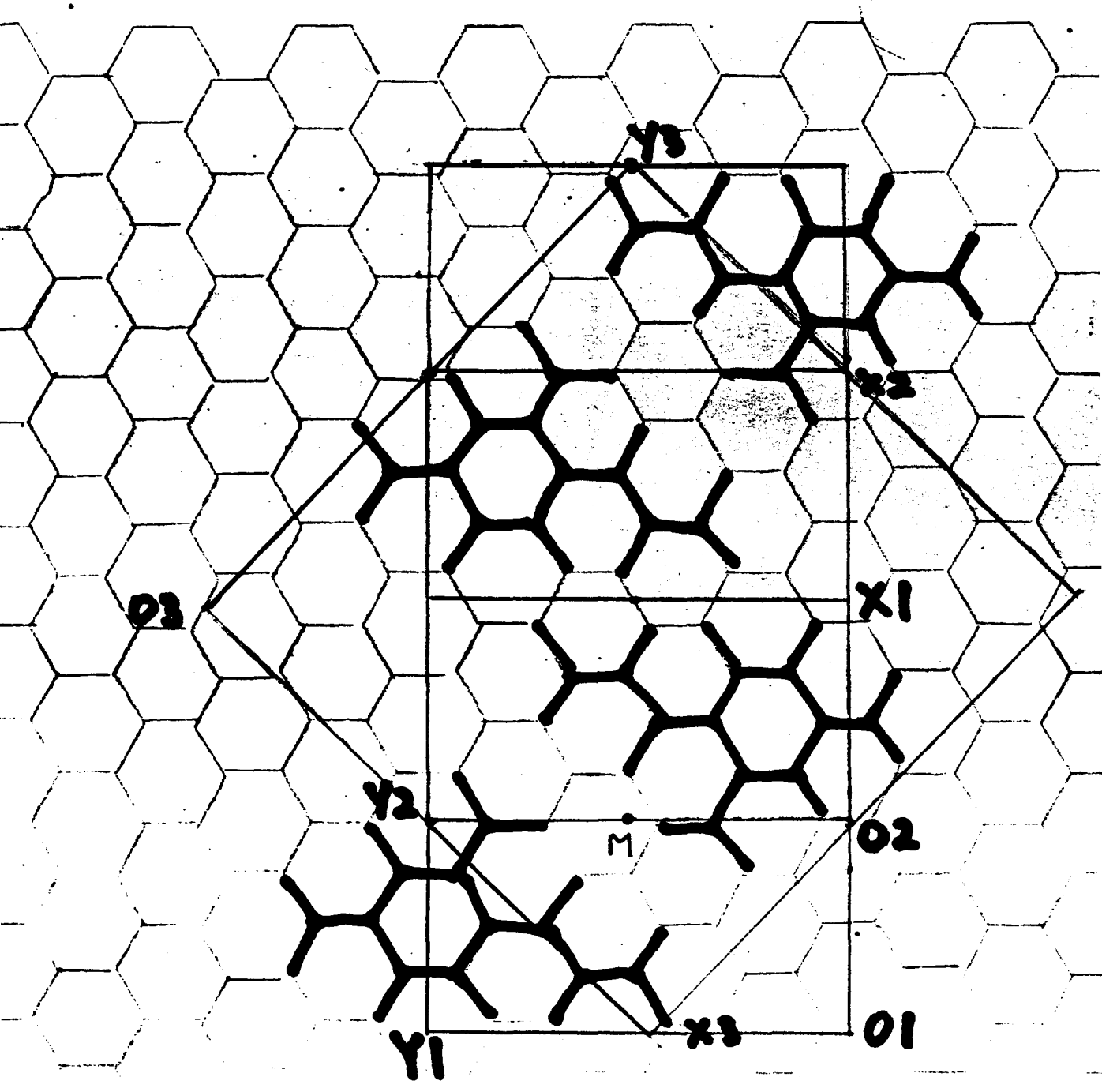

Fig. 5.1 O2....X2, and O2....Y2 are the x and y axes of an MNA-2 unit cell. Similarly, the x and y axes of the MNA-3 unit cell are O3...X3, and O3...Y3 and those of MNA-1 are O1...X1 and O1...Y1.

This diagram also defines the relative positions of the unit cells in the MNA system of polymorphs.

$$1,1 \longrightarrow 0,0.5$$

Since the repeat distance along the z-axis is halved the relationship between the c coordinates is as follows:-

$$z(3) = 2*z(2) - 0.5$$

The transformation matrix is:-

$$\begin{bmatrix} -0.5 & 0.5 & 0 \\ -0.5 & -0.5 & 0 \\ 0 & 0 & 2 \\ 1 & 0.5 & -0.5 \end{bmatrix} M1$$

The MNA-2 crystal coordinates are multiplied, as a row vector x y z 1, by the matrix using the matrix as a post multiplier.

Some MNA-3 coordinates which have been calculated using this matrix are presented in table 5.1 .

Table 5.1 Matrix generated x,y,z coordinates for MNA-3

C(1)	0.7216	0.4662	0.5294
C(2)	0.8031	0.4501	0.3554
C(3)	0.8610	0.5113	0.3592
C(4)	0.8411	0.5903	0.5340
C(5)	0.7598	0.6068	0.7086
C(6)	0.7018	0.5473	0.7092
C(7)	0.9044	0.6568	0.5478
N(1)	0.6612	0.4062	0.5260
N(2)	0.8321	0.3688	0.1562

A comparison of the calculated and experimental coordinates shows that there is fair agreement to two decimal places in the case of the x and y coordinates but this is not the case with all the z coordinates. For example, there is agreement in the case of the z coordinates of C(4) i.e. 0.5340 (calculated) and 0.5231 (found) but there is a large difference in the case of N(1), 0.5260 (calculated) and 0.8596 (found).

This discrepancy may be explained on the basis of a minor reorientation of molecules which are involved in the weak

intercolumnar hydrogen bond. This reorientation in which the C(7)....N(1) axis of the molecule pivots to a small extent about C(4) with respect to the z-axis, is shown in fig. 5.2 .

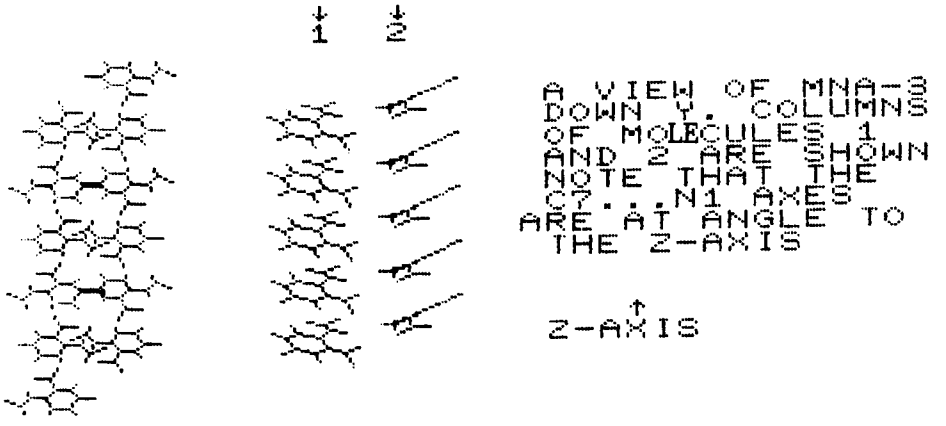

Fig. 5.2 This figure shows the orientation of the molecular axis N(1)....C(7) in MNA-2, where it is parallel to the y axis, and in MNA-3 where it is not parallel to the y axis.

A matrix transformation of the plane $\bar{2}02$ in MNA-2

The inverse of the matrix (M1) which was used to convert MNA-2 to MNA-3 coordinates is :-

$$\begin{bmatrix} -1 & 1 & 0 \\ 1 & -1 & 0 \\ 0 & 0 & 0.5 \end{bmatrix}$$

M2

The multiplication of -2 0 2, as a row vector by M2 gives the row vector 2 -2 1. Hence, the plane denoted by Miller indices $\bar{2}$ 0 2, in MNA-2 should transform to 2 $\bar{2}$ 1 in MNA-3.

This is confirmed by the equation of the plane of the calculated coordinates given in Table 5.1 . This equation is :-

$$1.8243X - 1.8414Y + 1.0282Z = 1$$

The ratio of these coefficients is approximately 2: -2 : 1. However, the experimental result for the indices of this plane is $3\bar{1}1$. The difference may be accounted for by the tilting of the C(7)...N(1) axis to accommodate the intercolumnar hydrogen bond.

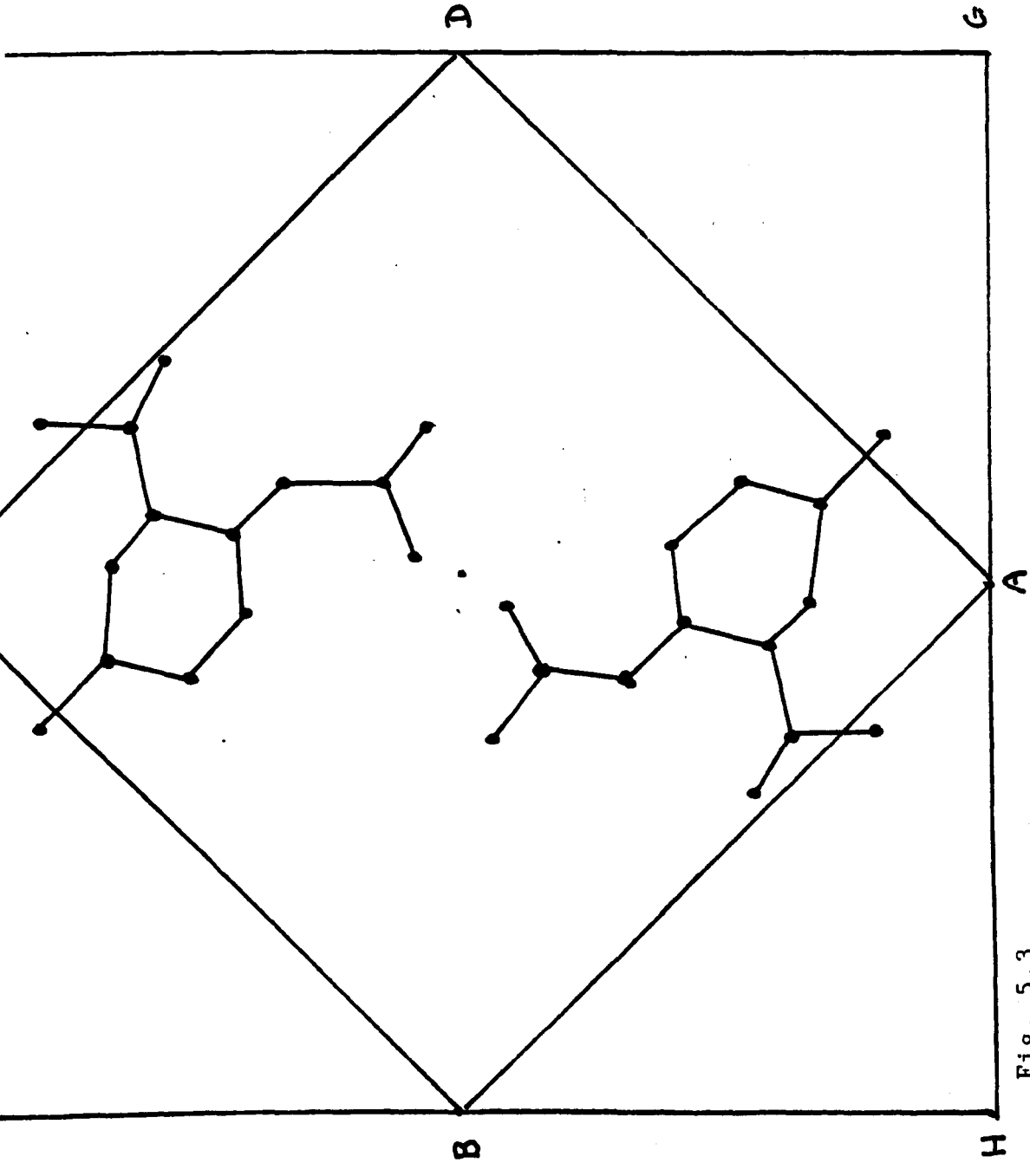

MNA-1 UNIT CELL ABCD

Fig. 5.3

Fig. 5.3

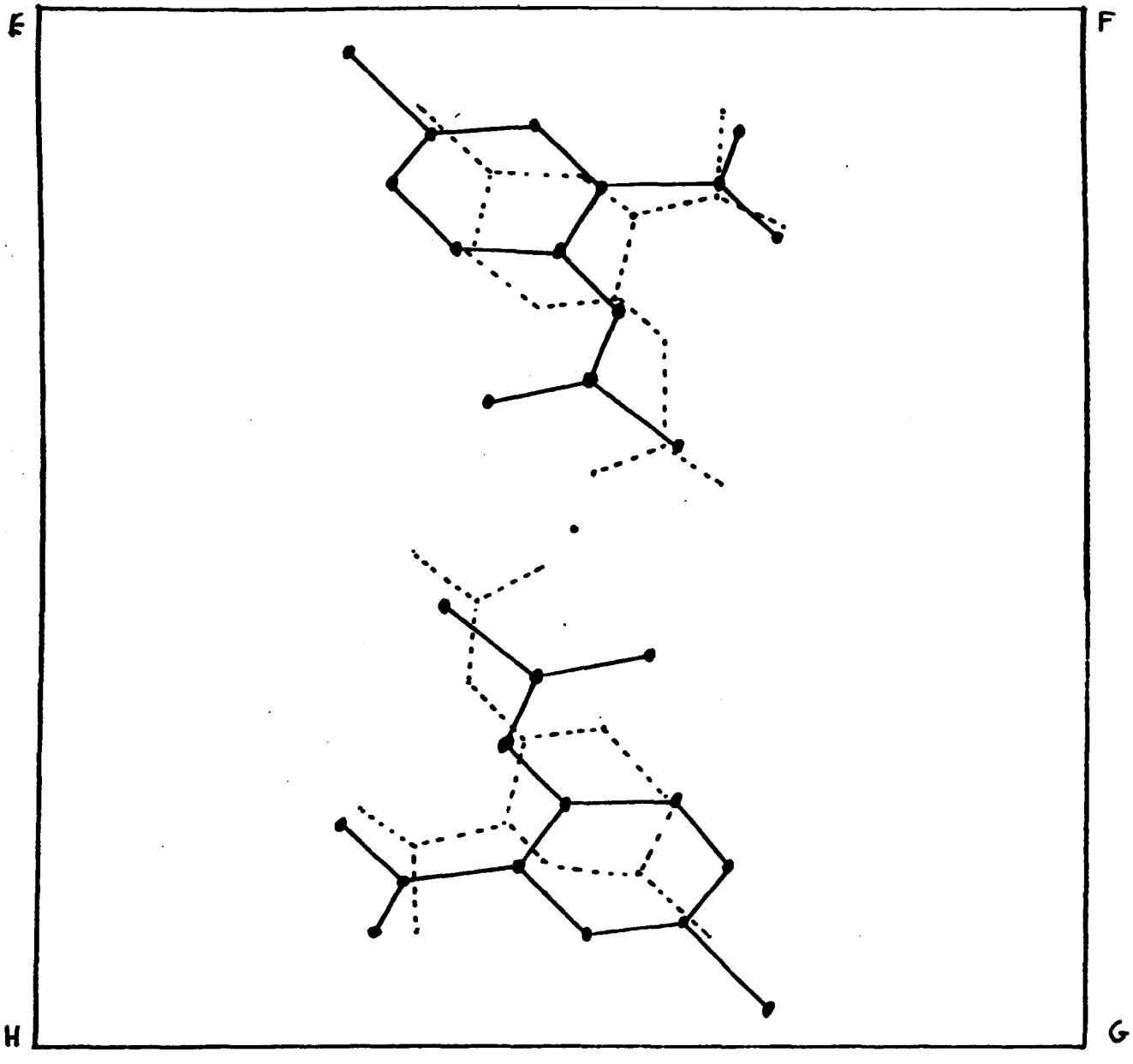

Fig. 5.4

RELATIVE POSITIONS OF MOLECULE I AND I' IN MNA-3 (full lines)
AND THEIR SUPERIMPOSED POSITIONS IN MNA-2 (dashed lines)

Conversion of MNA-3 coordinates to MNA-1 coordinates by matrix conversion

The ring coordinates and coordinates of N(1),N(2), and C(7) of MNA-3 may be converted to the equivalent MNA-1 coordinates by the following matrix :-

$$\begin{bmatrix} -1.0218 & 2.0186 & 0.3194 & 0 \\ -0.9733 & -0.9763 & -0.0442 & 0 \\ 0.0730 & 0.3340 & 0.6165 & 0 \\ 1.8734 & -0.9623 & -0.2727 & 1 \end{bmatrix}$$

M3

The approximate matrix is :-

$$\begin{bmatrix} -1 & 2 & 0.33 & 0 \\ -1 & -1 & 0 & 0 \\ 0 & 0.33 & 0.6 & 0 \\ 2 & -1 & -0.3 & 1 \end{bmatrix}$$

M4

Each of the above 4x4 matrices is premultiplied by x,y,z,1 i.e. the coordinates of the individual points of MNA-3. The conversion matrix was calculated with the aid of a computer program named GENINV by A. MacKay[189] which will produce a least squares solution to a series of simultaneous equations. The values of the columns are found by assuming them to be coefficients in the expression :-

$$ax + by + cz + d = x(\text{MNA-1})$$

where x,y,z are the nine MNA-3 coordinates. Thus there are nine equations and four unknowns which are calculated by the computer program. When this process is repeated for the y and z coordinates of MNA-1 the complete matrix can be calculated.

The transformation of MNA-3 to MNA-1 coordinates based on a clockwise rotation of molecules 1 and 1'.

A model for the conversion of MNA-3 to MNA-1 was considered in Chapter 4 in which pairs of molecules such as 1,1' and 2,2' rotated about centres of symmetry. If molecules 1 and 1' are rotated about 0.5,0.5,0.5, as indicated in fig. 5.5, then the resulting structure would be one based on fig. 5.6.

Calculated coordinates are shown in Table 5.2 and a comparison of these, with coordinates obtained from X-ray diffraction is shown in Fig. 5.8. Pairs of molecules at x,y,z+1 rotate in the same manner as those at x,y,z but the benzene rings must be rotated about the N(1)...C(1) axis in order to generate molecules C (x,0.5-y,0.5+z) and D (1-x,0.5+y,0.5+z).

Although this model is of interest because it enables fairly accurate ring coordinates to be calculated for MNA-1 molecules it does NOT agree with the observed orientations of crystals of MNA-1 which form in the solid state from MNA-3. The mechanism in which the molecules of MNA-3 fold about N(1) does not suffer from this disadvantage.

Transformation of MNA-3 coordinates to MNA-1 coordinates by matrix multiplication.

The rotation of the pairs of molecules 1 and 1' described above may be translated into a mathematical transformation which involves the following steps :-

1. move the origin of MNA-3 to 0.5,0.5;

2. rescale the x axis by a factor of 2 i.e. $x' = 2 \times x$;

3. rotate x and y axes around the z axis; (-45^{o})

4. $y' = -y$;

5. $x' = 1 - x$;

6. $z' = z \times 0.5$ in each case the coordinate marked (') refers to the new calculated coordinate.

The calculated coordinates are presented in table 5.2 .

Table 5.2 . Calculated MNA-1 coordinates

C(1)	0.6228	0.3783	0.3728
C(2)	0.5657	0.4923	0.2645
C(3)	0.4361	0.5355	0.2106

Table 5.2 (continued)

C(4)	0.3572	0.4690	0.2616
C(5)	0.4123	0.3564	0.3709
C(6)	0.5400	0.3127	0.4244
C(7)	0.2167	0.5135	0.2001
N(1)	0.7528	0.3335	0.4298
N(2)	0.6389	0.5711	0.2005

The equation for the new plane of the benzene ring is

$$-0.1684X + 1.3989Y + 1.5410Z = 1$$

The plane for the ring plane of molecule A in MNA-1 is

$$-0.1308X + 1.6658Y + 1.2206Z = 1$$

The angles between the normals to these planes is 11.55° . The angles between the z - axis and ring planes are 42.23° and 53.77° respectively. A comparison of the calculated coordinates and the equivalent coordinates obtained by X-ray diffraction studies on MNA-1 is presented in fig. 5.8 in which a view down z is presented.

Fig. 5.5 Molecules 1 and 1' in MNA-3. The theoretical conversion to MNA-1 might occur by rotation of such pairs around centres of symmetries 0.5,0.5,0.5

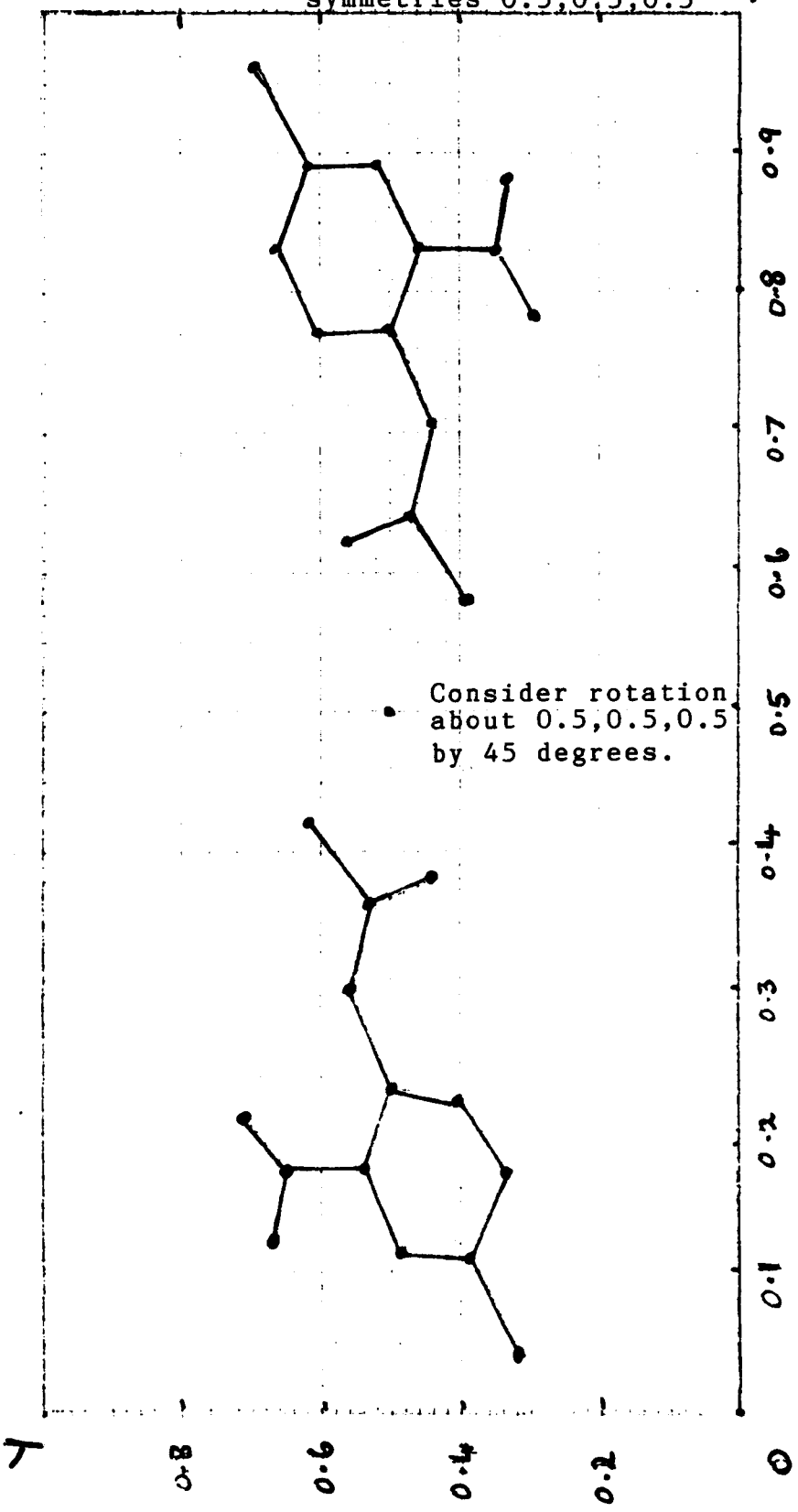

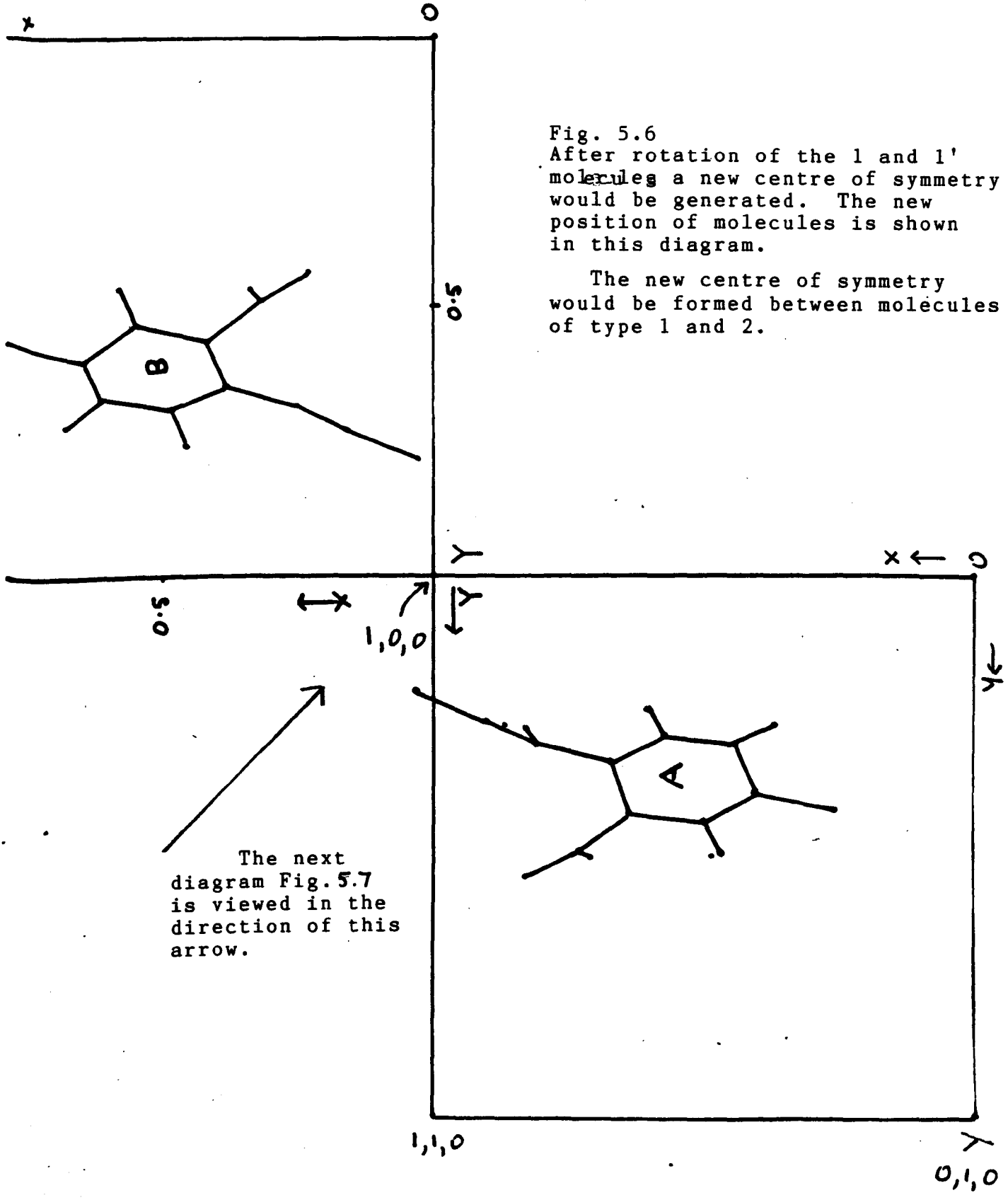

Fig. 5.6
After rotation of the 1 and 1' molecules a new centre of symmetry would be generated. The new position of molecules is shown in this diagram.

The new centre of symmetry would be formed between molecules of type 1 and 2.

The next diagram Fig. 5.7 is viewed in the direction of this arrow.

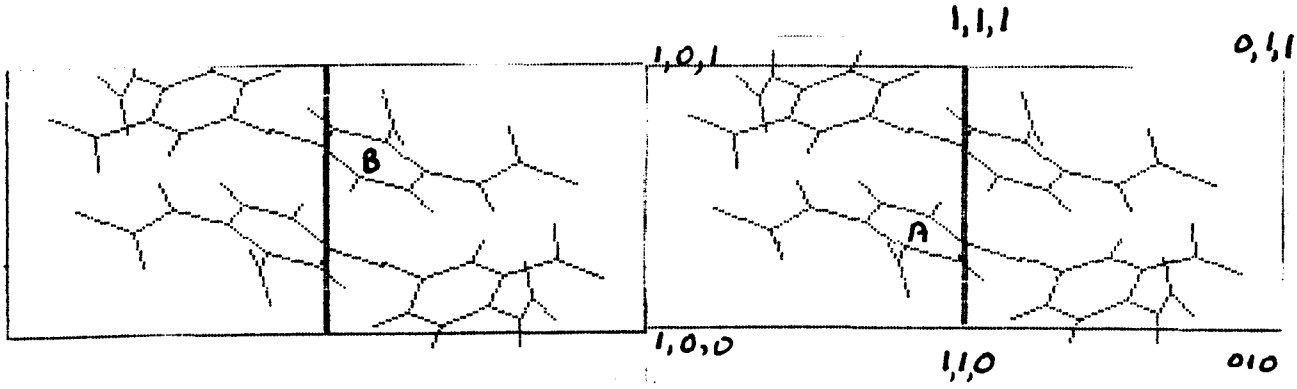

Fig. 5.7
This is a sideways view of two unit cells of MNA-1 which have an edge in common. It is a view down the unit cell diagonal i.e. from 1,1,0 to 0,0,0. The diagram shows molecules of type A and B which might be related to the rotated dimer unit originally in MNA-3. Molecule A would be equivalent to molecule 1 in MNA-3 and molecule B would be equivalent to molecule 1' in MNA-3.

Fig. 5.8
The calculated position of a type A molecule (dotted line) shown in comparison with the position of a molecule of type A based on experimentally determined coordinates.

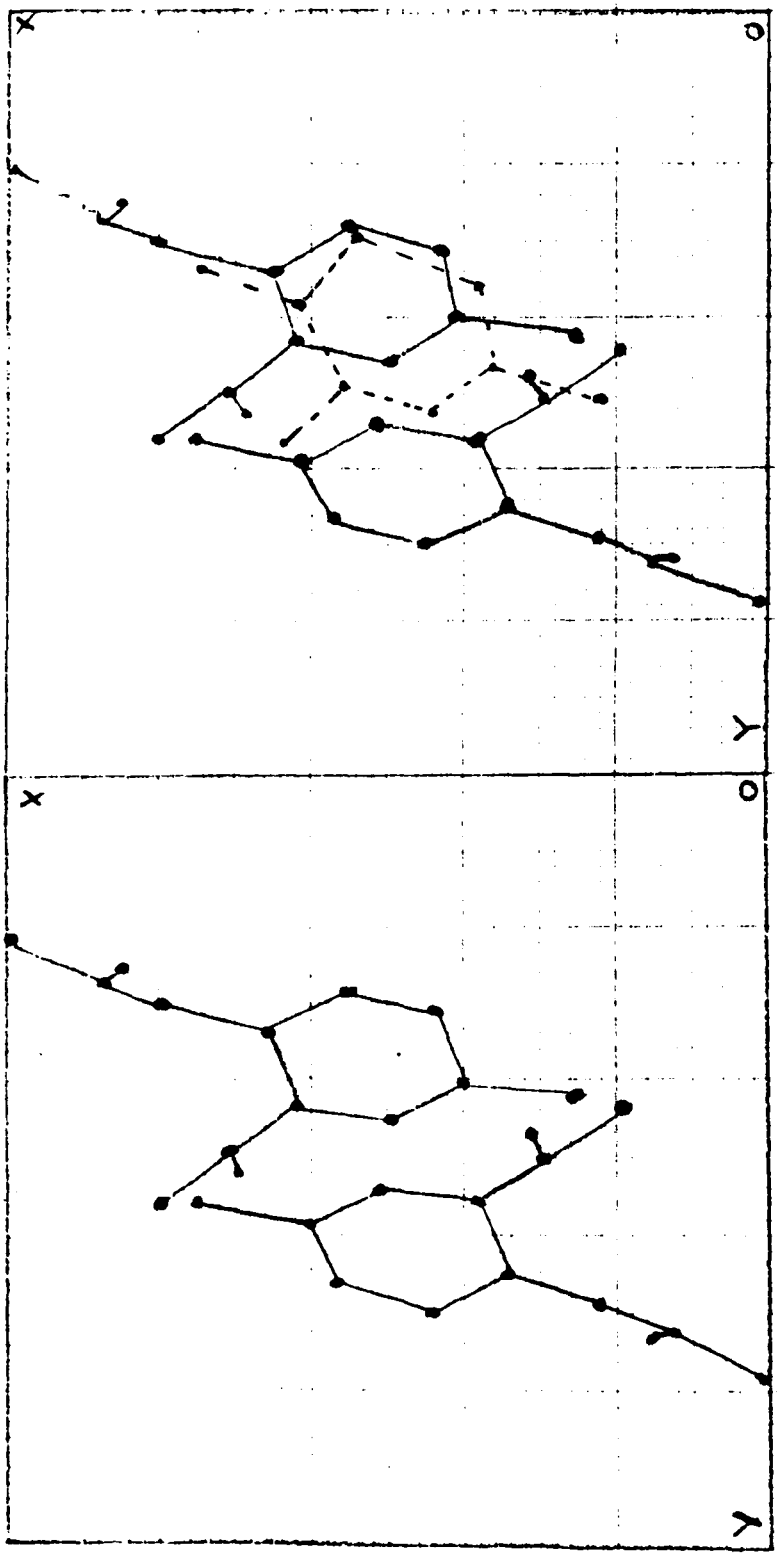

A summary of the relationship between the crystal lattices of MNA polymorphs.

It is convenient to regard the MNA-2 structure as the 'parent' structure. In fig. 5.1 molecules at x,y,z and 1-x,1-y,1-z are shown. The origin of the unit cell is O2 and x and y axes are shown by O2...X2 and O2...Y2 respectively. The transformation of MNA-2 to MNA-3 is thought to occur by alternate molecules in the columns parallel to the z axis rotating around the N(2)-C(2) bond. The MNA-3 unit cell is represented by the origin O3 and with x and y axes O3...X3 and O3...Y3 respectively. The common points occur where the two sets of axes intersect. The length of the c side of the unit cell in MNA-3 should be half that of MNA-2 and these values are 4.039 Å (found) and 8.041 * 0.5 = 4.2 Å (calculated from MNA-2 crystal data). The x and y coordinates of the MNA-2 can be converted to those of MNA-3 by a matrix which was presented in a previous section i.e. M1. This matrix allows for a rescaling and rotation of the reference axes.

Formation of MNA-1 from MNA-3 may be assumed to occur by molecules adopting a folded conformation with the N(1) atoms as pivots. The position of the MNA-1 unit cell is given by the origin at O1 and x and y axes at O1....X1 and O1...Y1

respectively. It is not possible to devise a simple rotation matrix to convert MNA-3 coordinates to MNA-1 coordinates since extensive folding of the molecules occurs but the transformation can be done graphically by means of fig. 4.22 . It is noted that the y coordinates of the ring atoms and N(1) and N(2) in MNA-2 are related by the approximate relationship :-

$$Y(MNA-2) = X(MNA-1) - 0.35$$

Another point of interest is that the points of pseudo-inversion between molecules of types 1 and 2 in MNA-3 viz. 0.75, 0.25 and 0.25, 0.75 transform to 0.5,0.5 in MNA-1.

In the diagram shown in fig. 4.21 formation of the folded conformation, with N(1) as stationary points, leads to a situation where the benzene rings overlap exactly. Comparison of this diagram with that obtained for the MNA-1 unit cell which has been rotated 45 degrees around the x axis shows a remarkable similarity*. Similarly, the positions of molecules obtained by rotation around the N(1) atoms followed by displacement along half the hexagonal grid leads to the projection which is very similar to that shown for the view of MNA-1 down the z axis (fig. 4.22). The lines G1 and G2 would represent the intersection of the glide planes with the xy plane. Approximate x and y coordinates can be obtained from the diagrams and they are in fair agreement with those obtained from x-ray diffraction experiments.

Another feature which is revealed by these diagrams is that the distance OX (the length of the a side of the unit cell) should be equal to that of half the longer diagonal of the MNA-3 unit cell. These values are

$$10.421\ \text{Å} \text{ and } 22.26 * 0.5 = 11.13\ \text{Å}$$

* see Fig. 5.9

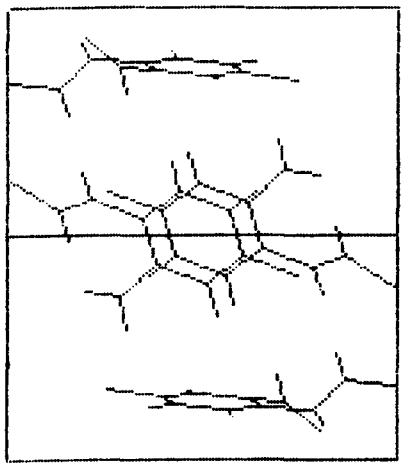

Fig. 5.9

A view of MNA-1 after rotation round the x axis by 45 degrees.

This Fig. is very similar to that in Fig. 4.21 obtained by pivoting MNA molecules about N(1)

A comparison of the relative positions of the MNA-3 and MNA-1 unit cells

In fig. 5.1 the larger squares with axes OY3 and OX3 represent the outlines of the unit cells of MNA-3 viewed down the z axis and O1...Y1 and O1...X1 represent the axes of the MNA-1 unit cell viewed down the z axis. The MNA-3 and MNA-1 z axes are parallel. The coordinates of the point M, repesented as a projection on the XY plane are 0.75,0.25 on the MNA-3 axes but become 0.5,0.5 on the MNA-1 set of axes. The significance of the point M is that it is an approximate point of inversion for the x and y coordinates of molecule 1 and molecule 2. When molecules of MNA-1 adopt the folded conformation i.e. when the transformation to MNA-1 occurs then M becomes a true centre of inversion since it is assumed to become the point 0.5,0.5,0.5 in MNA-1.

A matrix, which is used as a post multiplier, for the conversion of x,y,z coordinates based on Fig. 5.1 is given below :-

$$\begin{bmatrix} x & y & z & 1 \end{bmatrix} \begin{bmatrix} 1 & 1 & 0 & 0 \\ -1 & 1 & 0 & 0 \\ 0 & 0 & 0.5 & 0 \\ 0 & -0.5 & 0 & 1 \end{bmatrix} \quad \text{M5}$$

This matrix converts the coordinates of N(1) in molecules 1 and 2 in MNA-3 very nearly into those found for N(1) in MNA-1. The calculated and found values are shown in Table 5.3 .

Table 5.3 .

calculated conversions			
N(1) mol 1	0.2660	0.6443,	0.4298
N(1) mol 2	0.7591	0.3443	0.5257
found values for N(1) in MNA-1			
N(1) 1-x,1-y,1-z			
	0.2127	0.6878	0.5408
N(1) x,y,z			
	0.7873	0.3122	0.4592

It is concluded that molecular rotations can occur round N(1) and that N(1) in molecule 2 and molecule 1 can become equivalent to N(1) in MNA-1.

Diagrams which show these rotations are shown in fig.4.21 and fig. 4.22 . In each of these diagrams a view of MNA-3 is presented as viewed down the z axis and the flat face of the MNA-3 crystal is parallel to the line OP which is the a+b vector of the MNA-3 unit cell.

Similarly the length of the side of the unit cell represented by OY (the length of the b side) should be equal to half the length of the shorter diagonal of the MNA-3 unit cell and these values are

$$9.98\ \text{Å} \text{ and } 21.97 * 0.5 = 10.985\ \text{Å}$$

Thus contractions of approximately 6% and 10% are predicted in the MNA-1 x and y directions but since an expansion of 19% occurs in the z direction (i.e. from 2 * 4.039 = 8.078 Å to 9.568 Å) an overall expansion should occur. This is supported by the values of the volumes of the unit cells which are 929.1 Å^3 and 981.4 Å^3 for MNA-3 and MNA-1 respectively.

The type of phase change which is represented by the fig.4.21 shows that oblique or lateral growth of MNA-1 from MNA-3 involves an expansion in the direction of OP from

$$21.97 * 0.5 = 10.985 \text{ to } 13.83\ \text{Å}$$

where the value of 13.83 Å is the length of the diagonal of the bc face of MNA-1. A concomitant contraction of

$$4 * 4.039 = 16.156 \text{ A to } 13.83 \text{ A}$$

will occur in the c direction of MNA-3. These values amount to a 25% expansion in the original width of the needle shaped

MNA-3 crystal and a contraction of 14.4% along the length of the needle shaped crystal.

The formation of these two different orientations of MNA-1 unit cells are represented diagrammatically in fig. 5.10 where each block represents an edge-on view of a benzene ring.

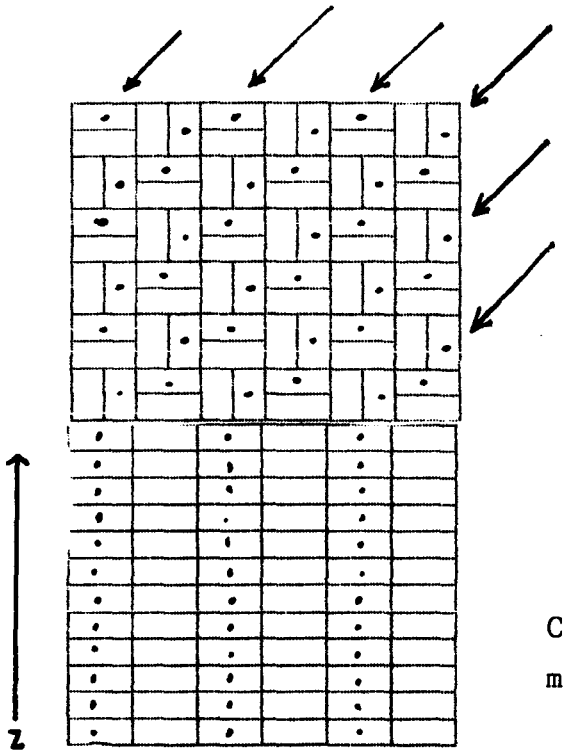

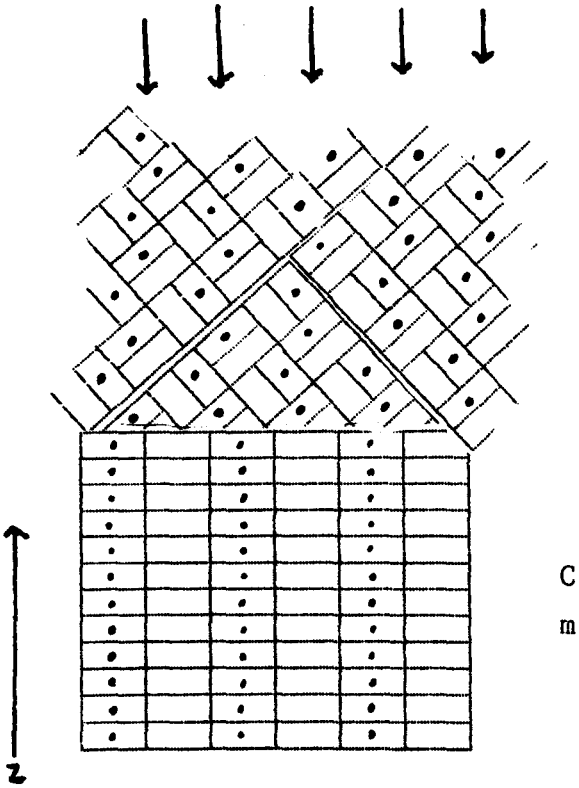

Fig. 5.10 Diagramatic schemes for the formation of intermolecular hydrogen bonds at 45° (upper) and parallel to z axis of MNA-3

Fig. 5.11 Computer simulation of the MNA-3 to MNA-1 change

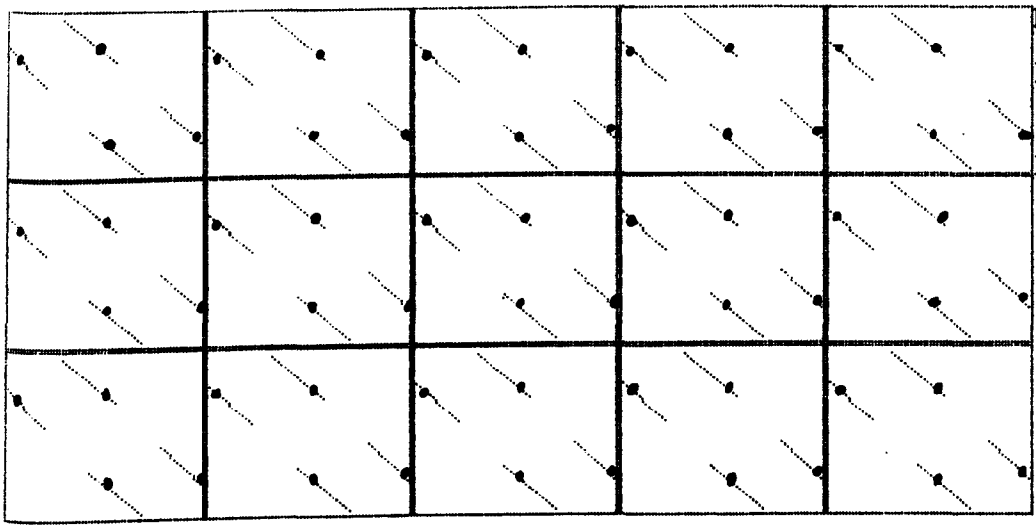

MNA -3 unit cells the dots locate N(1) atoms

The lines represent N(1)...C(7) axes

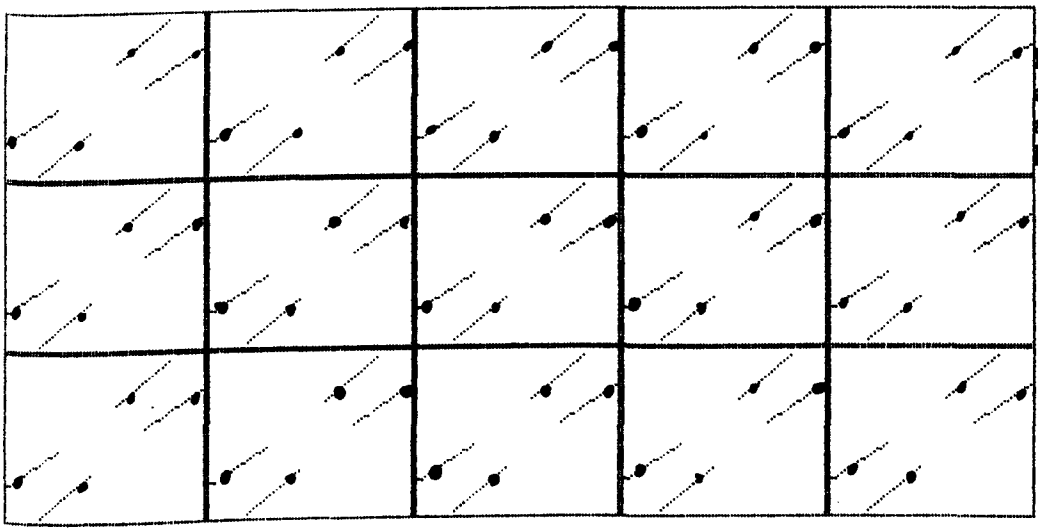

The positions of N(1)...C(7) axes after rotation around the pivot N(1)

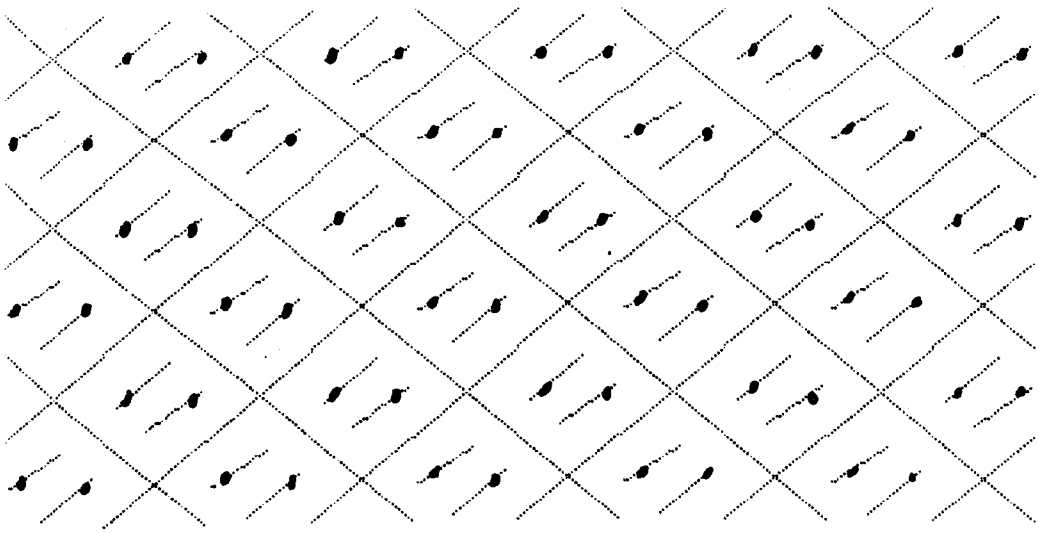

The outlines of the MNA-1 unit cells shown here.

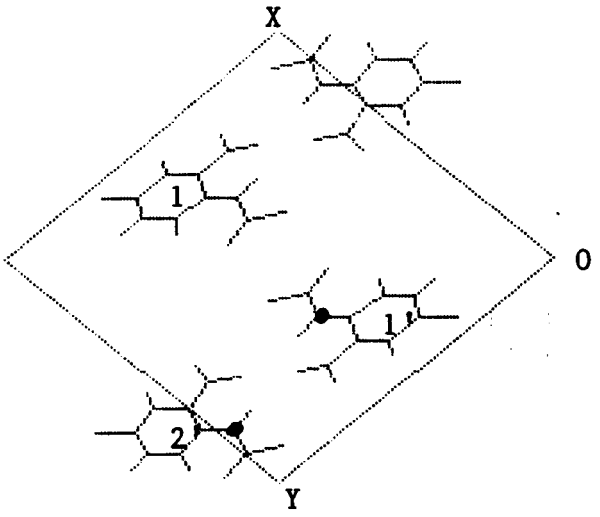

Four molecules in the MNA-3 unit cell as viewed down the z axis.

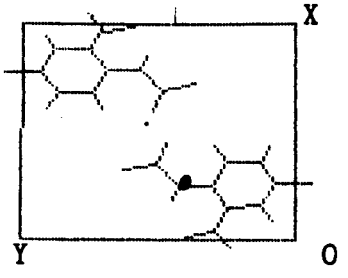

The MNA-2 unit cell viewed down the z axis The two molecules shown are regarded as equivalent to molecules 1 and 1' in MNA-3

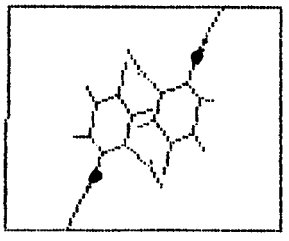

The MNA-1 unit cell viewed down the z axis.
Note the two N(1) atoms are regarded as equivalent to N(1) in molecules 1' and 2' in MNA-3
(N 1) = emphasised points)

Fig. 5.12 In each case the projections are based on the appropriate coordinates of each polymorph (crystal coordinates) and each cell is drawn to the same scale.

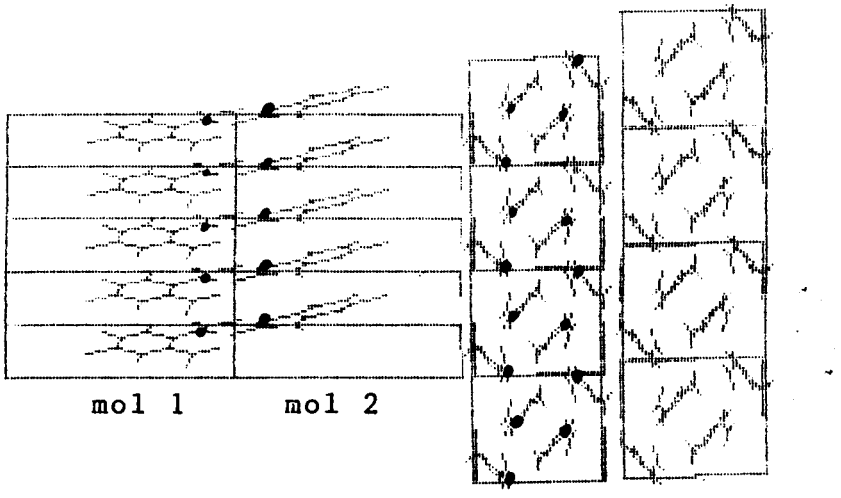

A

A view of MNA-3 perpendicular to the cell diagonal from 0,0,0 to 1,1,0. Several units shown stacked along z.

B

Two views of MNA-1 Four unit cells are stacked along z and views are perpendicular to the z axis.

The MNA-1 diagram (A) is drawn to the same scale as the diagram of MNA-3. Emphasised points which denote N(1), are shown and in each case they form the same pattern. This result is in accord with N(1) being the pivot for the change in conformation.

In diagram B an expansion of about 20% has occurred along the z direction. The expected expansion along z is 2 x 4.039 = 8.078 Å to 9.568 Å where 4.039 is the length of c in MNA-3 and 9.568 is the length of c in MNA-1 (i.e. an expansion of 18.5%)

Fig. 5.14

Fig. 5.13

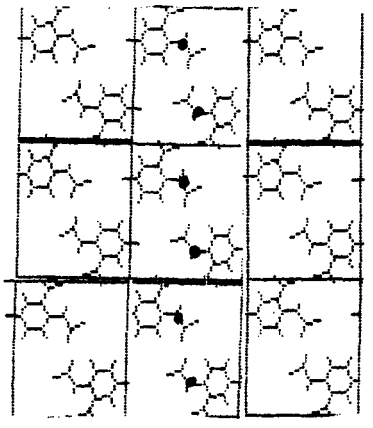

Nine unit cells of MNA-2 viewed down the z axis. Only molecules at x,y,z and 1-x,1-y,1-z are shown.

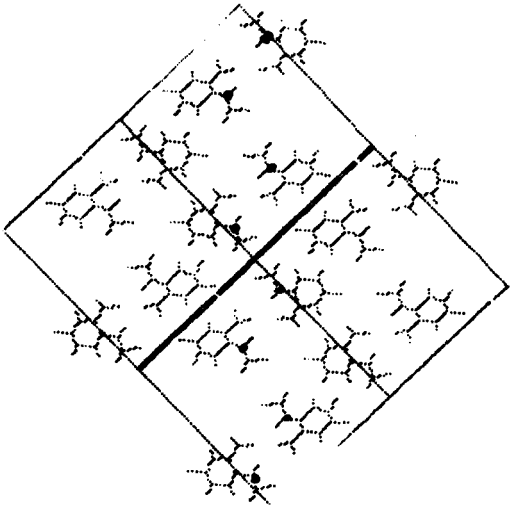

Four unit cells of MNA-3 viewed down the z axis. Note the similarity of this projection with that for MNA-2 .

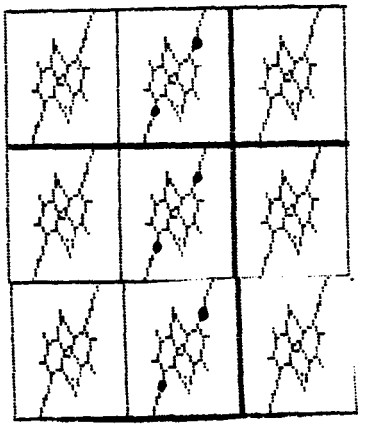

Nine unit cells of MNA-1 shown down the z axis. Note that the positions of the N(1) atoms in this case are equivalent to the N(1) positions in MNA-3. Only molecules at x,y,z and 1-x,1-y,1-z are shown.

Fig. 5.13 The relative positions of molecules in MNA-1, MNA-2, and MNA-3

Calculation of a pivot point for the transformation of MNA-3 to MNA-1

The matrix M3 will transform coordinates of atomic positions of ring atoms and N(1) and N(2) in MNA-3 to those found for equivalent positions in MNA-1.

The matrix M5 which was introduced in **this chapter** is one which merely allows for a change of position of the origin and a rescaling of the axes of the MNA-3 unit cell. The matrix M10 is obtained by multiplying matrix M5 by matrix M9 which converts coordinates x,y,z, to 1-x,1-y,1-z.

$$\begin{bmatrix} -1 & 0 & 0 & 0 \\ 0 & -1 & 0 & 0 \\ 0 & 0 & -1 & 0 \\ 1 & 1 & 1 & 1 \end{bmatrix}$$

M9

If it is assumed that the conversion of MNA-3 to MNA-1 does occur by a process involving molecular rotation then a point (i.e. the pivot) should exist which should convert to the same point when multiplied by either M3 or M10.

In mathematical terms :-

$$(x \; y \; z \; 1) * M3 = (x \; y \; z \; 1) * M10$$

The matrix M10 is :-

$$\begin{bmatrix} -1 & -1 & 0 & 0 \\ 1 & -1 & 0 & 0 \\ 0 & 0 & -0.5 & 0 \\ 1 & 1.5 & 1 & 1 \end{bmatrix}$$

M10

If the coordinates of the pivot point are multiplied by M3 and M10 and like terms are gathered together then three simultaneous equations result :-

$$-0.0218x - 1.9733y + 0.8734z = 0$$

$$3.0186x + 0.024y - 2.462z = 0$$

$$0.3194x - 0.0442y + 1.1617z = 0$$

These equations were solved using the general inverse program GENINV and gave the result :-

$$x = 0.7107$$

$$y = 0.4348$$

$$z = 0.9167$$

or approximately x=0.71, y=0.43, and z=0.92.

The coordinates for the atom N(1), in MNA-3, which were presented in Chapter 3 are x=0.7053, y=0.4390, z=0.8596.

Since there is a close correspondence between these coordinates it is concluded that the N(1) atoms in MNA-3 are the most likely pivot points when MNA-3 changes in the solid state into MNA-1.

A matrix conversion of MNA-2 (amber) coordinates to MNA-1 (white) coordinates

It is possible to construct a matrix for this conversion by assuming that a molecule at x,y,z in MNA-2 becomes a molecule (type A) at x,y,z in MNA-1. The following steps are involved in the construction of the elements of the matrix:-

a) re-position the origin of MNA-2 at 0.5,0,0

b) let x(1) = y(2)

c) let y(1) = 0.5 - x(2)

d) rotate the re-positioned axes by 20°

It is also assumed that the z-axes are parallel in both structures and that the z coordinates are related by the following relationship:-

$$z(1) = z(2)$$

A diagram showing the relative positions of the MNA-2 and MNA-1 axes are shown in fig. 5.1 .

A conversion matrix based on the above transformations is:-

$$\begin{bmatrix} x(2) & y(2) & 1 \end{bmatrix} \begin{bmatrix} 0 & -1 & 0 \\ 1 & 0 & 0 \\ 0 & 0.5 & 1 \end{bmatrix}$$

A transformation matrix for rotation of x and y axes around a z-axis is :-

$$\begin{bmatrix} x & y & 1 \end{bmatrix} \begin{bmatrix} \cos A & \sin A & 0 \\ -\sin A & \cos A & 0 \\ 0 & 0 & 1 \end{bmatrix}$$

Multiplication of these matrices gives a new matrix :-

$$\begin{bmatrix} \sin A & -\cos A & 0 \\ \cos A & \sin A & 0 \\ -0.5\sin A & 0.5\sin A & 1 \end{bmatrix}$$

If a value of 20° is assumed for the rotation then the actual transformation matrix is:-

$$\begin{bmatrix} -0.34 & -0.94 & 0 \\ 0.94 & -0.34 & 0 \\ 0.17 & 0.47 & 1 \end{bmatrix}$$

A transformation matrix has been calculated for the transformation of the x and y coordinates of MNA-2 to MNA-1 using the computer program GENINV[189] . The x and y coordinates of C(1),C(2),C(3),C(4),C(5),and C(6) were used as data and the following matrix was calculated:-

$$\begin{bmatrix} -0.3294 & -0.6862 & 0 \\ 1.0837 & -0.2369 & 0 \\ 0.4000 & 0.5932 & 1 \end{bmatrix}_{M7}$$

MATRIX 7

The elements of the matrices M6 and M7 are comparable in sign and magnitude. One element which differs is that element which corresponds to the translation along the x-axis of MNA-2 (or the y-axis of MNA-1). The predicted value is 0.171 but GENINV gives 0.400. This difference could be accounted for if molecules at x,y,z and 1-x,1-y,1-z in MNA-2 i.e. those molecules related by a centre of inversion at 0.5,0.5,0.5, rotated around this centre of inversion and moved apart while the molecule at x,y,z moved closer to a molecule at 1-x,1-y,1-z in the adjacent cell i.e. at -x,1-y,1-z.

The relationship between the z coordinates, as given by the equation :-

$$z(1) = z(2)$$

is an approximate one and it varies from giving a fairly close agreement for N(1) in MNA-2 (0.51) and N(1) in MNA-1 (0.46) to giving a poor agreement for C(7) which has values 0.52 in MNA-2 and 0.25 in MNA-1. This discrepancy can be explained on the same basis as that used when comparing the MNA-2 and MNA-3 structures when it was noted that the N(1)...C(7) axis is parallel to the y-axis in MNA-2 but is inclined to the equivalent (x-axis) in MNA-1.

A mathematical construction of a hypothetical crystal structure related to MNA-1

By means of a transformation matrix it is possible to construct a hypothetical crystal structure which is closely related to MNA-1 in that it will have the symmetry elements of MNA-1 (viz P 2_1/ c) but the molecules will have the conformation found in MNA-2 i.e. the molecules will be planar and contain intramolecular hydrogen bonds. Using the coordinates of the atoms C(1), C(2), C(3), C(4), C(5), and C(6) in MNA-2 and MNA-1 as data, the computer program GENINV provided a matrix which will convert MNA-2 coordinates into MNA-1 coordinates. By means of this matrix it is possible to calculate coordinates of atoms such as O(1) which would be in positions consistent with an intramolecularly hydrogen bonded system. The transformation matrix is shown as MATRIX 8:-

$$\begin{bmatrix} -1.1648 & -0.7330 & 1.2509 & 0 \\ 1.0754 & -0.2373 & 0.4431 & 0 \\ 0.9393 & 0.0523 & -0.3927 & 0 \\ 0.1232 & 0.5778 & 0.1681 & 1 \end{bmatrix} \quad \text{M8}$$

MATRIX 8

Using this matrix as a post-multiplier the following coordinates were obtained for the atoms specified:-

O(1)	0.7631	0.1822	0.6580
O(2)	0.8501	0.4859	0.2389
O(3)	0.6482	0.5618	0.1313
NH	0.8299	0.3588	0.4206
C(8)	0.8274	0.2417	0.5839
C(9)	0.9586	0.2331	0.6163

In this hypothetical structure the amide and nitro groups of molecules which are related by the glide plane are very close to each other and some close contacts are presented in Table 5.3 .

Table 5.3

Some important intermolecular distances (Å) in a hypothetical intramolecularly hydrogen bonded MNA-1.

using MNA-1 cell parameters

O(1)	O(2)	2.0
O(1)	O(3)	2.7
O(1)	NH	2.5
O(1)	C(8)	4.1
O(1)	C(9)	4.6

using MNA-2 cell parameters

O(1)	O(2)	2.2
O(1)	O(3)	3.1
O(1)	NH	2.1
O(1)	C(8)	3.55
O(1)	C(9)	4.2

The above distances show that the oxygen atom in the amide carbonyl group, O(1), would lie very close to one of the nitro-group oxygen atoms, O(2). Such a close proximity of these electron-rich atoms would lead to strong repulsive

forces between the amide and nitro groups which could be relieved by simultaneous rotation of the amide and nitro groups in such a way as to increase the O(1)....O(2) distance.

It is noted that O(1) is very close to the NH group in the adjacent molecule in this structure and this situation would assist in the formation of intermolecular hydrogen bonds between the glide plane related adjacent molecules.

A summary of the changes involved in the transformation of MNA-2 (amber) to MNA-3 (yellow) to MNA-1

The distribution of columns of MNA molecules which lie parallel to the z axis are arranged as shown in Fig. 5.13 and this distribution is shown diagramatically in Fig. 5.15. There is a similar distribution of columns in MNA-3 but in this case weak intermolecular hydrogen bonds link alternate columns. The formation of the most stable polymorph, MNA-1, from MNA-3 is thought to occur by intermolecular hydrogen bond formation along the column (i.e. in an intracolumnar fashion). Thus sheets or layers of MNA-1 molecules are formed in planes parallel to the plane formed by the a+b direction of MNA-3 (or the y direction in MNA-1) and the z axis. These sheets are then stacked along the x direction of MNA-1.

The positions of molecules in the various polymorphs can be visualised by the diagrams drawn on the hexagonal grids. The MNA-2 structure is shown in Fig. 4.16 and MNA-3 in Fig. 4.18. These diagrams represent the arrangement of coplanar molecules in these structures hence Fig. 4.16 should be viewed with OB horizontal and OA inclined at an angle of 45 degrees to the horizontal plane whereas Fig. 4.18 should be held with AP horizontal and inclined at about 30 degrees to the horizontal.

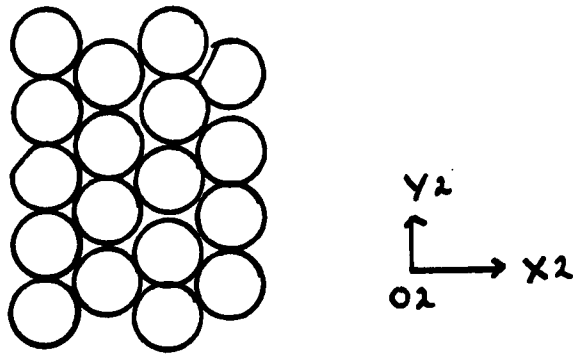

The relative positions of columns in MNA-2

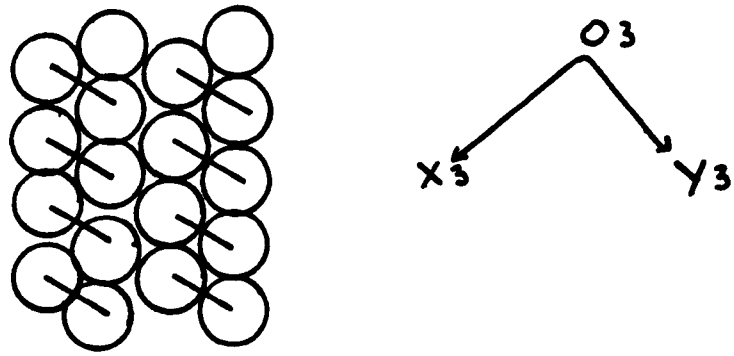

The relative positions of columns in MNA-3
The oblique lines represent columns linked by hydrogen bonds.

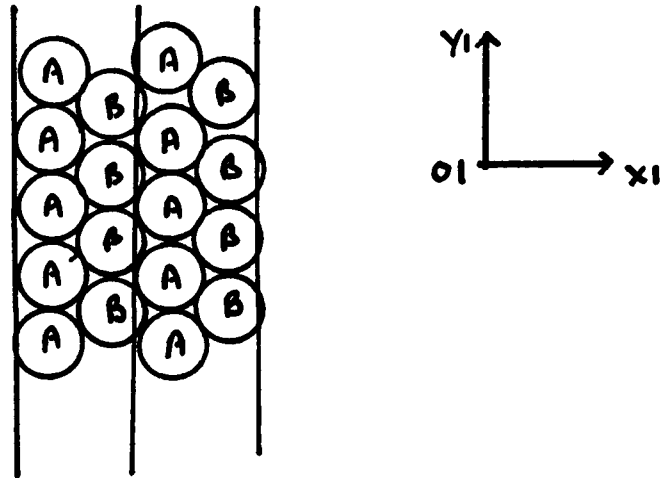

Two sheets or layers packed along x. A and B represent molecules at x,y,z (A) and 1-x,1-y,1-z(B)

Fig. 5.15

The diagram for MNA-1 is shown in Fig. 5.16 where OA represents the projection of the a side of the unit and OC the projection of c. The atoms involved in the hydrogen bonding system are in the plane of the diagram and the rings should be viewed as projections onto this plane which coincides with the glide plane. The directions of the hydrogen bonds are (i) along the columns so as to be parallel to the z axis, and (ii) inclined at an angle of about 45 degrees to the z axis. The edges of these planes coincide with arrows in Fig. 5.10.

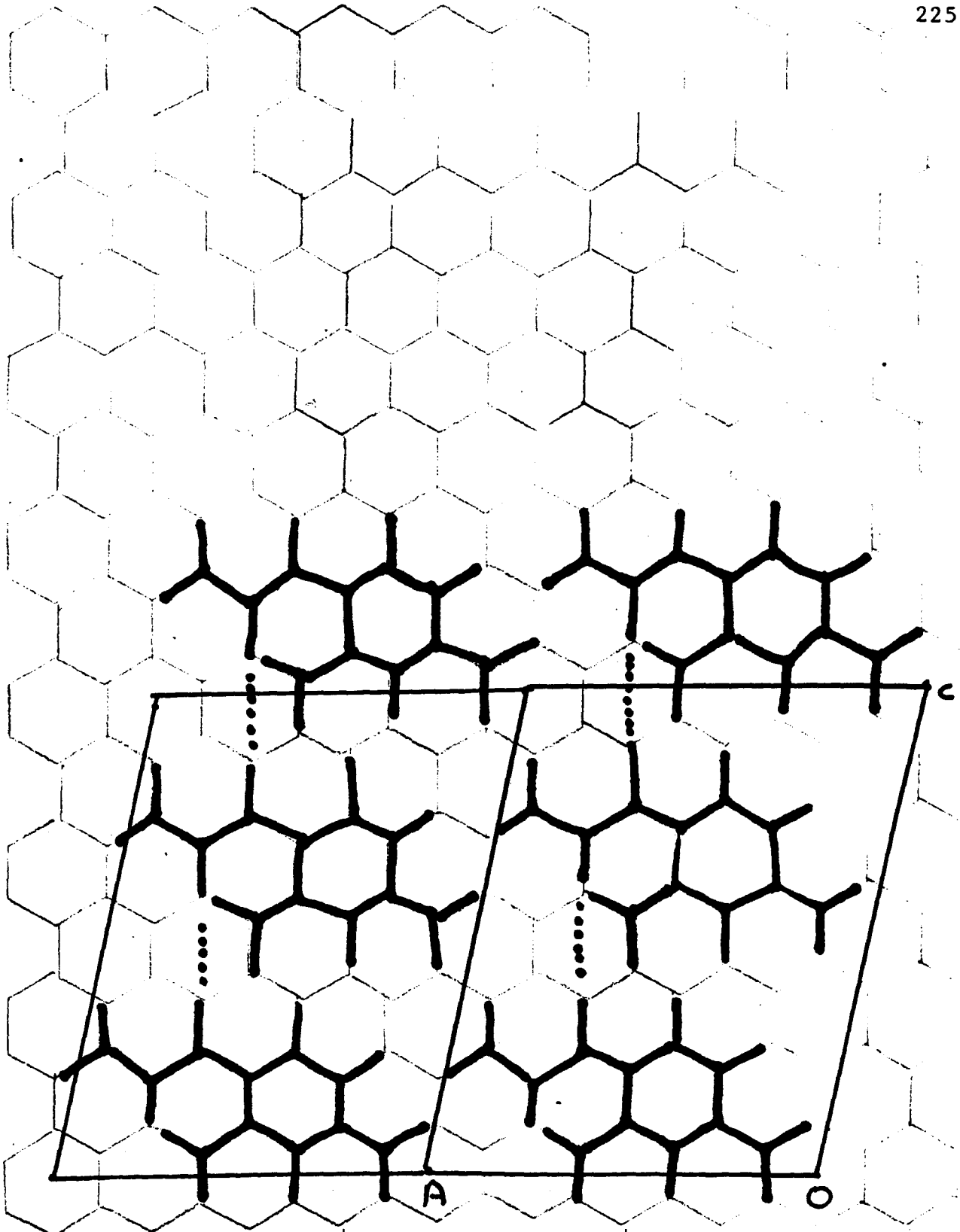

Fig. 5.16 A projection of MNA-1 structure on to the glide plane. The β angle in this projection is 102° compared to that of 99.51(5)° determined experimentally.

Powder Diffraction Studies.

Powder photographs of the three polymorphs were recorded and Debye-Scherrer photographs are shown in Fig. 5.17 . A sample of MNA-2 which was heated at 80°C for 5 minutes gave a powder pattern which was identical to that of MNA-3 showing that the phase change MNA-2 to MNA-3 occurs rapidly on heating. However a powder sample of MNA-3 was stable at 80° C for 72 hours. A possible explanation for stability under these conditions is that in order for MNA-1 to be formed an expansion of about 20% must occur along the direction in which the new intermolecular hydrogen bonds are formed. In a powder sample which is packed into a capillary tube the orientaion of crystallites is random and they are tightly packed making expansion unlikely.

Samples of MNA-2 and MNA-3 both gave MNA-1 powder patterns after ultrasonic vibration whilst suspended in water.

The positions of powder lines were measured using a transparent vernier scale and the corresponding d-spacings were calculated on a Sharp microcomputer. The measurements along the films were estimated to be accurate to within 0.2 mm and the calculated d spacings, together with line intensity estimates have been correlated with single crystal diffraction data.

Apparatus and conditions used for powder photographs.

A Raymax 60 XRD unit was used which has a 9 cm diameter camera (linear correction factor, 0.977) and 0.3 mm diameter sample holder. Exposures lasted two hours and chromium $K\bar{\alpha}$ radiation (wavelength 2.290 Å) was used with a vanadium foil β-filter.

The results from the powder photographs are presented in Table 5.4 Intensity values (I) are vs = very strong; s = strong; m = medium; w = weak; vw = very weak; br = broad.

POWDER PHOTOGRAPHS OF MNA POLYMORPHS

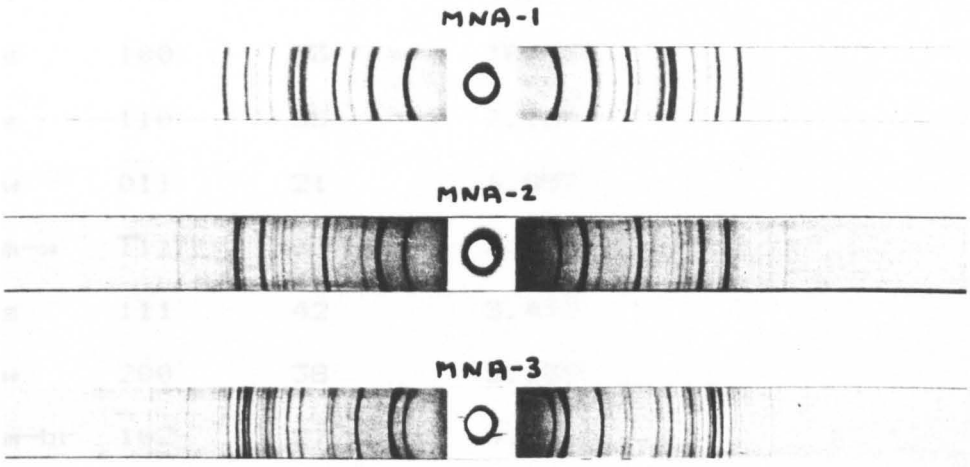

Fig. 5.17

Table 5.4

Correlation between powder and single crystal diffraction data.

MNA-1

Powder data		single crystal data		
d(Å)	I	hkl	F(obs)	d(calc)
10.31(3)	s	100	33	10.278
7.14(2)	s	110	35	7.160
6.80(2)	w	011	21	6.857
6.04(2)	m-w	$\bar{1}11$	30	6.049
5.41(1)	s	111	42	5.412
5.15	w	200	38	5.139
4.45(1)	m-br	$\bar{1}02$	27	4.585
		210	32	4.569
		120	47	4.489
		021	48	4.411
4.27(1)	m-s	021	54	4.266
4.16(1)	m	$\bar{1}21$	48	4.172
3.80(1)	m	$\bar{2}02$	61	3.803
3.58(1)	m-w	220	44	3.580
		$\bar{2}12$	30	3.553
3.43(1)	s	022	66	3.428
3.22(1)	w	$\bar{3}11$	35	3.223
3.15(1)	s-br	130	56	3.165
		122	51	3.141
		031	53	3.137

MNA-2

Powder data		Single crystal data		
10.13(3)	m	100	35	10.126
7.64(2)	vs	110&1$\bar{1}$0	69	7.638
6.61(2)	m-w	011	26	6.601
5.38(1)	w	111	23	5.372
5.05(1)	m-s	200	44	5.063
		120	65	5.044
4.72(1)	w-br	021	28	4.708
		210	11	4.642
4.03(1)	m-w	002	63	4.008
3.82 (1)	w	220	36	3.819
3.65(1)	m-s	$\bar{1}$12	78	3.640
		102	69	3.629
3.38(1)	w	300	71	3.375
3.29(1)	vs	$\bar{2}$02	164	3.271

MNA-3

Powder data		Single crystal data		
10.49(3)	m	$\bar{1}10$	28	10.486
8.91(3)	vs	200	54	8.924
6.43(2)	s	020	52	6.444
5.40(1)	m	$\bar{3}10$	36	5.417
		310	14	5.386
5.23(1)	m	$\bar{2}20$	30	5.243
		220	25	5.206
4.46(1)	m	400	56	4.462
4.18(1)	m	$\bar{1}30$	44	4.184
		130	47	4.170
4.01	w	001	32	4.009
3.89(1)	m	$0\bar{1}1$	34	3.887
		$\bar{1}11$	51	3.887
3.77(1)	m	011	42	3.771
		111	71	3.767
3.61(1)	m	$\bar{1}11$	26	3.617
		211	59	3.606
3.50(1)	m	$\bar{3}30$	58	3.495
		$\bar{1}21$	49	3.498
		330	27	3.471
3.43(1)	s	$3\bar{1}1$	100	3.428
		311	20	3.428
3.33(1)	m	021	87	3.325
		$\bar{2}11$	50	3.355

A comparison of the powder photographs of MNA polymorphs and correlation with the proposed phase transformations.

An inspection of the powder photographs of MNA polymorphs shown in fig. 5.17 shows that MNA-2 (amber) shows 5 main lines whereas that of MNA-3 (yellow) shows lines in similar positions but occurring as closely spaced doublets. The powder photograph of MNA-1 (white) show lines at positions similar to that in MNA-2 but with the addition of two broad bands in the centre of the pattern.

If it is assumed that each polymorph consists of columns and layers of MNA molecules in the same relative positions then similarities in the powder photographs would be expected since the lines observed are caused by diffracting layers. However, equivalent layers would be labelled by different Miller indices which should be interconvertible by knowing the relative positions of the unit cells of MNA-2, MNA-3, and MNA-1 in the proposed transformation mechanism. This is shown in fig. 5.18 in which each of the projections of the x and y axes is viewed down parallel z axes. Using this diagram it is possible write the indices of equivalent layers which lie parallel to z and these are listed in table 5.5.

Fig. 5.19

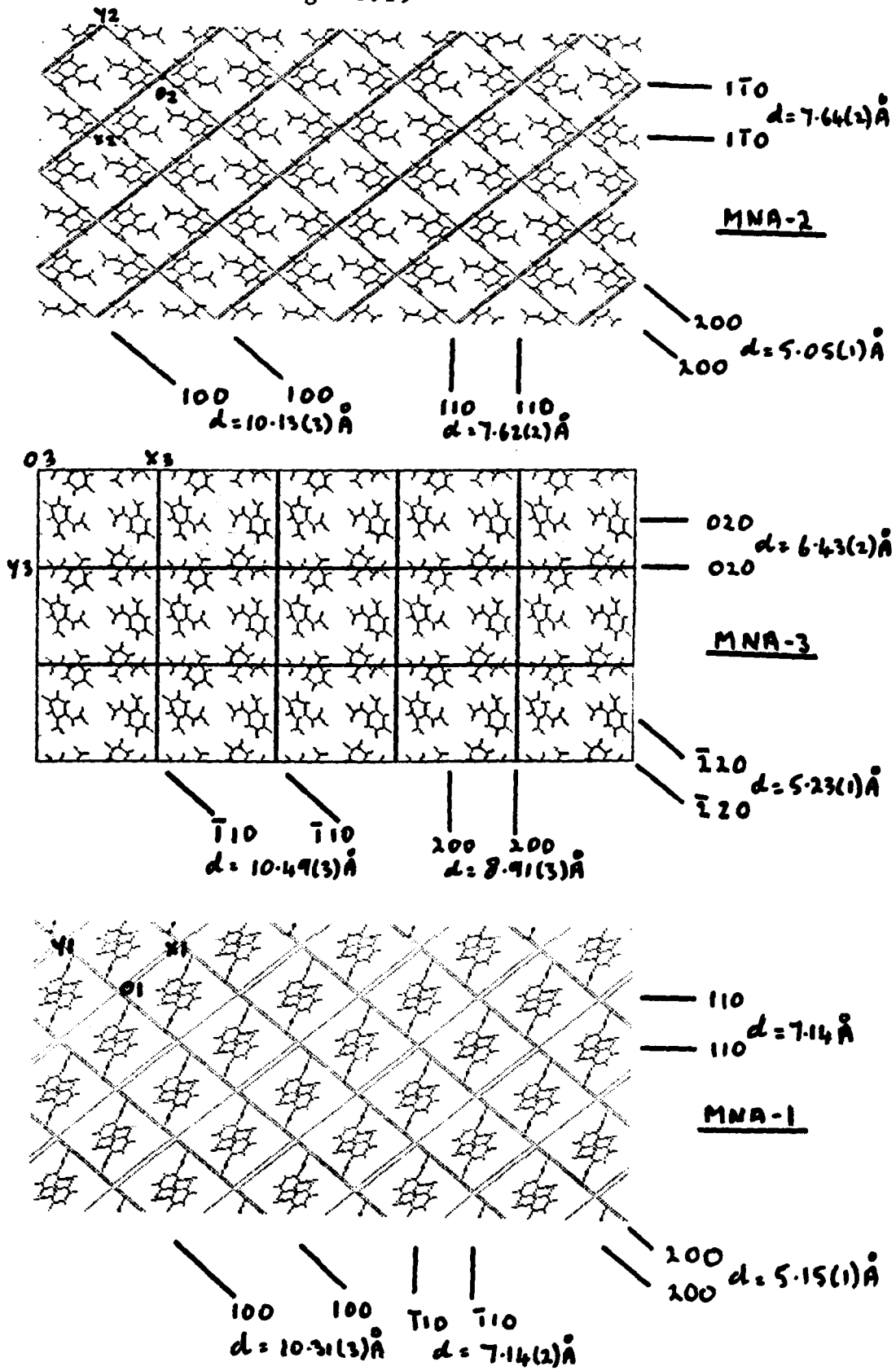

Fig. 5.19 Projections on to the xy planes of MNA polymorph crystal structures. The positions of parallel equivalent planes is shown with their d-spacings.

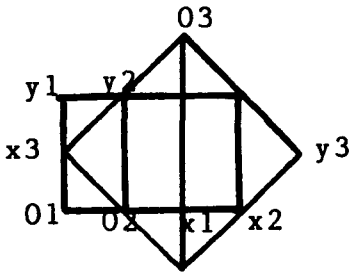

Fig. 5.18 The relative orientations of unit cells of MNA-1, MNA-2, and MNA-3. Each cell is viewed down a z axis.

Table 5.5

Equivalent layers in MNA polymorphs with their corresponding observed d-spacings.

MNA-2	MNA-3	MNA-1
100	$\bar{1}10$	100
10.13(3)	10.49(3)	10.31(3)
110	200	$\bar{1}10$
7.62(2)	8.91(3)	7.14(2)
$1\bar{1}0$	020	110
7.64(2)	6.43(2)	7.14(2)
200	$\bar{2}20$	200
5.05(1)	5.23(1)	5.15(1)

The layers referred to in this table are shown in fig. 5.19, in small scale crystal projection structures (all viewed down z) to enable the layers to be easily observed.

The presence of lines due to layers of parallel benzene rings in the various polymorphs are :-

MNA-2	$\bar{2}02$	3.29(1)Å
MNA-3(mol 1)	$3\bar{1}1$	3.43(1)Å
MNA-3(mol 2)	021	3.33(1)Å
MNA-1	022	3.43(1)Å.

Two broad bands occur in the powder photographs of MNA-1 which do not correspond to any lines in MNA-2 or MNA-3 powder photographs. Some of these additional lines are due to new layers due to intermolecular hydrogen bonds e.g. a plane with Miller indices of 120 has d = 4.45(1)Å and a plane with indices 012 has d = 4.27(1)Å. These sets of planes would give rise to lines which would not be expected of the MNA-2 and MNA-3 structures which do not possess intermolecular hydrogen bonds. Comparison of indices of equivalent planes is once more in agreement with the proposed transformation of MNA-2 to MNA-3 to MNA-1.

CHAPTER SIX

The infrared and Raman spectra of polymorphs of MNA and its deuterated derivatives.

Interpretation of the Infrared spectrum of the yellow triclinic form of 4-methyl-2-nitroacetanilide

1,2,4-trisubstituted benzenes have at most only the molecular plane of symmetry, and the fundamentals, apart from the additional vibrations of substituents, consist of 21 in plane vibrations (a') and 9 out-of-plane vibrations (a"). Examples of the interpretation of such spectra are presented in the collection of interpreted spectra by Varsanyi [199]. Green *et al.* have also interpreted several such spectra [200]. The present assignments are based on these works as well as on the shift of bands concomitant with the phase change and on the spectra of isotopically labelled compounds. The bands are listed in three tables, one assigning the fundamental frequencies associated with the benzene ring (Table 6.1), and the others listing the frequencies associated with the nitro group (Table 6.3) and with the amide group (Table 6.3). The vibrations are numbered according to the Mulliken notation [201], in order of decreasing wavenumbers for the a' modes followed by the a" modes. The Wilson nomenclature with reference to the Varsanyi scheme [202] is also used for the benzene ring modes.

Benzene ring modes

The weak but sharp absorptions between 3100 and 3000cm-1 were attributed to three aromatic C-H stretches expected in this region. The location of four of the C-C ring stretching and three of the C-H in-plane bending modes are located at frequencies within the accepted range for a 1,2,4-trisubstituted benzene derivative. The assignment of the C-X stretching vibrations in the region 1300-1200 cm-1 is difficult because of the broad absorption near 1240 cm-1. Bands at 1280 cm-1, 1210 cm-1 and 920 cm-1 are unaffected either by deuteration of the aromatic C-H groups or by deuteration of the N-H group. These bands have counterparts in the Raman spectrum and the strong Raman line at 1220 cm-1 is assigned to the vibration 7a in which the substituents vibrate in phase. The band near 1240 cm-1 which is strong in the Raman and infrared spectra is assigned to the amide III vibration.

The highest γ(CH) mode, 17b, is detected as a medium band in the infrared spectrum at 960 cm-1 and its position is confirmed by the combination bands in region 1750-2000 cm-1. The doublet near 880 cm-1 and the band at 828 cm-1 were also assigned to γ(CH) modes. Five bands due to radial skeleton vibrations were assigned on the basis that they were unaffected by ring or side chain

deuteration, both in the infrared and Raman spectra.

Nitro group frequencies

The assignments in Table 6.3 are based on well established values in the literature and in particular on those given by Green.[207]

Amide group frequencies

The strong band near 3370 cm-1 and the band near 1710 cm-1 which both appear as distinct doublets (separation 24 and 12 cm-1 respectively) were assigned to ν(NH) and ν(CO). On amide deuteration the doublet near 3370 cm-1 is replaced by doublet near 2500 cm-1. This ratio of the two wavenumbers (0.742) is close to that (0.707) expected for the behaviour of a pure N-H stretching vibration. The identification of bands corresponding to δ(NH) (Amide II) and γ (NH) (Amide V) has proved to be unexpectedly difficult. Some of the problems encountered were :-(a) some aromatic bands changed intensity and position slightly on amide deuteration, (b) the nitro group stretching vibrations obscured regions of interest and (c) more bands were observed in some regions of the spectra of deuterated compounds than was anticipated. The strong and broad band near 1460 cm-1 was assigned

the amide II band since (a) this band disappeared on amide deuteration and (b) a band at this position was observed in the spectra of other ortho-nitroacetanilides. The Amide III band was assigned to the band near 1240 cm-1 since the intensity of this band, which is strong in the infrared spectrum and very strong in the Raman spectrum, was markedly reduced on deuteration of the N-H group. The N-H out-of-plane bending vibration could not be assigned to one band. After amide deuteration the broad band near 650 cm-1 and the strong band at 600 cm-1 were replaced by a new band near 470 cm-1. Amide IV and Amide VI bands were assigned to the absorptions at 650 cm-1 and 590 cm-1 respectively.

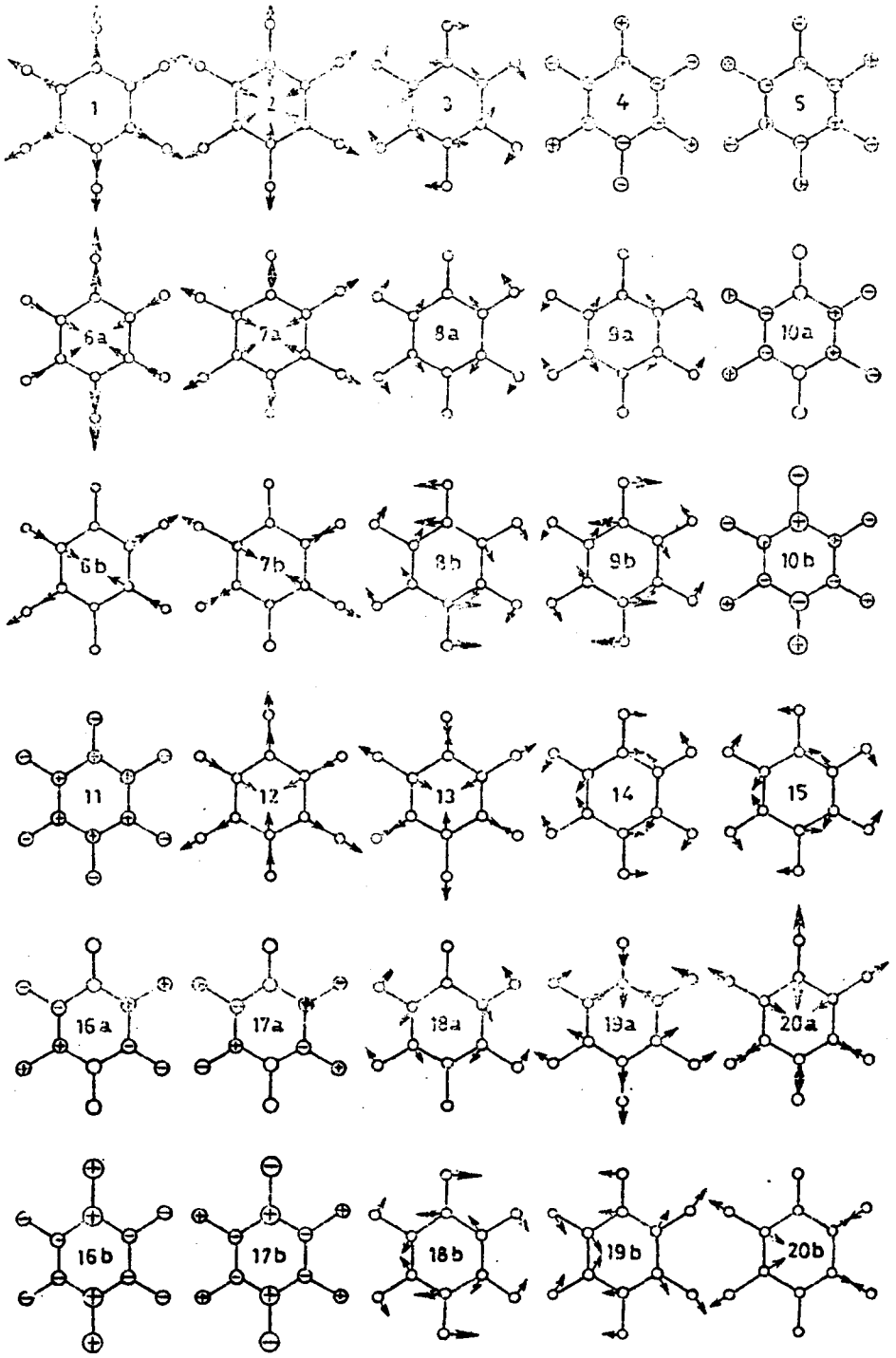

Normal vibrations of benzene

Fig. 6.1

Bands which appear as doublets are assigned to (a) N-H stretching, (b) C=O stretching and in-plane and out-of-plane bending (c) NO2 wagging (d) two of the three C-H in-plane bending vibrations, and (e) three out-of-plane bending vibrations of symmetry a". Of the above items, (a) and (b) can be explained on the basis that the yellow triclinic form consists of two distinct molecules whose amide groups are conjugated to the ring to different extents. Item (e) can be explained on the basis that the associated vibrations viz. 5, 4, and 16a all have N(1) and N(2) vibrating out-of-phase and out of plane of the benzene ring. This is presumably a reflection of a difference in interaction of the nitro and amide groups in the two types of molecules which is at a maximum in the out-of-plane vibrations. Item (c) can be explained if coupling between the NO2 wagging vibration and vibration 4 is assumed as stated by Varsanyi [203]. Since vibrations 15 and 18b, which involve in-plane C-H bending vibrations, also have N(1) and N(2) vibrating out of phase a similar explanation of the splitting of absorption bands is possible.

The spectrum of 4-methyl-2-nitroacetanilide at low temperature

X-ray diffraction studies on crystals of this compound have shown that the triclinic form has an asymmetric unit consisting of two molecules of 4-methyl-2-nitroacetanilide. The nitro group and amide group in each of these molecules lie in planes at different angles to the benzene ring in each case. Hence the doublet nature of N-H stretching could be explained on the basis of two amide groups which differ by virtue of their different conjugation to the benzene ring. The doublet nature of the band near 1700 cm^{-1} would be then explained on the same basis i.e. the two different amide groups would have different C=O stretching vibrations. Only one other closely spaced doublet is evident and this occurs near 888 cm-1. This is identified as due to a γ(C-H) mode since an overtone occurs at 2 x 888 = 1776. Also this band disappears on ring deuteration. This band is assigned to the out-of-phase vibrations of H(5) and H(6) (normal mode 5).

It is possible, therefore to account for three doublets but since the amide and nitro groups have several bands associated with them, other doublets should be present if the conformations of the amide and

nitro groups differ. When the infrared spectrum is recorded at 77K several bands are transformed into closely spaced doublets. These are the bands near 1150 cm-1 and 1080 cm-1 δ(C-H), 1040 cm-1 and 1000 cm-1 (CH_3 rocking), 760 cm-1 ($\gamma_s NO_2$) and 530 cm-1 (δNO_2), 700 cm-1 (normal vibration 4 which may be coupled to a NO_2 vibration [203], 640 cm-1 and 590 cm-1 (δC=O and γC=O respectively). There is no evidence for the doubling of bands due to Amide II and Amide V. Since the ring stretching and bending modes do not occur as doublets in the low temperature spectrum these vibrations can be distinguished from others due to substituent groups.

The low temperature spectrum of the white form of MNA contained sharper bands than that obtained at ambient temperature but no splitting of bands occurred.

A spectrum of the yellow monoclinic form of MNA could not be obtained at 77K. The unstable monoclinic form partially changed to the yellow triclinic form and hence a spectrum of a mixture of polymorphs was obtained. However, examination of the spectrum revealed that certain bands, particularly those associated with the nitro group, were slightly different in the two yellow forms **and this is accordance with the nitro groups in MNA-2 and MNA-3 having minor differences of conjugation with the benzene ring.**

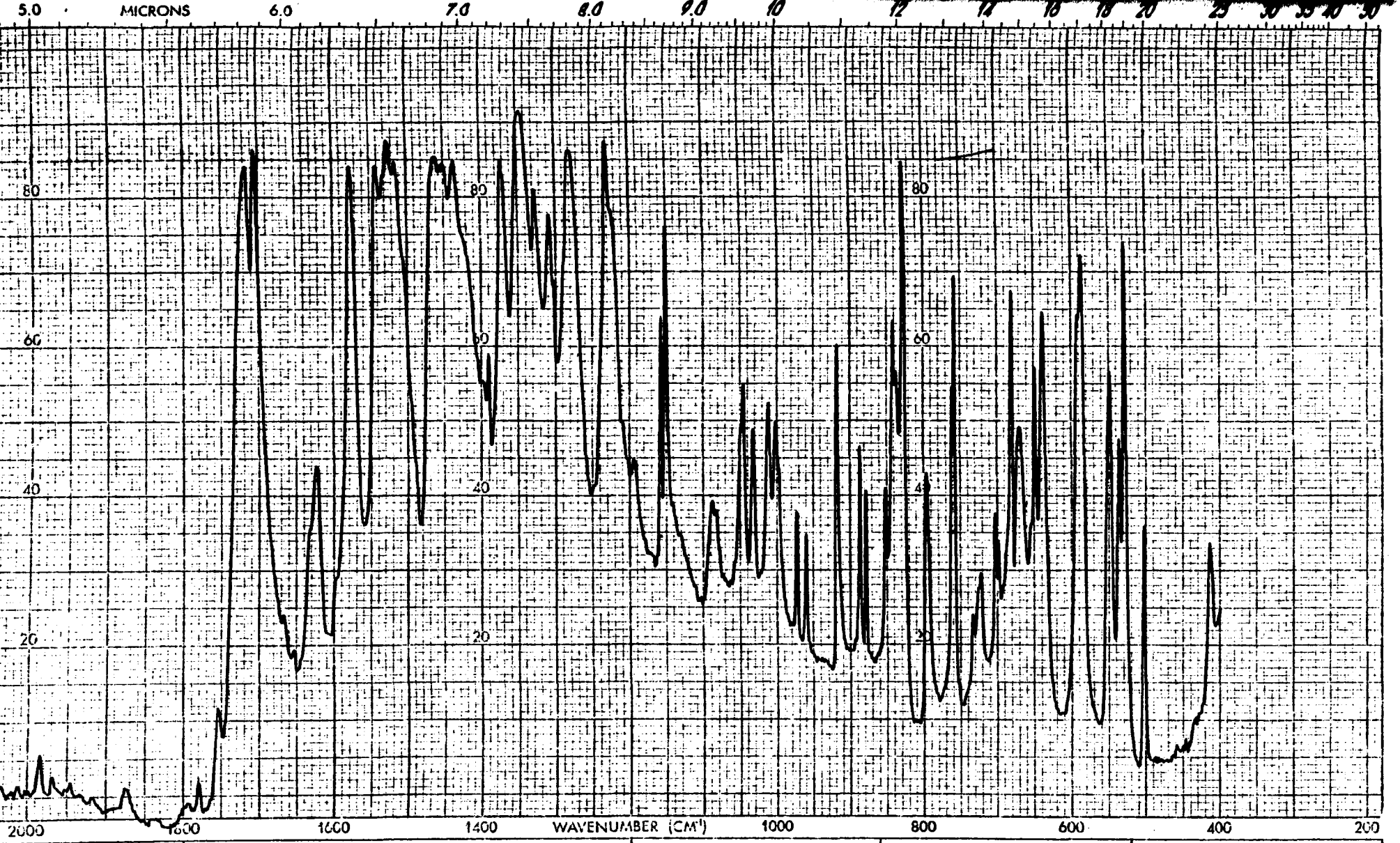

REMARKS "Yellow" Form 77K.

MNA-3 in nujol (Liq. N₂)

1458 N ↑ 1378 N

INT. SCAN MODE 6

SCAN TIME 20

RESOLUTION 1.4.

T. ✓ A. S.B.

ORDINATE EXP.

OPERATOR RWS DATE 9-2-82

CHART No. 5101-3600

REF. No.

Perkin Elmer 580B

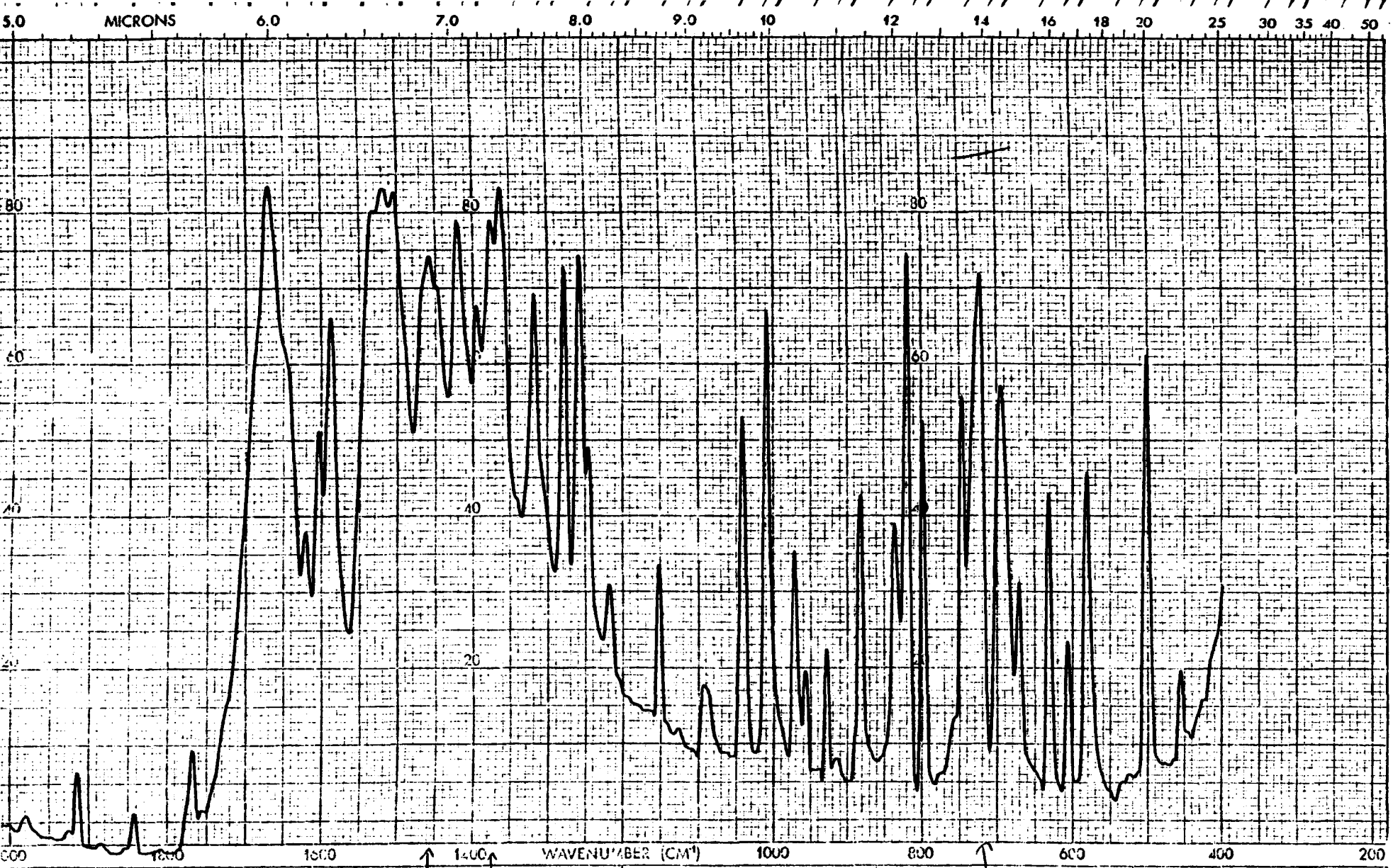

Perkin Elmer 580B

The infrared spectrum and Raman spectrum of the amber form of MNA

The amber form showed bands in the infrared spectrum at very nearly the same wavenumbers as the corresponding ones in the spectrum of the yellow triclinic form. The differences, although small, were measurable since an infrared spectrum of a mixture of amber and yellow forms was obtained at 77K. It proved impossible to obtain an infrared spectrum of the amber form at 77K. In the spectrum of the mixture several peaks occurred as closely spaced doublets and their significance will be discussed later. It was possible to obtain a spectrum of the amber form in a potassium bromide disc providing the grinding period was of the order of a few seconds.

However certain differences were evident. The band due to ν(N-H) now appears as a single band indicating only one type of NH group. The band near 1710 cm-1 due to ν(C=O) appears as a closely spaced doublet (separation 10 cm-1) presumably due to crystal field splitting. The crystal structure is such that C=O groups are only 3.5 Å apart across a centre of inversion. Hence the ν(C=O) band may be split into asymmetric and symmetric components. This idea is supported by the strong line

in the Raman spectrum at 1710 cm-1 and the absence of a line at 1720 cm-1.

The bands at 1530 cm-1 and 1340 cm-1 due to the $N-O_2$ stretching vibration in the nitro group are less intense. The γ(C-H) mode at 892 cm-1 now appears as a single line and that at 828 cm-1 is greatly reduced in intensity. The band due to γ(N-H) now has its maximum absorption at 680 cm-1 so that this broad band is nearly symmetrical (except for a shoulder at 660 cm-1).

The infrared spectrum of the amber form is in accordance with the presence in the crystal, of only one type of molecule, which contains an intramolecular hydrogen bond.

A summary of the changes in appearance of the infrared spectrum of yellow and white forms of MNA

Although infrared spectroscopy has been used to characterise polymorphic forms of steroids[204], and other compounds of pharmaceutical interest[205], only minor differences between the spectra of the polymorphs have been apparent. However, in the case of MNA, the infrared spectra of the yellow and white forms appear at first glance to be quite different. Changes in intensities of bands have occurred and certain bands have appeared in new positions and some bands have apparently disappeared. Since the yellow form changes to the white form on standing the following discussion will assume a change of yellow to white form occurring.

Bands due to ν(C-H) decrease whereas those due to ν(C-X) vibrations increase slightly as if the substituents, which may be regarded as point masses, decrease in mass. The bond order of C(1)-N(1) and C(2)-N(2) which decreases during the observed change is not the major factor involved.

The positions of bands due to vibrations involving the C-H in-plane and out-of-plane bending vibrations do not change. A similar situation applies to the radial

skeletal vibrations. The out-of-plane ring bending vibrations (16a and 16b) appear to move to lower wavenumbers indicating a rather less rigid ring system. As a general comment the bands due to the benzene ring become sharper although they lose some intensity and their position is hardly affected.

The positions of bands due to the nitro group are also hardly affected inspite of the loss in conjugation between the nitro and amide groups. Comparison of the νas and νs wavenumbers reveals that the former has decreased and the latter has increased (this conclusion is based on the more accurate Raman wavenumbers). Such a conclusion was reached by Murray et al. regarding the effect of steric hindrance on such vibrations[206]. The slight upward shift on the νs band is also in accordance with reduced conjugation as stated by Varsanyi[203] (p389). This slight increase is also in accordance with the model of an in-plane vibration of the oxygen atoms rather than a C-N stretching vibration.

The downward shift of the δs vibration could be due to loss of coupling with $\nu 25$ (vibration 4) whilst the increase in the δas vibration is most likely due to steric hindrance. The value for the latter vibration (near 580 cm-1) is very close to those of o-nitro

compounds investigated by Green[207].

The most easily recognised changes are those associated with the amide group. The intense doublet near 3380 cm-1 becomes the broad band near 3250 cm-1. This value is typical for the N-H stretching band in an anilide[13]. The increase in intensity and broadening is in accordance with the formation of a stronger intermolecular hydrogen bond. The value of 1670 cm-1 is typical of the νC=O in anilides[13] and again the change from 1720 cm-1 to 1670 cm-1 is accounted for by a stronger hydrogen bond being formed.

The location of the band which can be ascribed to AMIDE II, which is mainly δ(N-H) with ν(C-N), is not straightforward in either case. As mentioned in the introductory work, the interpretation of this and the AMIDE III band has been the subject of numerous investigations. In the yellow form, a broad band near 1450 cm-1 disappears on deuteration (N-H to N-D). This value would be low for the AMIDE II band and also a band due to C-C ring stretching (19b) is expected in this region. However, it has been shown by Miyazawa[4], that this band and the AMIDE III band is sensitive to changes of state. For example, the wavenumbers of these bands in N-methylacetamide, increase by 67 and 39

cm-1 respectively on changing from a nonpolar solvent to the liquid form. Therefore the low values quoted for the AMIDE II and III bands may be a reflection of the weak intramolecular hydrogen bond and the complete absence of any hydrogen bond to the carbonyl group in the yellow form. On changing to the white form the AMIDE II and III bands increase to positions normally associated with anilides. Hence the broad band at 1450 cm-1 shifts to near 1530 cm-1 so that this band becomes broad and intense and the AMIDE III band shifts to a lower position at 1260 cm-1. A more detailed account of the results of N-H deuteration follows in the next section.

The wavenumber of the broad band due to γ(N-H) increases to about 700 cm-1. Here this band couples with a ring bending mode (both of symmetry a") and two broad bands result. It is not clear whether the γ(N-H) vibration in the yellow form is associated with two bands or not since it is such a wide band and covers other aromatic vibrations. If present, these two bands would imply different γ(N-H) vibrations for the two types of molecules in the yellow triclinic form. There is some evidence from the spectrum of the N-D compound that two γ(N-D) bands occur. If present, one vibration would occur at 680 cm-1 and this band is clearly revealed in the low temperature spectrum and the other one would be

assigned to the shoulder at 630 cm-1.

The bands assigned to AMIDE IV and VI change little and this is the expected result for an increase in hydrogen bonding [4].

In the spectrum of the yellow and white forms several bands due to combinations of frequncies can be seen. Three of these viz. 1780,1845, and 1920 cm-1 can be accounted for by combinations of γ(C-H) wavenumbers (2 x 885, 885 + 960, 2 x 960). In many amides an overtone is present near 3100 cm-1 and this has been assigned (and criticised) to 2 x AMIDE II [13]. In all of the polymorphs of MNA a combination band near 3000 cm-1 may be accounted for either by 2 x AMIDE II or by ν(C=O) + 2 x γ(N-H). The latter combination has the advantage of explaining the position of the overtone near 3100 cm-1 in lactams which do not have an AMIDE II band near 1550 cm-1.

Analysis of the spectra of deuterated forms of MNA

Several deuterated forms of MNA were prepared in order to fulfil some of the following objectives:-

1. analysis of the spectra of deuterated compounds would aid in the interpretation of the spectra of normal polymorphic forms of MNA.

2. the deuterated forms were examined to see if they existed in equivalent polymorphic forms.

3. the ability of the deuterated forms to undergo a phase change equivalent to yellow triclinic changing to white monoclinic was examined.

4. The position of the AMIDE II and AMIDE III bands in the yellow forms was not clear. Comparison of the changes occurring with those reported for other amides should aid in the determination of the positions of the amide bands.

The following deuterated MNA derivatives were prepared

(only the position of the deuterium is specified; all other R = H)

a) $^{1}R = D$

b) $^{2}R = D$

c) $^{3}R = D$

d) ^{3}R and $^{4}R = D$

Changes in the infrared and Raman spectra upon amide deuteration of MNA-3.

1. The doublet at 3382 and 3358 cm-1 has been replaced by one at 2520 and 2500 cm-1.

2. the position of the strong doublet near 1700 cm-1 has shifted slightly to lower wavenumbers.

3. the band at 1445 cm-1 has disappeared.

4. a new strong band has appeared at 1380 cm-1.

5. the intense peak at 1230 cm-1 has been replaced by two peaks of medium intensity at 1215 cm-1 and 1230 cm-1.

6. a shoulder has appeared on the band at 1085 cm-1.

7. it appears that the medium band near 1000 cm-1 has

shifted to 970 cm-1.

8. a weak to medium band has appeared at 900 cm-1.

9. the shoulder at 836 cm-1 has shifted to become a stronger peak at 822 cm-1.

10. the broad peak around 650 cm-1 has disappeared.

11. the strong peak at 600 cm-1 has been greatly reduced in intensity.

12. the intensity of the strong band at 530 cm-1 has been reduced.

13. medium and strong broad bands have appeared at 485 and 462 cm-1

The following changes in the Raman spectrum of the yellow triclinc form are itemised below:-

1. a new doublet appears at 2470 and 2460 cm-1.

2. the very strong band at 1235 cm-1 has almost completely disappeared.

3. a new sharp band has appeared at 1100 cm-1.

4. a new weak band has appeared at 1060 cm-1.

5. a weak to medium band has appeared at 980 cm-1.

6. a strong band has appeared at 908 cm-1.

7. a band of medium intensity has appeared at 530 cm-1.

These changes in the infrared and Raman spectra are ones which are associated with the changes in the amide group and the wavenumbers of amide and N-deuteroamide correlations are listed in Table 6.5 . The position of bands due to the nitro group hardly change. Some bands, which are associated with the benzene ring, change with regard to position and intensity. For example, the band at 1578 cm-1, decreases in intensity and shifts to 1565 cm-1. Also the band at 1300 cm-1 intensifies whilst the very strong band at 530 cm-1 apparently decreases in intensity. The broad band near 1520 cm-1 sharpens to a marked degree. Such changes complicate the interpretation and it has been only possible to assign the amide bands with confidence after studying the deuteration of amide groups in several other intramolecularly hydrogen bonded amides. The spectra of these amides are discussed in a later section of this chapter.

Some of the difficulties which occur with the interpretation of these spectra are now listed :-

a) The position of the AMIDE II band could be either near 1580 cm-1, or 1520 cm-1 or 1445 cm-1 since

changes occur at all of these positions and it is well known that the position of the band due to δ(N-H) in amines is difficult to locate .

b) several bands overlap in the 1230 cm-1 region.

c) there are more bands appearing in the region 1100 cm-1 to 900 cm-1 than can be accounted for by simply assuming that the AMIDE III' would now be expected to occur in this region.

d) complex changes occur in the region of 500 cm-1 other than the expected one of the appearance of the AMIDE V' band.

All subsequent i.r. spectra were recorded on a Perkin Elmer 683 infrared spectrophotometer using the potassium bromide disc technique.

Raman spectra were recorded on a Spex Ramalab laser spectromer using finely powdered samples in the solid state.

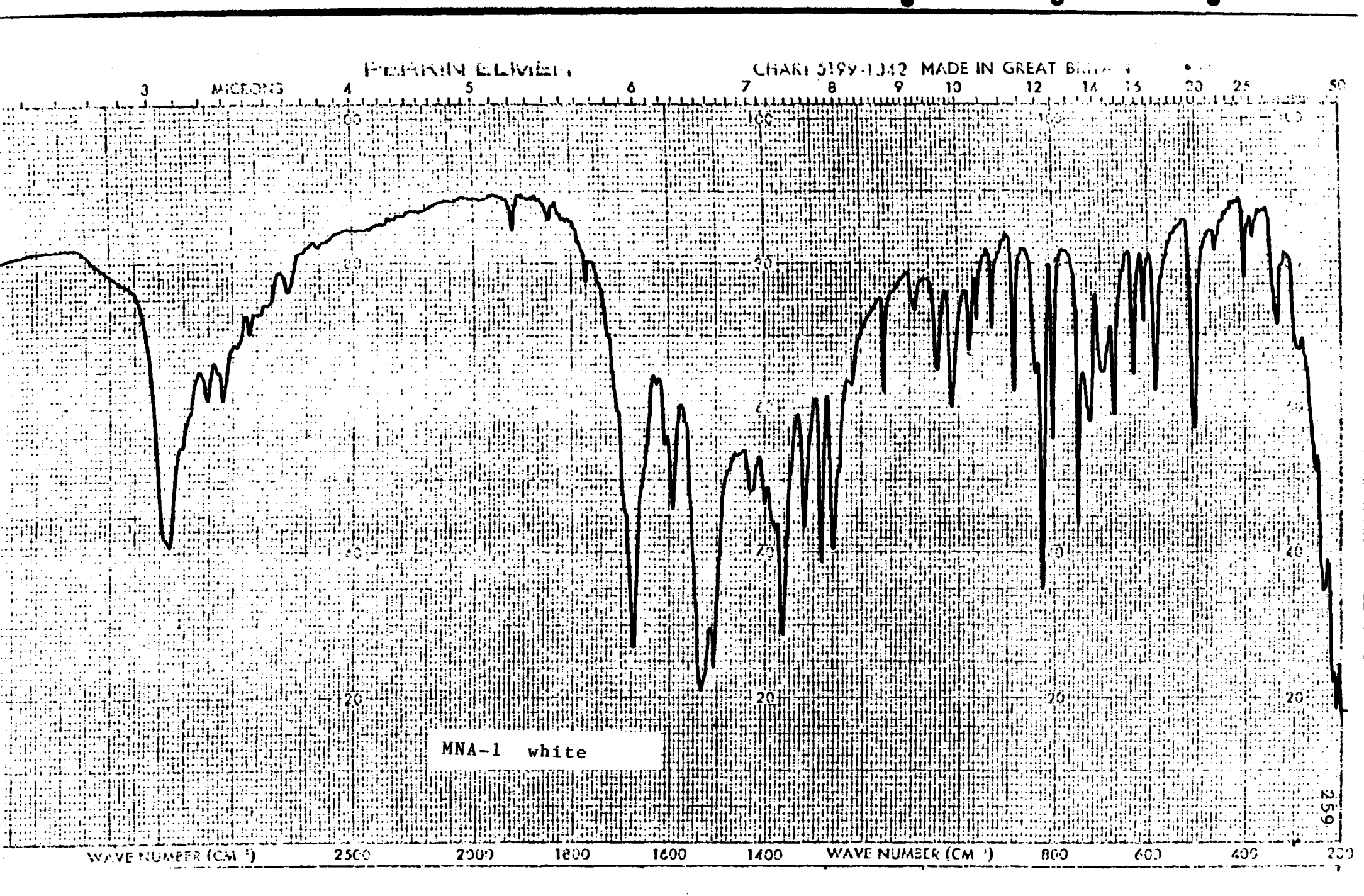
PERKIN ELMER
CHART 5199-1342 MADE IN GREAT BRITAIN
3 MICRONS 4 5 6 7 8 9 10 12 14 15 20 25 50
100 80 60 40 20 0
MNA-1 white
2.59
WAVE NUMBER (CM⁻¹) 2500 2000 1800 1600 1400 WAVE NUMBER (CM⁻¹) 800 600 400 200

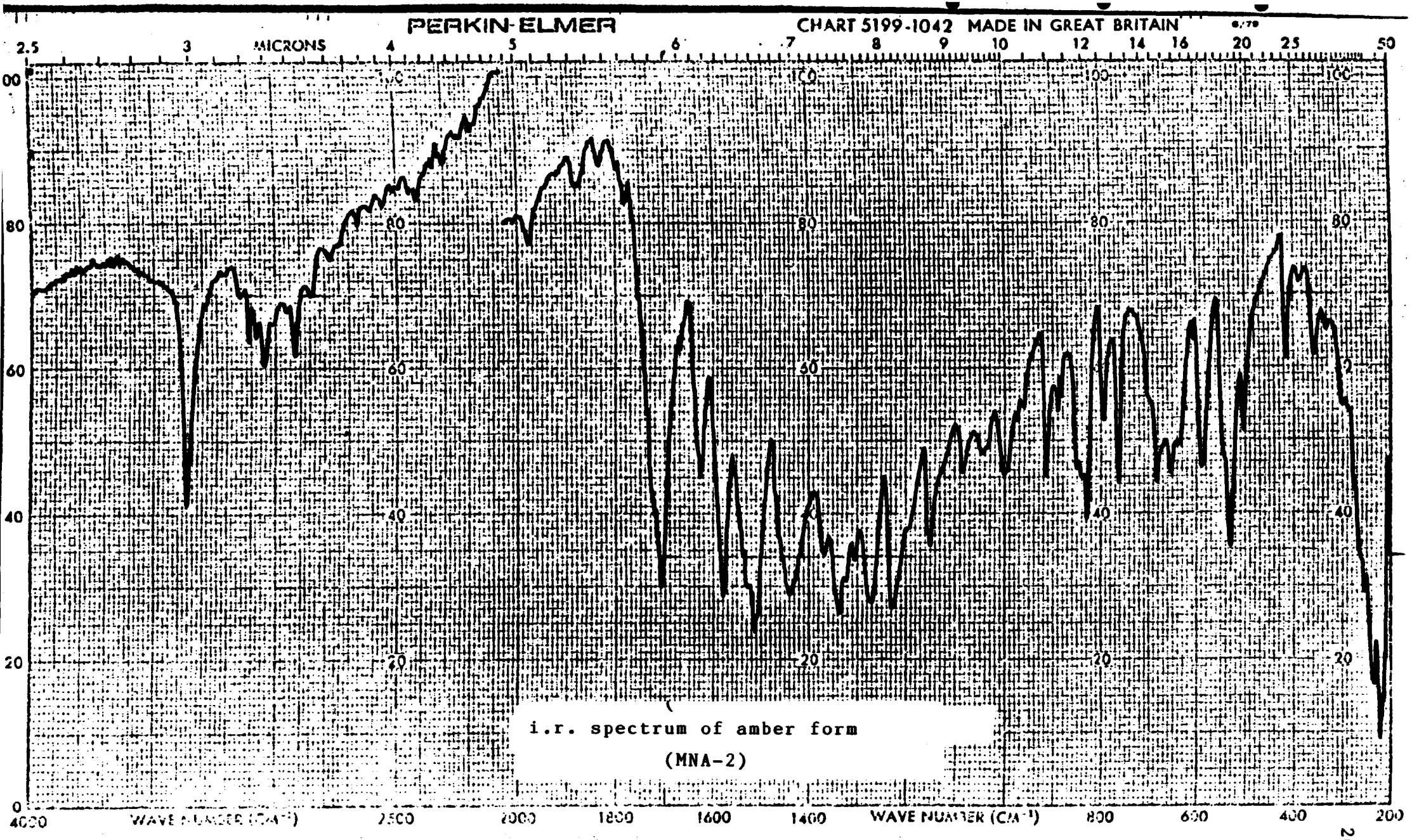

i.r. spectrum of amber form

(MNA-2)

260

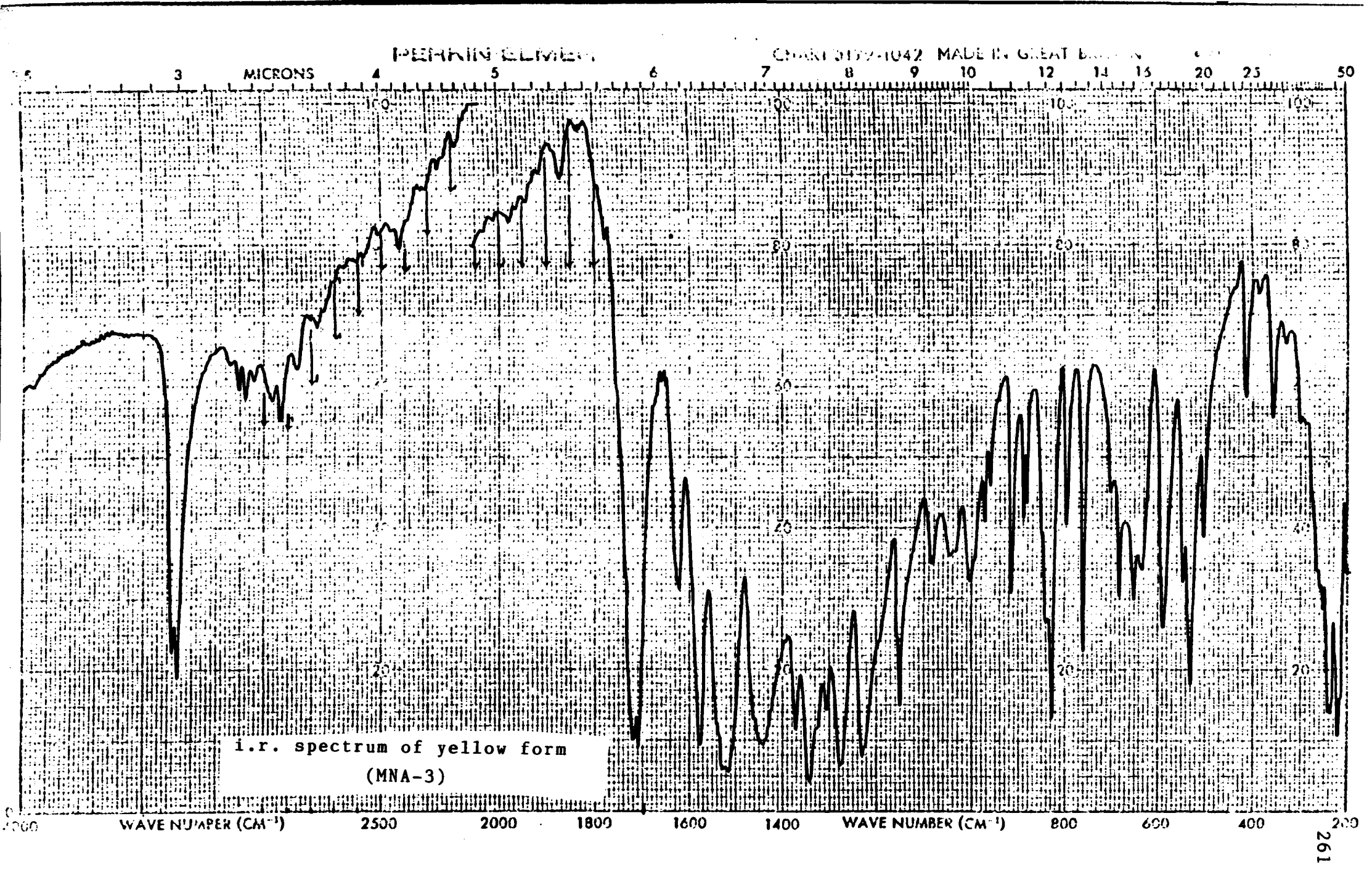

i.r. spectrum of yellow form

(MNA-3)

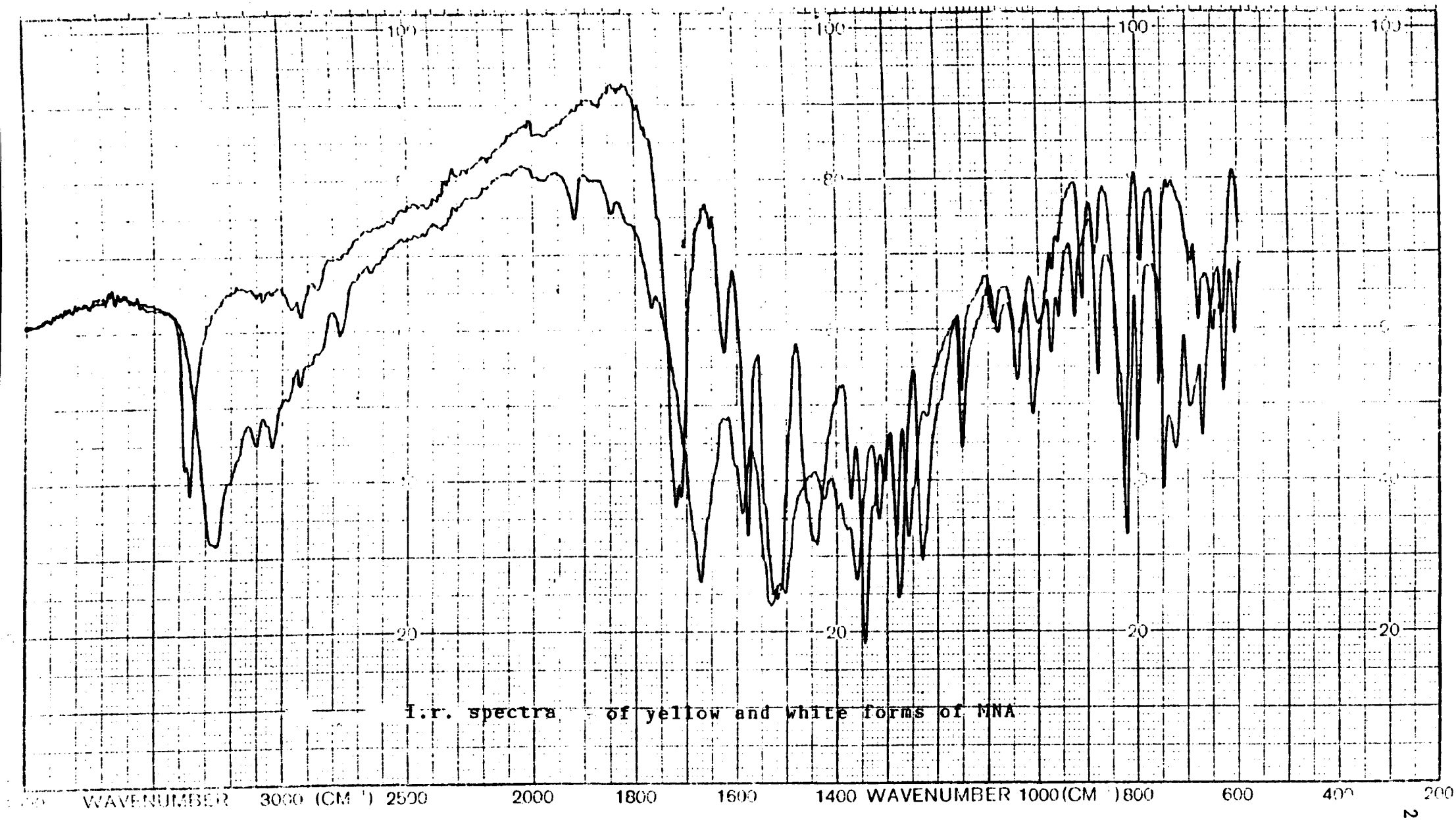

i.r. spectra of yellow and white forms of MNA

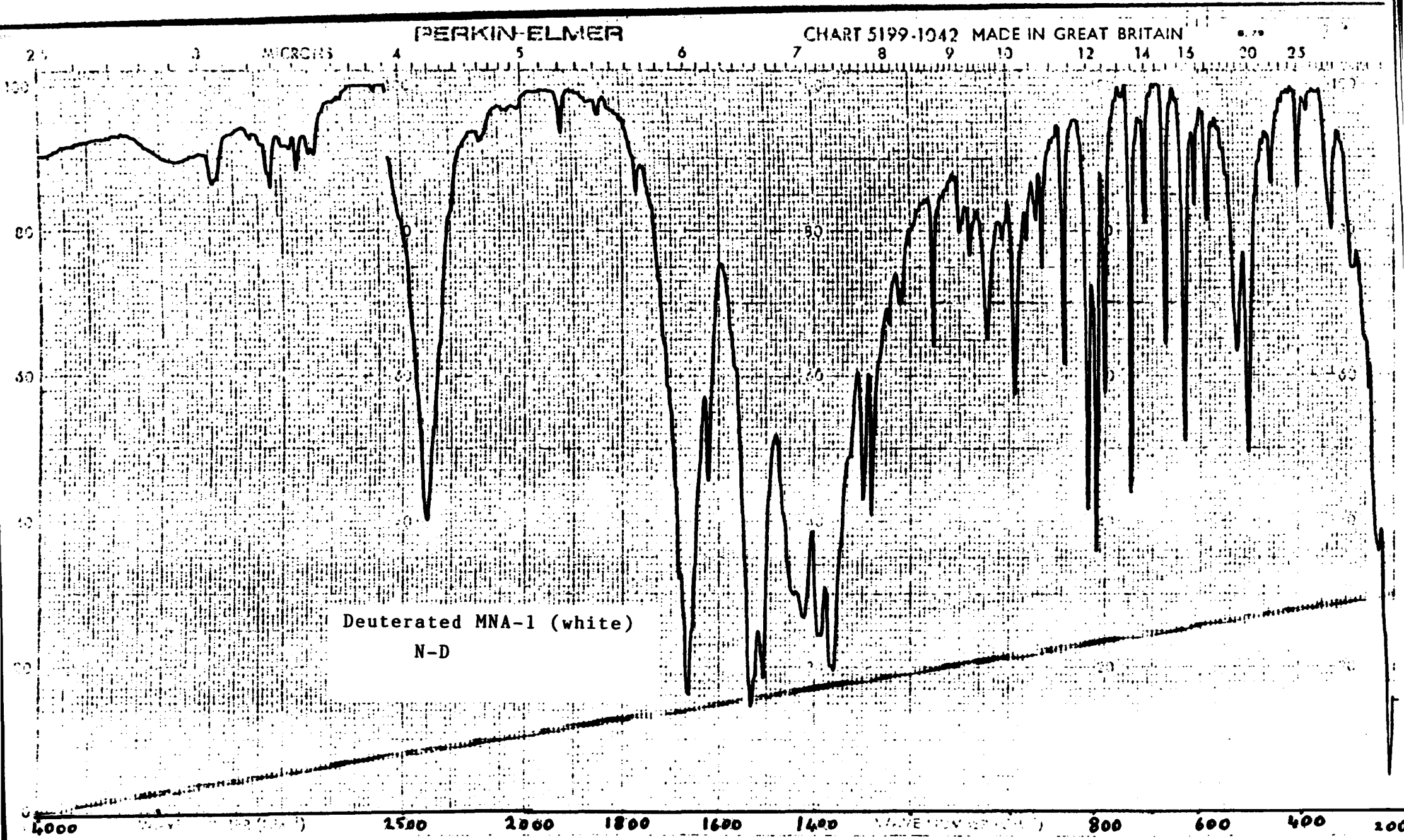
PERKIN-ELMER
CHART 5199-1042 MADE IN GREAT BRITAIN
MICRONS
2
3
4
5
6
7
8
9
10
12
14
15
20
25
100
80
60
40
20
0
Deuterated MNA-1 (white)
N-D
4000
2500
2000
1800
1600
1400
800
600
400
200

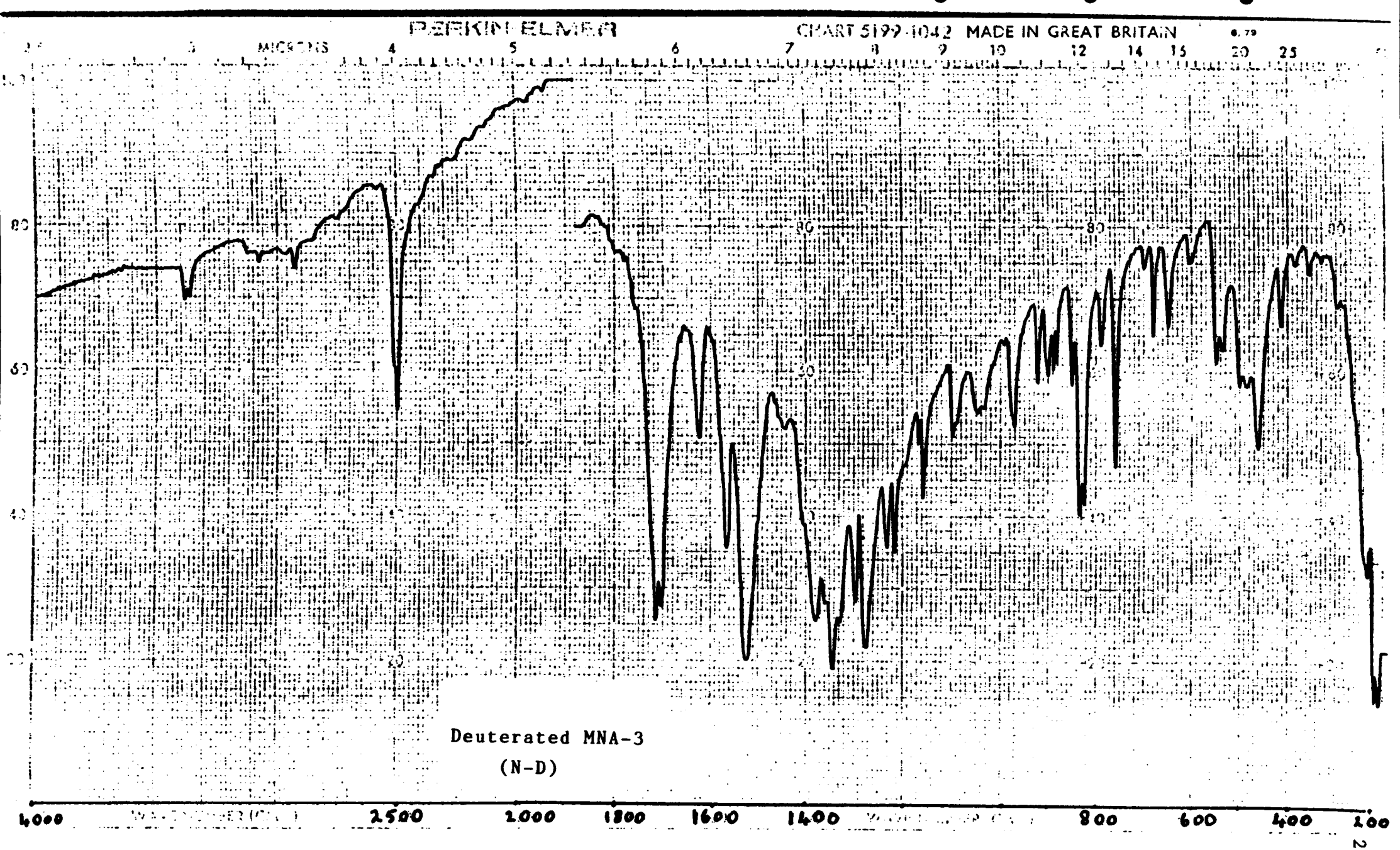
PERKIN ELMER
CHART 5199-1042 MADE IN GREAT BRITAIN
MICRONS
4
5
6
7
8
9
10
12
14
15
20
25
Deuterated MNA-3
(N-D)
4000
2500
2000
1800
1600
1400
800
600
400
200

Raman spectrum of MNA-1 (white)
208
292
346
384
393
440
560
512
612
632
676
725
743
828
848
920
980
1018

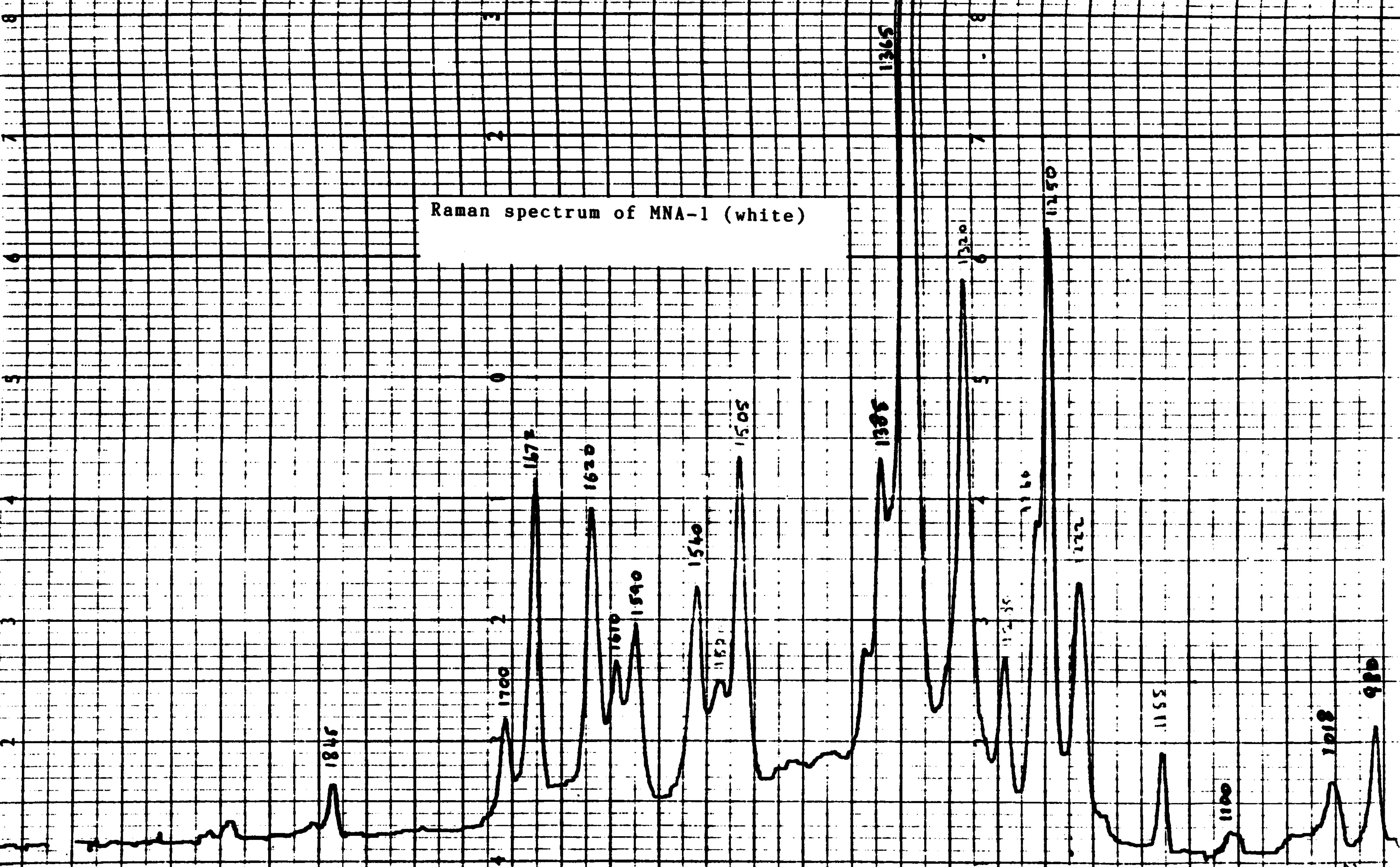

RAMAN SPECTRUM WHITE MNA

Raman spectrum of MNA-3 (yellow)

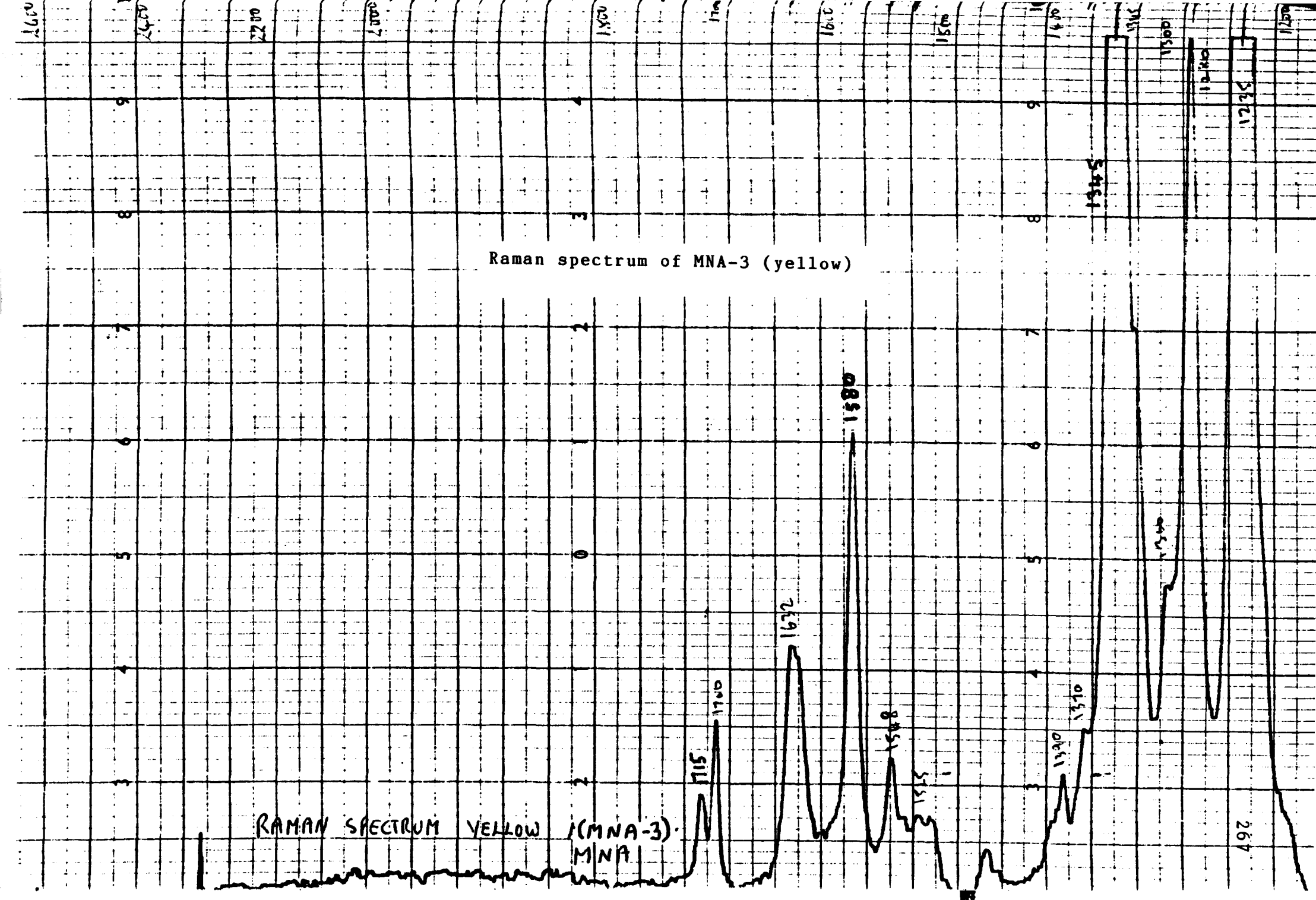

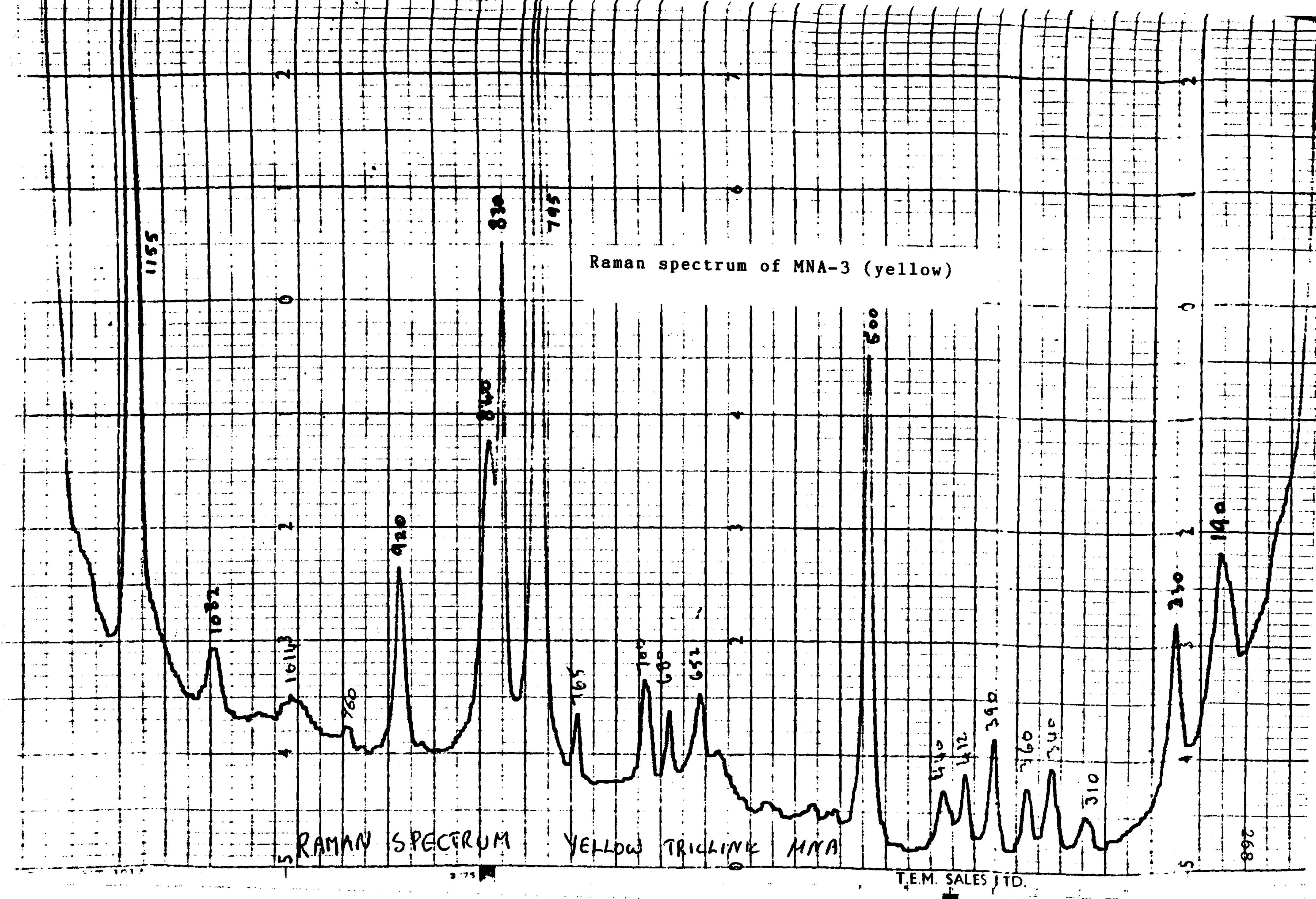

Raman spectrum of MNA-3 (yellow)

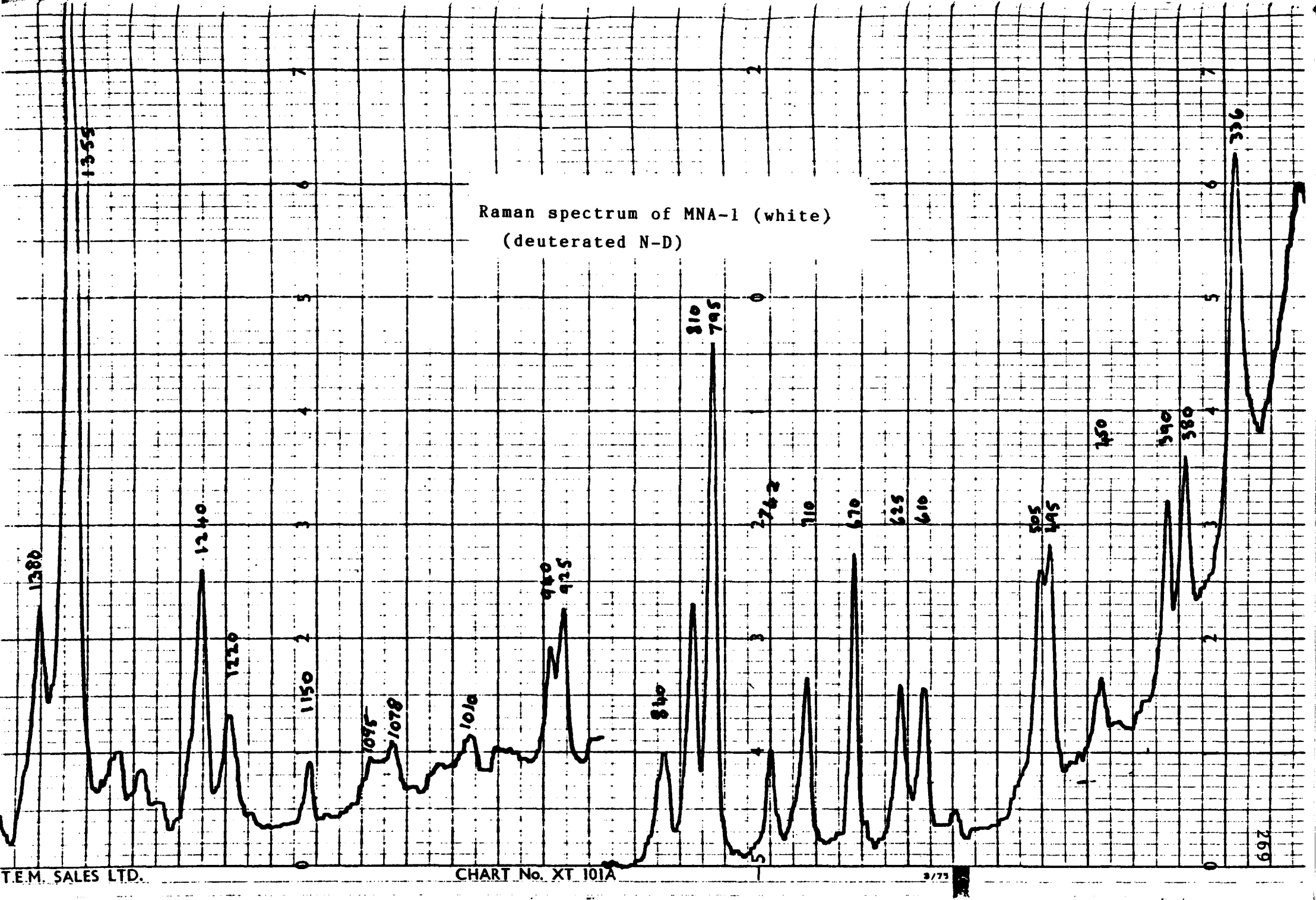
Raman spectrum of MNA-1 (white)
(deuterated N-D)
1355
1380
1240
1220
1150
1045
1078
1010
940
925
840
810
795
742
710
670
625
610
505
495
450
390
380
336
269
T.E.M. SALES LTD.
CHART No. XT 101A
3/73

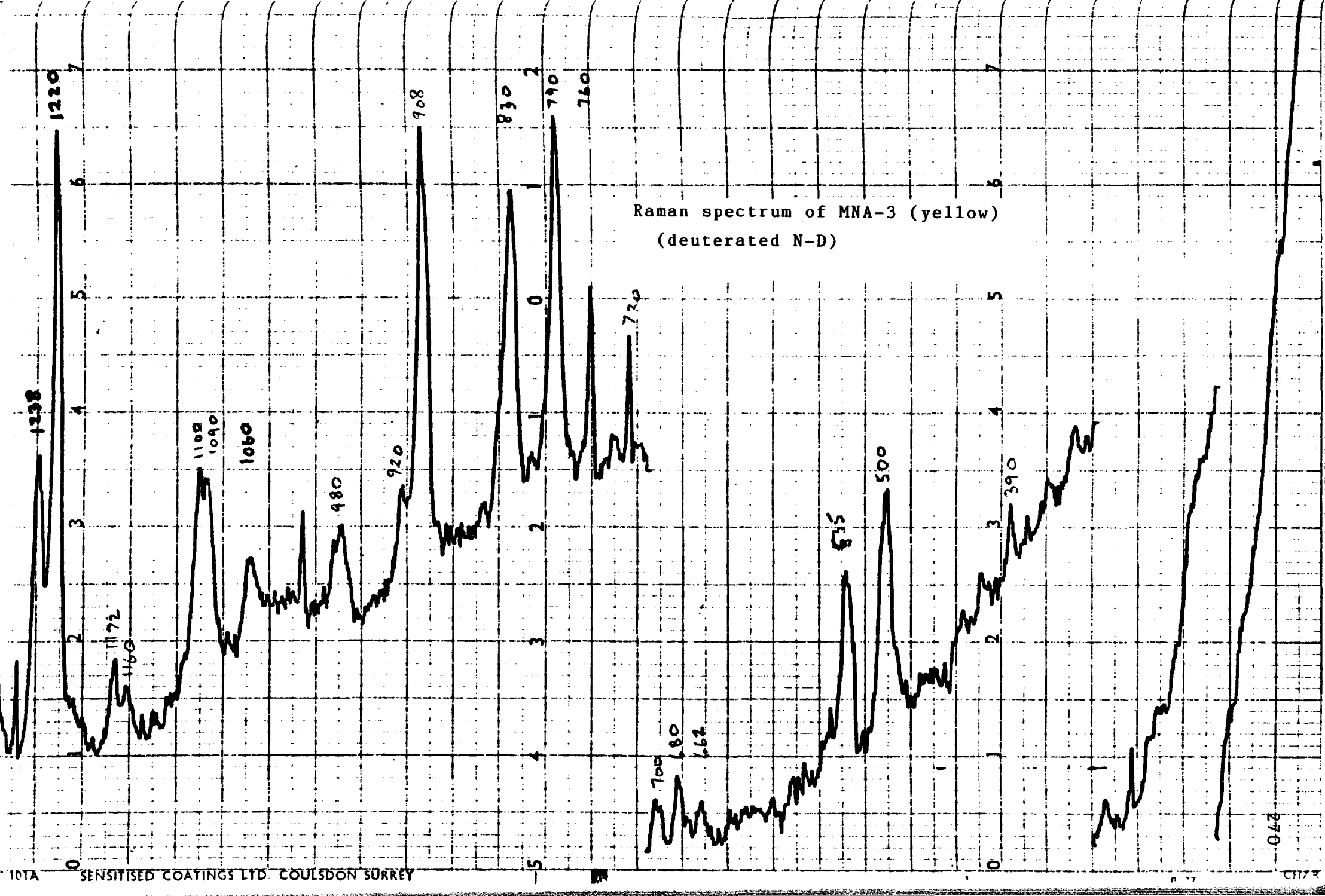
Raman spectrum of MNA-3 (yellow)
(deuterated N-D)
1220
1238
1172
1160
1109
1090
1060
980
920
908
830
790
760
730
700
680
664
565
500
390
270
SENSITISED COATINGS LTD COULSDON SURREY

Fundamental frequencies for yellow and white MNA

		yellow		white		Wilson
a'	ν_1	3108	-	3100	-	20a
	ν_2	3080	3070	3065	3070	2
	ν_3	3040	3055	3035	-	20b
	ν_4	1622	1630	1605	1610	8b
	ν_5	1578	1580	1588	1590	8a
	ν_6	1525	1525	1505	1505	19b
	ν_7	1460	1460	1450	-	19a
	ν_8	1310	1300	1320	1320	3
	ν_9	1280	1280	1280	1285	14
	ν_{10}	1220	-	1245	1250	7a
	ν_{11}	1210	-	1218	1222	13
	ν_{12}	1150	1155	1155	1155	15
	ν_{13}	1085	1082	1090	1100	18b
	ν_{14}	920	920	930	930	7b
	ν_{15}	796	795	800	800	12
	ν_{16}	680	680	670	676	1
	ν_{17}	500	500	500	500	6a
	ν_{18}	430	440	455	460	6b
	ν_{19}	390	390	380	382	9b
	ν_{20}	360	360	340	340	9a
	ν_{21}	230	230	230	224	18a
a''	ν_{22}	960	960	958	-	17b
	ν_{23}	885	-	882	-	5
	ν_{24}	828	830	820	828	11
	ν_{25}	700	700	715	725	4
	ν_{26}	530	-	500	-	16a
	ν_{27}	412	412	400	398	16b
	ν_{28}	300	300	290	292	10a
	ν_{29}	-	-	-	-	10b
	ν_{30}	-	-	-	-	17a
		i.r.	Raman	i.r.	Raman	

Table 6.1 The in-plane (a') and out of plane (a'') vibrations of MNA

Fundamental frequencies for amber MNA (MNA-2)

		i.r.	Raman
a'	ν_1	3110	-
	ν_2	3080	-
	ν_3	3045	-
	ν_4	1625	1630
	ν_5	1580	1580
	ν_6	1515	1510
	ν_7	-	1460
	ν_8	1305	1310
	ν_9	1275	1275
	ν_{10}	1215	-
	ν_{11}	1195	1198
	ν_{12}	1155	1158
	ν_{13}	1085	1090
	ν_{14}	912	918
	ν_{15}	790	795
	ν_{16}	680	680
	ν_{17}	500	500
	ν_{18}	-	-
	ν_{19}	380	390
	ν_{20}	345	-
	ν_{21}	-	230
a''			
	ν_{22}	965	-
	ν_{23}	894	-
	ν_{24}	828	-
	ν_{25}	-	-
	ν_{26}	530	-
	ν_{27}	412	-
	ν_{28}	300	-
	ν_{29}	-	-
	ν_{30}	-	-

Table 6.2
The in-plane (a') and out-of-plane (a'') vibrations of MNA-2 (amber form).

Table 6.3

Assignments of the bands due to the nitro, amide and methyl groups in yellow (MNA-3) and white (MNA-1)

	yellow		white	
Nitro group				
	i.r.	Raman	i.r.	Raman
ν_{as}	1542	1548	1530	1540
ν_{s}	1347	1345	1362	1365
δ_{s}	840	840	848	848
γ_{s}	762	765	748	748
δ_{as}	550	550	580	585
Amide group				
ν NH	3382	3390	3250	3265
ν NH	3358	3320		
ν CO	1720	1715	1670	1672
ν CO	1708	1710		
Amide II	1445		1520	1520
Amide III	1230	1235	1320	1320
δCO	645	652	630	632
γNH	680	680	725,695	725
γCO	592		608	612
ν C-CH_3	918	920	980	980
Methyl groups				
(i) acetyl methyl group				
ν_{as}			2980	2988
ν_{s}	2930	2935		2930
δ_{s}	1372	1370	1380	1385
r$\perp$	1045,1032	-	1040	-
r //	1010,1000	1014	1014	1018
(ii) 4-methyl group				
δ_{s}	1390	-	1395	1395
r //	972	-	972	980

Table 6.4

Assignments of bands to the nitro, amide, and methyl groups in the amber form. (MNA-2)

	i.r.	Raman
Nitro group		
ν_{as}	1530	1535
ν_{s}	1340	1340
δ_{s}	850	840
γ_{s}	768	-
δ_{as}	540	-
Amide group		
νNH	3360	3370
νCO	1720,1710	1710
Amide II	1435	-
Amide III	1230*	1230
δCO	658	660
γNH	670	-
γCO	595	-
$\nu C-CH_3$	915	918
Methyl groups		
(i) acetyl		
ν_{as}	2950	-
ν_{s}	2920	2930
δ_{s}	1362	-
$r_{\perp}$	1045	-
r//	992	1000
(ii) 4-methyl		
δ_{s}	-	1390
r//	-	-

* exact position uncertain due to overlap of bands

Assignments of bands due to the amide groups in deuterated (N-D) yellow (MNA-3) and white (MNA-1) forms.

Vibration	Yellow	White
νN-D	2520	2400
	2500	
amide I	1720	1665
	1700	
amide II'	1380	1420
amide III'	1085	1080
amide V'	460	530
r // CH_3	980	990
νC-C	900	945

The assignment of two of the bands given above was assisted by the corresponding Raman spectra

amide III'	1100(m)	1078(m)
νC-C	908(s)	940(m)

Since the bands assigned to the CH_3 rocking vibration and νC-C are sensitive to deuteration it is concluded that these vibrations are coupled to δN-D.

Table 6.5

The infrared and Raman spectrum of deuterated white monoclinic MNA

The changes in the infrared spectrum of white monoclinic MNA accompanying deuteration are as follows:-

1. a broad band at 2400 cm-1 replaces the strong band at 3250 cm-1.

2. the band of medium intensity at 1590 cm-1 disappears.

3. a broad band with a shoulder appears at 1420 cm-1.

4. the band at 1390 cm-1 intensifies.

5. the band at 1320 cm-1 becomes obscured by the broading of the band around 1350 cm-1.

6. the complex band at 1260 cm-1 decreases in intensity and closely spaced bands at 1245 cm-1 and 1220 cm-1 remain.

7. new bands at 1178 cm-1 and 944 cm-1 appear whilst the medium band at 1014 cm-1 apparently shifts to give a medium band at 988 cm-1.

8. the strong band at 820 cm-1 separates into two sharp bands at 835 cm-1 and 818 cm-1.

9. the two broad bands at 725 cm-1 and 695 cm-1 are replaced by a strong broad band at 525 cm-1

These changes can be explained by the following points:-

a) the major changes are associated with N-H becoming N-D so that the amide bands change.

b) the nitro group bands do not change position.

c) some bands due to ring vibrations shift and change in intensity viz. the bands at 1588 cm-1 which becomes a less prominent shoulder at 1570 cm-1, the broad band around 1520 cm-1 sharpens and the band at 1245 cm-1 which appears as a shoulder becomes a weak but sharp band at 1242 cm-1. The latter band which is strong in the Raman spectrum has been assigned to an in-phase C-X stretching vibration. A new band appears at 715 cm-1 which is sharp and is of medium intensity. Presumably this band is due to an out-of-plane ring vibration which couples with the γ(N-H) vibration.

The changes in the Raman spectrum on deuteration of the white form are as follows:-

1. a weak broad band appears at 1420 cm-1.

2. the strong band at 1320 cm-1 and medium band at 1260 cm-1 are greatly reduced in intensity.

3. bands of weak to medium intensity appear at 1078 cm-1 and 940 cm-1

4. the weak to medium bands at 1018 cm-1 and 980 cm-1 almost disappear.

5. the band at 828 cm-1 intensifies and shifts to 810 cm-1.

6. the broad band at 725 cm-1 becomes narrower and shifts to 710 cm-1.

Some problems of assignment exist. For example, the position of the AMIDE II band could be either at 1588 cm-1 or amongst the broad absorption near 1520 cm-1. Also the AMIDE III band position is obscured by other bands near 1240 cm-1. Also, as in the case of the yellow form, more bands occur in the 1100 cm-1 to 900 cm-1 range than might be expected from the possible appearance of a new AMIDE III' band. The final assignments of the amide bands were based on the following evidence:-

a) assignments made by Miyazawa[3] on N-methylacetamide

b) assignments by Chalapathi and Ramiah[25] on acetanilide

c) examination of the spectra of several anilides and their N-D derivatives, and

d) an examination of the spectra of several trideuteroacetyl derivatives of anilides (i.e. CD_3CO group has replaced the acetyl group) and their N-D derivatives.

Several important conclusions were reached and these are listed :-

a) the AMIDE II band , in anilides occurs near 1550 cm-1

b) the AMIDE II' band occurs near 1420 cm-1

c) the AMIDE III' occurs near1080 cm-1.

A comparison of the infrared and Raman spectra of yellow and white forms of deuterated MNA.

The compound N-deutero-4-methyl-2-nitroacetanilide can exist in white and yellow forms which are equivalent to white and yellow forms of the undeuterated MNA. The i.r. and Raman spectra of these polymorphs show marked differences and the reason is again due to differences in the type of hydrogen bonding which occurs in these compounds. The bands near 2500 cm-1 are due to N-D stretching whilst that near 1700 cm-1 is due to C=O stretching. The bands due to AMIDE II' and AMIDE III' occur at higher wavenumbers in the white form. This is a consequence of the stronger hydrogen bonding in MNA-1 and a shorter amide C-N bond in MNA-1. It is noted that bands due to AMIDE III' are more intense in the Raman spectrum than in the i.r. spectrum.

The positions of the AMIDE IV and VI bands are hardly affected by deuteration [3]. The AMIDE V' band in both cases occurs near 530 cm-1 in the white form and near 460 cm-1 in the yellow form. The higher value in the case of the white form again is a reflection of the stronger hydrogen bonding in the white form.

Interpretation of the infrared spectrum of the trideuteroacetyl derivative of 4-methyl-2-nitroaniline

This derivative was only obtained in one form. Since the infrared spectrum showed two closely spaced doublets near 3300 cm-1 and 1710 cm-1 it was concluded that the crystals of the compound were in the triclinic form. No attempt was made to obtain the form equivalent to the amber monoclinic form of the nondeuterated material. However, attempts were made to convert it to a white intermolecularly hydrogen bonded form and these included grinding the crystals for about 30 minutes with potassium bromide, suspending the crystals in water and subjecting them to ultrasonic vibration or allowing the crystals to stand at ambient temperature for about three years. The first two of the above methods also failed to convert an approximately 50:50 mixture (obtained by evaporation of a solution of the mixture) of the trideuteroacetyl and acetyl derivatives into the white form. This loss of ability to transform into the white form is not due to an increase in the strength of the intramolecular hydrogen bond since the bands due to N-H stretching and C=O stretching are at the same frequencies as those in the undeuterated material. The ability of the amide group

to rotate out of the plane of the benzene ring may be affected and this would be the case if the initial movement was that of a rotation of the acetyl group around the amide C-N bond giving a cis (E) amide intermediate. A trideuteroacetyl group would be harder to rotate because of its greater mass.

The changes in the infrared spectra are as follows :-

a) the sharp band near 1370 cm-1 disappears.

b) the band near 1000 cm-1 disappears.

c) a sharp band near 1070 cm-1 appears.

d) new peaks appear near 920 cm-1 and 780 cm-1 and peaks near 920 cm-1 and 800 cm-1 shift to 942 cm-1 and 818 cm-1.

e) the strong peak originally at 590 cm-1 is now absent.

f) a peak of medium intensity appears at 535 cm-1.

g) the strong peak at 530cm-1 shifts to 510 cm-1 and the peak of medium intensity shifts to 482 cm-1

The first two changes are in accord with the bands at 1370 cm-1 and 1000 cm-1 being assigned to the methyl

bending and rocking vibrations respectively. Hence bands occurring at 1070 cm-1 and 1050 cm-1 in the deuterated form can be assigned to CD_3 bending vibrations. The CD_3 rocking vibrations are accidentally degenerate with and couple with aromatic ring vibrations near 920 cm-1 and 800 cm-1. These changes are in agreement with those found by Rey-Lafon et al.[208] who examined the infrared spectra of amides containing the CD_3CO group. These workers also found that AMIDE IV and AMIDE VI bands shift on formation of the trideuteroacetyl derivative and in N-methylacetamide the latter can shift by about 70 cm-1

Hence the new band at 535cm-1 is assigned to the new AMIDE VI band. The final shift of peaks mentioned above can be explained by these bands being assigned to X-sensitive out-of-plane vibrations (16b) and an X-sensitive radial skeletal vibration (6a).

The infrared spectrum of 4-trideuteromethyl-2,3,5,6-tetradeuteroacetanilide

The CD3 stretching modes appear at 2100 cm^{-1}. Comparison of the spectrum of this compound with that of the 2,3,5,6-tetradeutero-acetotoluidide reveals the bands due to the 4-methyl group in p-acetotoluidide. The bending modes are assigned to the bands at 1430 and 1380 cm-1 and the rocking modes to those at 960 cm-1 and (possibly) 1018 cm-1. The position of the latter band would coincide with a rocking mode of the methyl group in the acetyl group. The new bands near 900 cm-1 can be assigned to the CD3 rocking modes. The infrared spectrum of the N-D derivative confirms the presence of the AMIDE II and AMIDE III bands near 1520 cm-1 and 1260 cm-1.

The band due to AMIDE III' occurs near 1080 cm^{-1}.

The infrared spectrum of p-acetotoluidide and its deuterated derivatives

Several deuterated derivatives of MNA have been prepared and examined for polymorphism by infrared spectroscopy. Some of these derivatives were prepared from deuterated p-acetotoluidides and the interpretation of the infrared spectra of the latter compounds was an important step towards interpreting the infrared spectra of the deuterated MNA compounds.

Varsanyi has presented an interpretation of the infrared spectrum of p-acetotoluidide [199], p 138. These assignments were checked by comparison with the infrared spectra of 2,3,5,6-tetradeutero-acetotoluidide **I**, 4-trideuteromethyl-2,3,5,6-tetradeutero-acetotoluidide **II**, trideuteroacetotoluidide **III**, and N-D acetotoluidide.

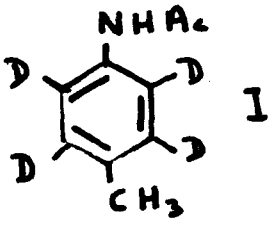

I

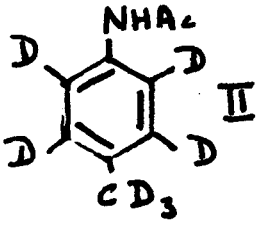

II

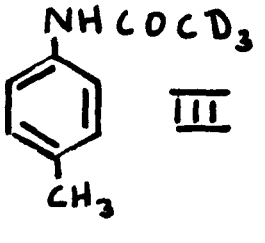

III

Some re-assignments were necessary, particularly with those bands associated with the amide group and therefore a re-assignment of certain bands to aromatic vibrations was necessary. The conclusions arising from a study of

the spectra of three deutero-amides are presented in Table 6.7. These values for the amide group vibrations are in good agreement with those values previously published for secondary amides. The positions of the C-H in-plane and out-of-plane bending vibrations were assigned to those bands which were removed on ring deuteration. The ring C-C stretching modes were slightly affected by ring deuteration. The shifts are comparable to thoses reported for ring deuteration of 1,4-difluorobenzene[199], p-cresol[199], and p-xylene[199]. The radial skeletal vibrations and ring bending vibrations were also slightly affected and moved to lower wavenumbers.

Three bands near 3200 cm-1 occur in the spectrum of p-acetotoluidide and similar bands occur in the infrared spectrum of other anilides. These bands can be explained as combinations and overtones of amide bands whilst the band at 1900 cm-1 is most likely an overtone of a γ(C-H) vibration.

Another important reason for studying the infrared spectrum of p-acetotoluidide is that it shows a strong resemblance to that of the white form of MNA with, of course, allowance for the bands due to the nitro group.

Infrared spectrum of p-acetotoluidide N-D

The positions of the AMIDE II and III bands at 1540 cm-1 and 1260 cm-1 are clearly established. The new band at 1450 cm-1 is due to AMIDE II'. A complex pattern of peaks results in the region 1000-1100 cm-1 and AMIDE III is assigned to the band near 1080 cm-1. The band assigned to νC-C falls to 955 cm-1 whilst the strong broad band at 755 cm-1 disappears and is replaced by a strong peak at 555 cm-1 which must be due to AMIDE V'. The bands due to the C=O bending vibrations are hardly affected by deuteration. However, the band assigned to AMIDE VI'decreases in intensity.

p-acet-D3-toluidide

The infrared spectrum of this compound was used to locate bands due to the amide-methyl group and the results are listed in Table 6.7 . An important result was that the methyl rocking vibration was established at 1020 cm-1. This derivative was also useful in locating the C=O bending vibrations since it is known that such vibrations in the CD_3CO-derivatives move to lower wavenumbers and are reduced in intensity [209] . Similar behaviour is apparent when the spectra of acetophenone and aceto-D3-phenone are

compared [209]. A new band appears at 480 cm-1. This band was assigned to a radial skeletal vibration which was substituent sensitive (6a). The peak assigned to another radial skeletal mode behaved in a similar manner and shifted by about 20 cm-1. In the infrared spectra of four para-substituted anilides a slight shift of about 20 cm-1 was observed in a band of medium intensity near 500 cm-1.[210]

Infrared spectrum of p-acetotoluidide-D4

Replacement of the aromatic protons by deuterium causes those bands due to all types of C-H vibrations to shift. νC-D appears as an unresolved group of bands near 2250 cm-1. Although it is possible to detect bands due to νC-H and δC-H by their disappearance after deuteration it is difficult to assign these to specific vibrations without recourse to a normal coordinate analysis. It seems probable that bands due to δC-D occur in the region 1100-850 cm-1 whilst those due to γ C-D appear in the region 850-700 cm-1. The strong band near 500 cm-1 shifts to 438 cm-1 while a rather less intense band remains at 500 cm-1. The latter band and the one at 625 cm-1 which are assigned to radial skeletal modes are expected to be only slightly affected by ring deuteration.

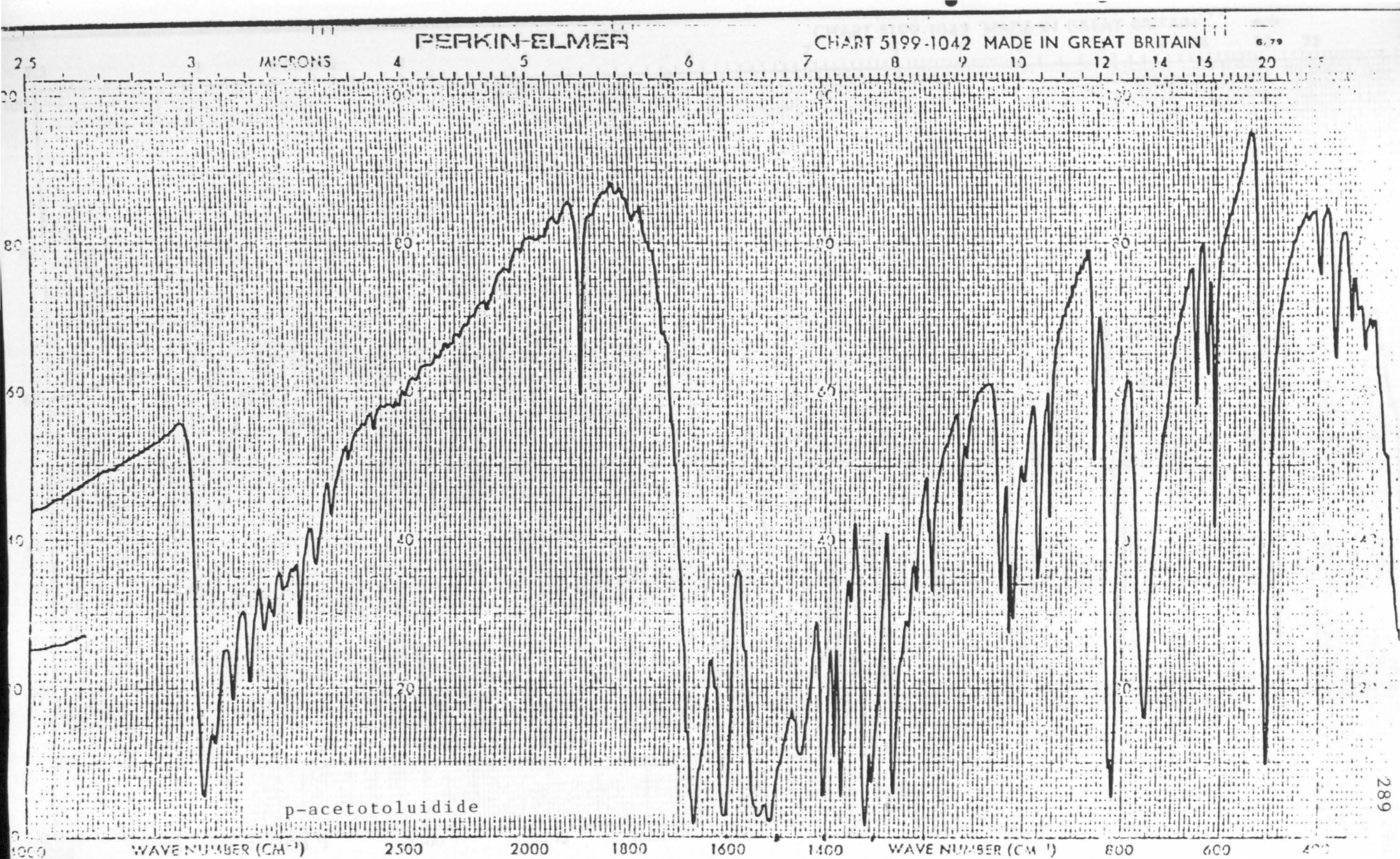
PERKIN-ELMER
CHART 5199-1042 MADE IN GREAT BRITAIN
6.79
2.5
3
MICRONS
4
5
6
7
8
9
10
12
14
15
20
p-acetotoluidide
WAVE NUMBER (CM⁻¹)
2500
2000
1800
1600
1400
WAVE NUMBER (CM⁻¹)
800
600

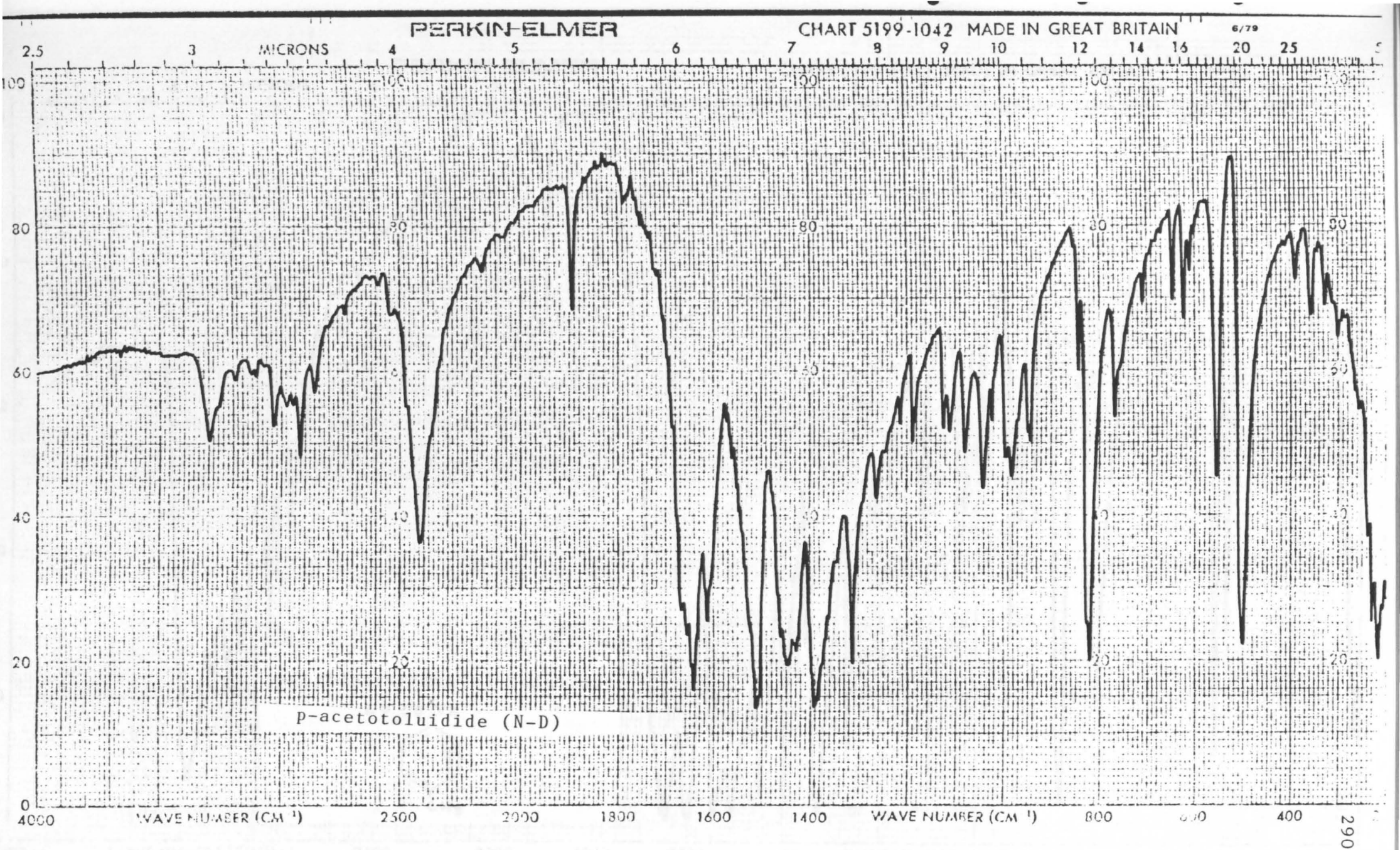
PERKIN-ELMER
CHART 5199-1042 MADE IN GREAT BRITAIN
6/79
2.5
3
MICRONS
4
5
6
7
8
9
10
12
14
16
20
25
100
80
60
40
20
0
p-acetotoluidide (N-D)
4000
WAVE NUMBER (CM ⁻¹)
2500
2000
1800
1600
1400
WAVE NUMBER (CM ⁻¹)
800
400
290

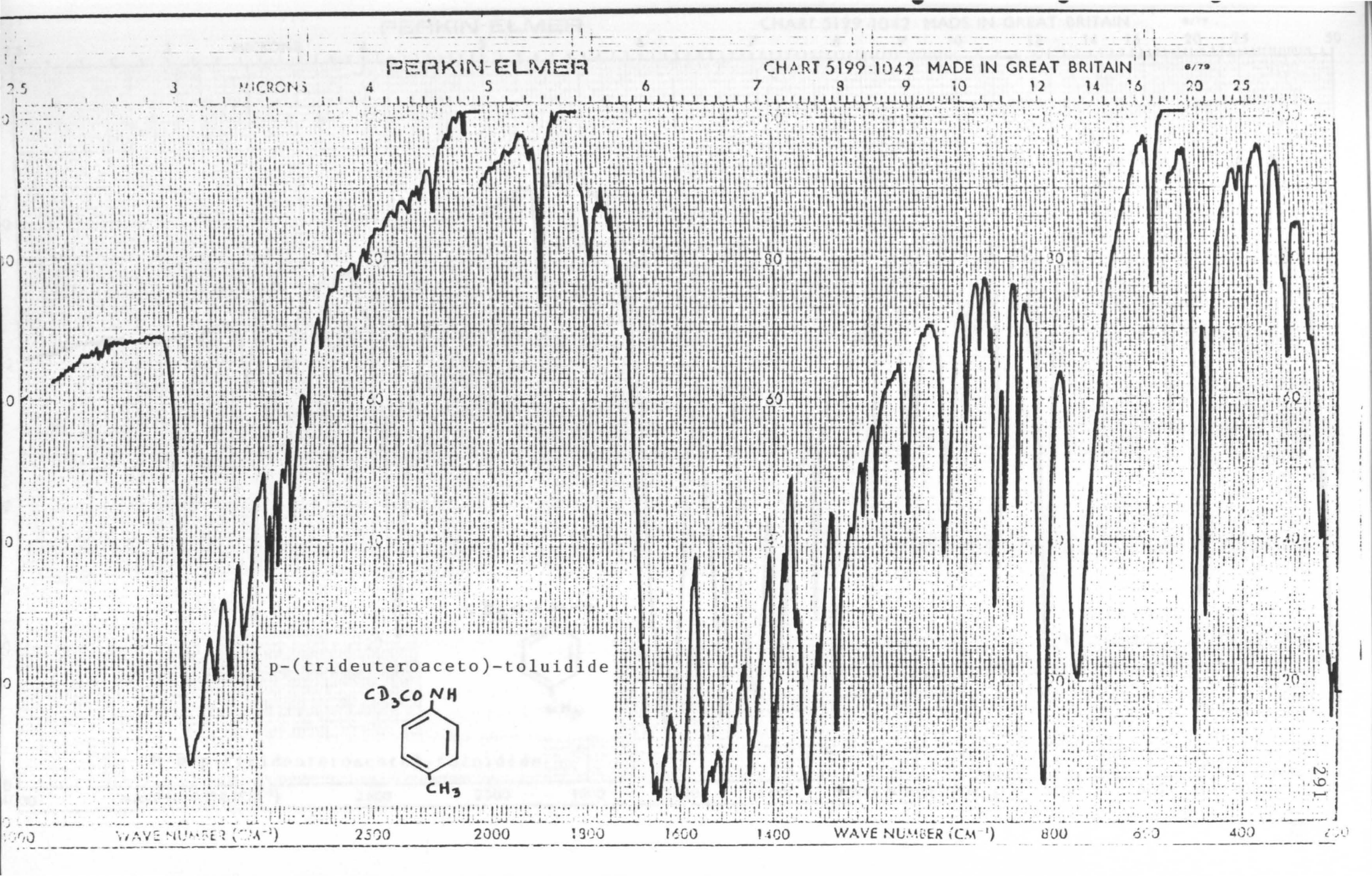
PERKIN-ELMER
CHART 5199-1042 MADE IN GREAT BRITAIN
MICRONS
WAVE NUMBER (CM⁻¹)
p-(trideuteroaceto)-toluidide
CD3CO NH
CH3
291

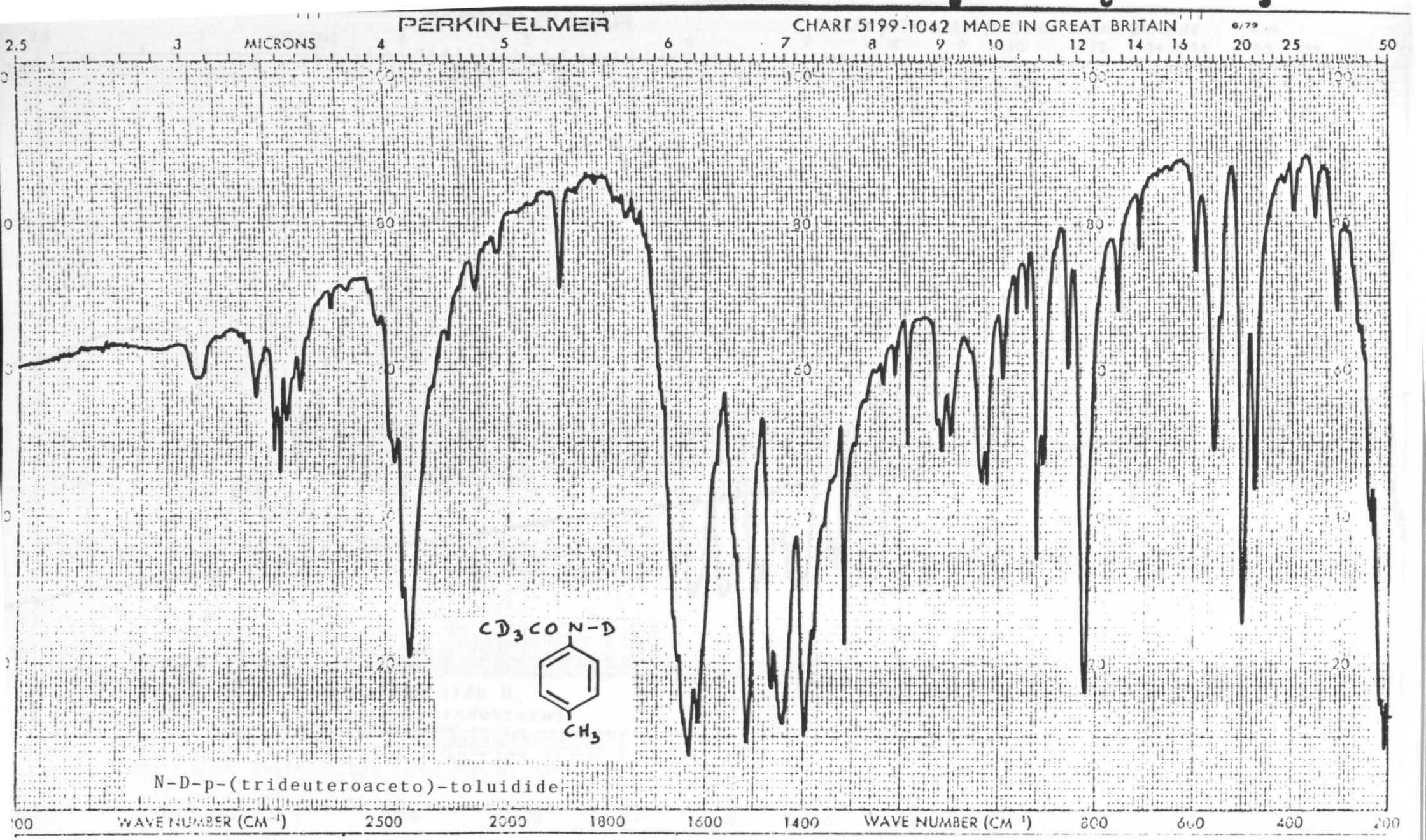
PERKIN-ELMER
CHART 5199-1042 MADE IN GREAT BRITAIN
6/79
2.5
3
MICRONS
4
5
6
7
8
9
10
12
14
16
20
25
50
100
80
60
40
20
0
$CD_3CO\,N\text{-}D$
CH_3
N-D-p-(trideuteroaceto)-toluidide
00
WAVE NUMBER (CM^{-1})
2500
2000
1800
1600
1400
WAVE NUMBER (CM^{-1})
800
600
400
200

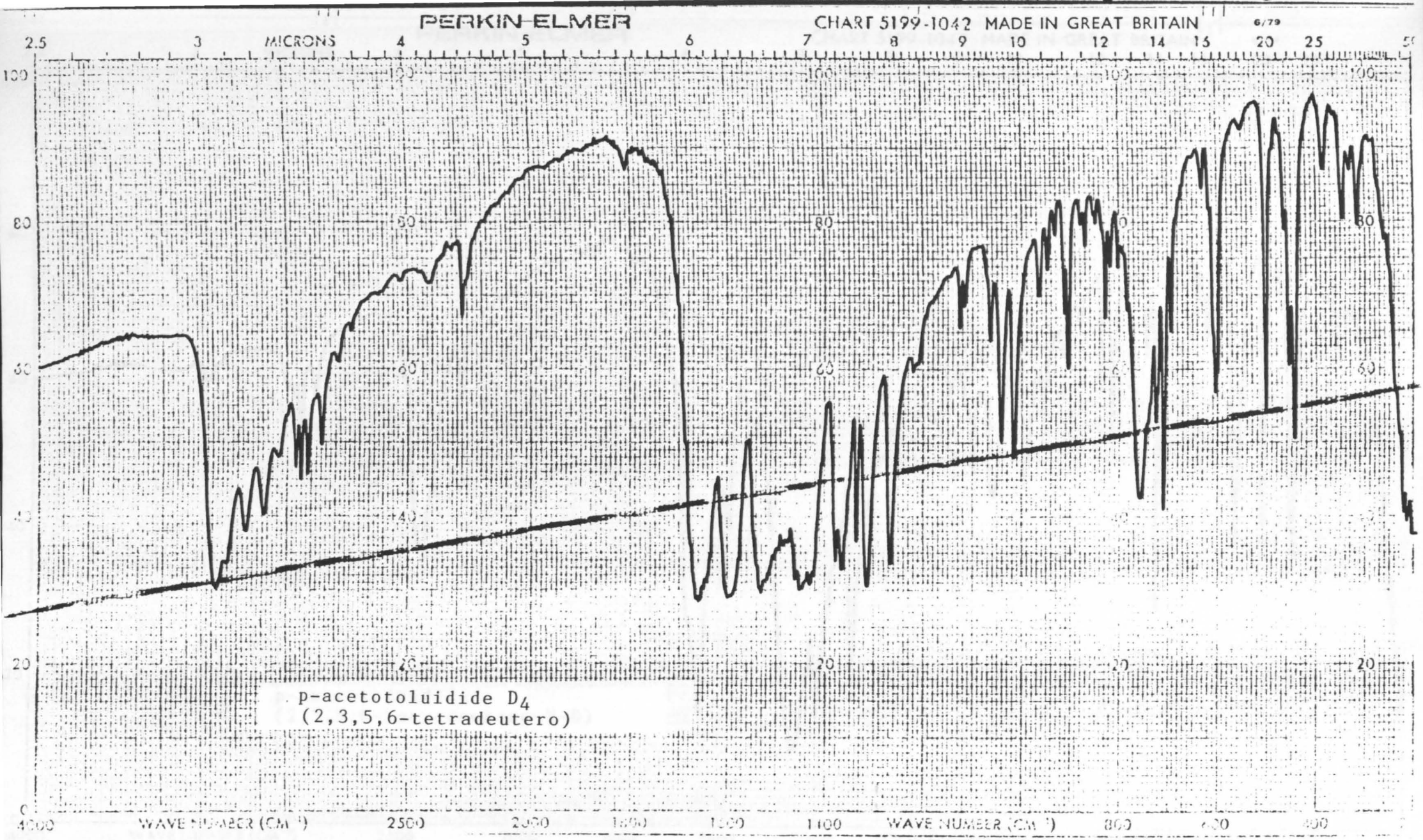
PERKIN-ELMER
CHART 5199-1042 MADE IN GREAT BRITAIN
6/79
2.5
3
MICRONS
4
5
6
7
8
9
10
12
14
15
20
25
100
80
60
40
20
0
4000
WAVE NUMBER (CM⁻¹)
2500
1100
WAVE NUMBER (CM⁻¹)
800
p-acetotoluidide D4
(2,3,5,6-tetradeutero)

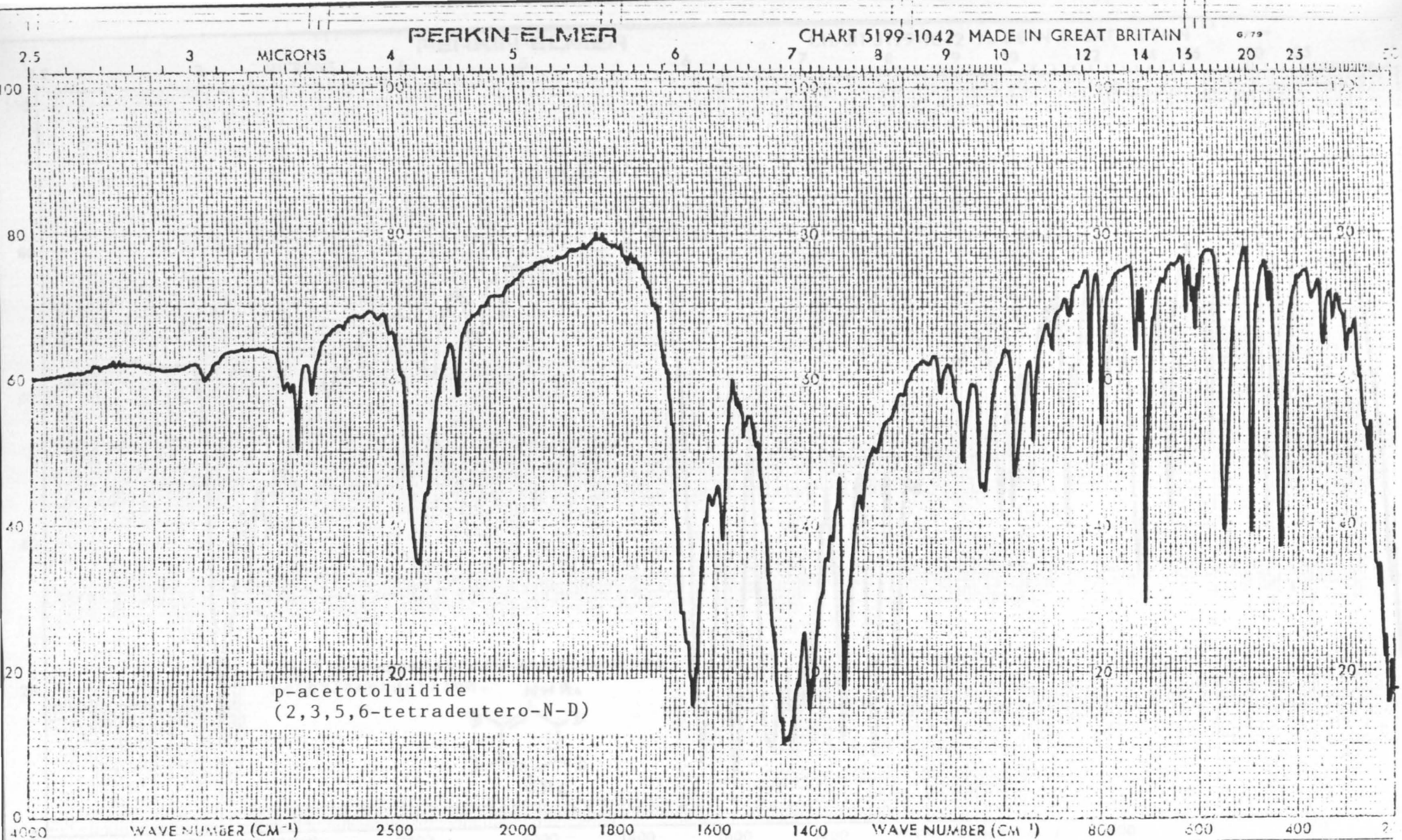
PERKIN-ELMER
CHART 5199-1042 MADE IN GREAT BRITAIN
MICRONS
WAVE NUMBER (CM⁻¹)
WAVE NUMBER (CM⁻¹)
p-acetotoluidide
(2,3,5,6-tetradeutero-N-D)

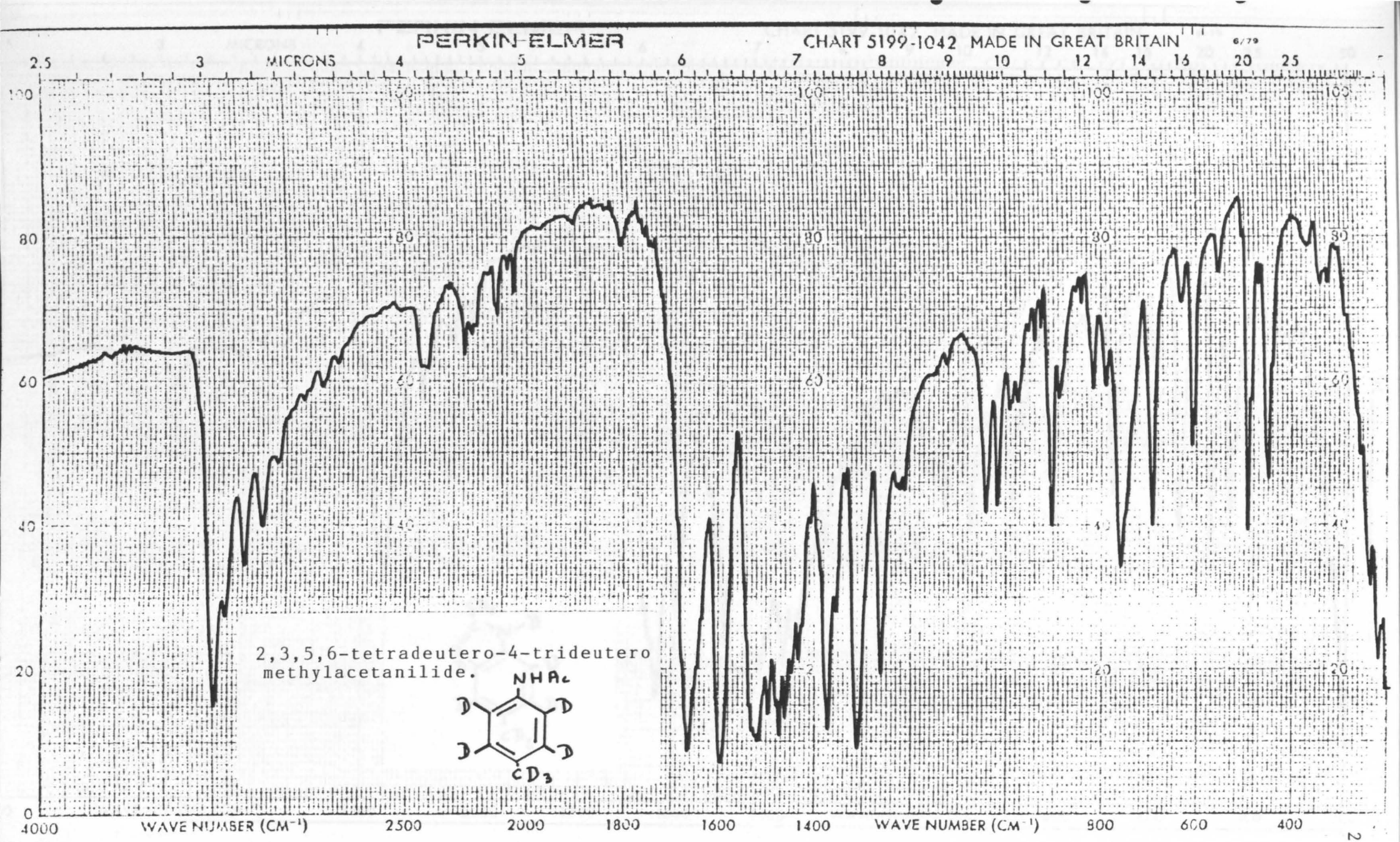
PERKIN-ELMER
CHART 5199-1042 MADE IN GREAT BRITAIN
6/79
2.5
3
MICRONS
4
5
6
7
8
9
10
12
14
16
20
25
100
80
60
40
20
0
4000
WAVE NUMBER (CM⁻¹)
2500
2000
1800
1600
1400
WAVE NUMBER (CM⁻¹)
800
600
400
2,3,5,6-tetradeutero-4-trideutero
methylacetanilide.
NHAc
D
D
D
D
CD3

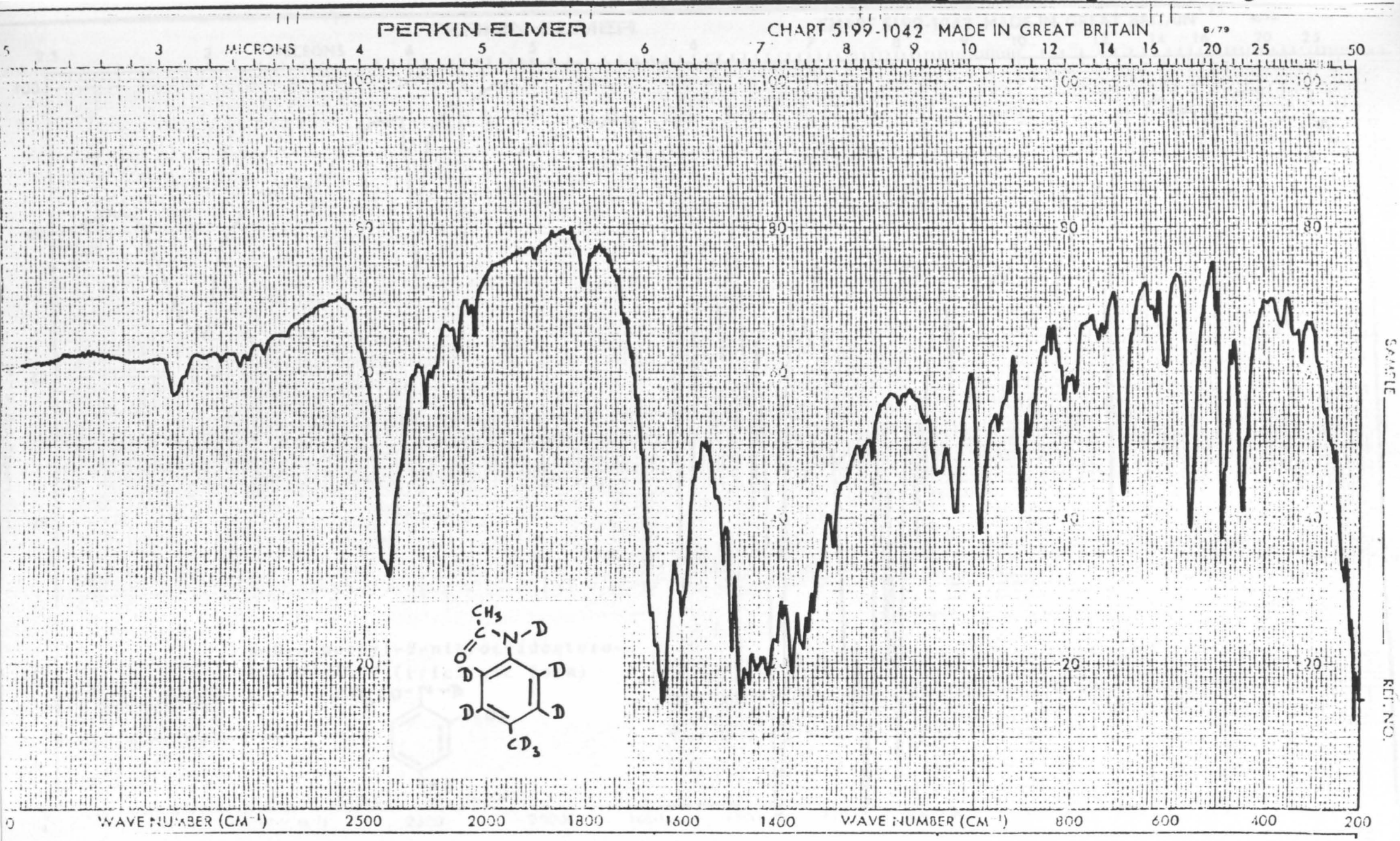
PERKIN-ELMER
CHART 5199-1042 MADE IN GREAT BRITAIN
6/79
MICRONS
3
4
5
6
7
8
9
10
12
14
16
20
25
50
100
80
60
40
20
0
WAVE NUMBER (CM⁻¹)
2500
2000
1800
1600
1400
WAVE NUMBER (CM⁻¹)
800
600
400
200
SAMPLE
REF. NO.

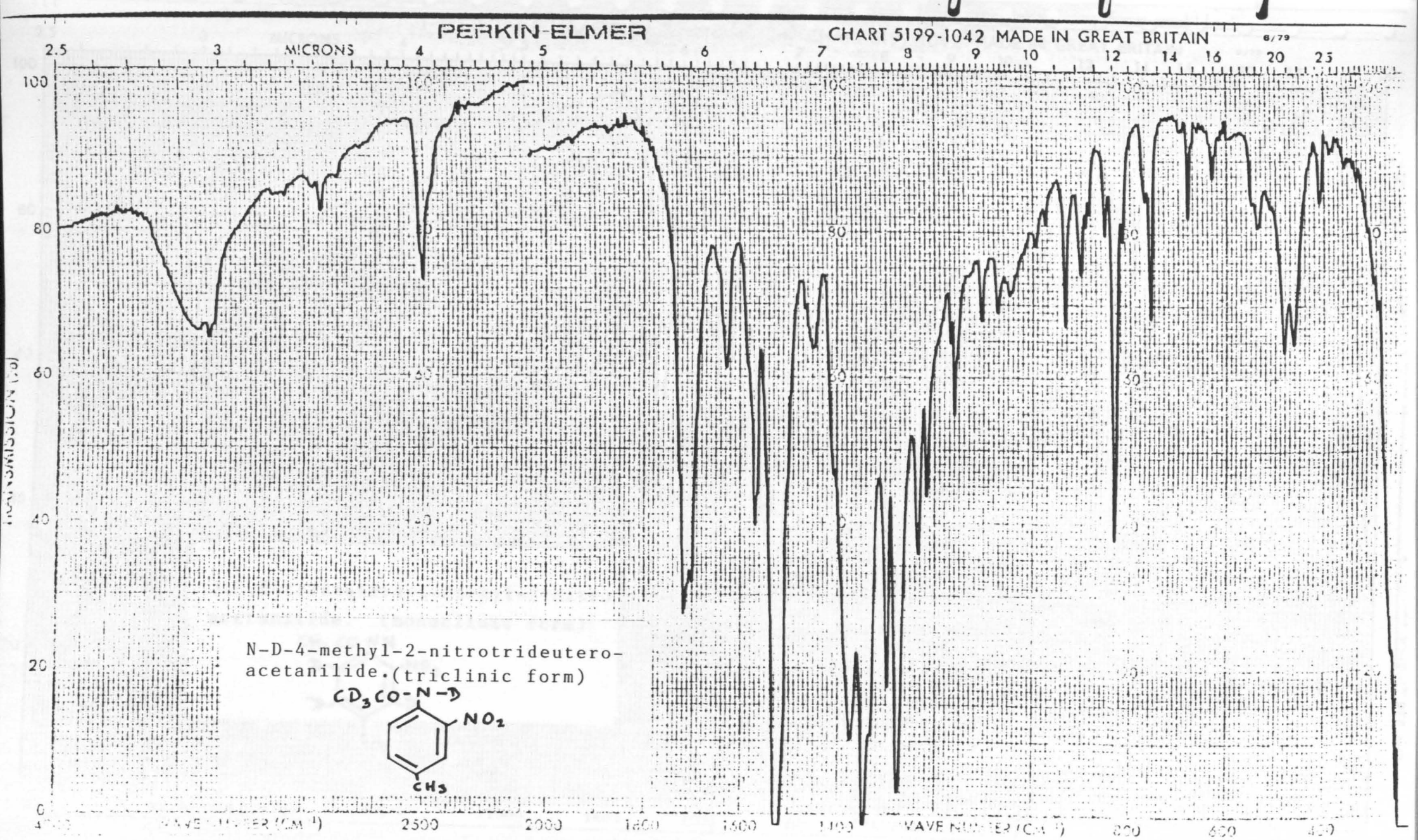
PERKIN-ELMER
CHART 5199-1042 MADE IN GREAT BRITAIN
6/79
MICRONS
2.5
3
4
5
6
7
8
9
10
12
14
16
20
25
100
80
60
40
20
0
TRANSMISSION (%)
2500
2000
1800
1600
1100
800
600
N-D-4-methyl-2-nitrotrideutero-
acetanilide.(triclinic form)
$CD_3CO-N-D$
NO_2
CH_3

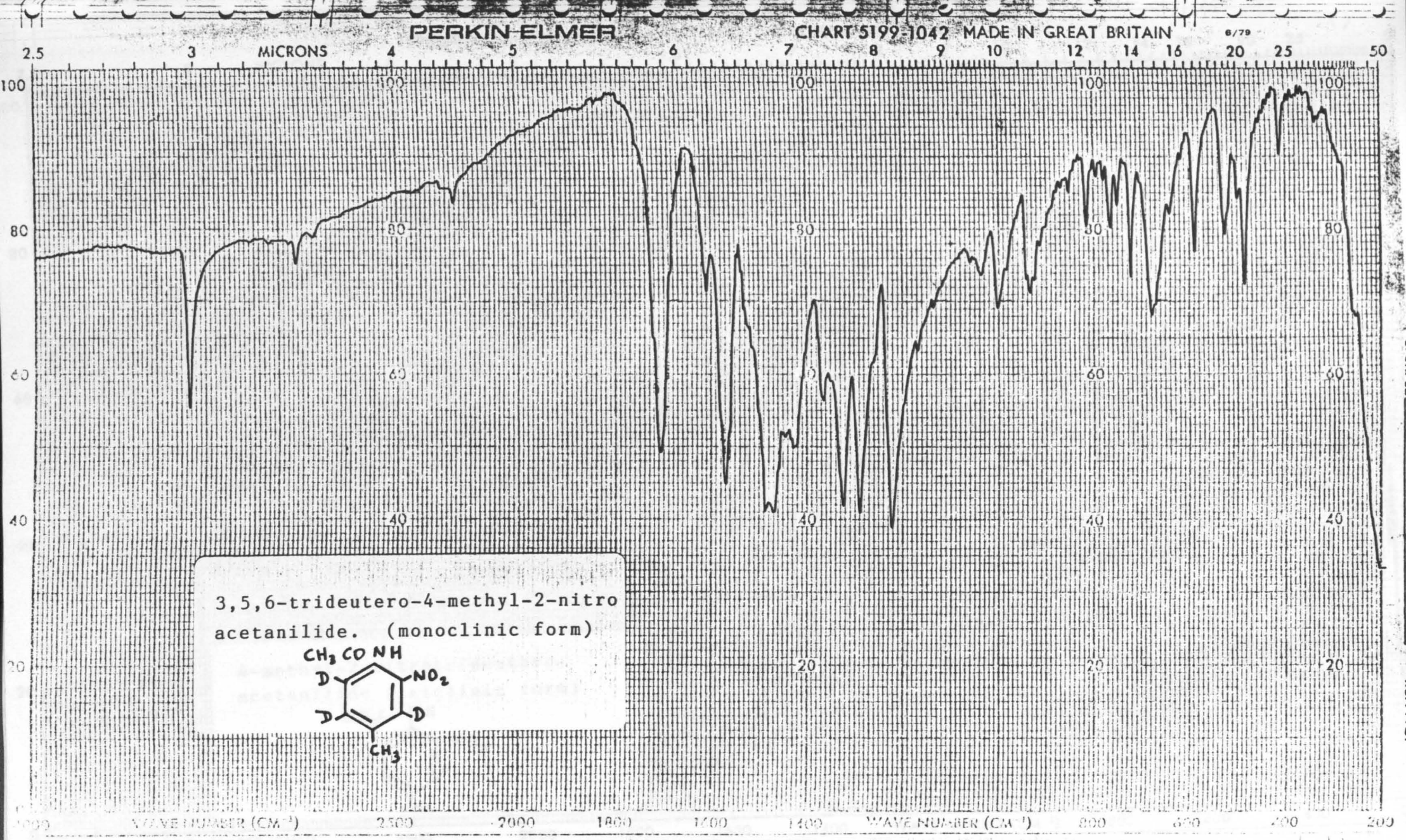
PERKIN-ELMER
CHART 5199-1042 MADE IN GREAT BRITAIN
6/79
MICRONS
2.5
3
4
5
6
7
8
9
10
12
14
16
20
25
50
100
80
60
40
20
3,5,6-trideutero-4-methyl-2-nitro acetanilide. (monoclinic form)
CH3 CO NH
NO2
D
D
D
CH3
WAVE NUMBER (CM-1)
2500
2000
1800
1600
1400
WAVE NUMBER (CM-1)
800
600
400
200

REF. NO.

298

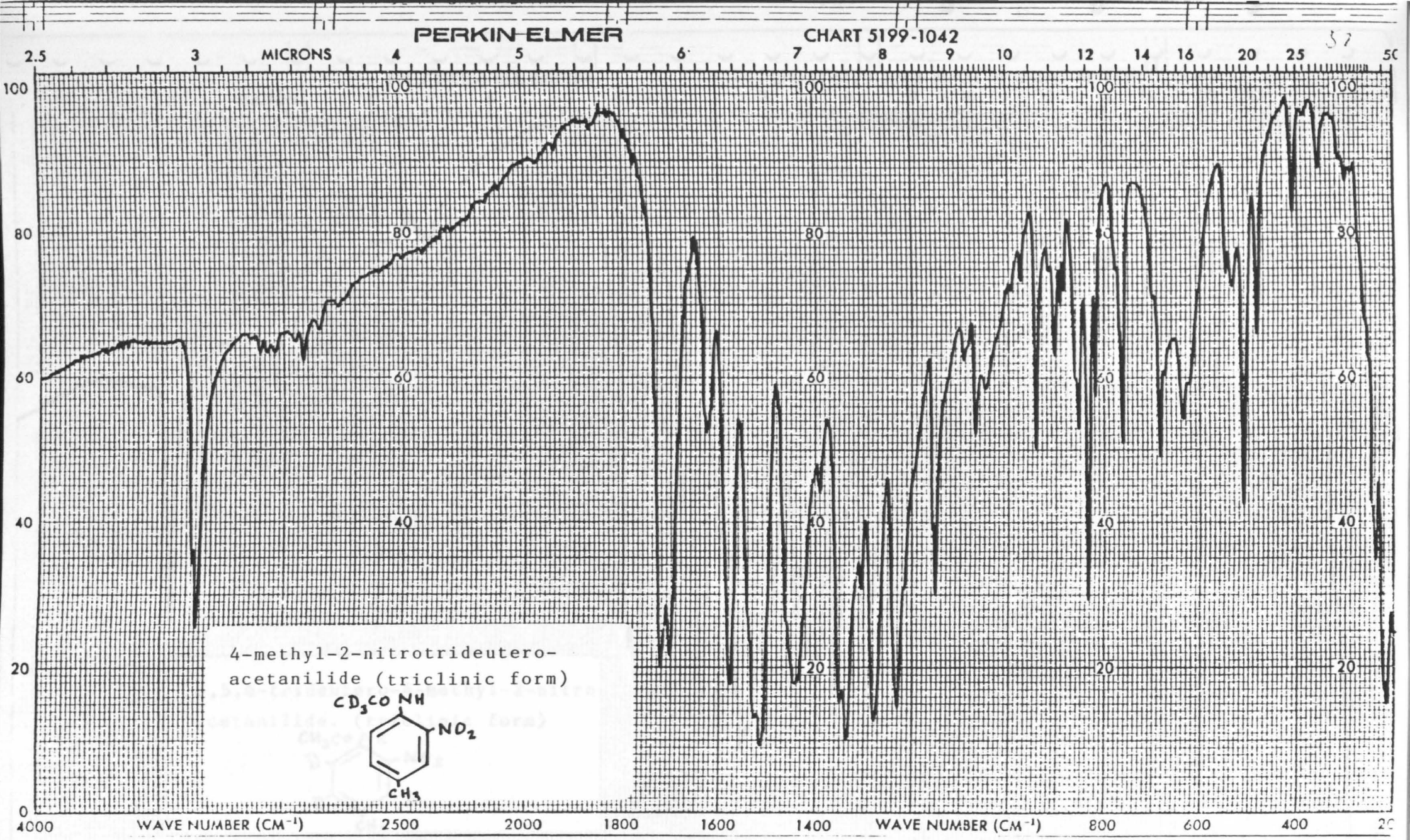
PERKIN-ELMER
CHART 5199-1042
MICRONS
2.5
3
4
5
6
7
8
9
10
12
14
16
20
25
50
100
80
60
40
20
0
4000
WAVE NUMBER (CM⁻¹)
2500
2000
1800
1600
1400
WAVE NUMBER (CM⁻¹)
800
600
400
4-methyl-2-nitrotrideutero-
acetanilide (triclinic form)
CD3CO NH
NO2
CH3

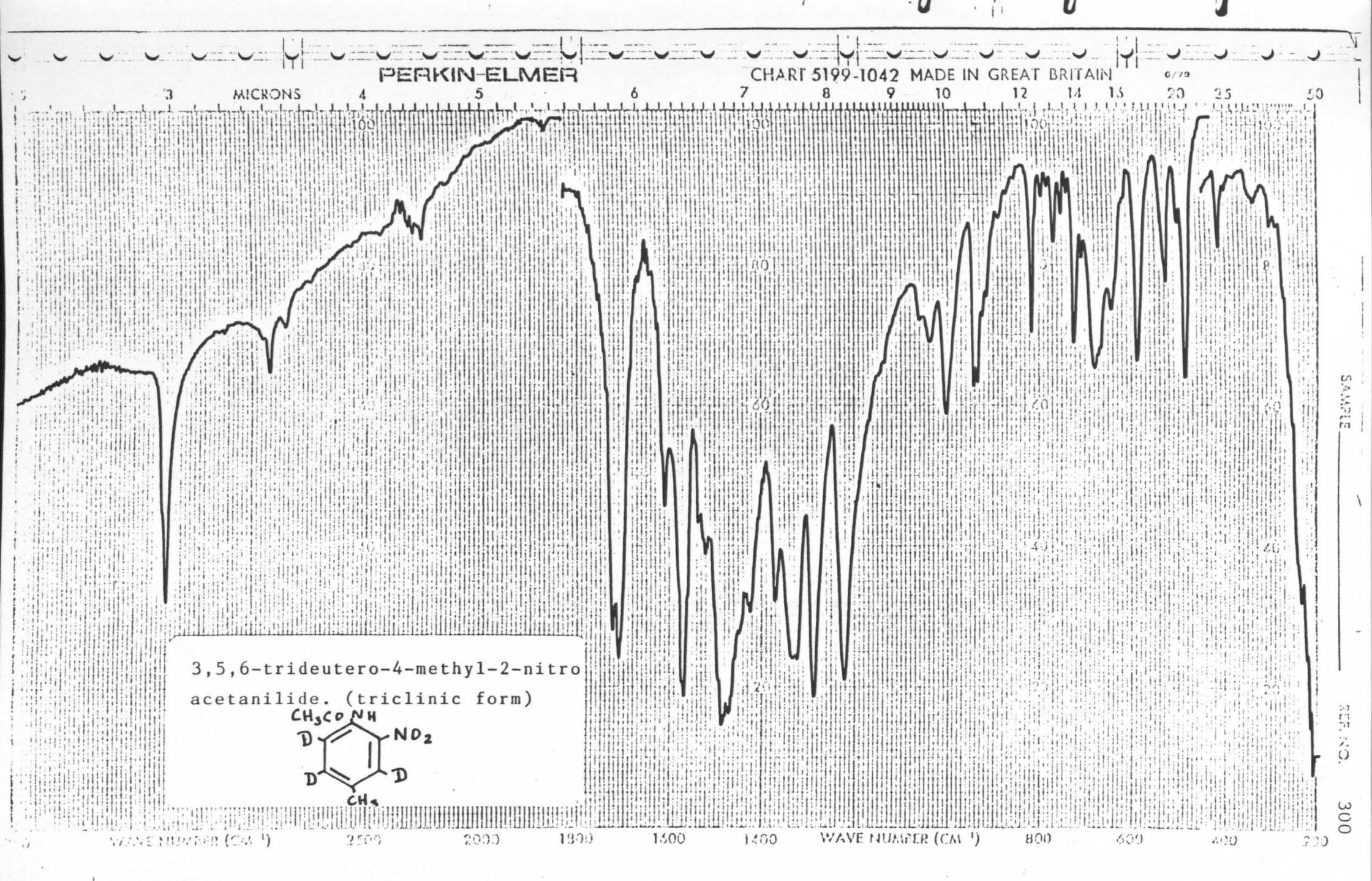
PERKIN-ELMER
CHART 5199-1042 MADE IN GREAT BRITAIN
MICRONS
3
4
5
6
7
8
9
10
12
14
15
20
25
50
100
80
60
40
20
3,5,6-trideutero-4-methyl-2-nitro
acetanilide. (triclinic form)
CH3CO NH
D
NO2
D
D
CH3
WAVE NUMBER (CM -1)
2500
2000
1900
1500
1400
WAVE NUMBER (CM -1)
800
600
400
SAMPLE
REF. NO. 300

Table 6.6

Observed fundamental frequencies for p-acetotoluidide and p-acetotoluidide (2,3,5,6-tetradeutero)

	Ring vibrations		
a'	p-acetotoluidide		2,3,5,6-tetradeutero-
ν_1	3080	νC-H	2260
ν_2	3050	"	"
ν_3	3040	"	"
ν_4	3000	"	"
ν_5	1613	νC=C(8a)	1595
ν_6	-	" (8b)	1585
ν_7	1515	" (19a)	1430?
ν_8	1408	" (19b)	1335
ν_9	1320	" (14)	1310
ν_{10}	1305	δC-H(3)	950
ν_{11}	1210	νC-X(13)	1210
ν_{12}	1182	δC-H(9a)	900
ν_{13}	1125	νC-X(7a)	1125
ν_{14}	1112	δC-H(18b)	875
ν_{15}	1028	δC-H(18a)	-
ν_{16}	-	δC-C (1)	-
ν_{17}	755	"	-
ν_{18}	620	" (6b)	600
ν_{19}	510	"(6a)	500
ν_{20}	360	δC-X(15 or 9b)	350
ν_{21}	-	-	-
a"			
ν_{22}	960	γC-H(17a)	800
ν_{23}	945	"(5)	780
ν_{24}	828	"(10a)	738
ν_{25}	820	"(17b)	710
ν_{26}	710	γC-C (4)	650
ν_{27}	510	"(16b)	438
ν_{28}	390	"(16a)	370
ν_{29}	300	γC-X(10b)	-
ν_{30}	-	-	-

Table 6.7

Assignments of methyl group vibrations in p-acetotoluidide

$C-CH_3$ in the amide group

	I	II	III
δ_{as}	1450	-	1115
δ_s	1370	1372	1030
r	1020, 970	1018, 972	910
νCH_3-C	970	970	930

4-methyl

	I	II	III
δ_{as}	1450	-	1450
δ_s	1380	1040	1380sh
r	1040,995	905,888	1040,995

CH_3 and CD_3 stretching vibrations

I	2980, 2960, 2930	
II	2980, 2960, 2930	2130, 2110,2050
III	2960, 2940, 2120	- - -

Assignments of amide group vibrations in p-acetotoluidide

	CH_3CONH	CH_3COND	CD_3CONH	CD_3COND
NH	3290	2420	3290	2400
amide I	1670	1640	1655	1632
amide II	1540	1450	1555	1450
amide III	1260	1080	1270	1095
amide IV	648	648	-	595
amide V	755	555	855	560
amide VI	610	610	-	540
$\nu C-CH_3$	970	950	930	920

Overtone and combination bands.

3250 2 x amide I
3200 amide I + amide II or amide I + 2 x amide V
3100 2 x amide III
2860 2 x C-N
2800 amide II + amide III
1900 2 x 945 (2 x γ C-H)

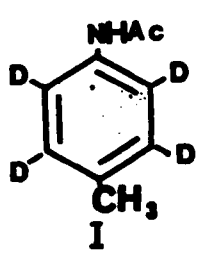

I

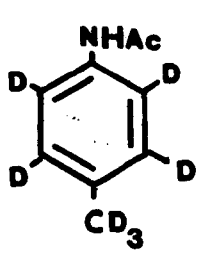

II

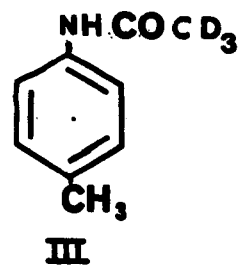

III

Table 6.8

An assignment of the trideuteroacetyl and amide group vibrations in 4-methyl-2-nitro-trideuteroacetanilide

	CD_3CONH	CD_3COND
νNH	3380,3360	2520, 2500
Amide I	1720, 1700	1720, 1700
Amide II	1440	1375
Amide III	1230	1100
Amide IV	630	630
Amide V	650	460
Amide VI	635	635
$\nu_{as}CD_3$	-	
$\nu_s\ CD_3$	-	
$\delta_{as}CD_3$	1095	1105
$\delta_s\ CD_3$	1070	1072
$r_{\perp}\ CD_3$	942*	932
r //	820*	815
$\nu C\text{-}CH_3$	905*	900

* The shift of νC-C on formation of the CD_3CO derivative and positions of the CD_3 rocking vibrations indicate that a mixing of these vibrations occur.

Chapter Seven

A study of the nuclear magnetic resonance spectra of MNA

A study of the nuclear magnetic resonance spectra of MNA

Although the three polymorphs of MNA give the same n.m.r. spectrum in any given solvent in which MNA is soluble it has been found that the n.m.r spectrum varies according to the nature of the solvent. Thus both the ^{1}H n.m.r. and the ^{13}C n.m.r. spectra of MNA are solvent dependent. One important factor which affects the ^{1}H n.m.r. is the anisotropic effect of the amide carbonyl group. This effect, which causes a marked variation in the chemical shift of H(6), has been extensively investigated in many aromatic anilides and the topic has been reviewed in Chapter 1.

In general terms, the chemical shift of H(6) decreases on increasing the relative permittivity of the solvent. The chemical shift of H(6) in various solvents is given in Table 7.1 and a plot of chemical shift against relative permittivity is shown in fig. 7.1 . The change of chemical shift of H(6) in various solvents in related 4-substituted-2-nitroacetanilides(4-X-2-nitroacetanilides) is also presented in this Table.

Table 7.1

The variation of chemical Shift (p.p.m.) of proton H(6) with relative permittivity (Er) and donor number (D_N)

solvent	CCl_4	$CDCl_3$	Me_2CO	EtOH	MeOH	MeCN	DMSO
Er*	2.2	4.8	21.3	25.7	33.0	38.8	45.0
D_N**	2	-	17	31.5	25.7	14.1	29.8
Chemical shifts. X = 4-substituent in MNA							
X							
H	531	525	511	487	483	504	480
NO_2	-	561	524	-	-	521	508
Cl	527	523	510	483	483	503	464
Me	519	516	500	476	474	493	468
OMe	520	513	493	470	464	485	454

* The values for the relative permittivity were taken from the "Book of Data for Chemistry and Physical Science and Physics", Longman and the Merck Index (7th Edition).

** D_N = Donicity Number. This solvent parameter is a measure of the nucleophilic properties of a solvent. Values were taken from a table compiled by Dr.D.Waters, Brunel University. A list of D values can be found in a text by V.Gutmann, "Coordination Chemistry in Nonaqueous Solvents", Springer Verlag, Vienna, 1968.

Fig. 7.1 A plot of relative permittivity (E_r) of solvent against the chemical shift of H(6)

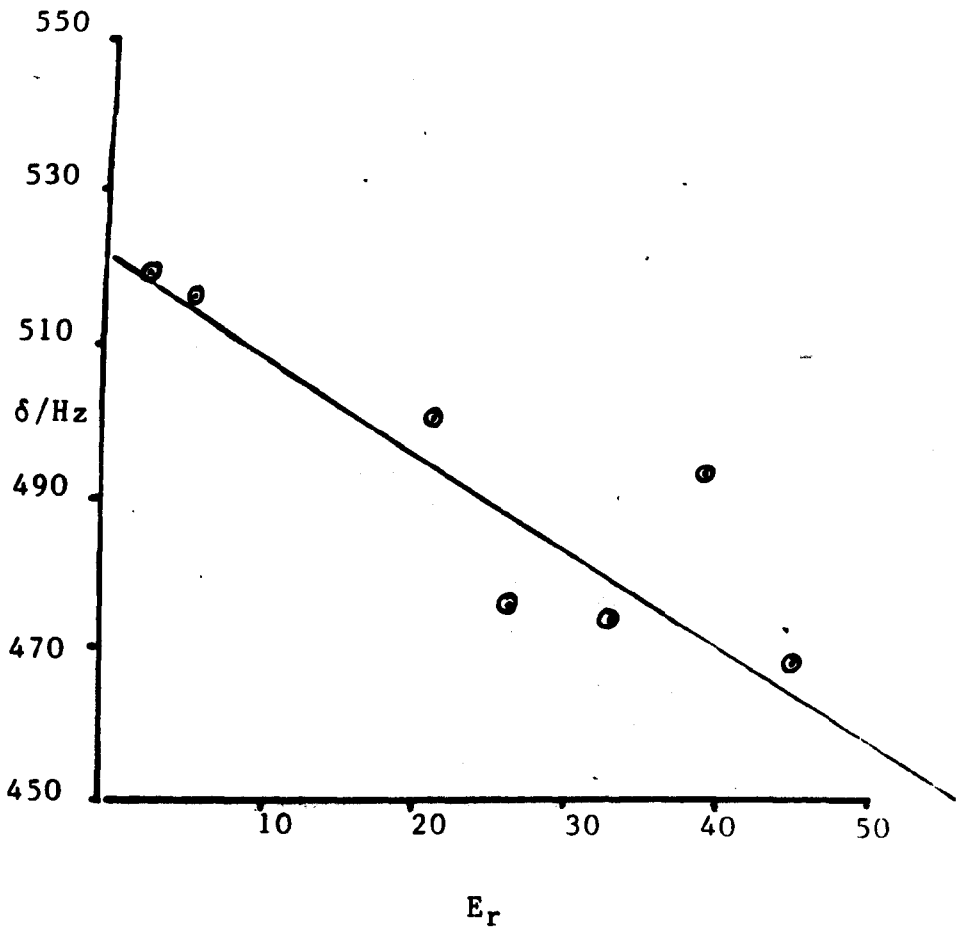

A least squares computer calculation gives the following results :-

	1	2
y intercept	519	521.7
slope	-1.10	-1.33
R	0.76	0.91

Results in column 1 take the acetonitrile data into account but neglect it in column 2.

Fig. 7.1 (a) A plot of donicity number D_N of solvent against chemical shift of H(6) in MNA

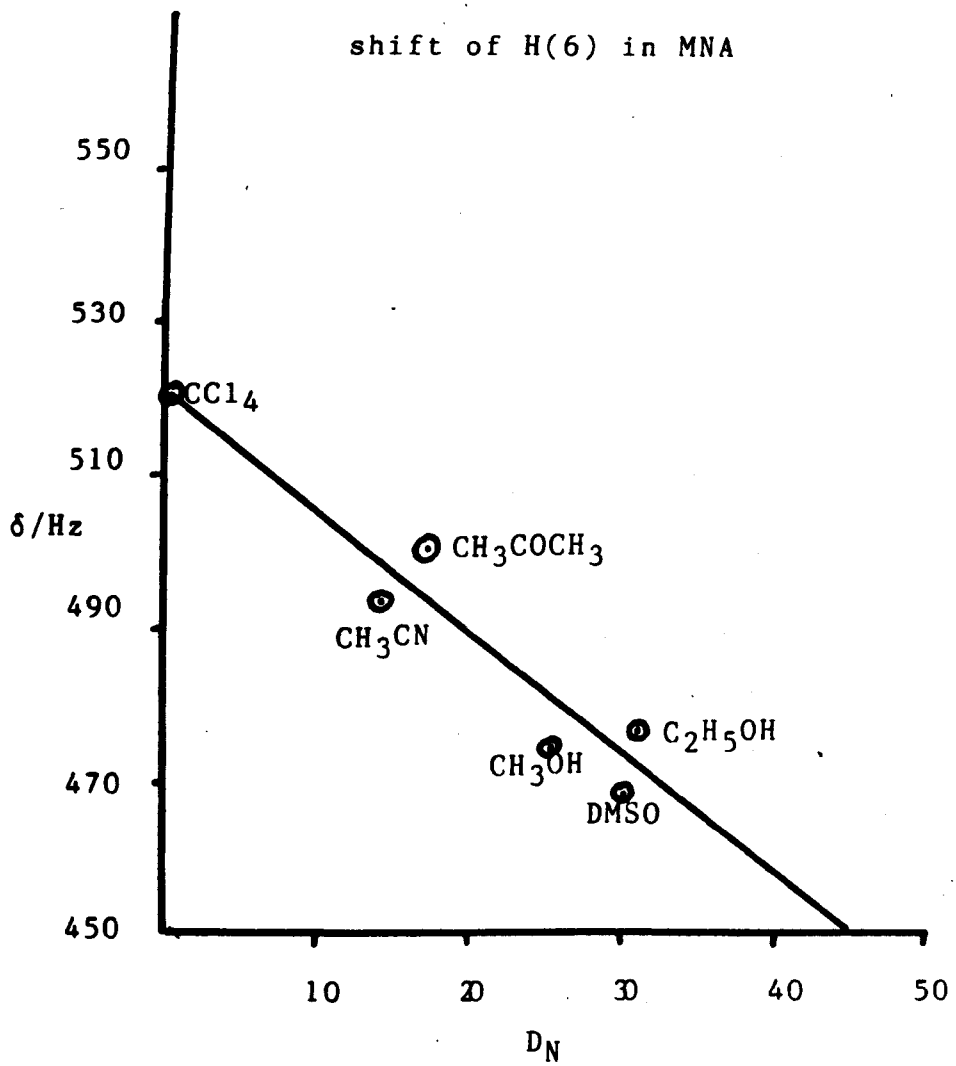

A least squares computer calculation gives the following results :-

y intercept 519.8

slope -1.59

R 0.92

It is concluded that a slightly better linear correlation exists between the chemical shift and D_N numbers than with relative permittivity (Fig. 7.1).

The ^{13}C n.m.r. spectrum of MNA has been recorded in several solvents and it has been found that the chemical shifts of C(2), C(4), and C(6) increase with increasing relative permittivity whilst the chemical shift of C(1), and C(5) decrease slightly. The chemical shift of C(3) increases slightly with increasing relative permittivity.

These changes may be explained on the basis that solvent molecules have variable degrees of ability to attach themselves to the amide group. A solvent such as DMSO should compete successfully with the nitro group in the molecule for the N-H group and solvate the amide groups by forming N-H....O-S linkages. The bulky amide-solvent complex formed in this manner is anticipated to force the plane of the amide group away from the plane of the benzene ring. Thus, the C=O group will move further away from H(6) and consequently the chemical shift would be expected to decrease as the amide group moves further out of the plane of the benzene ring. For example, the chemical shift of H(6) in MNA decreases from 8.6 ppm to approximately 7.6 ppm when the solvent is changed from deuterochloroform to DMSO. Since the chemical shift of H(5) is about 7.6 ppm and is affected to a very small extent by solvent the pattern of peaks observed for the coupled protons H(6) and H(5) varies from an AX type in deuterochlorform to an AB type in DMSO. The ^{1}H n.m.r. spectrum of the aromatic protons in other solvents are intermediate between these two types.

A twisting movement of the amide group from the plane of the benzene ring would also account for the variation in

chemical shift of C(2), C(4), and C(6) in the ^{13}C n.m.r spectrum since the electron density over these positions would be expected to decrease. This prediction can be made by a study of the canonical forms of MNA where the amide group can donate electrons to the 2,4, and 6 positions of the benzene ring. As the amide group moves from the plane of the ring so resonance interaction is inhibited by a factor of $\cos^2 \theta$ where θ is the dihedral angle between the ring and the amide plane [191]. The values of the chemical shifts of all carbon atoms of MNA are presented in Table 7.2.

Table 7.2

The assignment* of ^{13}C n.m.r. signals for MNA

solvent	$CDCl_3$	CD_2Cl_2	$(CD_3)_2CO$	CD_3OD	CD_3CN	DMSOd6	calc. ^{13}C n.m.r.
spectrum	1	2	3	4	5	6	
carbon 1	132.2	132.6	132.3	130.9	132.1	130.3	131.8
carbon 2	136.2	-	138.2	141.5	136.3	143.6	138.5
carbon 3	125.2	125.4	125.6	125.5	125.8	126.6	124.5
carbon 4	133.1	133.6	134.3	136.3	134.8	136.3	132.7
carbon 5	136.4	136.6	136.2	135.8	136.5	135.7	135.1
carbon 6	121.9	122.2	123.5	125.9	123.7	126.0	119.4
carbon 8	168.4	168.6	168.9	171.3	169.5	169.6	-
carbon 9	25.4	25.5	24.8	24.0	25.0	24.9	-
carbon 7	20.4	20.6	20.3	20.5	20.4	21.6	-

* chemical shifts are measured in ppm from TMS

Calculated values are based on substituent constants listed in Wehrli and Wirthlin [211].

The same numbering sequence is used for the assignments of the carbon atoms in the ^{13}C n.m.r. as in the crystal structures.

MNDO calculations on MNA

The charges on the various atoms in MNA were calculated using the computer program MNDO.* The values obtained are presented in Table 7.3. The atoms of the benzene ring C(1) to C(6) are alternately charged + and − . N(2), the nitro group nitrogen, is the most positive atom whereas the amide nitrogen atom, the nitro group oxygen atoms, and the oxygen atom in the carbonyl group are all negative.

Rotation of the amide group out of the plane of the benzene ring is seen to reduce the value of the negative charge on C(2), C(4), and C(6). This is a result which is expected from a reduced resonance interaction between the lone pair on the amide nitrogen and the ring π electrons. Rotation of amide and nitro groups from the plane of the benzene ring reduces the value (neglecting the sign) of the charge on all ring atoms and this could account for the more even distribution of the C-C bond lengths in the benzene ring in MNA-1 (white) compared with MNA-2 (amber) and MNA-3 (yellow). These bond lengths are presented in a graphical form in fig. 7.2.

* The help of Dr E. Short is gratefully acknowledged.

Fig. 7.2 A plot of bond length against the ring bonds in MNA

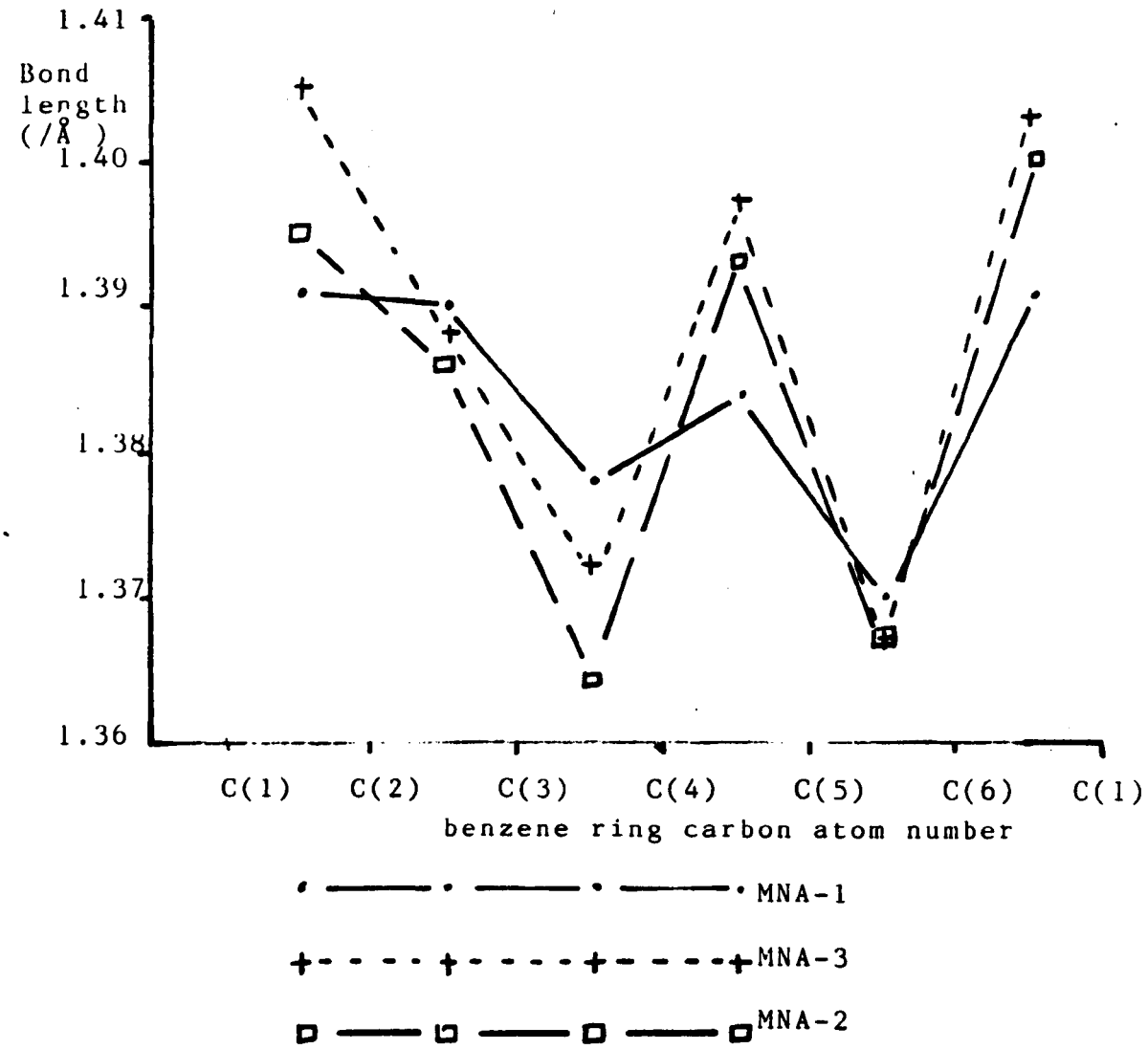

Table 7.3

Electron density calculations based on MNDO calculations

amide-ring*		0	45	90	30	150
nitro-ring*		0	0	0	30	50
1	C(1)	+0.2126	+0.1985	+0.1849	+0.1985	+0.1819
2	C(2)	-0.1691	-0.1379	-0.0952	-0.1458	-0.1093
3	C(3)	+0.0410	+0.0301	+0.0182	+0.0332	+0.0344
4	C(4)	-0.1490	-0.1303	-0.1100	-0.1353	-0.1336
5	C(5)	+0.0366	+0.0224	+0.0071	+0.0244	+0.0184
6	C(6)	-0.1380	-0.0820	-0.0783	-0.0967	-0.1177
7	H(3)	+0.0922	+0.0949	+0.0974	+0.0881	+0.0851
8	H(5)	+0.0710	+0.0711	+0.0710	+0.0718	+0.0768
9	H(6)	+0.1288	+0.0851	+0.0734	+0.0983	+0.0633
10	C(7)	+0.0874	+0.0847	+0.0816	+0.0858	+0.0860
11	H(71)	+0.0015	+0.0034	+0.0056	+0.0021	+0.0033
12	H(72)	+0.0034	+0.0065	+0.0084	+0.0034	+0.0026
13	H(73)	+0.0034	+0.0038	+0.0049	+0.0060	+0.0045

Table 7.3 continued

14 N(2)	+0.5155	+0.5085	+0.5044	+0.5086	+0.5294
15 O(2)	-0.3949	-0.3729	-0.3467	-0.3824	-0.3628
16 O(3)	-0.3248	-0.3355	-0.3421	-0.3235	-0.3179
17 N(1)	-0.3453	-0.3513	-0.3737	-0.3520	-0.3417
18 C(8)	+0.3365	+0.3389	+0.3519	+0.3349	+0.3406
19 O(1)	-0.3657	-0.3660	-0.3706	-0.3631	-0.3515
20 C(9)	+0.0146	+0.0174	+0.0203	+0.0154	+0.0206
21 H(91)	+0.0115	+0.0078	+0.0004	+0.0093	-0.0028
22 H(92)	+0.0338	+0.0294	+0.0259	+0.0349	+0.0428
23 H(93)	+0.0338	+0.0360	+0.0383	+0.0325	+0.0325
24 NH	+0.2635	+0.2411	+0.2229	+0.2514	+0.2240
dipole (Debye)	1.9664	3.5822	5.6744	2.7143	6.9275
Heat of Formation ($kcalmol^{-1}$)	34.95	19.05	16.58	21.34	43.66

Analysis of the solvent-dependent ^{1}H n.m.r. spectrum of MNA

The signals in the ^{1}H n.m.r. spectrum are due to protons NH, H(3), H(5), H(6) and the protons in the methyl groups which involve C(7) and C(9).

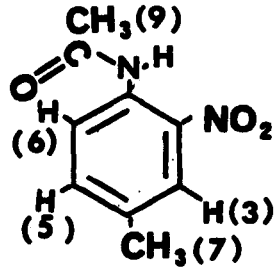

The latter protons give rise to singlets at 2.38 ppm and 2.30 ppm respectively in $CDCl_3$. The signals, due to the ring protons, in various solvents are shown in fig. 7.3 to 7.9 .

The explanation for the solvent dependence is mainly due to the variation of the chemical shift of H(6) which is strongly affected by its distance from O(1) i.e. the oxygen atom in the C=O group. The anisotropic effect of the C=O group is at its maximum when the amide group is in the same plane as the ring i.e. the H(6)...O(1) distance is at a minimum. Hence a decrease in the chemical shift of H(6) is consistent with a rotation of the amide group from the plane of the ring. This solvent shift is greater for solvents of greater relative permittivity and probably acts by reducing the electrostatic interaction between the amide NH and O(2) in the nitro group. A plot of the chemical shift of H(6) against solvent permittivity is shown in fig. 7.1 .

The splitting of signals due to the ring protons can be accounted for by spin-spin splitting. The extent of interaction is in the order

$$J(ortho) > J(meta) > J(para)$$

J(ortho) is about 9Hz when the chemical shift of H(6) differs from the chemical shift of H(5)by more than 0.5 ppm. J(meta) is of the order of 2Hz and J(para), which is observed when the spectrum is recorded in DMSO is 1Hz. The interaction of protons H(6) and H(5) varies from an AX type in deuterochloroform to an AB type in DMSO when the chemical shifts of H(6) and H(5) are approximately equal. The spin-spin splitting by the ring protons, which is shown in figs. 7.3 to 7.7, has been checked by specifying the chemical shifts and couplings shown in these figs. in the Pascal computer program NMR which is available from the Quantum Chemistry Program Exchange and has been described as a tried and tested computer program for the calculation of line positions and relative intensities for up to six interacting protons [212]. The calculated positions and intensities of lines obtained from this program are shown in figs. 7.3- 7.9.

The n.m.r. spectrum of the N,N-diacetyl derivative of 2-nitro-4-methylaniline shows a doublet at 7.12 ppm (J=8Hz) which must be due to the protons of type H(6). Inspection of molecular models shows that the most likely conformation

of this molecule is one with the amide group perpendicular to the ring. The upfield shift of the chemical shift of H(6) could be due to H(6) escaping from the deshielding effect of the anisotropic effect of the C=O group or perhaps H(6) enters the shielding zone of the C=O group or perhaps these two effects could be operating simultaneously. However, it would appear that the amide group is not perpendicular to the ring when MNA is in DMSO and has not attained the conformation of the amide group in MNA-1 (white) in which the amide group has moved 135° from the plane of the benzene ring. It is concluded that the chemical shift of H(6) is sensitive to the dihedral angle which the amide group makes with the ring plane but it is not possible to make a direct correlation between the chemical shift of H(6) and the dihedral angle between the amide and ring.

MNA is not sufficiently soluble in hexane solution to enable the n.m.r. spectrum to be recorded using a single sweep technique without interference from background noise. This problem was overcome by using a JEOL 400MHz instrument fitted with a data accumulation system. The spectrum collected from a saturated solution of MNA in deuterohexane + 5% deuterodichloromethane is shown in fig. 7.10 . The chemical shift of the protons of type H(6) is 9 ppm. This is the highest chemical shift recorded for this type of proton and is consistent with an inverse relationship between

the chemical shift of proton H(6) and the relative permittivity of the solvent. However, since the relative permittivity of this mixed solvent is not known the corresponding point is omitted from the graph shown in fig.7.1.

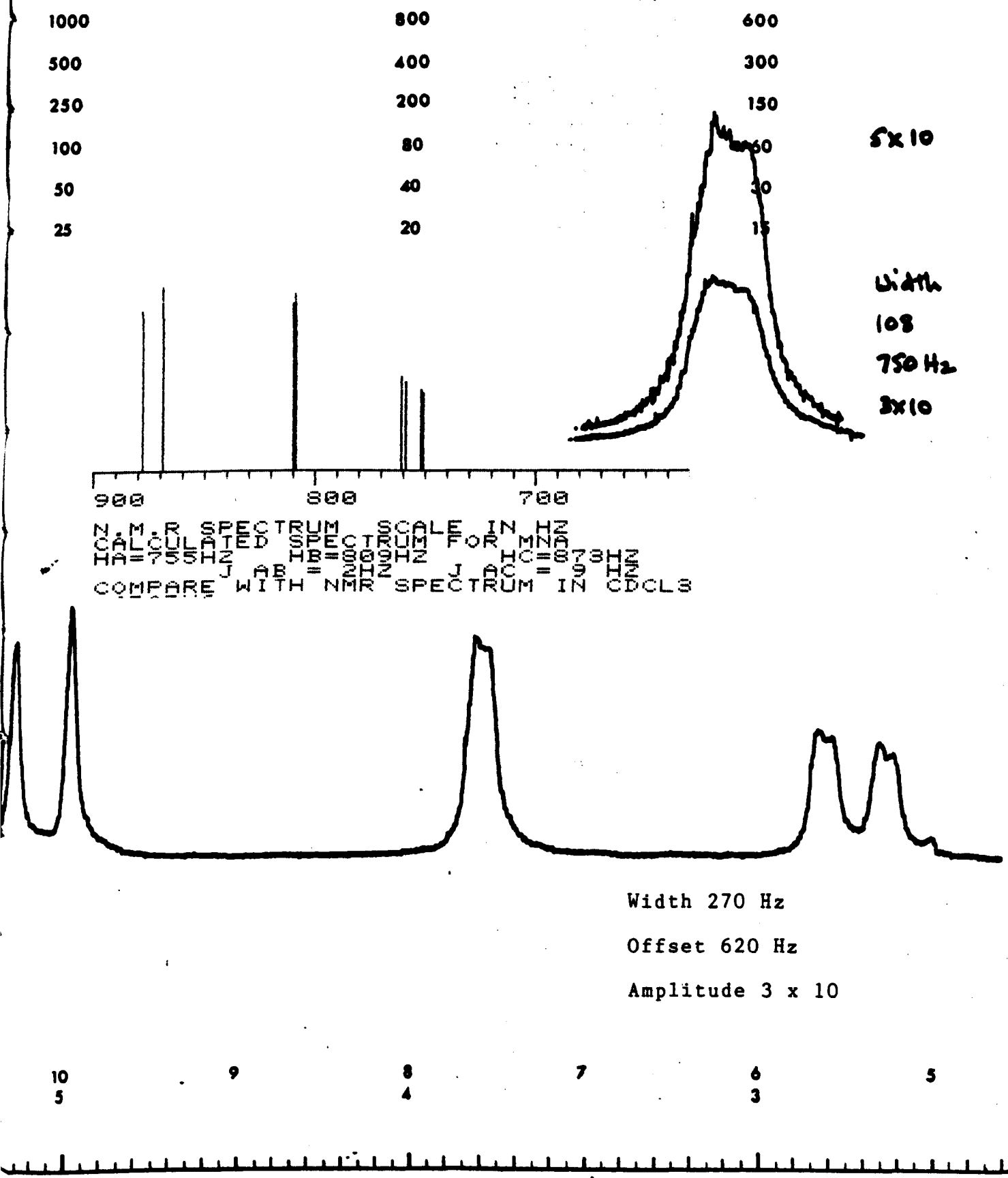

Fig. 7.3

The ^{1}H n.m.r. spectrum of MNA in $CDCl_3$

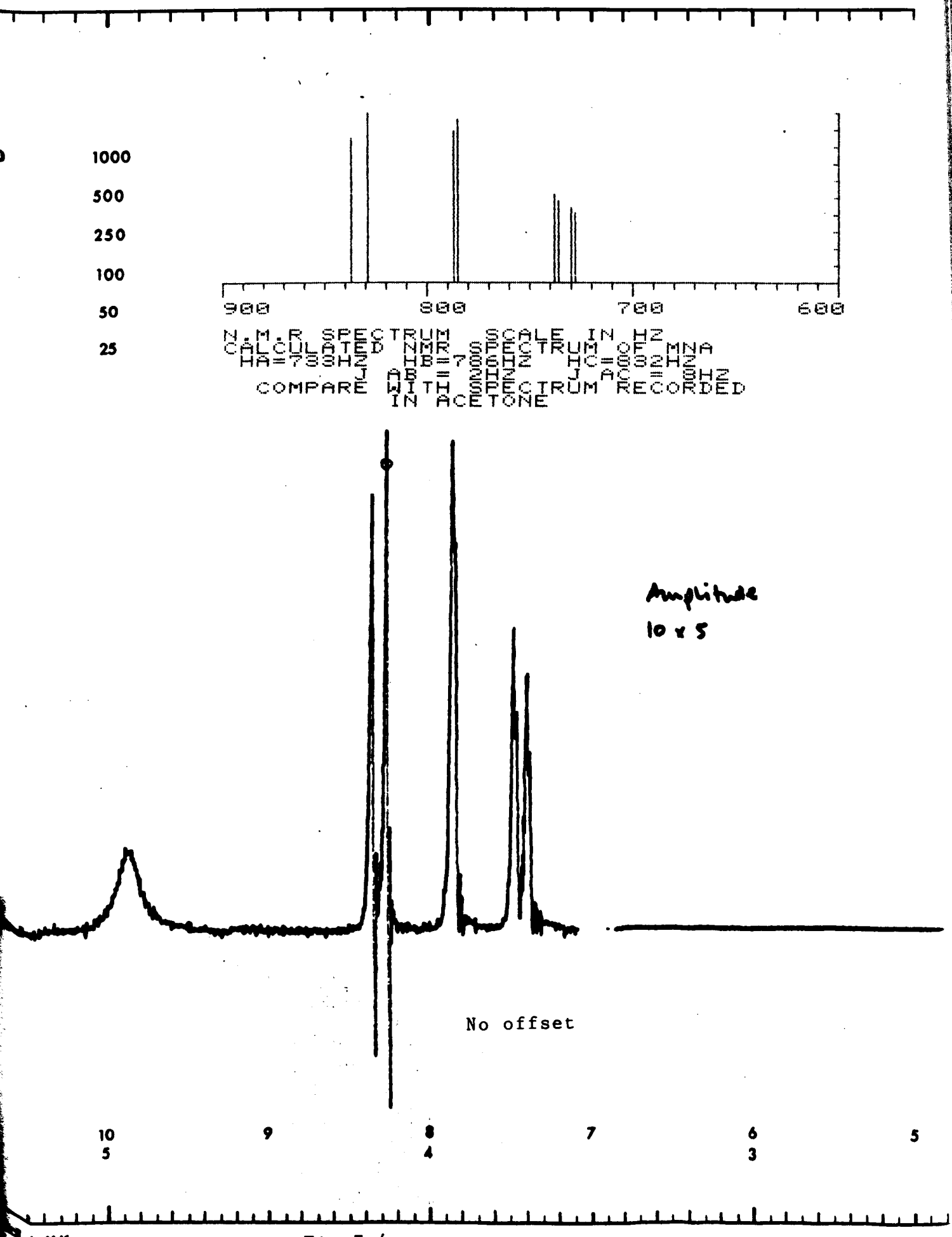

Fig 7.4

The ^{1}H n.m.r. spectrum of MNA in acetone

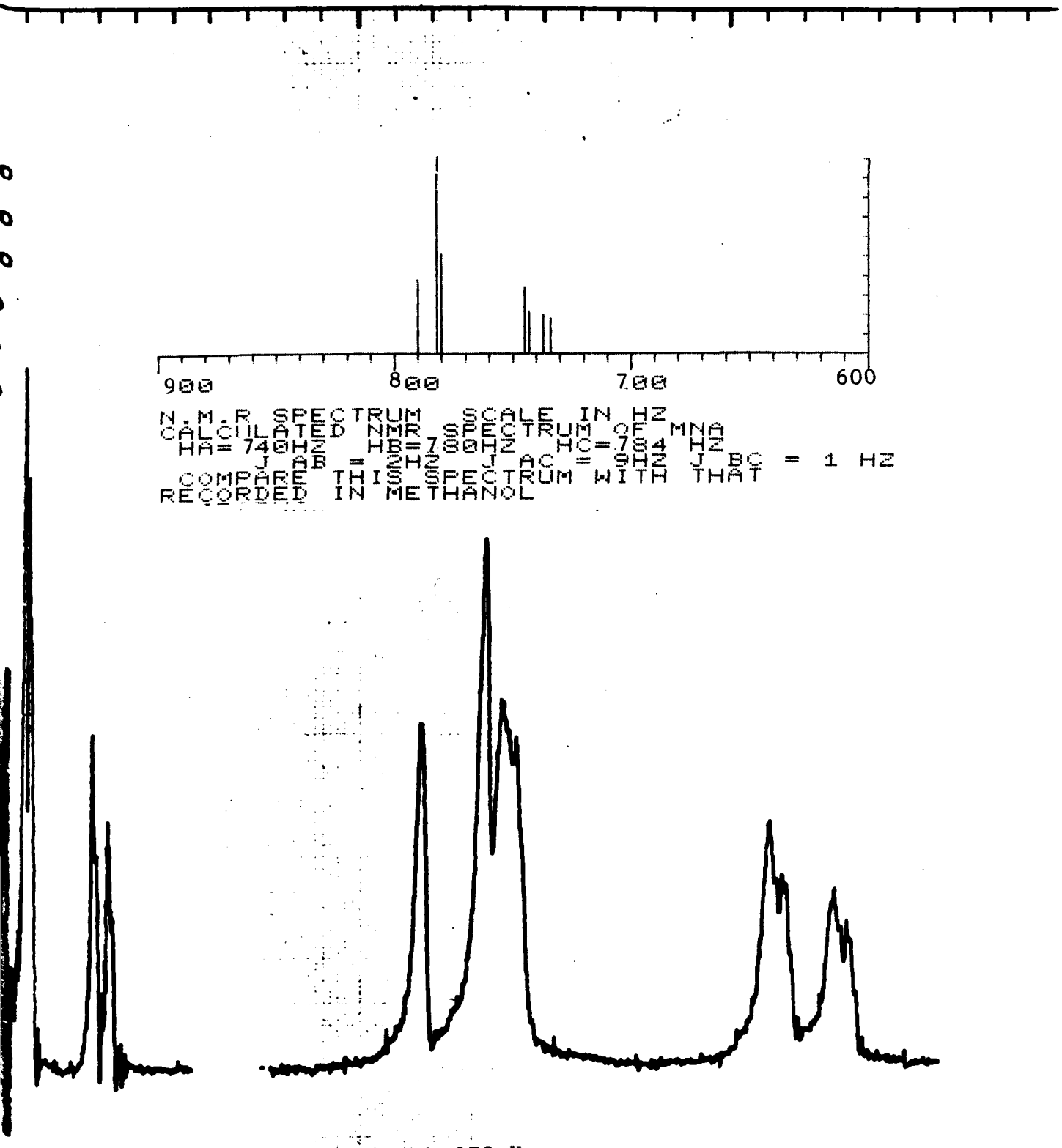

Fig. 7.5
The ^{1}H n.m.r spectrum of MNA in methanol

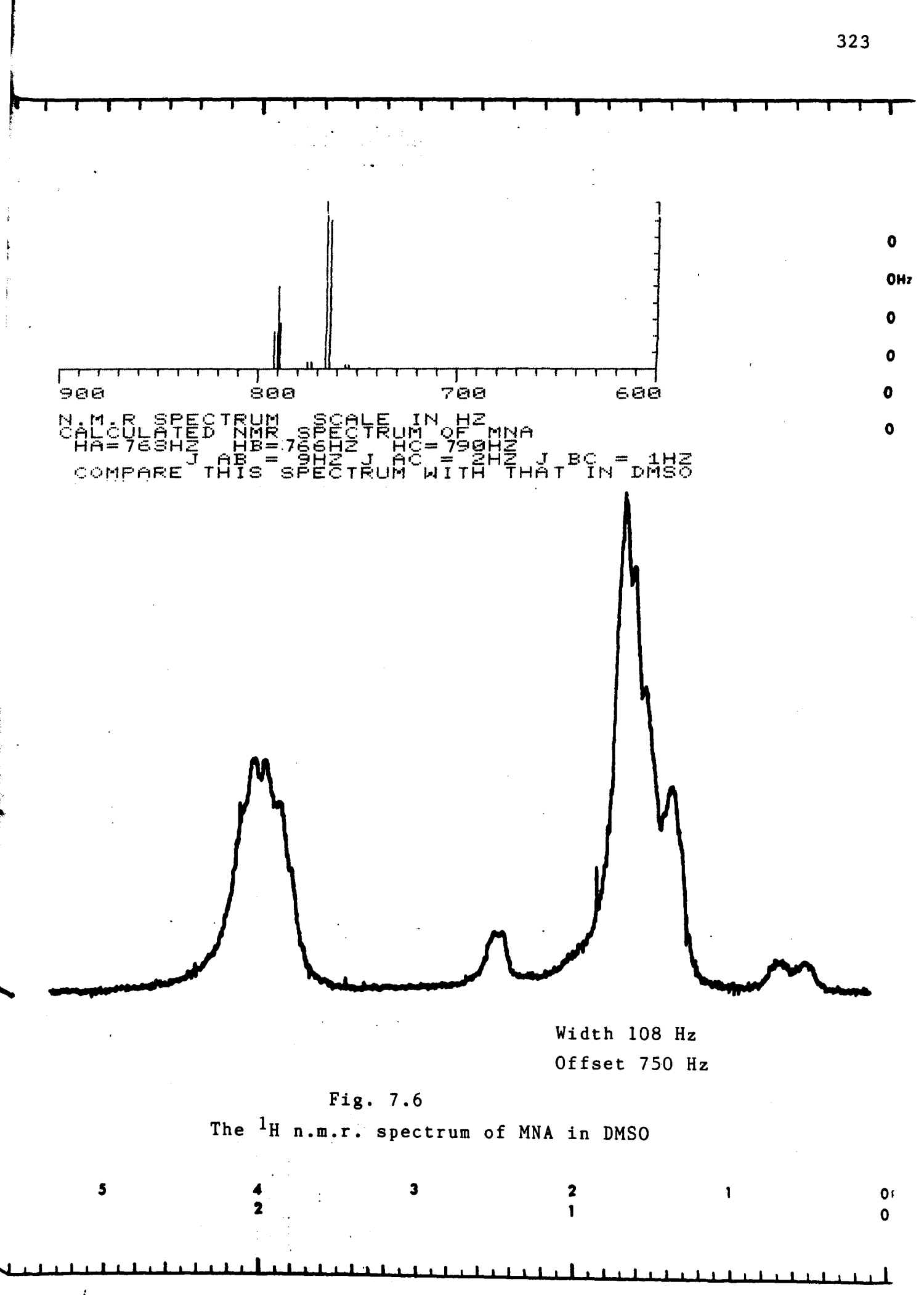

Fig. 7.6

The ^{1}H n.m.r. spectrum of MNA in DMSO

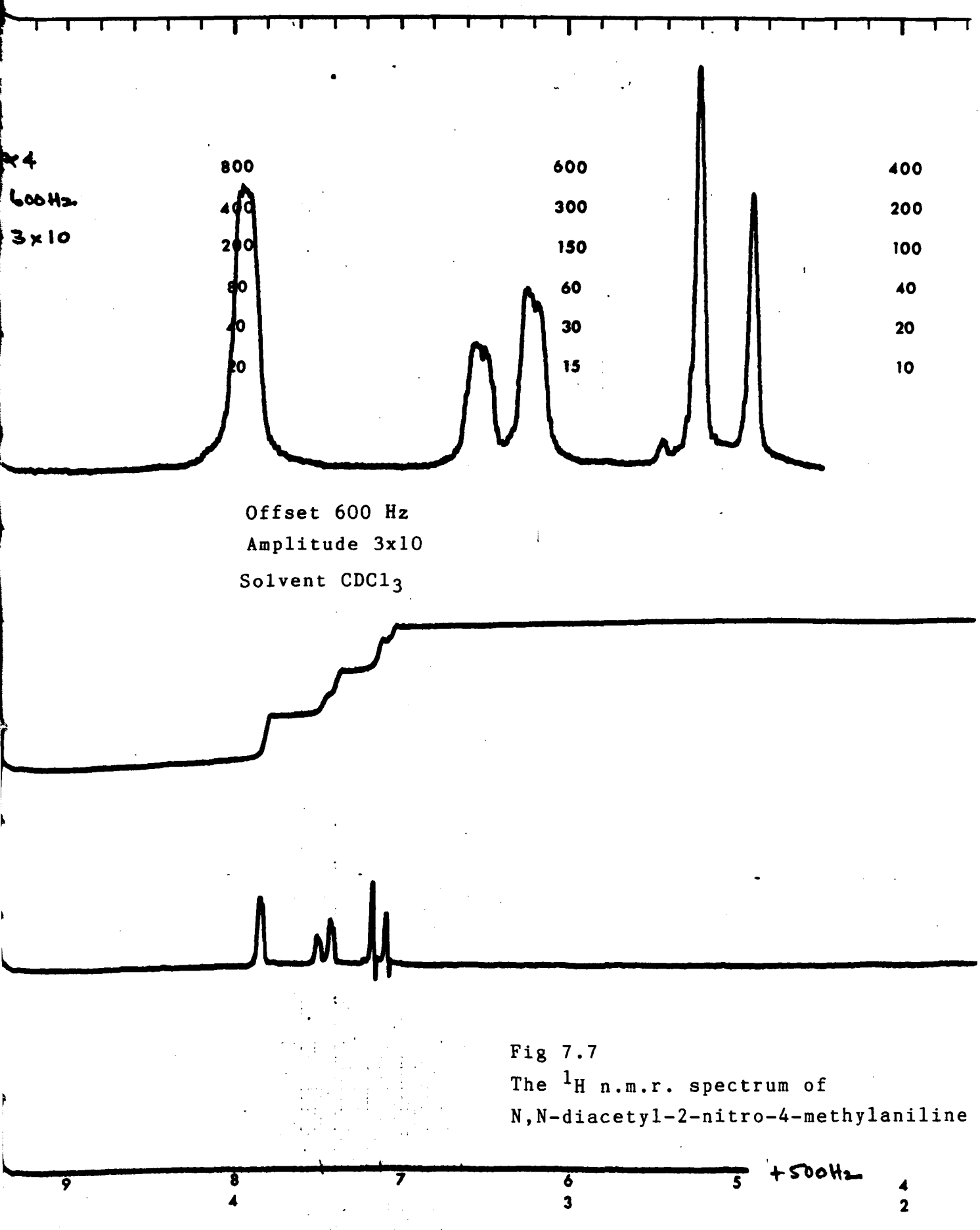

Fig 7.7
The ^{1}H n.m.r. spectrum of
N,N-diacetyl-2-nitro-4-methylaniline

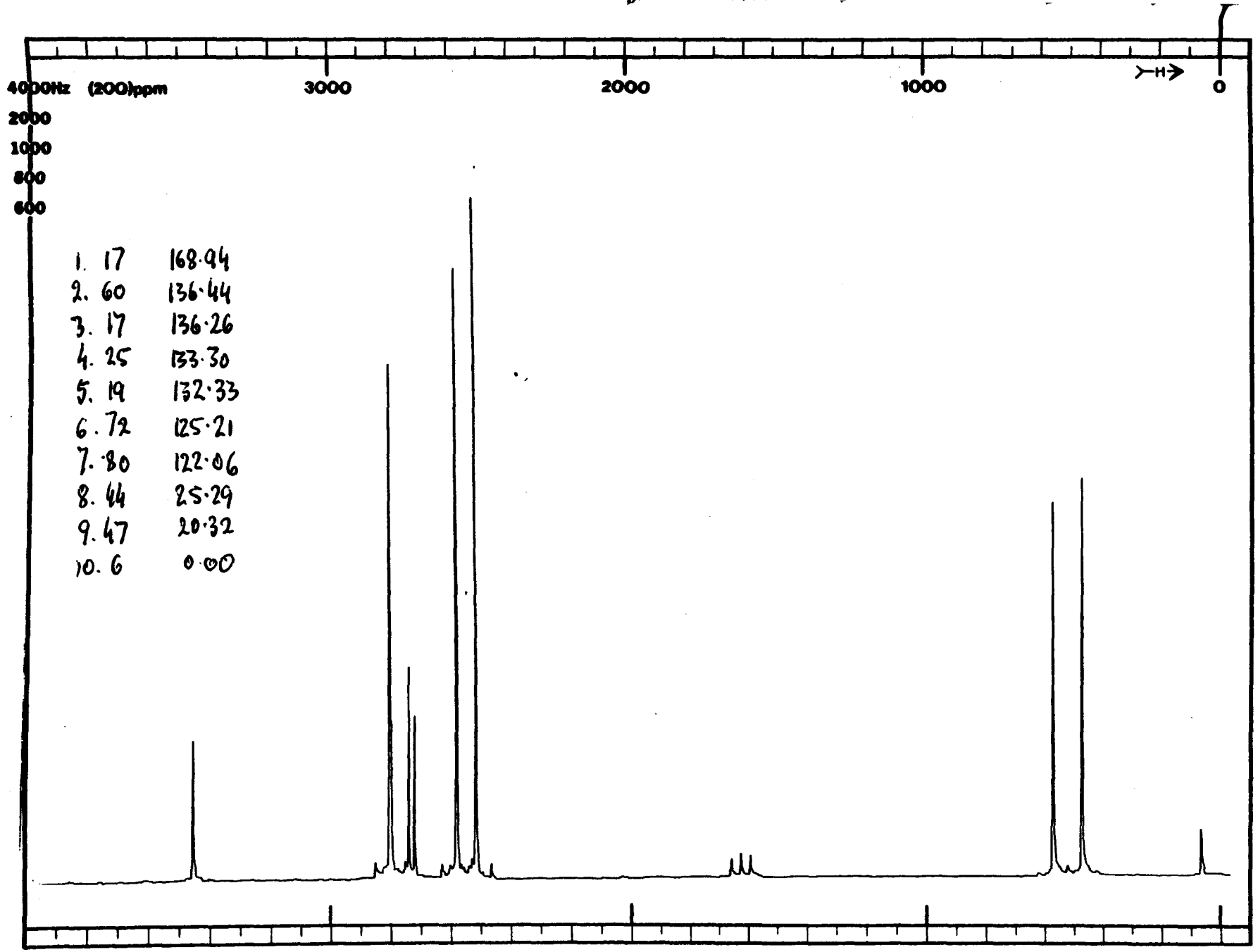

CFT-20 SPECTRUM NO.

OPERATOR lk DATE 22·11·

SAMPLE

4-methyl-2-nitro-acetanilide

Fig. 7.8

^{13}C n.m.r. spectrum of MNA in $CDCl_3$

LOCK SIGNAL $CDCl_3$

SPIN RATE 20 rps. TEMP RT °C

ACQUISITION

SPECTRAL WIDTH (SW) 4000 Hz

NO. OF TRANSIENTS (NT) 10000

ACQUISITION TIME (AT) ·511 sec.

PULSE WIDTH (PW) 10 µsec.

PULSE DELAY (PD) 2 sec.

DATA POINTS (DP) 4096

TRANSMITTER OFFSET (TO) 50

HIGH FIELD LOW FIELD

RECEIVER GAIN (RG)

DECOUPLER MODE (DM) 1

DECOUPLER OFFSET (DO) 57

NOISE BANDWIDTH (NB) 2 kHz

DISPLAY

SENS. ENHANCEMENT (SE) ·4 sec.

WIDTH OF PLOT (WP) 4000 Hz

END OF PLOT (EP) -75 Hz

WIDTH OF CHART (WC) 5678 Hz

END OF CHART (EC) -75 Hz

VERTICAL SCALE (VS) 80

REFERENCE LINE (RL) 0

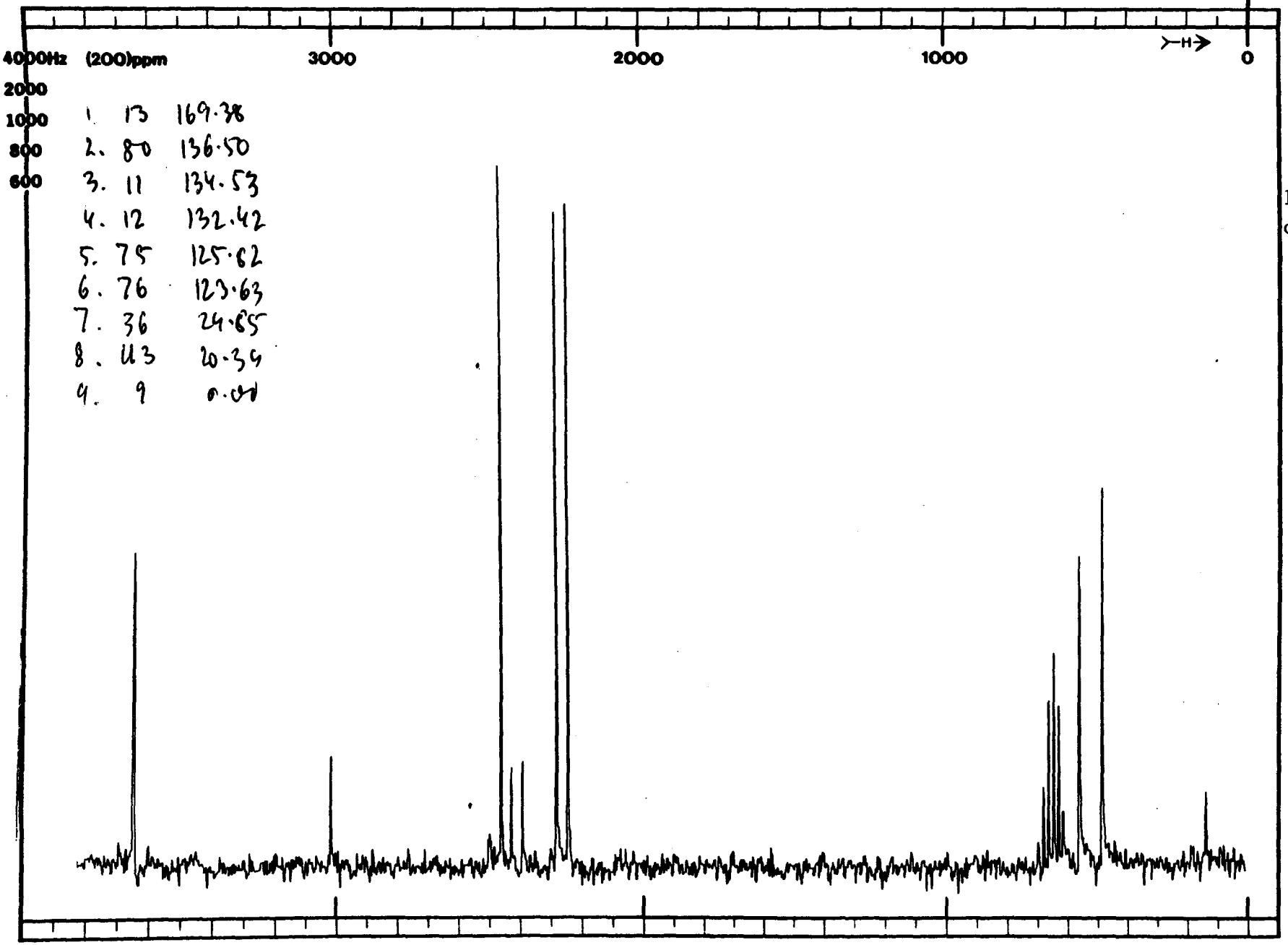

OPERATOR ..... DATE 4.86

SAMPLE 4-Me2NC6H4-CO-CD3

D_3C-CO-CD_3

Fig. 7.9

^{13}C n.m.r. spectrum of MNA in acetone-d_6

LOCK SIGNAL .....
SPIN RATE ..... rps. TEMP ..... °C

ACQUISITION
SPECTRAL WIDTH (SW) 4500 Hz
NO. OF TRANSIENTS (NT) 1336
ACQUISITION TIME (AT) 4 sec.
PULSE WIDTH (PW) 8 μsec.
PULSE DELAY (PD) 2 sec.
DATA POINTS (DP) .....

TRANSMITTER OFFSET (TO) .....
HIGH FIELD ..... LOW FIELD .....
RECEIVER GAIN (RG) .....

DECOUPLER MODE (DM) .....
DECOUPLER OFFSET (DO) .....
NOISE BANDWIDTH (NB) ..... kHz

DISPLAY
SENS. ENHANCEMENT (SE) ..... sec.
WIDTH OF PLOT (WP) ..... Hz
END OF PLOT (EP) ..... Hz
WIDTH OF CHART (WC) ..... Hz
END OF CHART (EC) ..... Hz
VERTICAL SCALE (VS) .....
REFERENCE LINE (RL) .....

Fig. 7.10
The ^{1}H n.m.r. spectrum recorded on a JEOL 400MHz instrument.

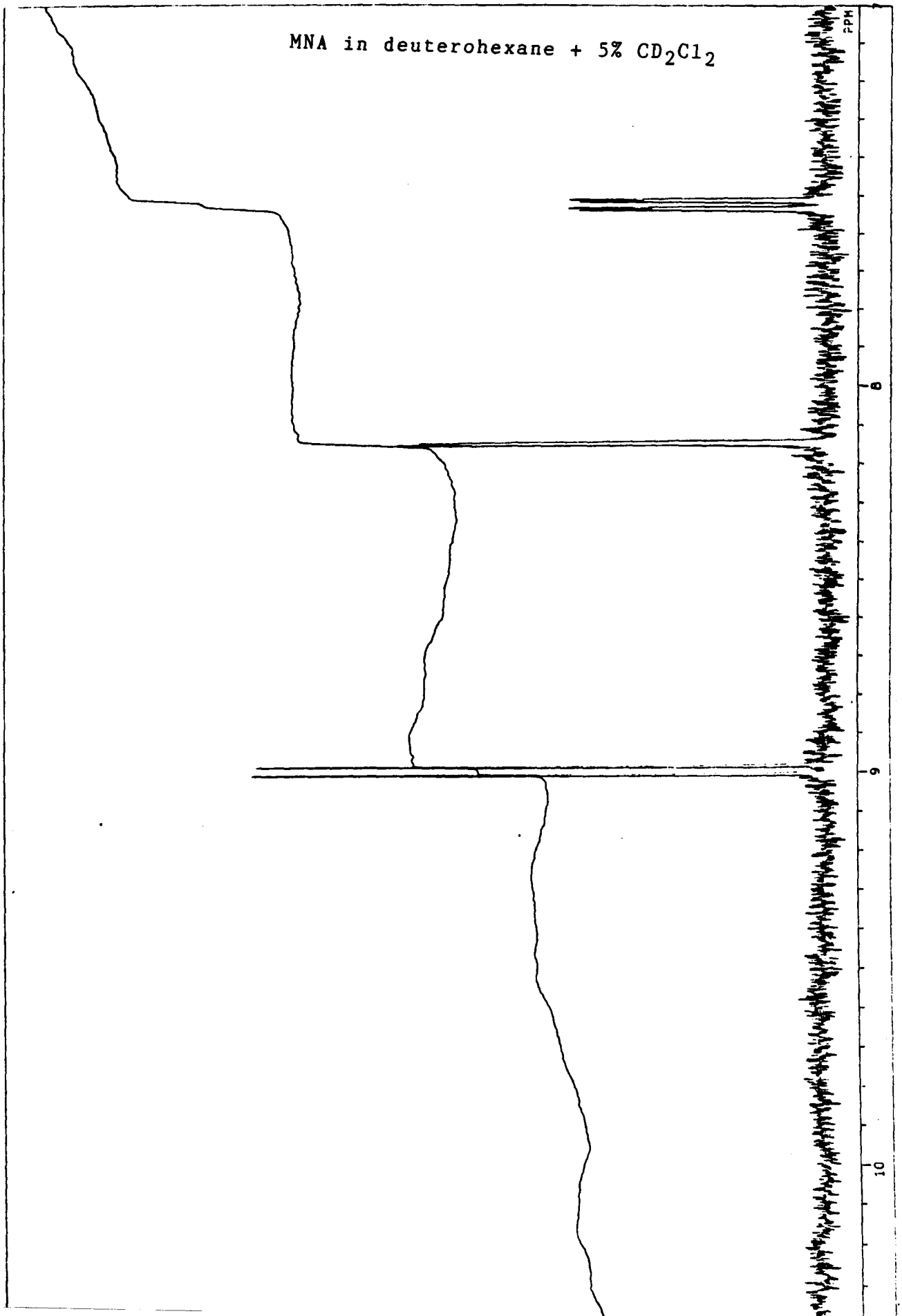

Chapter Eight

A search for polymorphism in a series of substituted nitroacetanilides.

A search for polymorphism in a series of substituted nitroacetanilides

The compounds investigated can be divided into five categories :-

1. 4-substituted 2-nitroacetanilides (I, Y = H; R = Me) ;

2. 5-substituted 2-nitroacetanilides (I, X = H; R = Me);

3. 4,5-disubstituted 2-nitroacetanilides (I, R = Me) ;

4. acyl derivatives of 4-methyl-2-nitroacetanilide (I, X = Me; Y = H) ;

5. a miscellaneous collection of nitroamides.

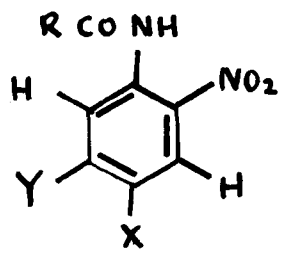

I

These compounds were prepared by means of one of three general methods :-

1. acetylation or acylation of a commercially available primary aromatic nitroamine (METHOD 1) ;

2. nitration of an acetamide derivative in acetic anhydride using the method of Lynch[213] (METHOD 2) ;

3. nitration of an acetamide using a mixture of concentrated nitric acid and concentrated sulphuric acid (METHOD 3) ;

Since these methods are classical synthetic methods and lead mainly to compounds which have been described in the chemical literature, only one example of each type of method is included in the experimental section.

The use of METHOD 3 often led to the formation of mixtures which were examined by TLC and separated by column chromatography using alumina as the separating material and this is indicated briefly in the experimental section.

The identity of each compound was established by

a) comparison with the literature m.p. ;

b) examination of the i.r. spectrum (KBr disc) ;

c) examination of the n.m.r. spectrum .

Methods used to test for polymorphism in nitroacetanilides and related compounds.

Each compound was recrystallised from light petrol (boiling range 40 - 60°C, or 60 - 80° C) as well as from a polar solvent such as methanol or a methanol-water mixture. The appearance and colour of the resulting crystals were examined under the microscope and the i.r. spectrum of each form was recorded. In many cases polymorphism could be detected simply by noting the colour of the crystals obtained from the two types of solvent since the form which consisted of molecules which contained intramolecular hydrogen bonds was pale yellow whereas crystals containing intermolecular hydrogen bonds were white or very pale yellow. Crystals containing intramolecular hydrogen bonds (yellow) were often obtained using petrol as crystallising solvent whereas those containing intermolecular hydrogen bonds (white form) were formed from solvents such as methanol or water.

Infrared spectroscopy proved to be a valuable tool for distinguishing between the two possible types of hydrogen bonding since the intramolecular hydrogen bonded form showed a band of medium intensity near 3400 cm-1 due to N-H stretching and also a band just above 1700 cm-1 due to a non-hydrogen bonded carbonyl group. The presence of the

intermolecularly hydrogen bonded form was characterised by a strong broad band near 3200 cm-1 and a strong band about 1680 cm-1 due to N-H and C=O stretching bands. In some cases the yellow form could not be obtained by recrystallisation from petrol but was formed by rapidly cooling the molten form. In cases where yellow and white forms were obtained it was found that grinding with potassium bromide could rapidly change the yellow form into the white form and intermediate stages have been observed in which the two forms were present. Hence, when using the potassium bromide disc technique it was necessary to use gentle grinding to avoid changing the yellow into the white form. Since the yellow and white forms are only stable in the crystalline state, techniques such as n.m.r. or UV are not suitable for the detection of this type of polymorphism. The last comment cannot of course be applied to reflectance UV which could be used to detect polymorphism resulting from intra- and intermolecular hydrogen bonds.

Table 8.1

An examination of some 4-substituted-2-nitroacetanilides for polymorphism

substituent	m.p.*	lit. m.p.	yellow form νN-H	yellow form νC=O	white form νN-H	white form νC=O	polymorphism
H	92	93(B)	3375	1705	-	-	no
Me	94	94(B)	3380	1720	3260	1675	yes
			3360	1710			
Et	45	46(B)	3300	1700	-	-	yes[Δ]
				1680			
Pr	70	77(B)	3360	1705	-	-	no
n-Bu	73	76(CA)	3360	1702	-	-	no
i-Pr	80	81(CA)	3350	1705	-	-	no
t-Bu	107	104.5(B)	3350	1710	-	-	no
F	70	71(D)	3360	1705	-	-	no
Cl	98	100(B)	3375	1718	-	-	no
Br	98	102(B)	3370	1715	-	-	no
CN	131	131(D)	3340	1715	-	-	no
nitro	121	120(B)	3340	1712	-	-	no(1)
acetyl	139	141(D)	3350	1725	-	-	no
OMe	117	120(D)	3380	1708	-	-	no

[Δ] After standing at ambient temperature for about five years, colourless hexagonal plates had formed and i.r. spectroscopy confirmed them as a "white" form.

* all m.p.s are reported in degrees centigrade. Experimental determinations were made on a Kofler Hot Stage. The sources of m.p.s are given in Table 8.2

(1) see Appendix 11.1 for details of unit cell dimensions and symmetries for yellow polymorphs of this compound.

Table 8.2

An examination of some 5-substituted-4-methyl-2-nitroacetanilides for polymorphism

5-substituent			yellow form		white form		polymorphism
	m.p.*	lit. m.p.	νN-H	νC=O	νN-H	νC=O	
Me	106	107(D)	2250	1715(s) 1700(m)	-	-	no
F	96	94(B)	3335	1710	-	-	no
Cl	112	112(B)	3360	1700	3220	1680	yes(3)
Br	121	120(D)	3320	1700	3220	1680	yes(1)
I	152	-	3340	1695	3330	1665	yes(2)
nitro	135	132(H)	detectable		3240	1685	yes(4)

(1) yellow form obtained from a melt.

(2) i.r. reveals yellow form from methanol-water and a mixture of forms from petrol.

(3) yellow and white forms obtained by recrystallisation from petrol and methanol-water respectively.

(4) yellow form mixed with white form.

* The sources of literature values for melting points are: B = Beilstein; D = Dictionary of Organic Compounds; CA = Chemical Abstracts; L = Lynch (Reference 213); H = Hickinbottom (Reference 216).

Table 8.3

An examination of some acyl derivatives (R.C=O) of 4-methyl-2-nitroacetanilide for polymorphism

substituent			yellow form		white form		polymorphism
R	m.p.	lit m.p.	νN-H	νC=O	νN-H	νC=O	
H	124	-	-	-	3260	1680(s)	no(1)
PhCO	144	143(B)	3360	1690	-	-	no
o-ClC6H4	139	139(B)	3370	1690	-	-	no
Et	85	-	3340	1680	-	-	no
Pr	59	62(B)	3350	1700	-	-	no(3)
n-Bu	59	-	3340	1675	-	-	no
n-pentyl	54	-	3355	1705	-	-	no
t-Bu	64	-	3400	1690	-	-	no
i-Bu	88	88(B)	-	-	3270	1660	no(2)
CH2Cl	118	122(B)	3290		1685	-	- no

(1) perhaps Z and E forms of this compound are present.

(2) only the white form of the compound was obtainable.

(3) crystals of this compound were obtained in the form of needles as well as plates.

Table 8.4

An examination of some 5-substituted-2-nitroacetanilides for polymorphism

substituent			yellow form		white form		polymorphism
	m.p.	lit. m.p.	νN-H	νC=O	νN-H	νC=O	
Me	84	87(L)	3355	1695	-	-	no
F	87	90(L)	3335	1705	-	-	no
Cl	114	118(L)	3335	1695	-	-	no
Br	143	138(L)	3350	1700	-	-	no
CN	135	132(D)	3360	1720	3260	1675	yes
nitro	116(Y) 121(white)	121(L)	3370	1715	3260	1670	yes
acetyl	118	121	3350	1690	3280	1675	yes
OMe	121	125(L)	3330	1700	-	-	no
CF_3	65	-	-	-	3300	1685	no
COOH	205	205(D)	-	-	3260	1680*	yes
COOMe	95(petrol) 104(MeOH)	-	3390	1730	-	-	yes

* the 5-COOH derivatives hydrolyses very easily on grinding with KBr and a yellow form was only made on melting.

* Different crystalline forms of the 5-COOMe were obtained by crystallisation from either petrol or methanol. The value for N-H stretching was the same in both cases but the form from methanol shows a distinct doublet near 1700 cm-1 as well as additional differences.

Table 8.5

Data on miscellaneous amides which have been examined for purposes of comparison.

name	yellow form			white form		polymorphism
	m.p.	lit.m.p.	νN-H	νC=O	νN-H	νC=O	
2-nitro-4-ethylpropionanilide							
	78	-	3350	1710	-	-	no
2-methyl-5-nitroacetanilide							
	155	150(D)	-	-	3280	1670	no(5)
3-chloro-4-methylacetanilide							
	88	83(B)	-	-	3300	1670	yes(1)
	102	104(B)	-	-	3300	1670	
2-chloro-4-methylacetanilide							
	110	118(B)			3280	1660	no
N-benzenesulphonyl-4-methyl-2-nitroaniline							
	99	99(B)	3260	-	3260	-	yes(2)
3-nitro-4-methylacetanilide							
	143	144(D)			3280	1660	no
2-nitro-1-acetamidonaphthalene							
	195	199(B)	-	-	3290	1660	?(3)
1-nitro-2-acetamidonaphthalene							
	124	124(B)	-	-	3200	1670	yes(4)
6-methyl-2-nitroacetanilide							
	158	158(B)	-	-	3250	1660	no

(1) this compound was obtained as needles from ethanol-water (m.p. 88°C) and as plates from toluene (m.p. 110°C) The i.r. spectrum of each form was the same. The polymorphism of this compound has been reported earlier [214] .

(2) well formed yellow (rectangles) and white crystals were formed simultaneously by slow evaporation of an ethanol solution. Yellow and white forms of this compound have been reported [215] .

(3) the infrared spectrum of a sample of 2-nitro-1-acetamidonaphthalene which crystallised from methanol as yellow needles showed only one band near 1700 cm-1 whereas another batch showed two strong bands (1670 and 1725 cm-1) in this region as well as additional bands in other regions. The latter sample could be a mixture of polymorphic forms but only one polymorphic form corresponding to an intermolecularly hydrogen bonded form was obtained in a homogeneous form.

(4) 1-nitro-2-acetamidonaphthalene crystallised as fine needles from petrol or rods from methanol and in each case the i.r. spectrum showed only one band near 1670 cm-1 and a cluster of sharp unresolved peaks near 3200 cm-1 which would indicate intermolecular hydrogen bonding. However a sample recrystallised from methanol-water showed strong bands at 1730 and 1670 cm-1 and additional new peaks but a homogeneous polymorph was not isolated.

(5) a mixture of two different crystalline forms was obtained using methanol as a crystallising solvent.

Table 8.6

Some deuterated MNA species which have been examined for polymorphism

name	νN-H	νC=O	crystal type(5)
N-D MNA	2520	1720	MNA-3
	2500	1700	
	2400	1670	MNA-1
trideuteroacetyl derivative of MNA			
MNA-d3	3380	1720	MNA-3
	3360	1700	(1)
3',5',6'-trideuteroMNA (ring deuterated)			
	3365	1710	MNA-2
	3380	1720	MNA-3
	3360	1705	(2)
3',5',6',7',7',7'-hexadeuteroMNA (ring deuterated and a 4-CD3 group)	3360	1710	MNA-2
	3380	1720	MNA-3
	3360	1700	(3)
	3370	1670	MNA-1(4)

(1) Both N-D compounds were made by crystallising MNA from deuterium oxide.

(2) The characteristic doublets of the triclinic form are clearly observed. Crystallisation from aqueous ethanol gave crystals which gave an i.r. spectrum of the same type as MNA-2 and after standing for two years a portion of the sample had changed to hair-like crystals which gave the MNA-3 type of i.r. spectrum.

(3) Crystallisation from petrol gave a sample which gave an i.r. spectrum which is similar to that of MNA-2. Crystallisation of a sample from aqueous ethanol gave a sample which had an i.r. spectrum showing the characteristic doublets of the MNA-3 crystal structure.

(4) Vigorous grinding of the sample with KBr gave a spectrum which was characteristic of the white form i.e. MNA-1

(5) The crystal type (i.e. either MNA-1 or MNA-2 or MNA-3 type) was assigned by comparison with the i.r. spectrum of the appropriate polymorph.

Comments on the polymorphism of deuterated MNA.

The replacement of H(10) i.e. the amide hydrogen, by deuterium does not affect the ability of MNA to exist in yellow (MNA-3) and white forms (MNA-1) and a similar result was obtained when the aromatic hydrogen atoms and the hydrogen atoms in the ring methyl group were replaced by deuterium. In marked contrast to this behaviour, the trideuteroacetyl derivative i.e. where $CH_3C{=}O$ was replaced by $CD_3C{=}O$, no method could be found which would convert the yellow crystalline material (which had an i.r. showing the characteristic doublets of the MNA-3 form) into the white form. The methods which were used to attempt the conversion were those which rapidly convert MNA-3 into MNA-1 and include (i) treatment with ultrasonic sound waves for 30 minutes, (ii) prolonged grinding with KBr and, (iii) crystallisation from water.

It is concluded that the conversion of MNA-3 to MNA-1 goes via an intermediate which contains a cis amide structure as shown in fig. 4.20 . This shows that the more bulky CD_3 group will be sterically hindered by the nitro group. This, together with the increased energy required to rotate the heavier amide group may make the polymorphic change far less likely to occur in this case. Also a crystalline sample containing an approximately 50:50 mixture of trideuteroacetyl MNA and unlabelled MNA would not undergo the conversion of MNA-3 to MNA-1. This behaviour , in which a deuterated analogue has a totally different physical property from its

undeuterated analogue, is unusual.

Another important aspect of the deuterated compounds is that they provide i.r. spectra which may be compared with those of the various types of MNA and are an important aid in interpreting the i.r. spectra of MNA.

A discussion of the factors affecting the occurrence of white and yellow forms of o-nitroacetanilides

Until the work described in this thesis was published no data existed in the literature concerning the crystal structure of an o-nitroacetanilide and hence comparison of the crystal structure of MNA with this type of compound is not possible. However, from a study of the yellow and amber forms of MNA it is possible to postulate some generalisations which are likely to affect the stabilities of white and yellow forms.

In molecules where the amide group is intramolecularly bonded to the nitro group the general shape is that of a planar system and if the resulting crystal involves ring - ring interactions along a column with a possibility of intercolumnar molecules being nearly coplanar then the resulting crystal will be needle or rod shaped. Such crystals will be yellow or orange due to the extended conjugation due to resonance interaction between the benzene ring, the amide group, the nitro group, and the other substituent group(s). The latter could give rise to additional strong dipole-dipole interactions which would stabilise the columnar structure. It is likely that these factors influence the crystal structures of the compounds

given in table **8.1.** In this series of compounds, containing one substituent in the 4 position, the intramolecularly hydrogen bonded (yellow) form is favoured. The substituent is too remote to cause an intramolecular steric effect and any electronic effects on the strength of the hydrogen bond, caused by inductive and resonance effects, are probably insignificant compared to those of the adjacent nitro group. The only compound bearing a substituent in the 4 position which shows yellow and white polymorphism is MNA which contains a methyl group in this position. In this case additional dipole - dipole interactions would be expected to be small. However the inductive effect of the methyl group may reduce the partial charges on the ring which may be involved in ring - ring interaction and an induced inductive effect (an inductiomeric) effect of the methyl group may assist in off-setting a reduction of conjugation with the nitrogen in the amide group as the folded conformation is being formed.

The presence of an electron withdrawing group in the 5 position reduces the stability of the yellow form and four compounds bearing a 5 substituent were found which possessed the ability to exist in white and yellow forms. The i.r. spectrum of the yellow and white form of each compound were different and the shifts in bands were very similar to those noted for yellow and white forms of MNA.

A possible reason for the reduced stability of the yellow form may be the presence of electron withdrawing groups in positions which would withdraw electron density from the same positions in the benzene ring. In order to counteract this effect the groups may prefer to twist out of the plane of the benzene ring as is found in molecules of 1,4 dinitrobenzene.[219] If the 2-nitro substituent is in the ring plane then the 5 substituent will be distorted from the plane of the ring. It is also possible that the 5 substituent could exert an inductive effect on the 2-nitro group which would weaken its ability to form the intramolecular hydrogen bond.

The presence of electron donating groups in the 5 position stabilises the yellow form. In this case, the resonance interaction between the substituent and the nitro group is favoured if the nitro group is coplanar with the ring.

The compounds listed in Table 8.3 contain a variable acyl side chain. The majority of these compounds exist in the yellow form with their i.r. spectra showing bands near 3350cm-1 and 1700 cm-1. However, two compounds, viz. the formyl derivative (R = H) and the 3-methylbutanoyl (isovaleryl) derivatives could only be obtained in crystalline forms whose i.r. spectra suggested that the white form was present. The i.r. spectrum of the formyl derivative showed strong bands at 1680 cm-1 and 1710 cm-1 which might indicate that the amide group was present in Z and E forms but no explanation can be offered as to the absence of a yellow form. The formation of the E (or cis) conformation is favoured by the replacement of the methyl group by H which will not be sterically hindered by the ring H(6) as much as a larger carbonyl oxygen (O1). In the case of the isovaleryl derivative the intramolecularly hydrogen bonded form may be destabilised by the side chain methyl group as shown in the formula below :-

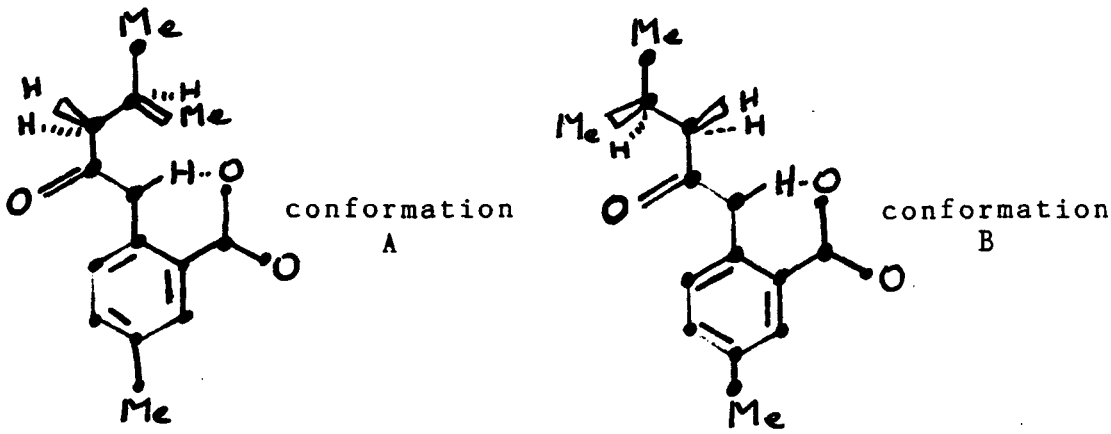

Fig. 8.1 Two possible conformations of the isovaleryl derivative are shown. The atoms which are emphasised lie in one plane. In conformation A the intramolecular hydrogen bond is sterically hindered whereas in B a side chain Me group lies close to the C=O group.

Of the 4,5-disubstituted-2-nitroacetanilides which were examined for polymorphism only the 4-methyl-5-chloro and 4-methyl-5-bromo compounds were obtained in separate crystalline forms. In each case the yellow form consisted of yellow needles whilst the white form consisted of plates which were similar in appearance to the white form of MNA. The i.r. spectra of these polymorphs were consistent with intramolecular hydrogen bonding in the yellow form and intermolecular hydrogen bonding in the white form.

The iodo derivative and nitro derivative listed in Table 8.2 were obtained in the yellow and white forms respectively but evidence was obtained for the existence of the alternative forms in each case (see notes (2) and (4) in Table 8.2).

A tentative conclusion from this series of compounds is that the presence of a methyl group situated para with respect to the amide group assists in the ease with which the amide group can rotate out of the plane of the benzene ring.

Several of the miscellaneous amides which are mentioned in Table 8.5 cannot exist in white and yellow forms since they do not possess ortho nitro and amide groups. Polymorphic forms of the chloro derivatives were obtained. These compounds had different crystalline forms but their i.r. spectra were identical.

A clear case of yellow and white polymorphism was found in the case of the N-benzenesulphonyl derivative.[215] Yellow and white crystalline forms were obtained and each form had a different i.r. spectrum although the wavenumber of the N-H stretching band for the two forms was the same.

In the cases of the acetamidonitronaphthalenes the form which was readily obtained by crystallisation from solvent was the white form. However, in each case, there was clear evidence from the presence of two bands near 1700 cm-1, that two forms of each compound were possble in the solid state but only the form having intermolecular hydrogen bonds was obtained in a homogeneous form. Since the hydrogen attached to C(8) in the naphthalene ring would be expected to cause steric hindrance to both adjacent 1- nitro as well as 1-amide groups it is predicted that the yellow forms of these compounds would be relatively unstable.

CHAPTER NINE

Experimental methods and d.s.c. experiments.

Experimental details

Nitration techniques used to prepare nitroacetanilides.

METHOD 1

Acetylation of primary aromatic amines.

The amine (1 g) was heated with acetic anhydride (4 cm^3) and concentrated sulphuric acid (1 drop) for 30 minutes. The mixture was cooled and poured into water. The resulting oil was stirred with a glass rod until crystallisation occurred and the crude acetyl derivative was recrystallised from aqueous ethanol.

METHOD 2

A solution of nitric acid (d, 1.52, 6 cm^3) in acetic anhydride was prepared at 0°C and a saturated solution of the substituted acetanilide(5 g) was added portionwise so that the temperature was maintained at 0°C. The solution was kept for one hour at 0°C and then poured into water. The crude nitroacetanilide was collected at the pump, washed with water and recrystallised from ethanol-water.

METHOD 3.

The substituted acetanilide(5 g) was dissolved in concentrated sulphuric acid and the mixture cooled to 0°C and a mixture of concentrated nitric acid (10 cm^3) and sulphuric acid(13 cm^3) was added. The mixture was kept at 0°C for one hour and poured into water. The crude solid nitroacetanilide was collected at the pump and recrystallised from aqueous ethanol.

Equations for METHODS 1,2, and 3.

METHOD 1.

$$RNH_2 + Ac_2O \longrightarrow RNHAc + HOAc$$

METHOD 2.

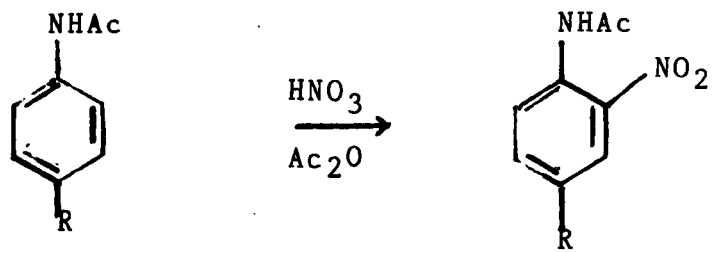

METHOD 3.

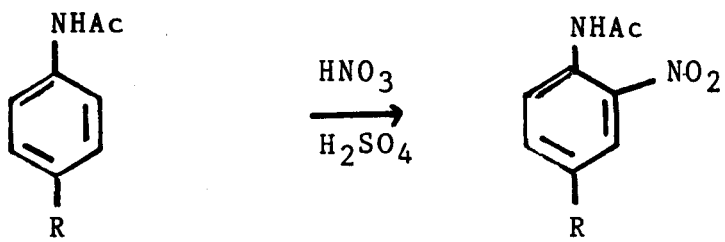

Experimental details for the preparation of deuterated derivatives of MNA

Preparation of N-d MNA.

MNA(ca 0.1 g) was boiled with D_2O for several minutes. Yellow (MNA-3) crystals form rapidly from the hot solution and were collected on filter paper after decanting the excess liquid. If the white form was required then the cycle of heating to effect solution and reprecipitation was repeated until the white form precipitated. Alternatively the hot clear solution was seeded with a trace of the white form.

Preparation of 4-methyl-2-nitroacet-d_3-anilide.

To a mixture of acetic -d_3-acid-d (2 g) [ALDRICH GOLD LABEL] and DMF (2 drops) surrounded by an ice bath, thionyl chloride (2.4 cm^3) was added and the mixture was allowed to stand for 30 minutes. A solution of 4-methyl-2-nitroaniline (0.4 g) in pyridine (4 cm^3) was then added dropwise. A yellow product separated from the reaction mixture and this was recrystallised from water to yield small yellow needles. The i.r. spectrum of this product is shown in spectrum . The n.m.r. spectrum of this compound showed no peak at 2.28 ppm which confirms the absence of the protonated form of

the acetyl group. The mass spectrum of the compound showed peaks at the following m/z values 197, M+; base peak 153, M+ $-COCD_2$; 46, $COCD_3$. No peak was observed at m/z 194 which would correspond to an undeuterated MNA. [The mass spectrum and n.m.r. of 4-methyl-2-nitroacet-d_3-anilide were recorded by Mr. B.G.Dalgarno, Kodak Ltd Harrow]

Reactions involved in the preparation of 4-methyl-2-nitroacet-d_3-anilide

$$CD_3CO_2D + SOCl_2 \longrightarrow CD_3COCl + SO_2 + DCl$$

$$CD_3COCl + \text{4-methyl-2-nitroaniline} \longrightarrow \text{4-methyl-2-nitroacet-}d_3\text{-anilide}$$

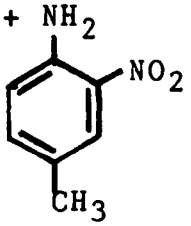

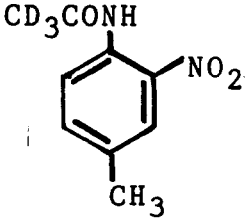

Preparation of 3,5,6-trideutero-4-methyl-2-nitroacetanilide.

The reactions which were used to prepare the title compound include replacement of the aromatic hydrogens in p-acetotoluidide by deuterium followed by a nitration in acetic anhydride.

Preparation of 2,3,5,6-tetradeutero-4-methylacetanilide.

p-Acetotoluidide (0.2 g) was added to dideuterosulphuric acid (2.0 cm^3) [ALDRICH GOLD LABEL] and the solution was heated to 60°C, with exclusion of moisture for two hours. The solution was cooled, poured into water and the precipitate collected at the pump. Recrystallisation from ethanol gave white crystals m.p. 149.5°C. This procedure was repeated since the n.m.r. spectrum of the product revealed small peaks due to residual aromatic protons but a second treatment with deuterosulphuric acid gave a product which gave an n.m.r. spectrum which showed aromatic protons to be absent.

The product from the above reaction was added to a mixture of concentrated nitric acid (1 drop) and acetic anhydride (4 drops) surrounded by an ice-water mixture. Water was added

to the reaction mixture after 30 minutes and the yellow product was filtered off and recrystallised from ethanol to give yellow crytals m.p. 93°C.

The product obtained showed no aromatic signals in the n.m.r. spectrum and the mass spectrum of the compound showed peaks at the following m/z values 197, M+; base peak 155, (M-COCH2)+; 109, 155-NO2. These peaks are consistent with the replacement of the three aromatic protons of MNA by three deuterium atoms. The i.r. spectrum, n.m.r. spectrum and mass spectrum showed that only a trace of aromatic protons could be detected.

[The MS and n.m.r. of this product was recorded on an AEI MS 30 and Jeol 100Mz n.m.r by Mr. D. Langton of ICI, Jealotts Hill, Bracknell]

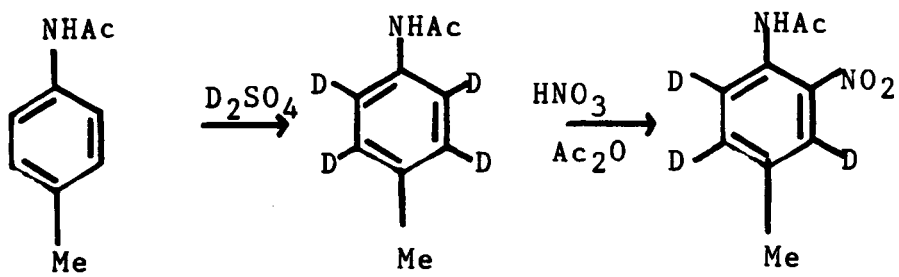

Preparation of the labelled acetophenone (B)

Aluminium chloride (17.5 g) was mixed with toluene-d_8 (5 cm^3) and carbon disulphide (10 cm^3). The mixture was stirred and cooled by an ice-water bath whilst acetic anhydride (5 cm^3) was added. After heating the mixture under reflux for 30 minutes the reaction mixture was cooled, poured into water and extracted with dichloromethane. The dichloromethane layer was washed with water (3 x 25 cm^3), filtered through phase separating paper and evaporated to give a light amber oil (4.3 g). The i.r. spectrum had a complex system of bands near 2200 cm^{-1} which is characteristic of C-D stretching bands in aromatic systems and a strong band near 1700 cm^{-1} due to C=O stretching.

Preparation of the oxime (C).

The ketone (2 g) was heated with hydroxylamine hydrochloride (2 g), and sodium hydroxide (4 g) in a solution of water (15 cm^3) and ethanol (10 cm^3) for 45 minutes. The crude oxime was precipitated by acidification with hydrochloric acid and collected at the pump.

The Beckmann rearrangement of the oxime

The crude oxime was heated with the minimum of polyphosphoric acid which would effect solution at 130° C. After heating for 10 minutes the solution was cooled, diluted with water and the precipitate was collected at the pump and washed thoroughly to remove the acid. A buff solid (ca 0.8 g) was obtained which was heated with dideuterosulphuric acid in order to attempt to replace any aromatic protons, which had been introduced by the acidic conditions of the rearrangement reaction, by deuterium. The i.r. spectrum of this compound showed many bands which were present in the i.r. spectrum of an authentic specimen of p-acetotoluidide but the differences noted were as follows :-

(i) the compound showed a complex series of bands of medium intensity near 2200 cm^{-1} which could be due to the C-D stretching bands.

(ii) a sharp band at 1400 cm^{-1} present in p-acetotoluidide was missing. This identifies the band at 1400 cm^{-1} as due to the 4-methyl group in p-acetotoluidide.

(iii) The strong band at 810 cm^{-1}, due to the out of plane bending vibrations of aromatic hydrogen atoms, was replaced by a weak peak at this wavenumber which indicates the presence of residual hydrogen atoms on the aromatic ring.

Preparation of 4-trideuteromethyl-3,5,6-trideutero-2-nitroacetanilide (6D-MNA).

This material was synthesised starting from perdeuterotoluene (toluene - d_8) which is available from ALDRICH. The synthetic route involved a Friedel Crafts reaction of the labelled toluene with acetic anhydride using aluminium chloride as the catalyst. This reaction gave a labelled acetophenone (B) which was converted to its oxime derivative (C). A Beckmann rearrangement of the oxime using polyphosphoric acid gave a labelled p-acetotoluidide (D) which was nitrated, using concentrated nitric acid in acetic anhydride, to yield the required labelled MNA (6D-MNA).

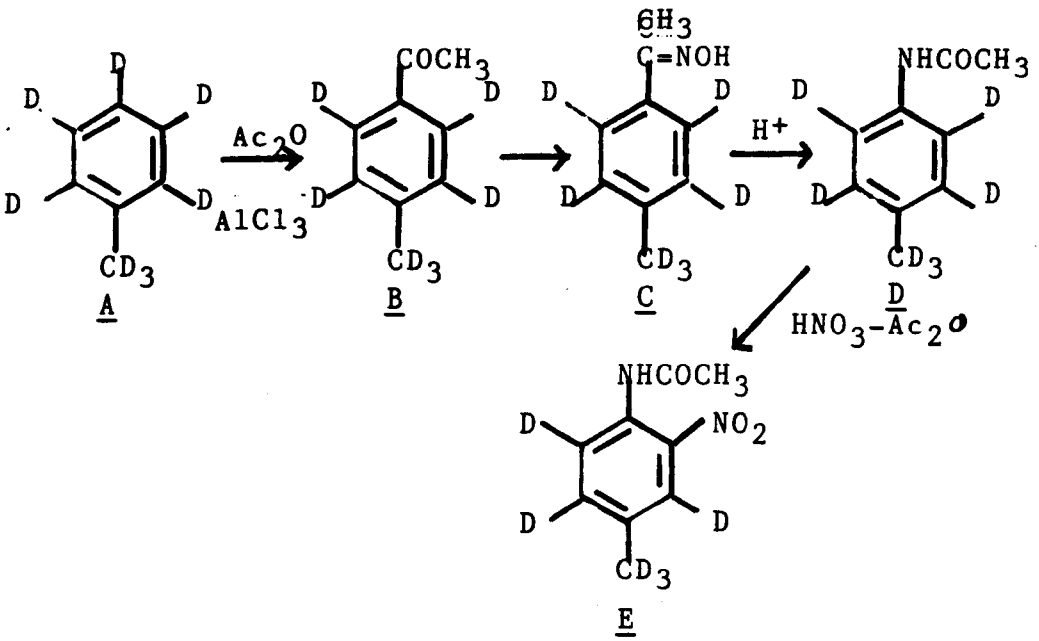

The deuterated p-acetotoluidide (**D**, 0.5 g) was added to a cooled solution of concentrated nitric acid (d 1.5 gcm^{-3}; 0.5 g) in acetic anhydride (2 cm^{3}) at 0^{o} C. After standing at ambient temperature for 45 minutes water was added and a yellow precipitate was collected at the pump, washed with water and recrystallised from ethanol-water to give a yellow crystalline solid. The compound showed strong bands in the i.r. spectrum near 1530 cm^{-1} and 1350 cm^{-1} which is consistent with the introduction of a nitro group. Some bands present in the i.r. spectrum of MNA-3 such as a sharp medium band near 1150 cm^{-1} which can be assigned to an in plane bending vibration of aromatic C-H and the strong band near 820 cm^{-} (out of plane bending of aromatic C-H), were weak. This is consistent with much of the aromatic hydrogen being replaced by deuterium.

The mass spectrum of the product showed that a mixture of MNA molecules of varying deuterium content was present. In the molecular ion region peaks at m/z 197.05, 198.05, 199.05 and 200.05 at relative abundances 6.1, 13.8, 16.3 and 6.1 were observed and this corresponds approximately to 14% 3D, 33% 4D, 38.5% 5D, and 14% 6D respectively . It is concluded that the product could only be regarded as partially deuterated but inspite of this, the material, which could be obtained in three polymorphic forms, provided useful i.r. data.

An examination of the polymorphic forms of MNA by differential scanning calorimetry

Three different batches of each polymorph were examined by differential scanning calorimetry (d.s.c.) using a DuPont thermal analyser to examine one batch and a Perkin-Elmer DSC-2 differential scanning calorimeter to examine two later batches. The results presented in Table 9.1 are from the examination of the last batch which was examined on a Perkin-Elmer instrument.

Although the general character and shape of curves obtained from each polymorph were similar, slightly different results were obtained for each polymorph from different batches. The d.s.c. curve obtained from the amber polymorph (MNA-2) showed a small exotherm near 82°C followed by a melting endotherm with an extrapolated onset at 92.07°C . When samples of the amber form were heated to approximately 80°C for about fifteen minutes and examined by infrared spectroscopy and by X-ray powder diffraction techniques it was clear that a phase change had occurred and now the solid sample consisted of the yellow form. When amber crystals of MNA were examined on a Kofler hot-stage microscope at about 85°C the initially clear amber crystals become opaque and yellow and the phase change did not appear to travel along

distinct boundary fronts.

Hence it is concluded that the solid amber form changes, on heating to about 80°C, into the yellow form. However, the melting point endotherm has a lower enthalpy change than that for the yellow form but the onset temperatures are similar. The values for the melting point endotherms show that the order of stability of the three polymorphs is, in order of increasing stabilty,

MNA-2 (amber) < MNA-3 (yellow) < MNA-1 (white)

The d.s.c. curves do not show one aspect of the effect of heat on MNA-3, which is easily observed on the Kofler hot-stage. This is the change of the yellow to the white form, which is seen to occur at about 90°C. It is possible that the enthalpy change associated with this phase change is slightly endothermic and may account for the relatively low starting point for the endotherm at 74.6°C as well as the asymmetric nature of the melting point endotherm.

Table 9.1

Results of the d.s.c. studies

polymorph	amber	yellow	white
melting onset (°C)	90.64	90.69	93.94
maximum temp. (°C)	92.07	93.92	96.31
melting endotherm ($calg^{-1}$)	24.81	27.57	30.52
melting endotherm ($kcalmol^{-1}$)	4.82	5.35	5.93
melting endotherm ($kJmole^{-1}$)	20.14	22.38	24.78
exothermic change			
($kcalmol^{-1}$)	0.25		
($kJmole^{-1}$)	1.05		

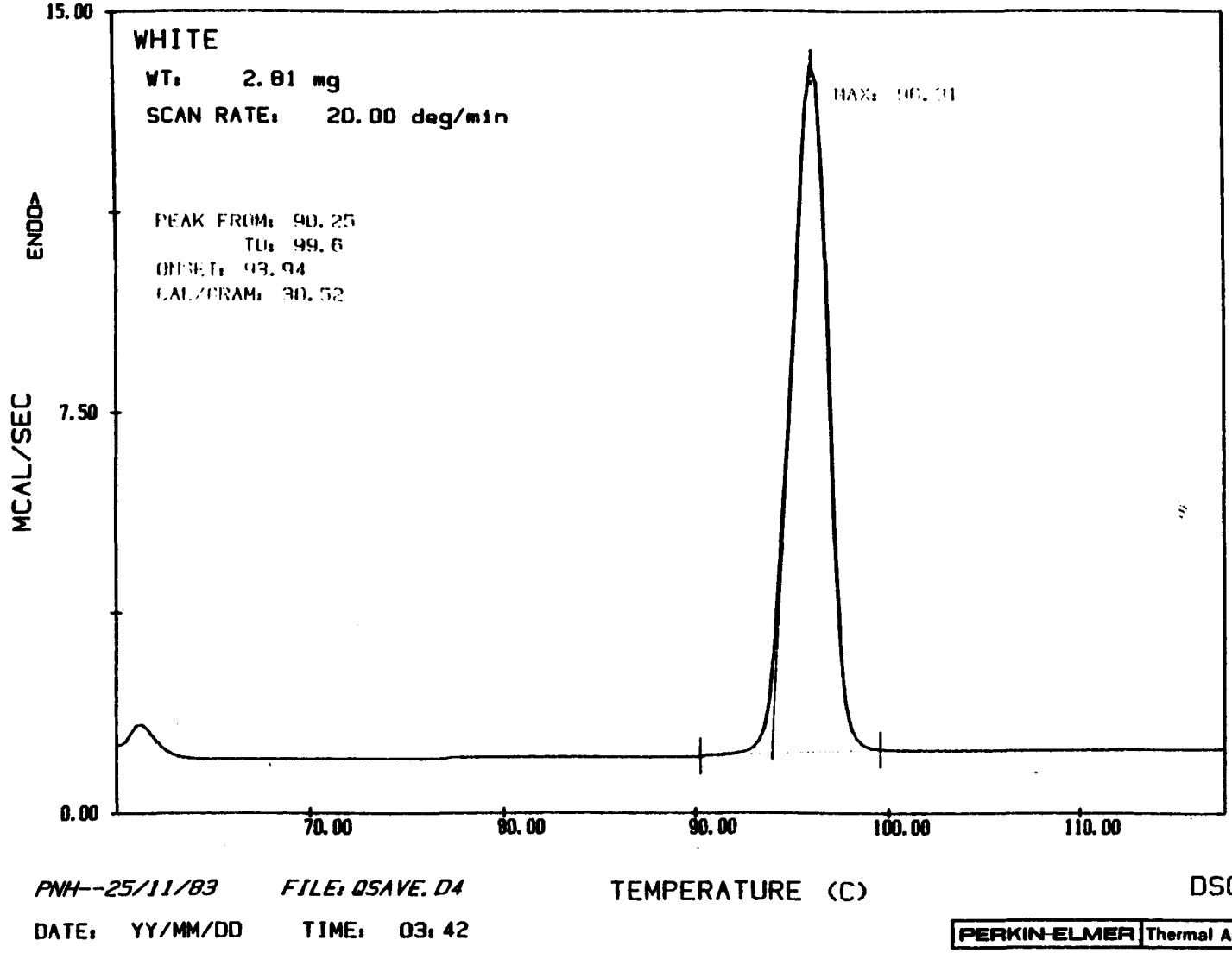

Fig. 9.1 DSC curve of the white (MNA-1) form.

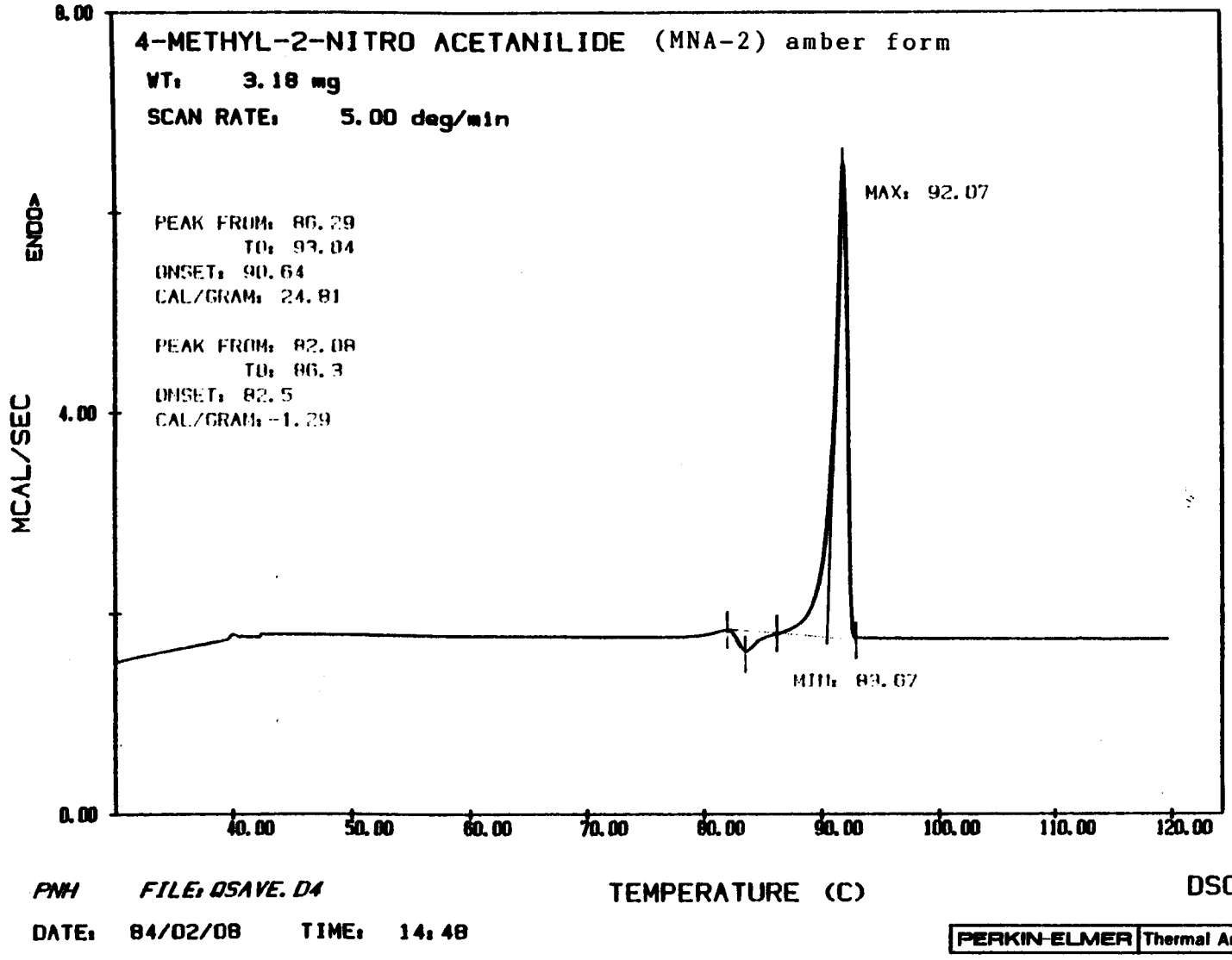

DSC curve of the amber form (MNA-2).

Fig. 9.2

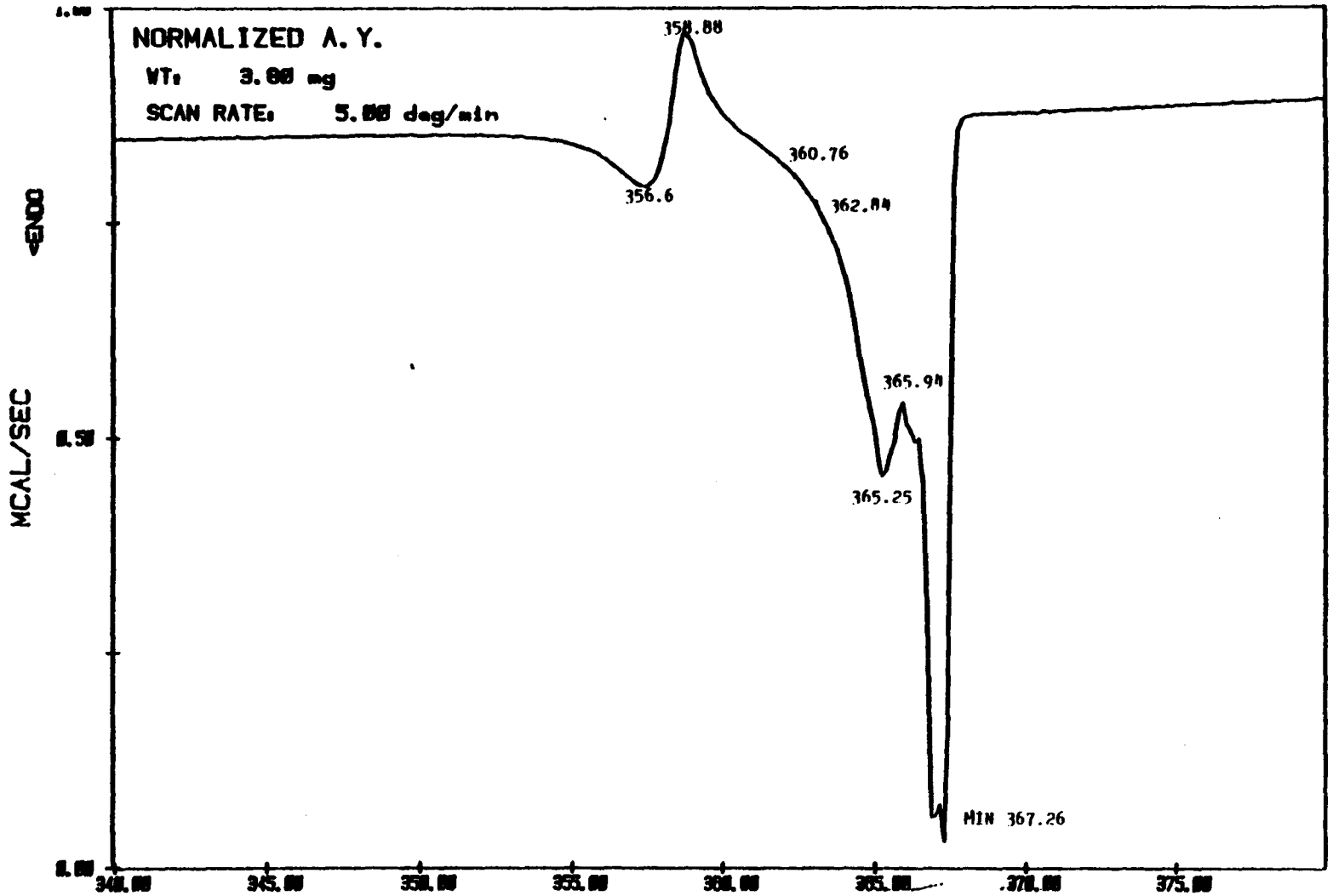

Fig. 9.3 DSC curve of amber form (MNA-2)

DSC curve of the AMBER (MNA-2) form.

Fig 9.4

DSC curve of YELLOW (MNA-3) form

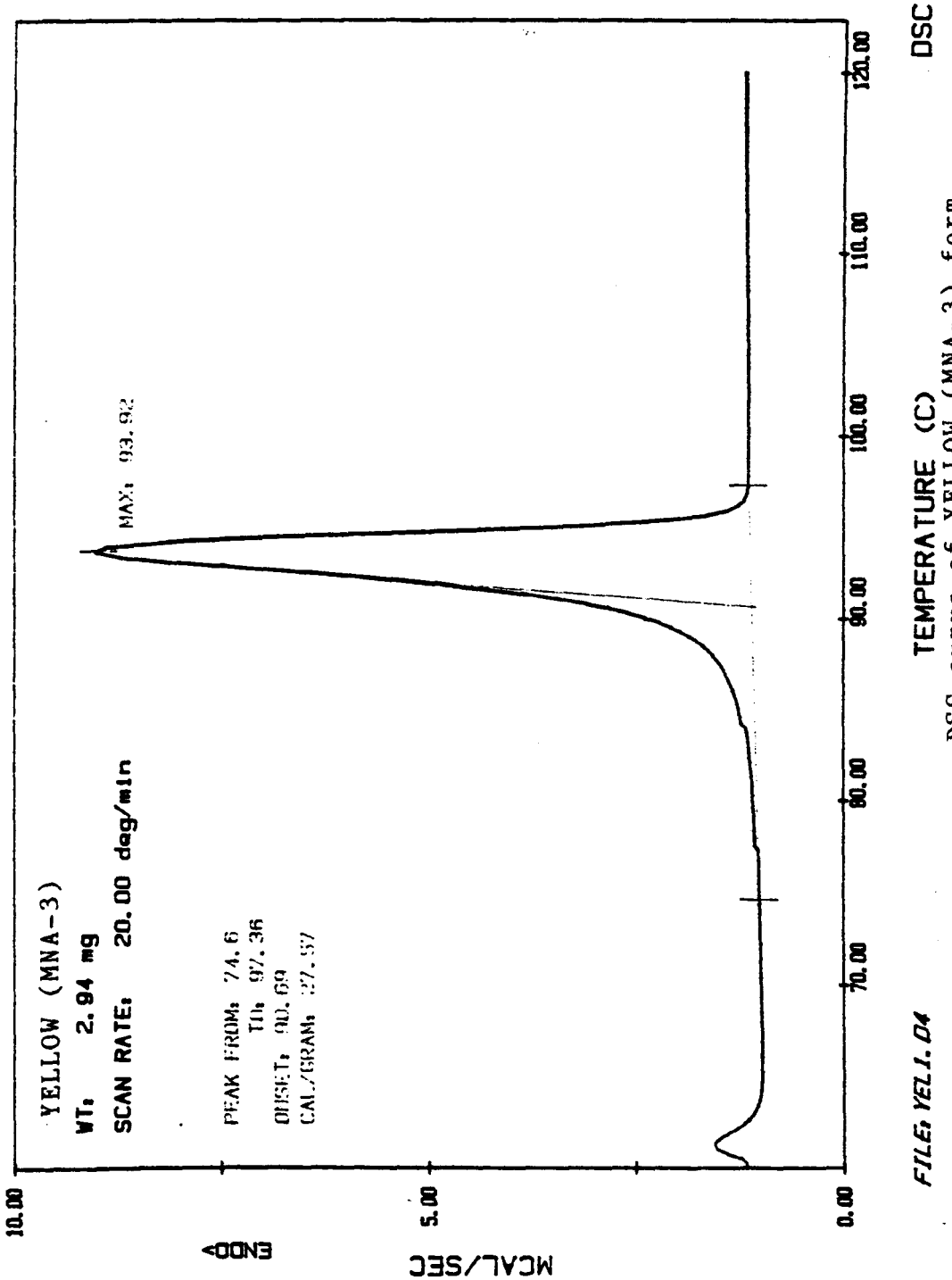

Fig. 9.5

DSC curve of YELLOW (MNA-3) - slow heating rate.

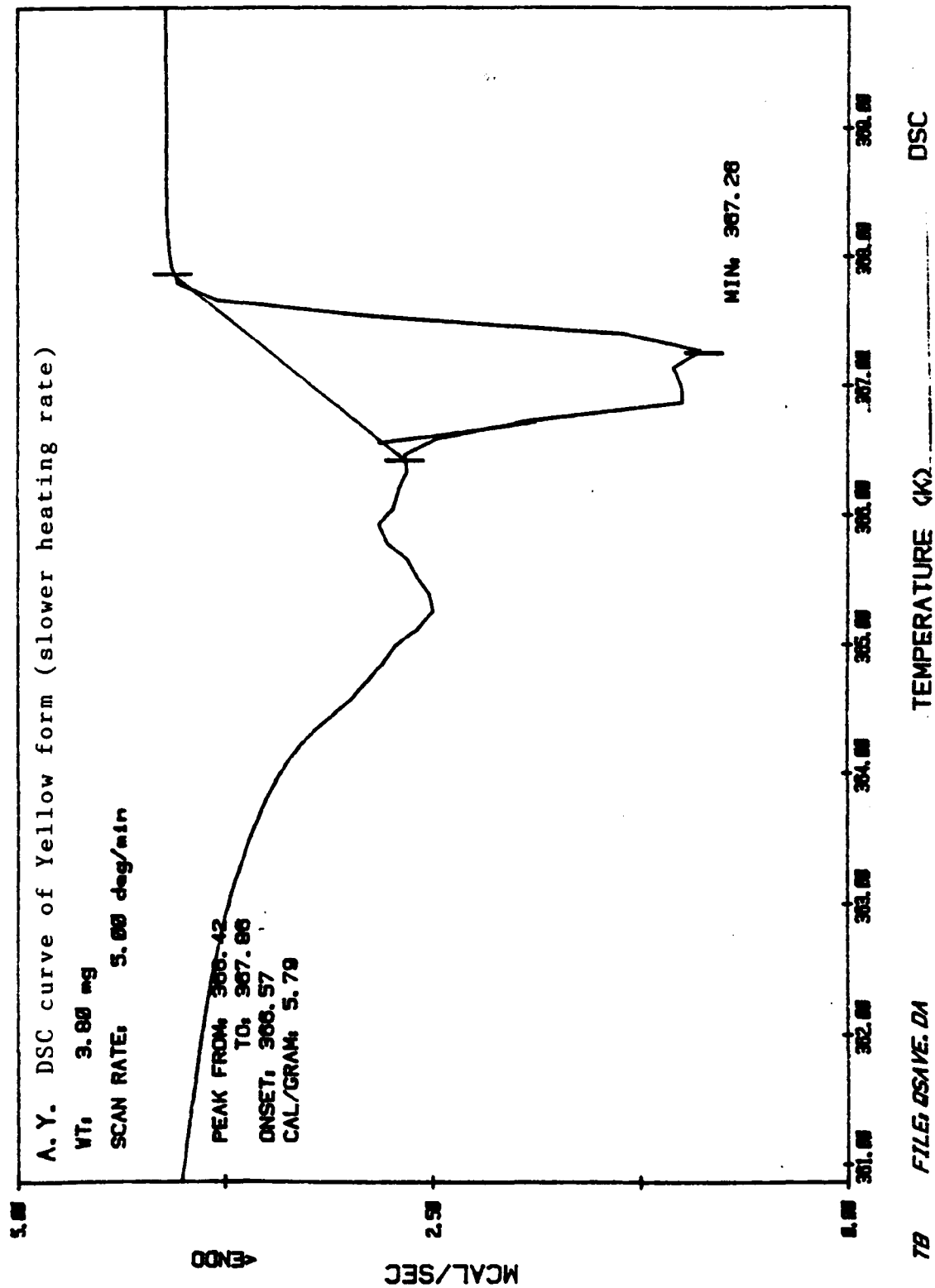

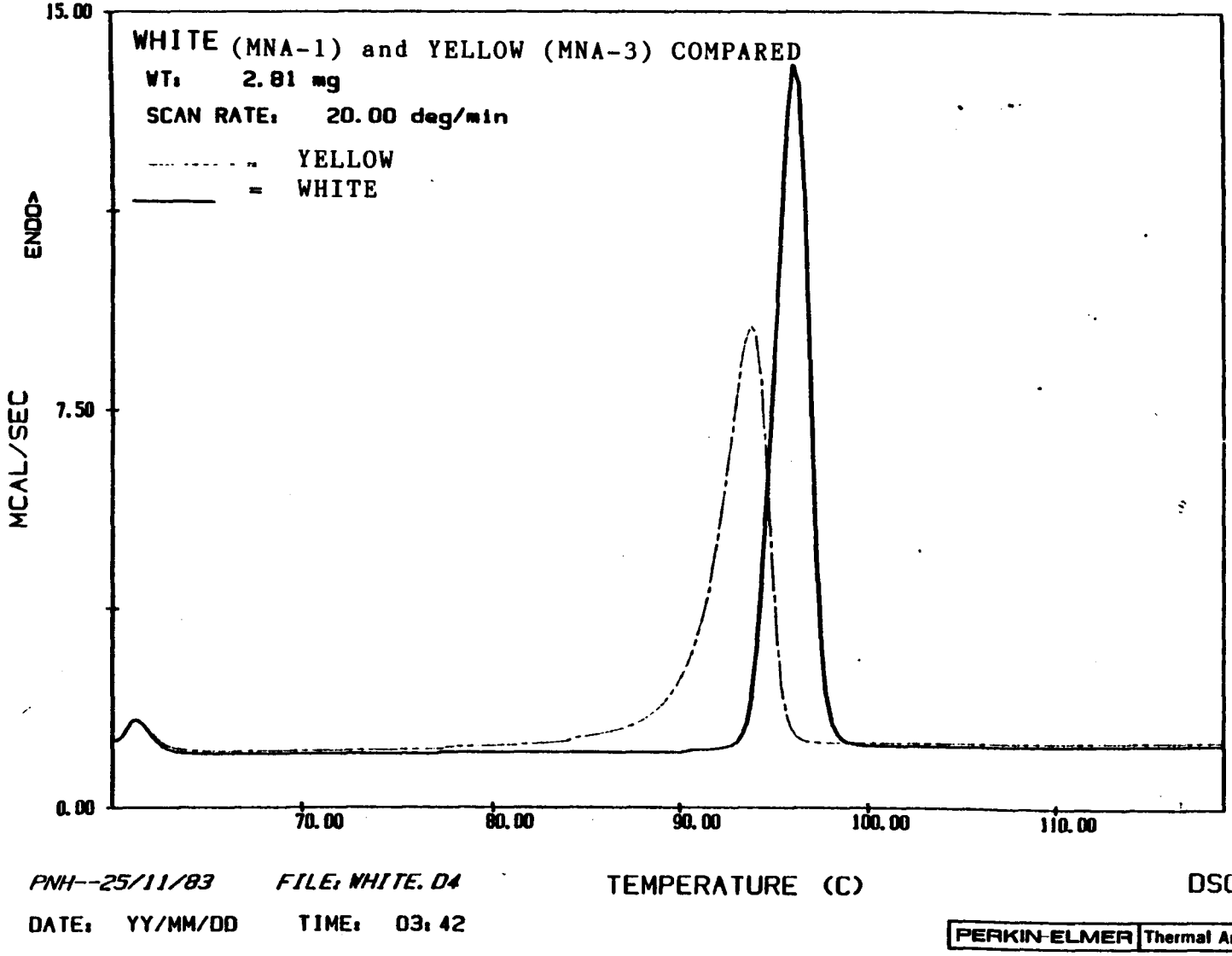

Fig. 9.6 DSC curves of the WHITE and YELLOW forms.

CHAPTER TEN

References.

References

1. S.Mizushima, T.Shimanouchi, S.Nagakura, K.Kuratani, M.Tsuboi, H.Baba,, and O.Fujioka, J.Amer.Chem.Soc, 1950,72,3490.

2. M.Tsuboi, Bull. Chem.Soc.Japan, 1949,22,215,255.

3. T.Miyazawa, T.Shimanouchi, and S.Mizushima, J.Chem.Phys., 1956,24,408.

4. T.Miyazawa, T.Shimanouchi, and S.Mizushima, J.Chem.Phys., 1958,29,611.

5. R.B.Corey and L.Pauling, Proc.Roy.Soc., 1953,B141,10.

6. R.A.Russell and H.W.Thompson, Spectrochim. Acta, 1956,8,138.

7. R.L.Jones, J.Mol.Spec., 1958,2,581.

8. I.Suzuki, M.Tsuboi, T.Shimanouchi, and S.Mizushima, Spectrochim. Acta, 1960,16,471-478.

9. T.Miyazawa, J.Chem.Soc. Japan, 1955,76,821.

10. I.Suzuki, Bull.Chem.Soc. Japan, 1960,33,1359.

11. C.H.Smith and R.H.Thompson, J.Mol.Spectroscopy, 1972,42,227-238.

12. I.Suzuki, Bull.Chem.Soc. Japan, 1962,35,540.

13. L.J.Bellamy, "The Infrared Spectroscopy of Complex Molecules", Methuen, London, 1984.

14. R.E.Richards and H.W.Thompson, J.Chem.Soc., 1947,1248.

15. H.M.Randall, R.G.Fowler, N.Fuson, and J.R.Dangl, "Infrared Determination of Organic Structures", D. van Nostrand, New York, 1949.

16. H.Letow Jnr. and A.H.Gropp, J.Chem.Phys., 1953,21,1621.

17. R.D.B.Fraser and W.C.Price, Nature, 1952, 170,490.

18. H.K.Kessler and G.B.B.M.Sutherland, J.Chem.Phys., 1953,21,570.

19. A.Warshel, M.Levitt, and S.Lifson, J.Mol.Spectroscopy, 1970,33,84.

20. N.B.Abbott and A.Elliott, Proc.Roy.Soc.,1956,234A,247.

21. D.A.Crooks, Nature, 1947,160,17.

22. J.Mann and H.W.Thompson, Proc.Roy.Soc., 1948,192A,489.

23. C.H.Bamford, L.Brown, A.Elliott, W.E.Hanby, and I.F.Trotter, Proc.Roy.Soc. 1953,141B,49.

24. A.Gierer, Z.Naturforsch., 1954,8B,654.

25. V.V.Chalapathi and K.V.Ramiah, Proc.Indian Acad. Sci., 1968,67A,184.

26. E.J.Forbes, K.J.Morgan, and J.Newton, J.Chem.Soc., 1963,835.

27. M.St.C.Flett, Trans. Faraday Soc.,1948,44,767.
D.E.Hathaway and M.St.C.Flett, Trans. Faraday Soc. 1949,45,818.
A.Bryson and R.L.Werner, Austal.J.Chem. 19,13,456.
V.C.Farmer and R.H.Thompson, Spectrochim. Acta, 1960,16,559.
A.G.Moritz, Spectrochim. Acta, 1960,16,1176 & 1962,18,671.
L.K.Dyall and A.N.Hambly, Austral. J.Chem., 1958,11,513.
L.K.Dyall, Spectrochim. Acta, 1961,17,291.

28. D.Peltier, A.Pichevin, and A.Bonnin, Bull.Soc.Chim.France 1961,1619.

29. M.Gomel and H.Lumbroso, Bull.Soc.Chim.France, 1962,1203.

30. J.W.Smith, J.Chem.Soc., 1961,4700.

31. H.E.Hallam and C.M.Jones, J.Mol.Structure, 1970,5,1-19
B.F.Pederson and B.Pederson, Tetrahedron Letters 1965,2995.

32. L.K.Dyall and J.E.Kemp, Spectrochim. Acta, 1966,22,483.

33. T.H.Siddall III, W.E.Steward, and A.L.Marston, J.Phys.Chem. 1968,72,2135.

34. R.E.Carter, Acta Chem.Scand., 1968,22,2643.

35. A.G.Moritz, Spectrochim. Acta, 1960,16,1176.

36. L.J.Bellamy, H.E.Hallam, and R.L.Williams, Trans. Faraday Soc., 1958,54,1120.

37. J.W.Emsley, J.Feeney, and L.H.Sutcliffe, "High Resolution Nuclear Magnetic Resonance Spectroscopy", Pergamon Press, New York, 1965.

38. J.R. Bartels-Keith, and R.F. Cieciuch, Can.J.Chem., 1968,46,2593.

39. H.Paulsen and K.Todt, Angew.Chem.Int.Ed.Eng., 1965,5,899.
Chem.Ber. 1967,100,3385.
Chem.Ber. 1967,100,3397.
Z.Anal.Chem. 1968,235,30.

40. T.H.Siddall III and W.E.Stewart, J.Mol.Spec. 1967,24,290-301.

41. A.Ribera and M.Rico, Tetrahedron Letters, 1968,5,535.

42. W.E.Stewart and T.H.Siddall III, Chem.Rev. 1970,70(5),517.

43. H.E.Hallam and C.M.Jones, J.Mol.Structure, 1970,5,1.

44. J.M.Appleton, B.D.Andrews, I.D.Rae, and B.E.Reichert, Aust.J.Chem.,1970,23,1667.

45. B.M.Lynch, C.M.Chen, and Y-Y.Wigfield, Canad.J.Chem.,1968,46,1141.

46. L.K.Dyall and J.E.Kemp, Spectrochim. Acta, 1966,22,483.

47. R.E.Carter, Acta Chem. Scand., 1968,22,2643.

48. I.D.Rae, Canad.J.Chem., 1966,44,1334.

49. A.Mannschrenck, A.Matthews, and G.Rissman, J.Mol.Spec., 1967,23,15.

50. A.J.R.Bourn, D.G.Gillies, and E.W.Randall, Tetrahedron, 1964,20,1811.

51. R.F.C.Brown, L.Radom, S.Sternhell, and I.D.Rae, Canad.J.Chem., 1968,46,2577.

52. R.E.Carter, Acta Chem.Scand. 1967,21,75.

53. M.Zanger,W.W.Simons, A.R.Gennaro, J.Org.Chem.1968,33,3673.

54. H.Kessler and A.Rieker, Ann.Chem. 1967,708,57.

55. H.Kessler and A.Rieker, Z.Naturforsch., 1967,22,456.

56. R.Adams, Rec.Chem.Progr. 1949,10,91.

57. H.Kessler, Tetrahedron, 1968,24,1857.

58. T.H.Siddall and W.E.Stewart, J.Phys.Chem.,1969,73(1),40.

59. B.F.Pedersen and B.Pedersen, Tetrahedron Letters, 1965,2995.

60. H.B.Thompson and K.M.Hollberg, J.Phys.Chem., 1963,67,2486.

61. H.S.Gutowsky and C.H.Holm, J.Chem.Phys., 1956,25,1228.

62. I.D.Rae, Canad.J.Chem., 1967,45(1),1.

63. M.Kondo, Bull.Chem.Soc.Japan, 1978,51(6),1905.

64. D.Sugden GRSC Part 2 Project, Slough College, 1979.

65. I.D.Rae, Aust.J.Chem., 1978,31,1851-4.

66. W.Brugel, Z.Elektrochem., 1962,66,159.

67. C.J.Brown and D.E.C.Corbridge, Acta Cryst., 1954,7,711.

68. C.J.Brown, Acta Cryst., 1966,21,442.

69. B.F.Pedersen and B.Pedersen, Tetrahedron Letters, 1965,34,2995.

70. R.E.Carter, Acta Chem.Scand., 1967,21(2),75-86.

71. M.Haisa, S.Kashino,Y.Matsusaki, R.Kwai and K.Kunitomi, Acta Cryst. 1977,B33,2455-2459.

72. M.Haisa, S,Kashino, Y.Matsuzaki, R.Kawai, and K.Kunitomi, Acta Cryst., 1977,B33,2455-2459.

73. M.Haisa, S.Kashino, and H.Maeda, Acta Cryst., 1974,B30,2510-2512.
1976,B32,1283-1285.

74. E.Subramanian, Z.Krist., 1966,222-234.

75. G.D.Andretti,L.Cavalca, P.Domiano, and A.Musatti, Acta Cryst., 1968,B24,1195-1198.

76. S.Kashino, K.Ito, and M.Haisa, Bull.Chem.Soc.Japan, 1979,52(2),365-369.
K.Tashino, M.Kabayshi, and H.Tadokoro, Macromolecules, 1977,10,413.
M.Haisa, S.Kashino, and H.Maeda, Acta Cryst., 1974,30B,2510
1976,32B,1283.

77. L.Leiserowitz and M.Tuval, Acta Cryst., 1978,B34,1230-1247.

78. W.A.Denne, M.F.MacKay, J.Cryst.Mol.Struc., 1974,4,141.

79. H.D.Block,H.-D.Lockenhof, R.Allmann, Cryst.Struc.Comm., 1975,4,77.

80. A.G.Michel, F.Durant, Acta Cryst., 1976,B32,1574.

81. T.Ozawa, Y.IItaka,M.Hirobe,T.Okamoto, Chem.Pharm.Bull., 1974,22,2069.

82. C.Cohen-Addad, J.Lajzerowicz, J.-L.Benoit-Guyod, A.Boucherle, Chim.Ther., 1972,7,384.

83. P.Singh, F.R.Ahmed, Acta Cryst., 1969,B25,1901.

84. C.Bonnemer, J.A.Hamilton, L.K.Steinrauf, J.Knappe, Biochemistry, 1965,4,240.

85. C.Cohen-Addad, Acta Cryst., 1973,B29,157.

86. C.Cohen-Addad, Acta Cryst., 1973,B29,157.

87. C.Miravitlles,F.Plana, J.L.Brisansc, M.Font-Altaba, Cryst.Struc.Comm., 1974,3,439.

88. N.W.Gilman, J.F.Blount R.I.Fryer, J.Org.Chem., 1976,41,737.

89. J.P.Schaefer and L.L.Reed, Acta Cryst., 1972,B28,1743.

90. G.Precigoux,B.Busetta, M.Hospital, Acta Cryst., 1976,B32,943.

91. W.R.Krigbaum, R.-J.Roe,J.D.Woods, Acta Cryst., 1968,B24,1304.

92. F.Plana, C.Miravitlles, J.L.Brisano, M.Font-Altaba, Cryst.Struc.Comm., 1973,2,573.

93. J.L.Brianso,C.Miravirlles, F.Plana,M.Font-Altaba,

Cryst.Struct.Comm., 1973,2,551.

94. M.H.J.Koch,G.Evrard, Acta Cryst. 1974,B30,237.

95. J.L.Brianso,C.Miravtlles,M.Font-Altaba, J.P.Declerc, G.G.Germain, Cryst.Struc.Comm., 1973,2,319.

96. A.V.Hanson,D.W.Eanner, Acta Cryst. 1974,B30,2486.

97. C.S.Yoo, E.Abola, M.K.Wood, N.Sax, J.Fletcher, Acta Cryst., 1975,B31,1354.

98. A.W.Hanson, Acta Cryst., 1972,B28,672.

99. A.W.Hanson and M.Rohrl, Acta Cryst., 1972,B28,3567.

100. L.P.Zalukaev, N.A.Ignat'ev, E.I.Zavalishin, Zh.Strukt.Khim., 1975,16,237.

101. F.Plana, C.Miravitlles, J.L.Brianso, M.Font-Altaba, Cryst.Struc.Comm., 1974,3,135.

102. F.Plana,J.L.Brianso, C.Miravitlles,X.Solans,M.Font-Altaba, O.Dideberg,J.P.Declerc, G.G.Germain, Acta Cryst., 1976,B32,2660.

103. C.J.Brown, J.Chem.Soc.(A),1967,405.

104. G.Reck, Krist.Tech., 1975,10,511.

105. L.Kutschaesky, C.Zerbe, Krist.Tech., 1976,11,5.

106. G.Reck,H.Schmittler-Fichtner,P.Leibnitz, J.prakt.Chem., 1973,315,483.

107. G.Reck,P.Leibnitz,J.-P.Wenzel, Kristal und Technik, 1974,9,345.

108. G.Reck and G.Bannier, Kristal und Technik, 1975,10,951.

109. G.G.Christoph, E.B.Fleischer, Acta Cryst. 1973,B29,121.

110. J.L.Brianso,C.Miravitlles, F.Plana, M.Font-Altaba, Estud.Geol.(Madrid), 1974,30,423.

112. M.H.Koch,C.J. de Ranter, M.Rolies, O.Dideberg, Acta Cryst., 1976,B32,2529.

113. H.-C.Mez, Ber.Bunsengesellsch.Phys.Chem., 1968,72,389.

114. J.P.Collman,F.R.Gagne,C.A.Reed,W.T.Robinson,G.A.Rodley, Proc.Nat.Acad.Sci. U.S.A., 1974,71,1326.

115. K.A.Kerr,J.P.Ashmore, Stockholm Symp.Biol.Struc., 1973,91.

116. L.Kutschaesky,P.Leibnitz,J.Wenzel, Kristal und Technik, 1974,9,605.

117. Y.Kai,N.Yasucka,N.Kasai,T.Minami, K.Yamataka,Y.Ohshiro,T.Agawa, J.Chem.Soc., (D), 1971,1532.

118. S.Paul-Roy,H.Schenk C.H.Macgillavry, J.Chem.Soc.(D), 1969,1517.

119. M.Brufani, W.Fedeli, G.Giacomello, A.Vaciago, Experientia, 1964,20,339.

120. M.Brufani,W.Fedeli, G.Giacomello, A.Vaciago, Experientia, 1967,23,508.

121. W.T.Robinson, G.A.Rodley, G.B.Jameson, Acta Cryst., 1975,A31,S49.

122. J.Haleblain and W.McCrone, J.Pham.Sci., 1969,58(8),911-929.

123. E.W.Jenkins, "The Polymorphism of Elements and their Compounds", Methuen Educational Ltd., 1973.

124. L.T.O'Connor in "Fatty Acids", Ed. K.S.Markley, 2nd. Ed. Pt.I, Interscience N.Y. 1960,285-378.

125. N.H.Hartshorn and A.Stuart "Crystals and the Polarising Microscope", 3rd. Ed. Edward Arnold Ltd., London, 1960,20.

126. L.Kofler and A.Kofler, "Mikro Methoden zur Kernzeichung Organisher Stoffe und Stoffe Gemische", Wagner, Innsbruck, Austria, 1954.

127. W.C.McCrone, "Fusion Methods inChemical Microscopy", Interscience, N.Y., 1957.
W.C.MsCrone, "Physics and Chemistry of the Organic Solid State", Vol II, Ed. A.Weissberger, Interscience, N.Y., 1965,725-767.

128. A.R.Verma and P.Krishna, "Polymorphism and Polytypism in Crystals", Wiley, N.Y., 1966,7-60.

129. L.Deffet,"Repertoire Des Composes Organiques

Polymorphes", Desoer, Liege, 1942.

130. L.Gattermann, Ber., 1885,18,1482.
L.Gattermann, Ber., 1890,23,1733.

131. R.Schenk, Z.phys.Chem., 1894,15,33; 1897,23,449.

132. K.Auwers, Z.phys.Chem., 1894,15,33; 1897,23,449.

133. E.C.C.Baly, W.B.Tuck and E.G.Marsden, J.Chem.Soc., 1910,97,581.

134. A.Hantzsch, Ann, 1911,384,135; 1913,398,381.

135. A.Hantzsch, Ann., 1932,492,65.

136. A.H.R.Muller, Z.phys.Chem., 1913,86,222.

137. K.Schaum, Ann., 1928,462,194.

138. L.Hunter and H.O.Chaplin., Nature, 1937,140,896.

139. L.Skulksi, J.Org.Chem., 1963,28(12),3565.

140. L.Skulski, Zeszyty Naukowe Politechnika Warszawska Chemia, 1966,5,160-212.

141. D.N.Kendall, Anal.Chem., 1953,25,382.

142. R.J.Messley, Spectrochim. Acta, 1966,22,889-917.

143. G.P.Bettinetti, F.Giordano, A.La Manna, and G.Giuseppetti, J.Pharm.Pharmac., 1976,28,87.

144. R.J.Mesley and C.A.Johnson, J.Pharm.Pharmac., 1965,17,329.

145. R.J.Mesley and E.E.Houghton, J.Pharm.Pharmac., 1967,19,295.

146. J.H.Chapman, J.E.Page, A.C.Parker, D.Rogers, C.J.Sharp, and S.E.Stanforth., J.Pharm.Pharmac., 1968,20,418-429.

147. R.J.Mesley, R.L.Clements, B.Flaherty, and K.Goodhead, J.Pharm.Pharmac., 1968,20,325-340.

148. B.W.Muller and M.Lagas, Pharmaceutisch Weekblad, 1979,114,449.

149. M.F.Grostic and G.E.Bronson, Applied Spectroscopy, 1961,

15(6),157-9.

150. A.W.Baker, J.Phys.Chem., 1957,61,450.

151. J.C.P.Schwarz "Physical Methods in Organic Chemistry", Oliver and Boyd, 1963,57.

152. E.J.Graeber and B.Morosin, Acta Cryst., 1976,b32,310.

153. P.Prusiner and M.Sundaralingam, Acta Cryst., 1976,B32,419.

154. S.Needle, W.Kuhlbrandt, and Achari, Acta Cryst., 1976,B32,1850;
J.Kraut and L.H.Jensen, Acta Cryst., 1963,16,79.

155. A.I.Kitaigorodskii, Adv.Struct.Res.Diffr. Methods, 1970,3,173.

156. M.K.Kaloustian, J.Chem.Educ., 1974,51(12),777.

157. J.Bernstien and A.T.Hagler, J.Amer.Chem.Soc., 1978,100(3),673.

158. J.Bernstein and A.T.Hagler, Mol.Cryst.Liq.Cryst., 1979,50,223-234.

159. I.Bar and J.Bernstein, J.Phys.Chem., 1982,86,3223-3231.

160. J.Bernstein and G.M.J.Schmidt, J.Chem.Soc.(Perkin 2), 1972,2,951.

161. J.Bernstein, I.Bar, and A.Christensen, Acta Cryst., 1976,B32,1609.

162.
D.Y.Curtin,I.C.Paul,E.N.Duesler,T.W.Lewis,B.J.Mann,W.Shiau, Mol.Cryst.Liq.Cryst., 1979,50,25-42.

163. G.M.J.Schmidt, Pure Appl.Chem., 1971,27,647

164. M.D.Cohen and B.S.Green, Chem. in Britain, 1973,9,490.

165. J.M.Thomas, Phil.Trans.Roy.Soc., 1974,277,251.

166. I.C.Paul and K.T.Go, J.Chem.Soc.(B), 1969,33.

167.
G.M.Parkinson,J.M.Thomas,J.O.Williams,M.J.Goringe,L.W.Hobbs, J.Chem.Soc., Perkin II, 1976,836.

168. J.Bregman, J.Leiserowitz and G.M.J.Schmidt, J.Chem.Soc., 1964,2068.

169. J.Z.Gougoutas, Pure and Applied Chem., 1971,27,305-325.

170. A.I.Kitaigorodsky, Yu.V.Mnyukh, and Yu.A.Asadov, J.Phys.Chem.Solids, 1965,26,463.
Yu.V.Mnyukh,N.A.Panifilova,N.N.Petropavlov, and N.S.Uchvatova, J.Phys.Chem.Solids, 1975,36,127.
P.A.Reynolds, Acta Cryst., 1977,A33,185.

171. P.Coppens and G.M.J.Schmidt, Acta Cryst., 1965,18,62.

172. D.Y.Curtin and S.R.Byrn, J.Amer.Chem.Soc., 1969,91,6102.
S.R.Byrn, "Solid State Chemistry of Drugs", Academic Press, New York, 1982.

173. S.R.Byrn, D.Y.Curtin, and I.C.Paul, J.Amer.Chem.Soc., 1972,94,890.

174. J.Swiatkiewicz and P.N.Prasad, J.Amer.Chem.Soc., 1982,104,6913-6918.

175. G.R.Dsiraju, I.C.Paul, and D.Y.Curtin, J.Amer.Chem.Soc., 1977,99,1594.

176. B.J.Mann,E.N.Duesler,I.C.Paul and D.Y.Curtin, J.Chem.Soc. Perkin II, 1981,1577.

177. B.J.Mann, I.C.Paul,D.Y.Curtin, J.Chem.Soc., Perkin II, 1981,1583.

178. C.Pascard-Billy, Bull.Soc.Chim.Fr., 1962,2293.
C.Pascard-Billy, Acta Cryst., 1962,15,519.
P.D.Cradwick and D.Hall, Acta Cryst., 1971,B27,1990.

179. L.A.Errede,M.C.Etter,R.C.Williams, and S.M.Darnauer, J.Chem.Soc., Perkin II, 1980,233.

180. C.N.Sukenik,J.A.P.Bonapace,N.S.Mandel,P-Y.Lau,G.Wood, and R.G.Bergman, J.Amer.Chem.Soc., 1977,99,851.

181. R.B.Wilson, Y-S.Chen,I.C.Paul, and D.Y.Curtin, J.Amer.Chem.Soc., 1983,105,1672-1674.

182. C.S.Chol and H.P.Boutin, Acta Cryst., 1970,B26,1235.

183. H.H.Cady,A.C.Larson, and D.T.Cromer, Acta Cryst., 1963,15,617.

184. R.E.Cobbledick and R.W.H.Small, Acta Cryst., 1974,B30,1918.

185. F.Goetz and T.B.Brill, J.Phys.Chem., 1979,83,340-346.

186. T.B.Brill and C.O.Reese, J.Phys.Chem., 1980,84,1376-1380.

187. T.B.Brill and R.J.Karpowicz, J.Phys.Chem., 1982,86,4260-4266.

188. M.C.Etter and A.R.Siedle, J.Amer.Chem.Soc., 1983,105,641-643.

189. A.T.Hagler and J.Bernstein, J.Amer.Chem.Soc., 1978, 100(20),6349.

190. W.C.Hamilton, Acta Cryst. 1965,18,502.

191. J.R.Holden and C.Dickinson, J.Phys.Chem., 1977,81(15),1505.

192. G.Kopfmann and R.Huber, Acta Cryst., 1968,A24,348.

193. A.C.T.North, D.C.Phillips, and S.S.Matthews, Acta Cryst., 1968,A24,351.

194. I.J.Tickle (personal communication to J.C.Moore).

195. P.B.Braun, J,Hornstra, and J.I.Leenhouts, Philips Res.Repts. 1969,24,85.

196. J.C.Moore, A.Yeadon, and R.A.Palmer, J.Crystallogr.Spectrosc.Res., 1983,13,279. (MNA-1;white and MNA-3;yellow)

J.C.Moore, A.Yeadon, and R.A.Palmer, J.Crystallogr.Spectrosc.Res., 1984,14(3),283. (MNA-2; amber form).

197. A.MacKay, Practical Computing, 1981,4(9),108.

198. 'International Tables for X-ray Crystallography ', Kynoch Press, Birmingham 1952, vol. 1.

199. G.Varsanyi, " Assignments for Vibrational Spectra of 700 benzene derivatives", Adam Hilger, London, 1974.

200. J.H.S.Green D.J.Harrison and W.Kynaston. Spectrochim.

Acta 1971,27A,807.

201. R.S.Mullikan, J.Chem.Phys., 1955,23,1997.

202. E.B.Wilson, I.C.Decius and P.C.Cross, "Molecular Vibrations", McGraw-Hill, London 1955.

203. G.Varsanyi, "Vibrational Spectra of Benzene Derivatives ", Academic Press. London. 1969.

204. M.F.Grostic and G.E.Bronson, Appl. Spectroscopy, 1961,15(6),157.

205. B.W.Muller and M.Lagas, Pharm. Weekblad, 1979,449.

206. M.J.Murray, and F.F.Cleveland, J.Amer.Chem.Soc., 1942,64,1181.

207. J.H.S.Green and D.J.Harrison, Spectrochim. Acta 1970,26A,1925.

208. M.Rey-Lafon, M.T.Forel and C.Garrigou-Lagrange, Spectrochim. Acta 1973,29A,471-486.

209. A.Gambi, S.Giorgianni, A.Passini, R.Visinoni, and S.Ghersetti, Spectrochim. Acta 1980, 36A,871.

210. D.Langton, GRSC Project, Slough College, 1982.

211. F.W.Wehrli and T.Wirthlin, "Interpretation of Carbon-13 NMR Spectra", Heyden, London, 1976.

212. A.Ellison, J.Chem.Educ., 1983,60(5),425.

213. B.M.Lynch, C.M.Chen, Y.Wigfield, Canad.J.Chem., 1968,46,1141.

214. M.Schofield, J.Chem.Soc., 1927,2903.

215. G.T.Morgan and G.E.Scharff, J.Chem.Soc., 1914,105,119.

216. W.J.Hickinbottom, "Reactions of Organic Compounds", Longmans, 3rd Edition,1959.

217. P.Gay, "The Crystalline State", Oliver and Boyd, Edinburgh, 1972, p. 231.

218. Y.Sugarawa, A.Y.Hirakawa, and M.Tsuboi, J.Mol.Spectrosc., 1984,108,206.

219. F. Di Rienzo and A.Domenicano, Acta Cryst.,1980,B36,586.

CHAPTER ELEVEN

Appendices.

Appendix 11.1

The cell parameters for 2,4-dinitroacetanilide have been determined by D. Manners during work for a project as part fulfilment for the GRSC Pt. 2(1980) course. The work was supervised by Mr. J.C. Moore and Mr. A.Yeadon. Although the data are incomplete it was established that at least two forms for this compound existed and both crystalline forms were monoclinic.

Yellow Form

Crystal system	Monoclinic
a,b,c (Å)	9.72(2),16.18 6.12(2)
α,β,γ (deg)	90,≠90,90
Space group	$P2_1/n$

White Form

Crystal system	Monoclinic
a,b,c,(Å)	4.725(5),9.72 18.02
α,β,γ(deg)	90,97,90
Space group	$P2_1$ type

Appendix 11.2

The unit cell parameters of o-nitroacetanilide have been determined by N.R.Sumption at Slough College of Higher Education during the GRSC Part 2 course. The work was supervised by Mr. J.C.Moore and Mr. A.Yeadon. The results were calculated from rotation and Weissenberg photographs and are as follows:-

Crystal system	Monoclinic
Habit	Yellow, tabular
a,b,c (Å)	15.61(1),4.99(1),11.04(1)
α,β,γ (deg)	90, 97.4(0.1),90
Space group	$P2_1/n$
Systematic absences	h + l = 2n

There are no reports of the crystal structure for o-nitroacetanilide in the literature.

Mr. Sumption reported his results in the form of a project in part fulfilment for GRSC Part 2, June 1982.

Comments on the above results

The lengths of the sides of the unit cell are similar to those for MNA-3. The b side has a relatively short distance of 4.99 Å compared with that for the c side in MNA-3 of 4.039(1) Å.

Appendix 11.3

References to some BASIC computer programs.

The following items give details of the use and sources of programs which have been used in the preparation of this thesis. All of the programs were modified to conform to SHARP BASIC (SP5025) for use on a SHARP MZ-80K personal computer. Three types of extended basic interpreters were used :-

1. SPEED BASIC

This modified basic has additional commands available such as APPEND and RENUMBER as well as facilities for tracing errors. Data storage with SPEED BASIC is relatively fast.

Supplier:-

SHARPSOFT LTD

86-90 PAUL STREET,

LONDON EC2A 4NE

2. High resolution graphics are available on the MZ-80K if a Quantum Micros HI-RES graphics board is fitted. This gives a screen with 320 X 200 pixels. A modified BASIC is required viz. QUANTUM HI RES BASIC, which contains additional commands to control the high resolution graphics e.g.:-

GRAPH 0 resets high resolution.

GRAPH 1 enables high resolution.

GRAPH 6 high resolution screen dump to an Epson MX-80FT dot matrix printer.

LINE x1,y1,x2,y2 this instruction draws a line from the point x1,y1 to x2,y2.

Supplier:-

QUANTUM MICROS,

55 WADE LANE,

MERRION CENTRE,

LEEDS LS2 8NJ

3. The third variety of BASIC, called APOLLO BAS MOD, which was used incorporates an extended BASIC interpreter. It offers high speed operation and is very similar to BBC BASIC.

BAS MOD is available from

KUMA COMPUTERS,

12, HORSESHOE PARK,

HORSESHOE ROAD, PANGBOURNE,

BERKSHIRE RG8 7JW

Programs.

1. A program to calculate bond lengths, bond angles, torsion angles, and interatomic distances from atomic coordinates.

J.Dunitz, "X-Ray Analysis and the Structure of Organic Molecules", Cornell University Press, 1979, page 495.

2. A program to calculate cartesian coordinates from internal coordinates .

J.Dunitz, "X-ray Analysis and the Structure of Organic Molecules", Cornell University Press, 1979, page 498.

3. The solution of simultaneous equations by the generalised inverses of matrices.

A.Mackay, Practical Computing, 1981,4(9),108.

4. Using the transformation matrices presented in this reference it was possible to devise programs which would show molecules in one or more unit cells. An example of such a program follows this section and it shows four molecules of MNA in a unit cell. Scale, perspective, and angle of view can all be varied. An outline of the unit cell can be added by incorporating the coordinates of the corners of the unit

cell and drawing appropriate lines between them.

M.Shepherd, Personal Computer World, 1980,3(10),57.

5. The calculation of n.m.r. spectra was accomplished by a computer program written in PASCAL by Dr. A.Ellison, Hull College of Higher Education. The program enables the positions and intensities of lines due to six interacting protons to be predicted. The program is available from Quantum Chemistry Program Exchange, Department of Chemistry -- Room 204, Indiana University, Bloomington, Indiana 47405, U.S.A.

A description of this program occurs in the Journal of Chemical Education.

A.Ellison, J.Chem.Educ., 1983, 60(5),425.

6. A major part of this thesis was written and stored on cassette magnetic tape using a commercially available word processing program called WDPRO.

WDPRO is available from

KUMA COMPUTERS,

12, HORSESHOE PARK,

HORSE SHOE ROAD, PANGBOURNE, BERKSHIRE RG8 7JW.

Appendix 11.4

A BASIC computer program to view the contents of the unit cell of MNA-3

The program allows any scale to be adopted for the axes and will allow a perspective view. If RZ=0 a view from infinity is drawn.

```
1 REM A BASIC PROGRAM TO VIEW THE
2 REM ARRANGEMENT OF 4 MOLECULES
3 REM IN MNA-3 UNIT CELL. AXES NOT SHOWN
10 GOSUB 200
20 INPUT "ROTATION ANGLES";ALPHA,BETA,GAMMA
30 INPUT "LOCAL SCALING FACTORS";A,B,C
40 INPUT "TRANSLATIONS";U,V,W
50 INPUT"RECIPROCAL VIEWPOINT";RZ
60 GOSUB 300
70 GOSUB 500
80 GOSUB 600
90 GOSUB 700
100 GOSUB 800
120 END
197 REM N=NUMBER OF ATOMS
198 REM CRYSTAL COORDS OF ALL 4 MOLS
199 REM IN DATA STATEMENTS 200-224
200 READ N
201 DATA 72..7671,.4992,.7456,.8276,.4590,.5289,.8296,.3515,.4011
202 DATA .7857,.2887,.5192,.8762,.3265,.1716,.8887,.5201,.4212
203 DATA .9252,.4944,.2846,.8931,.6229,.5231,.9585,.6908,.4003
204 DATA .8338,.6636,.7418,.8333,.7369,.8261,.7732,.6042,.8488
205 DATA .7362,.6344,.9899,.7053,.4390,.8596,.7131,.3665,.8272
206 DATA.6362,.4736,.9910,.6198,.5643,1.0181,.5816,.3894,1.0974
207 DATA .7411,-.0198,1.1673,.6663,.006,1.141,.6469,.1015,.9939
208 DATA .6919,.1715,.9687,.5852,.1084,.8989,.6069,-.0577,1.2497
209 DATA .5593,-.0356,1.2311,.6186,-.1502,1.393,.5551,-.2201,1.5125
210 DATA .6927,-.1748,1.4239,.7003,-.2411,1.521,.7520,-.1123,1.3173
211 DATA .8043,-.1332,1.3415,.8017,.0426,1.0514,.7898,.107,1.0022
212 DATA .8716,.0092,.9204,.8899,-.081,.9083,.9233,.0934,.7933
213 DATA .2329,.5008,.2544,.1724,.541,.4711,.1704,.6485,.5989
214 DATA .2143,.7113,.4808,.1238,.6735,.8284,.113,.4799,.5788
215 DATA .0749,.5056,.7154,.1069,.3771,.4769,.0415,.3092,.5997
216 DATA .1662,.3364,.2582,.1667,.2631,.1739,.2268,.3958,.1512
217 DATA .2638,.3656,.0101,.2947,.561,.1404,.2869,.6335,.1728
218 DATA .3638,.5264,.0090,.3802,.4357,-.0181,.4184,.6106,-.0974
219 DATA .2589,1.0198,-.1673,.3337,.994,-.141,.3531,.8985,.0061
220 DATA .3061,.8285,.0313,.4148,.8916,.1011,.3931,1.0577,-.2497
221 DATA .4407,1.0356,-.2311,.3814,1.1502,-.393,.4449,1.2201,-.5125
222 DATA .3073,1.1748,-.4239,.2997,1.2411,-.521,.248,1.1123,-.3173
223 DATA .1957,1.1332,-.3415,.1983,.9574,-.0514,.2102,.893,-.0022
224 DATA .1284,.9908,.0796,.1101,1.081,.0917,.0767,.9066,.2067
```

```
225 DIM OC(N,4),TC(N,4),T(4,4),IC(N,2)
227 FOR R=1 TO N
230 FOR C=1 TO 3
240 READ OC(R,C)
245 NEXT C
250 OC(R,4)=1
255 NEXT R
260 RETURN
298 REM ROTATION MATRICES
300 F=3.141592/180
310 SA=SIN(ALPHA*F): CA=COS(ALPHA*F): SB=SIN(BETA*F)
320 CB=COS(BETA*F):SG=SIN(GAMMA*F):CG=COS(GAMMA*F)
330 T(1,1)=A*CB*CG
340 T(1,2)=B*CB*SG
350 T(1,4)=C*SB*RZ
360 T(2,1)=A*(SA*SB*CG-CA*SG)
370 T(2,2)=B*(SA*SB*SG+CA*CG)
380 T(2,4)=-C*SA*CB*RZ
390 T(3,1)=A*(CA*SB*CG+SA*SG)
400 T(3,2)=B*(CA*SB*SG-SA*CG)
410 T(3,4)=-C*CA*CB*RZ
420 T(4,1)=U:T(4,2)=V:T(4,4)=1-W*RZ
430 FOR R=1 TO 4:T(R,3)=0:NEXT R
440 RETURN
500 FOR R=1 TO N
510 FOR C=1 TO 4
515 S=0
520 FOR J=1 TO 4
525 S=S+OC(R,J)*T(J,C)
530 NEXT J
535 TC(R,C)=S
540 NEXT C
545 NEXT R
550 RETURN
```

```
598 REM CALCULATION OF SCREEN COORDS
600 FOR R=1 TO N
605 PRINT R
610 IC(R,1)=(TC(R,1))/TC(R,4)
620 IC(R,2)=TC(R,2)/TC(R,4)
630 PRINT IC(R,1),
635 PRINT IC(R,2)
640 NEXT R
650 RETURN
698 REM SCREEN X=320 Y=200
699 REM SC(N,2)=SCREEN COORDS
700 DIM SC(N,2)
710 P=320:Q=200:YD=10
720 FOR R=1 TO N
730 SC(R,1)=INT(TC(R,1)*Q/YD/TC(R,4)+P/2)
740 SC(R,2)=INT(TC(R,2)*Q/YD/TC(R,4)+Q/2)
750 NEXT R
755 RETURN
800 DATA 72,1,2,2,3,3,4,3,5,2,6,6,7
801 DATA 6,8,8,9,8,10,10,11,10,12
802 DATA 12,13,12,1,1,14,14,15
803 DATA 14,16,16,17,16,18
804 DATA 19,20,20,21,21,22,21,23
805 DATA 20,24,24,25,24,26,26,27
806 DATA 26,28,28,29,28,30,30,31
807 DATA 30,19,19,32,32,33,32,34
808 DATA 34,35,34,36,37,38,38,39,39,40
809 DATA 39,41,38,42,42,43,42,44,44,45,44,46,46,47,46,48
810 DATA 48,49,48,37,37,50,50,51,50,52,52,53,52,54
811 DATA 55,56,56,57,57,58,57,59,56,60,60,61,60,62,62,63
812 DATA 62,64,64,65,64,66,66,67,66,55,55,68,68,69,68,70,
813 DATA 70,71,70,72
814 GRAPH 1
815 GRAPH 0
820 READ NL
825 FOR L=1 TO NL
830 READ P1,P2
840 LINE SC(P1,1),SC(P1,2),SC(P2,1),SC(P2,2)
850 NEXT L
860 RETURN
```

Appendix 11.5

This simulation program shows the relative positions of MNA molecules in the MNA-3 unit cell (viewed down z) as lines which represent the C(7)...N(1) axes. The changes which occur in one unit cell (top left) are poked into 8 other unit cells so that the full screen shows the changes in 9 (3 x 3) unit cells. The statement LINE x1,y1,x2,y2 draws a line from x1,y1 to x2,y2 and the statement WIPE will delete a line.

```
100 REM A SIMULATION OF THE CHANGE
110 REM MNA-3 TO MNA-1
120 GRAPH 0:Q=320
130 FOR X=0 TO 63 STEP 8
140 FOR Y=0 TO 63 STEP 8
150 RESET X,Y:NEXT Y,X
160 FOR X=0 TO 7:FOR Y=0 TO 7
170 M=53248+X+(Y*40)
180 FOR Z=0 TO 2
190 T=PEEK(M)
200 POKE M+(Q*Z),T
210 POKE M+(Q*Z)+8,T
220 POKE M+(Q*Z)+16,T
230 POKE M+(Q*Z)+24,T
240 POKE M+(Q*Z)+32,T
250 NEXT Z,Y,X
260 REM OUTLINES UNIT CELL OF MNA-3
270 LINE 0,0,63,0
280 LINE 63,0,63,63
290 LINE 63,63,0,63
300 LINE 0,63,0,0
310 REM C1...N1 AXES OUTLINED
320 LINE 28,45,44,61
330 LINE 63,51,50,36
340 LINE 36,19,20,3
350 LINE 0,13,14,28
360 FOR TD=0 TO 10000:NEXT
```

```
370 REM C1...N1 AXES ROTATED ABOUT N1
380 FOR J=0 TO 32
390 LINE 28,45,44-J,61
400 WIPE 28,45,44-J,61
410 NEXT
420 LINE  28,45,12,61
430 FOR J=0 TO 32
440 LINE 63,51,50+J,36
450 WIPE 63,51,50+J,36
460 NEXT
470 LINE 63,51,82,36
480 FOR J= 0 TO 32
490 LINE 36,19,20+J,3
500 WIPE 36,19,20+J,3
510 NEXT
520 LINE 36,19,52,3
530 FOR J=0 TO 14
540 LINE  0,13,14-J,28
550 WIPE  0,13,14-J,28
560 NEXT J
570 FOR J=0 TO 18
580 LINE 63,13,63-J,28
590 WIPE 63,13,63-J,28
600 NEXT J
610 LINE 63,13,45,28
620 LINE 0,0,0,63
630 LINE 63,0,63,63
640 FOR TD=1 TO10000:NEXT
650 REM ERASE MNA-3 UNIT CELLS
660 WIPE 0,0,63,0
670 WIPE 63,0,63,63
680 WIPE 63,63,0,63
690 WIPE 0,63,0,0
700 FOR TD=0 TO 10000:NEXT
710 REM OUTLINE MNA-1 UNIT CELLS
720 LINE 0,0,63,63
730 LINE 32,0,0,32
740 LINE 63,32,32,63
750 END
```

Appendix 11.6

In order to assist in the identification of the flat face of the flat needle-shaped crystals of MNA-3, rotation photographs were obtained which showed a series of closely spaced layer lines.

A photocopy of such a rotation photograph is shown in fig. 11.1. The unit cell axis around which rotation occurs is given by the formula[217]

$$d = n\lambda / \cos(\tan^{-1} D/2y_n)$$

where d = the repeat distance of the unit cell axis around which rotation occurs;

λ = wavelength of X-rays used (1.542 Å)

D = cylindrical film diameter (60 mm)

y_n = separation of the 0 and nth layer ($2xy_{10}$ = 59.3 mm)

The calculated values for d based on 10,8 and 6 layers are 21.97, 21.95, and 21.94 Å respectively.

A value of 21.95 ± 0.05 Å was adopted for d. Comparison of this value with the MNA-3 unit cell diagonals from 0,0,0 to 1,1,0 (21.97 Å) and 1,0,0 to 0,1,0 (22.26 Å). This result led to the conclusion that the flat face of MNA was parallel to planes of Miller indices 1 $\bar{1}$ 0.

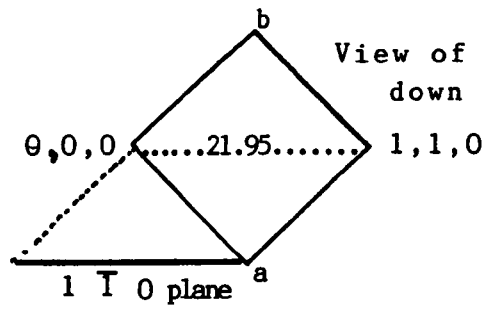

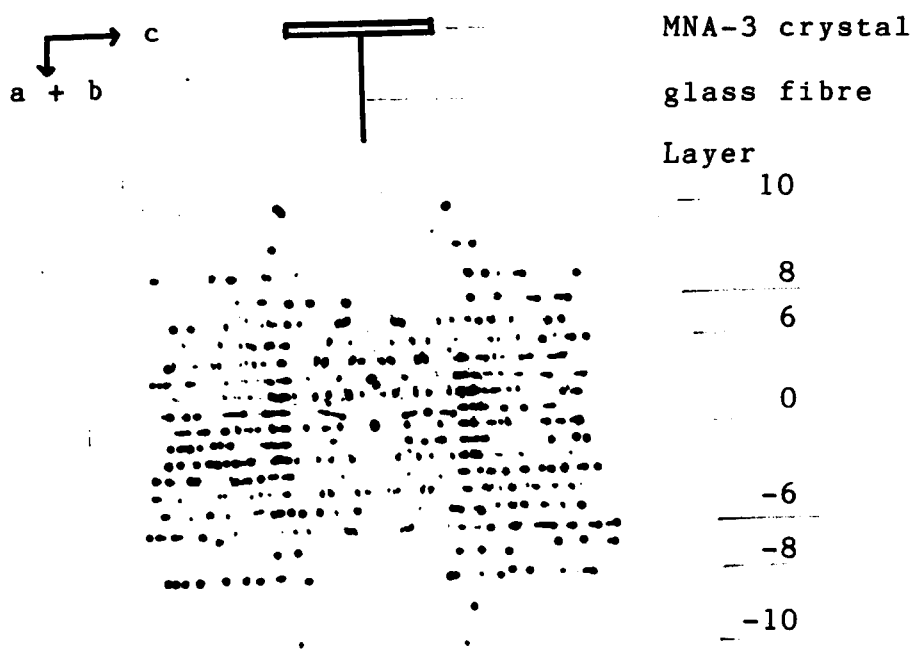

Fig. 11.1 A rotation photograph of MNA-3 with the needle axis of the crystal perpendicular to axis ofrotation. (this reproduction has lost its original good quality)